1-1-2013

Development Of Matrix Assisted Ionization Methods For Characterization Of Soluble And Insoluble Proteins From Native Environments By Mass Spectrometry

Ellen Dela Victoria Inutan
Wayne State University,

Follow this and additional works at: http://digitalcommons.wayne.edu/oa_dissertations

DEVELOPMENT OF MATRIX ASSISTED IONIZATION METHODS FOR CHARACTERIZATION OF SOLUBLE AND INSOLUBLE PROTEINS FROM NATIVE ENVIRONMENTS BY MASS SPECTROMETRY

by

ELLEN DELA VICTORIA INUTAN

DISSERTATION

Submitted to Graduate School

of Wayne State University,

Detroit, Michigan

in partial fulfillment of the requirements

for the degree of

DOCTOR OF PHILOSOPHY

2013

MAJOR: CHEMISTRY (Analytical)

Approved by:

_____

Advisor   Date

_____

_____

_____

DEDICATION

This dissertation is dedicated to

my parents: **Evangeline Herrero** *and* **Pacito dela Victoria Sr.***(deceased);*

my husband: **Rollie Montebon Inutan** *and my son* **Andrei Jullan**

ACKNOWLEDGEMENTS

To our collaborator, **Prof. Charles McEwen**, thank you for supporting and guiding me in every step of the way. You are a great help in my progress as a researcher.

To the members of my committee, **Prof. Colin Poole**, **Prof. Charles McEwen**, and **Prof. Wen Li** for their expertise and inputs for the completion of my dissertation. Thank for your time that has made me move towards this end.

To **Wayne State University, Department of Chemistry and its staff** (Melissa, Debbie, Erin, Diane, Bernie, Katlyn, Jackie, Nestor, Dr. Shay, Dr. Lew, **Dr. Coleman**) for providing all that I needed in fulfilling my Ph.D program requirements especially the financial support thru assistantships and fellowships (Schaap, Summer dissertation, and Rumble). I also thank Dr. Barber, Dr. Zibuck, Dr. Poole, and Dr. Munk, my mentors as a teaching assistant. The training you provided made me grow in this area equipped with the tools and character to excel in this field.

To the **TRIMPIN GROUP** (Alex, John, Beixi, Chris, Alicia, Darrell, Samantha, Jermel, Leonard, Chenchen, Danielle, Kristen, Corinne, Tarick, Dan, Steve, Lorelie) for without them, my life in the lab will never be as encouraging and uplifting. Thank you for all your help in the lab, the teamwork that you've shown, and the bits and pieces of advice you gave to me. To Andjoe, for all the time that we've been together in the lab. It was such an unforgettable moment. I am thankful that I've met you.

To my **Filipino friends**: Janir, Joel, Lalai, and Armando for their kindness, generosity, and invaluable time together. To my close friends: Thushani, Kanchana, Sadish, Asanka, Joe, Jing, Yinling, Fadia, and Calvin. Thank you for the precious moments that we shared together that made my graduate school exciting.

To my colleagues in the Department of Chemistry (**MSU-IIT, Philippines**) for all the support that they've provided that made me finish my Ph.D. Thank you for trusting and believing that I would be able to accomplish all of these.

To the **Cathedral church of St. Paul**, for accepting me as part of their family and for the spiritual support they've been providing that made me strong in every endeavor that I have along the way.

Above all, to the ***Almighty God*** to whom I bring back all the praises and thanksgiving for allowing all these achievements to be part of His will for me. All the strength, the knowledge, and wisdom, I owe everything to Him. I would never have been joyful and successful in this life without His presence and guidance. To **YOU**, I bring back all the glory and honor.

PREFACE

This dissertation is based closely on the following refereed publications:

Chapter 3: Trimpin, S.; Inutan, E.D.; Herath, T.N.; McEwen, C.N.; A Matrix-Assisted Laser Desorption/Ionization Mass Spectrometry Method for Selectively Producing Either Singly or Multiply Charged Molecular Ions, *Anal. Chem.* **2010**, *82*, 11-15.

Chapter 4: Trimpin, S.; Inutan, E.D.; Herath, T.N.; McEwen, C.N.; Laserspray Ionization - A New AP-MALDI Method for Producing Highly Charged Gas-Phase Ions of Peptides and Proteins Directly from Solid Solutions, *Mol. Cell. Proteomics* **2010**, *9*, 362-367.

Chapter 5: Inutan, E.D.; Trimpin, S. Laserspray Ionization (LSI) Ion Mobility Spectrometry (IMS) Mass Spectrometry (MS). *J. Am. Soc. Mass Spectrom.* **2010**, *21*, 1260-1264.

Chapter 6: Inutan, E.D.; Trimpin, S. Laserspray Ionization - Ion Mobility Spectrometry - Mass Spectrometry: Baseline Separation of Isomeric Amyloids without the Use of Solvents Desorbed and Ionized Directly from a Surface. *J. Proteome Res.* **2010**, *9*, 6077-6081.

Chapter 7: Inutan, E.D.; Richards, A.L.; Wager-Miller, J.; Mackie, K.; McEwen, C.N.; Trimpin, S. Laserspray Ionization - A New Method for Protein Analysis Directly from Tissue at Atmospheric Pressure and with Ultra-High Mass Resolution and Electron Transfer Dissociation Sequencing. *Mol. Cell. Proteomics* **2011**, *10*, 1-8.

Chapter 8: <u>Inutan, E.D.</u>; Wang, B.; Trimpin, S. Commercial Intermediate Pressure MALDI Ion Mobility Spectrometry Mass Spectrometer Capable of Producing Highly Charged Laserspray Ionization Ions. *Anal. Chem.* **2011**, *83*, 678-684.

Chapter 9: <u>Inutan, E.D.</u>; Wager-Miller, J.; Mackie, K.; Trimpin, S. Laserspray Ionization Imaging of Multiply Charged Ions using a Commercial Vacuum MALDI Ion Source. *Anal. Chem.* **2012**, *84*, 9079-9084.

Chapter 10: <u>Inutan, E.D.</u>; Trimpin, S. Matrix Assisted Ionization *Vacuum*, a New Ionization Method for Biological Materials Analysis using Mass Spectrometry. *Mol. Cell. Proteomics* **2013**, *12*, 792-796.

Chapter 11: Trimpin, S.; <u>Inutan, E.D.</u> Matrix Assisted Ionization in Vacuum, a Sensitive and Widely Applicable Ionization Method for Mass Spectrometry. *J. Am. Soc. Mass Spectrom.* **2013**, *24*, 722-732.

Chapter 12: <u>Inutan, E.D.</u>; Wager-Miller, J.; Narayan, S.; Mackie, K.; Trimpin, S. The Potential for Clinical Applications using a New Ionization Method Combined with Ion Mobility Spectrometry - Mass Spectrometry. *Int. J. Ion Mobility Spectrom.*, **2013**, *16*, 145-159.

TABLE OF CONTENTS

LIST OF SCHEMES

LIST OF TABLE

LIST OF FIGURES

xiii

CHAPTER 1

NEW INLET AND VACUUM IONIZATION METHODS

FOR MASS SPECTROMETRY

1.1 Introduction

Mass spectrometry (**MS**) is an important analytical tool because of its wide applicability, dynamic range, sensitivity, specificity, speed of analysis, and the ability to simultaneously observe many constituents in a mixture. Its advancement in analyzing nonvolatile and large biological molecules has made a huge impact in the area of biological research. Key to this advancement is the development of two commonly used ionization methods in MS: electrospray ionization (**ESI**) [1] and matrix-assisted laser/desorption ionization (**MALDI**) [2,3] to ionize nonvolatile and high-mass compounds such as peptides and proteins. ESI, with the production of multiply charged ions from solution at atmospheric pressure (**AP**), has gained much attention because of the simplicity to interfaced with chromatographic and electrophoretic liquid-phase separation techniques.[4] In addition, the formation of higher charge states can extend the mass range of high resolution mass range limited mass spectrometers and provide the advantage of better fragmentation for structural characterization and identification. On the other hand, MALDI with time-of-flight (**TOF**) mass analyzers [3,5] rapidly gained its popularity for analyzing large biomolecules. The production of predominantly singly charged ions makes data interpretation simpler. MALDI-TOF-MS, due to its high

sensitivity and analysis directly from the surface, is the chosen analytical tool for molecular tissue imaging [6,7], important for biomedical applications [8].

A long term interest of our research group is the analysis of solubility restricted materials, especially directly from surfaces. ESI is limited to samples that can be solubilized. It is in this area where ESI-MS has challenges when dealing with poorly soluble and insoluble compounds such as membrane proteins. Although MALDI can analyze directly from the surface, structural characterization is challenging because of poor fragmentation using singly charged ions. The limitation of ESI to analyze directly from the surface and the difficulty of MALDI to provide better fragmentation are reasons to develop ionization techniques that have the benefits of ESI and MALDI. Ionization developments described in this dissertation demonstrate the ability to detect and characterize compounds directly from a surface such as tissue, and use gas phase ion mobility separation to reduce complexity and improve the dynamic range of the experiment.

1.2 Motivation

Cellular membranes are important in the area of biological research to understand diseases associated with it. The available analytical tools have limitations in analyzing these compounds because of their complexity and limited solubility. Membrane proteins are an example of solubility restricted compounds in the cellular membrane for which the current understanding in relation to disease is limited because of the inability of current analytical technologies to unravel the chemical make-up of this complex system.[9,10] Approximately 70% of drugs are said to target membrane proteins and 20 to 30% of the

human genome encodes membrane proteins but less than 1% of the proteins of known structure are membrane proteins.[9,11,12] Diseases related to the membrane architecture are Alzheimer's disease (AD), Huntington's diseases, Parkinson's disease, and misfolding/aggregation (e.g. prion disease).[13-18]

Advances needed to better analyze membrane proteins include improved sample preparation to solubilize intact proteins, instrumentation to allow characterization and identification especially of protein isoforms, and better liquid chromatographic (**LC**) performance involving bottom up and top-down proteomics.[9,19] MS has been a powerful analytical approach in developing comprehensive analysis of membrane proteins. ESI and MALDI are the most used MS techniques in determining the molecular weights of intact proteins followed by enzyme digestion, separation, and tandem MS/MS for characterizing and identifying the proteins.[20] However, the approach of bottom up or shotgun proteomics which involves the use of high performance LC combined with MS requires solubilization of these compounds. In addition, analyzing membrane proteins directly from their native environment requires new analytical technologies especially when dealing with complex systems such as tissue which is important for pharmacology and disease treatments. Efficient ionization of these compounds still remains an issue due to their limited solubility.

AP-MALDI has been demonstrated [21] and offers advantages over vacuum MALDI, including speed of analysis and compatibility with instruments built for atmospheric pressure ionization (API) [22]; however, vacuum MALDI offers better sensitivity and the analysis of large biomolecules [23] than AP-MALDI. AP-MALDI is

limited in mass range because of the mass-to-charge (m/z) limitations of API instruments and the production of predominately singly charged ions. Thus, methods that have attributes of AP-MALDI, but provide improved sensitivity and/or multiply charged ions are needed. Sheehan and Willoughby modeled AP ionization and reported that if a high electric field is present in the AP region, >90% of the ions are lost to the walls (rim losses) entering the AP to vacuum orifice.[24] Willis and Grosu demonstrated a laser ablation experiment using the backside approach where the laser beam passes through the glass sample holder causing an explosive expansion of the material irradiated.[25] The feasibility of a backside (transmission geometry, **TG**) approach in AP-MALDI for laser ablation using a glass plate as a sample holder positioned close (1-3 mm) to the mass spectrometer ion entrance was also previously demonstrated.[26] Combining these configuration with field-free (**FF**) conditions was anticipated to ensure high transmission of ions into the mass analyzer. An ionization source was configured for AP-FF-TG MALDI.[27,28] The sample holder was a glass plate and the laser illuminates from the backside so the sample holder can be placed close (1-3 mm) in front of the MS orifice. This back-side laser ablation approach desorbs/ionizes similar to the front side (reflectron geometry, **RG**) approach. The laser ablates the matrix/analyte crystals from the surface and the expanding matrix plume brings them sufficiently close to the MS ion entrance inlet so that they become flow entrapped in the air entering the inlet to the vacuum of the mass spectrometer. With this transmission geometry (**TG**) approach, the spatial resolution is improved because shorter laser focal lengths can be used to provide a smaller laser spot at the point of ablation. Imaging can be achieved by moving the

sample through the laser beam focused on the sample and aligned with the MS inlet. Most important, however, was the discovery that multiply charged ions, similar to what is observed with ESI, were produced using laser ablation of a MALDI matrix. Initially, the methods was deemed to be a MALDI method,[27,28] but later was termed laser spray ionization (**LSI**) [29]. This initial discovery is the starting point of the research presented here in which a number of ionization methods were uncovered. For some, ionization occurs in a heated *inlet* and for others in *vacuum*.

1.3 LSI Inlet and Vacuum Ionizations

The newly discovered ionization methods are summarized in **Scheme 1.1**. LSII, the first inlet ionization method produces multiply charged ions similar to ESI at AP (**Scheme 1.1.IA)** but directly from the solid state similar to MALDI.[30] Ionization occurs in a heated inlet tube between AP and vacuum. Since LSII has similar attributes to MALDI, which uses a matrix to produce ions, initial understanding on the ion formation for LSII is that the laser results in a free jet expansion of the matrix producing highly charged matrix/analyte clusters that become desolvated in the heated inlet capillary of a mass spectrometer (**Scheme 1.1.IA**).

To understand the fundamental aspects of LSII, the ablated material was collected on a glass plate before it enters the ion entrance of the mass spectrometer and analyzed using microscopy. Microscope image of this ablated material shows particles and formation of liquid droplets [31] similar to what has been experimentally observed in vacuum MALDI [32-34] and theoretically shown through dynamic molecular modeling studies [35-38]. In addition, a temperature study on the heated inlet transfer capillary

shows that ion abundance of the multiply charged ions increased significantly as the transfer capillary is heated from 100 to ~350 °C.[29] Contrary to MALDI, a laser is not required as identical mass spectra were obtained by physical means (e.g. tapping) of transferring the matrix/analyte crystals into the heated transfer capillary of the mass spectrometer. This approach is called matrix assisted ionization *inlet* (**MAII**) (**Scheme 1.1.IB**).[39]
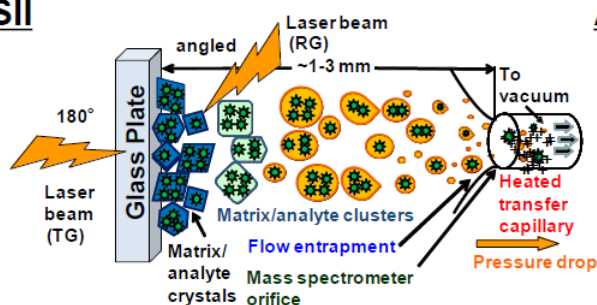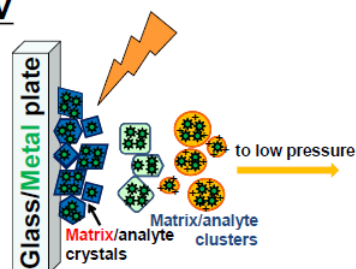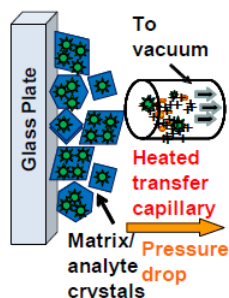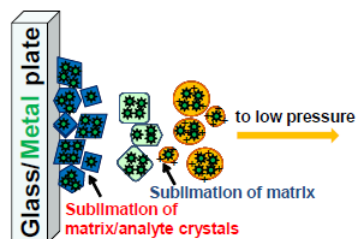
Scheme 1.1. (**I**) *Inlet* ionizations: (**A**) LSII and (**B**) MAII, and (**II**) *Vacuum* ionizations: (**A**) LSIV and (**B**) MAIV.

In addition, a study of over 200 small molecule matrices showed that aromaticity and functionality similar to that of common UV-MALDI matrices (e.g., 2,5-dihydroxyacetophenone, **2,5-DHAP** and 2,5-dihydroxybenzoic acid, **2,5-DHB**) (**Scheme 1.2**) is not a requirement to produce multiply charged ions since matrixes that are linear,

or aromatic compounds with no other functionality, produces multiply charged ions so as long as it is heated at ~450 °C.[40] A number of these matrixes worked at temperatures as low as 50 °C. Because LSII and MAII produce ions within a heated tube linking AP to the first vacuum region of the mass spectrometer and the ionization occurs within the heated inlet tube, these methods have been termed '*inlet* ionizations'.

A) 2,5-Dihydroxybenzoic acid

C) 2-Nitrophloroglucinol

B) 2,5-Dihydroxyacetophenone

D) 3-Nitrobenzonitrile
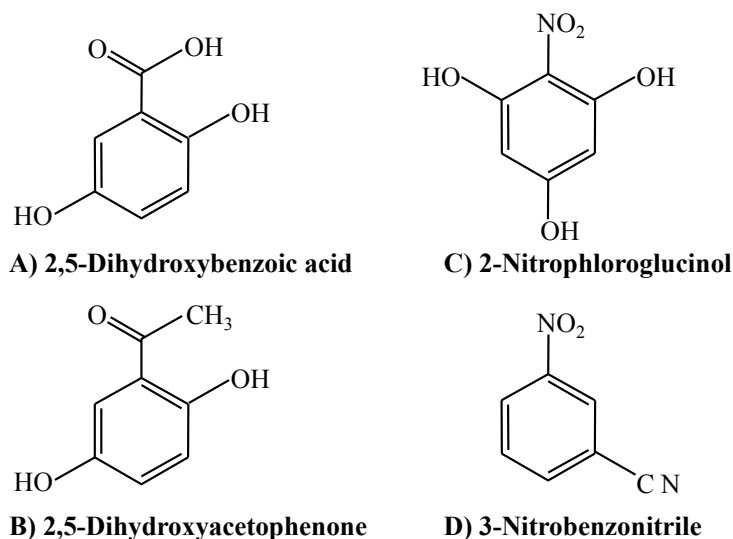
Scheme 1.2. Structures of LSII (**A,B,C**), LSIV (**B,C**) and MAIV (**D**) matrixes.

A number of these matrixes that have lower thermal requirement were tested on a SYNAPT G2 vacuum MALDI source that operates at intermediate pressure (**IP**) and the source uses RG laser alignment. The TG approach in LSII is not a limitation in the production of multiply charged ions because RG had previously been demonstrated using an AP-MALDI source for LSII.[41] With the vacuum MALDI source, the only source of thermal energy is the laser ablation event. The pressure drop for LSII still applies to this setup because the source operates from IP to vacuum. Two matrixes, 2,5-DHAP and 2-nitrophloroglucinol (**2-NPG**) (**Scheme 1.2**) were shown to produce multiply charged ions

in the IP-MALDI vacuum source with the use of a laser, similar to what has been obtained using LSII. This approach was thus called laserspray ionization *vacuum* (**LSIV**) (**Scheme 1.1.IIA**).[42,43]   2-NPG also produces stable multiply charged ions in high vacuum MALDI-TOF instruments.[44,45] Among the few matrixes that produced multiply charged ions at 50 °C, 3-nitrobenzonitrile (**3-NBN**) (**Scheme 1.2**) astonishingly produces multiply charged ions just by exposing the matrix/analyte crystals to the vacuum of the IP-MALDI source of the mass spectrometer without initiating the laser. This method is called matrix assisted ionization *vacuum* (**MAIV**) (**Scheme 1.1.IIB**) [46,47] in analogy to MAII. The classification defines the main driving force for the formation of the analyte ions by using a heated *inlet* (**Scheme 1.1.I**) or by the *vacuum* (**Scheme 1.1.II**) of the mass spectrometer.

This dissertation presents the results, application, and insights to the fundamental aspects of the three new ionization methods developed during the course of the work described here: LSII, LSIV, and MAIV in ten published papers. **Chapter 2** describes general experimental procedures including the materials, sample preparation, set-up, acquisition conditions, and instrumentation involved. Experimental methods relevant to each chapter are included in the chapter. **Chapters 3-7** shows the results obtained for LSII on three different mass spectrometers: Thermo Scientific Orbitrap Exactive [28,29,48] and LTQ Velos [48], and Waters SYNAPT G2 [49,50] documented in five published papers. **Chapter 3** reports the first FF-TG-AP-MALDI experiments using a 2,5-DHB, a matrix common to MALDI, to produce multiply charged ions. Singly or multiply charged ions can be selectively produced by changing the matrix or sample

preparation conditions for 2,5-DHB. Using 2,5-DHB matrix, multiply charged ions are produced from angiotensin I using solvent-based sample preparation while singly charged ions are formed using solvent-free sample preparation. ESI-like mass spectra are observed by applying as low as attomole amounts of the analyte with the matrix on the target plate. The production of multiply charged ions similar to ESI extends the mass range of high resolution mass spectrometers that have limited mass-to-charge (*m/z*) ratio (4000).

Chapter 4 discusses briefly the fundamental aspects and the conditions for LSII in producing ESI-like ions in MALDI-like sample preparation. ESI produces multiply charged ions by a mechanism involving highly charged solvent/analyte droplets.[1,51-53] In MALDI, the dominant production of singly charged ions was postulated to occur from multiply charged matrix:analyte clusters by the "lucky survivor" model [54] and latter modified to formation of singly charged ions from clusters [55]. Multiply charged cluster formation has been proposed in MALDI by a mechanism similar to ESI.[54,56,57] For LSII, the formation of liquid droplets and clusters of the laser ablated material was shown from the microscopy studies [31] at AP. These observations are similar to the droplets or cluster formation by MALDI and has been experimentally observed [32-34] and theoretically demonstrated thru molecular modeling studies [35-37]. For LSII, these liquid droplets and clusters are believed to be highly charged and with appropriate desolvation condition as shown from the temperature study of the heated transfer capillary produces abundant multiply charged ions. In vacuum MALDI, it is proposed that charged droplets/clusters are produced by laser ablation, but for LSII after the

discovery of MAII, it is shown that removing charged droplets/particle/ions with high voltage before they enter the inlet does not significantly alter the ion abundance in LSII. The tapping method to demonstrate MAII clearly shows that the charges are produced in the inlet for LSII. With the production of ESI-like mass spectra by LSII, the first protein fragmentation is reported from a MALDI-like sample preparation using electron transfer dissociation (**ETD**) [58]. Fundamental aspects in producing multiply charged ions by LSII includes the field-free and proper desolvation conditions using a heated transfer capillary in the presence of a pressure drop region from AP to vacuum.

MS methods are limited to the separation of ions measured and displayed by *m/z* ratios and ion intensities thus it becomes a challenge to analyze complex systems such as tissue by MS due to its complexity including solubility, volatility, hydrophobicity, isobaric, and isomeric compositions. Current technologies employ liquid based separation approaches coupled to MS, but perform poorly with solubility restricted materials [10,30]. Ion mobility spectrometry (**IMS**) MS has been noted for the ability to separate ions in the gas-phase according to the number of charges and cross-section defined by size and shape.[59-67] IMS-MS has many advantages compared with even high-resolution mass spectrometers because of its ability to extend the dynamic range and separate isomeric composition.[64-67]

With the ability of LSII to produce multiply charged ions, **Chapter 5** presents the results of LSII coupled to a Waters SYNAPT G2 mass spectrometer with IMS-MS capability. The Waters SYNAPT G2 has a source that can only be heated up to 150 °C. Fabrication of a desolvation device mounted on the z-spray ESI skimmer cone of the

SYNAPT G2 mass spectrometer provides the external heat needed to desolvate efficiently the 2,5-DHB matrix from the highly charged matrix/analyte clusters to produce the multiply charged molecular ions.[29] The total ion current displays almost no ion abundance when the external heat supply is off. With the IMS dimension, one can readily observed the separation of the components in the mixture from the pictorial snapshot [66] as displayed from the 2-dimensional plot of drift time *vs. m/z*. The 2-D plot display allows the extraction of drift time and/or *m/z* which is very useful for the separation of components in a complex mixture. In the absence of a heated inlet, another approach to efficiently desolvate the highly charged matrix/analyte clusters is to lower the thermal requirement of the matrix for the desolvation process.

Chapter 6 reports the use of 2,5-DHAP matrix that allows the operation of Waters SYNAPT G2 mass spectrometer at 150 °C without applying external heat to the fabricated desolvation device. The multiply charged ions produced from an isomeric mixture are well separated in the drift time dimension. Distinguishig isomers by MS alone is currently not possible. The extracted drift time information using LSII shows baseline separation of the isomeric mixture. The LSII drift times obtained from a surface are identical to the extracted drift times using solution ESI suggesting similar softness. Conditions that lower the thermal requirement in the formation of multiply charged ions by LSII are very important in retaining the structure of proteins during ionization and when coupled with IMS, provide the benefits of efficient separation and characterization of protein mixture including isomers as well as cross section analysis from surfaces which is important for biomedical application involving tissue samples.

Chapter 7 reports for the first time the detection of intact peptides and proteins of up to ~20 kDa by LSII directly from mouse brain tissue mounted on a microscopy glass plate and spotted with 2,5-DHAP matrix. The multiple charging of LSII allows the analysis of proteins from the mouse brain tissue on a high performance mass spectrometer that has limited m/z. The use of a high resolution mass spectrometer provides the mass accuracy which is useful in identifying the protein from the measured molecular weight. With sufficient ion abundance of the multiply charged ions from the tissue, ETD fragmentation is demonstrated for the first time directly from the tissue providing sequence coverage and identification of an endogenous peptide when combined with the high mass resolution and mass accuracy data obtained from the same tissue samples. With the TG approach for LSII, improved spatial resolution for tissue imaging can be attained. As shown in this study , ~15 μm diameter laser ablated areas on the tissue are seen thru microscopy images. In addition, the AP condition allows the analysis of tissue at ambient conditions and speed of analysis beneficial for tissue imaging.

Chapter 8 reports the first example of the production of highly charged ions in vacuum similar to LSII, thus termed LSIV using the commercial IP-MALDI vacuum source of the SYNAPT G2. In the absence of a heated inlet, important factors influencing the production of multiply charged peptide/proteins ions in a vacuum MALDI source at IP are the use of a suitable matrix and the appropriate settings and acquisition conditions (e.g. laser power, voltages) for ion acceleration and transmission. With IMS dimension, singly charged lipid ions are well separated from multiply charged

peptide/protein ions detected from mouse brain tissue. The extracted drift times of the identified endogenous peptide directly from the mouse brain tissue are identical to the synthesized standard using LSII and ESI confirming the presence of the endogenous peptide in the tissue.

In a search for more matrixes that have low thermal requirements for desolvation in the absence of a heated inlet, **Chapter 9** introduces another matrix, 2-NPG, that produces higher charge states than 2,5-DHAP in vacuum. Spotting 2-NPG on a delipified mouse brain tissue allows the detection of higher mass compound in the tissue than 2,5-DHAP using LSIV. The use of 2-NPG for tissue imaging by LSIV, which was not possible for 2,5-DHAP, shows the first example of images of multiply charged ions from delipified mouse brain tissue.

Another matrix, 3-NBN, produces multiply charged ions with high ion abundance even at very low temperature using MAII. **Chapters 10-12** reports for the first time the production of ions in vacuum without the use of a laser by using 3-NBN as the matrix on the IP-MALDI vacuum source of a SYNAPT G2 mass spectrometer. **Chapter 10** introduces this new ionization as MAIV and shows the ability to ionize a variety of samples from small molecule, lipids, peptides, to proteins up to ~66 kDa by simply exposing the matrix/analyte crystals to the vacuum of the mass spectrometer without the use of the laser. MAIV ionizes both in positive and negative mode measurements. Low femtomole concentration can be analyzed without optimization for small proteins. This new ionization in vacuum without the use of a laser is softer than MALDI for the analysis of fragile molecules, post translational modification, and molecular complexes. The

sublimation process makes it possible for MAIV to improve the spatial resolution in analyzing tissue samples since matrix deposition on the tissue can be miniaturized.

Chapter 11 presents a brief mechanistic aspect on the ion formation by MAIV. The conversion of the matrix/analyte crystals into gas-phase ions without the use of laser suggests that the ion formation is via a sublimation process in which 3-NBN has the property to sublime.[68]   In addition, 3-NBN is a triboluminescence compound [69,70] that produces a strong dinitrogen discharge emission as a result of the high electric field created during crystal fracturing leaving the opposing surfaces having opposite charges. This phenomenon also explains the ability of 3-NBN to ionize molecules both in positive and negative ion mode detection. Thus, the formation of ions by MAIV in vacuum using 3-NBN is hypothesized to be a sublimation driven triboluminescence process. Different surfaces can be used for MAIV including filter paper, foil, thin layer chromatography plates, and paper currency. Basic small molecules are ionized with less or no chemical background which is an advantage in comparison to MALDI for small molecule analysis. Sensitivity of basic small molecule is achieved at very low femtomol and with MS/MS high attomole concentrations in the positive ion mode. Analysis of mixture of lipid, peptides, and proteins by MAIV ionizes efficiently all the components in the mixture and with the IMS dimension are well separated and the charge state distribution are readily observed from the pictorial snapshot. Because ions are formed by using a suitable matrix, e.g. 3-NBN, and by exposing the matrix/analyte crystals to the vacuum of the mass spectrometer, MAIV extends its utility using a custom modified ESI source.[46,47,71]

Chapter 12 reports the utility of MAIV for real time applications in combination with IMS for ionization, separation, and characterization of small molecule such as drugs to lipids, peptides, and proteins. Mixtures of small molecules are ionized instantaneously by MAIV and separated by IMS. Characterization by MS/MS without precursor ion selection makes the method rapid for clinical applications. MAIV is very specific in ionizing small molecules such as drugs as shown from the results obtained from drug treated mouse brain tissue, and drugs with their metabolites from biological fluids such as urine. MAIV ionizes efficiently both in positive and negative mode measurements, and with IMS dimension, comparison of extracted drift times can be compared between positive and negative mode, and with ESI. Identical drift times are observed between MAIV from the surface and ESI from solution. The production of higher charge states is advantageous to improve fragmentation by CID. With IMS dimension, multiply charged ions formed from isomeric mixture are baseline separated and with IMS, characterized by MS/MS in the transfer region. The sublimation process in the ionization allows miniaturization of matrix deposition on the tissue and detection of the higher mass compounds from mouse brain tissue in vacuum compared to LSIV. MAIV stands out among the three ionization methods, but currently has its limitation for tissue imaging. Both LSII and LSIV have the potential for tissue imaging and with LSII improving the spatial resolution. The quest in searching for an ionization method to efficiently ionized solubility restricted materials directly from the surface leads to a discovery that encompasses both the benefits and advantages of the traditional ionization methods in mass spectrometry.

CHAPTER 2

MATERIALS AND METHODS

2.1 Materials and Sample Preparation

Salts, sugars, lipids, peptides, and proteins were purchased from Sigma Aldrich (St. Louis, MO) unless otherwise noted. Amyloid peptides were purchased from American Peptide Co. (Sunnyvale, CA), other lipids from Cayman Chemicals (Ann Arbor, MI), synthesized N-acetylated myelin basic protein fragment (**MBP**) from Anaspec (Fremont, CA), modified peptides from Protea Biosciences (Morgantown, WV), clozapine from Santa Cruz Biotechnology (Santa Cruz, CA), and commonly used illicit drugs from Cerilliant (Round Rock, TX). Waters Co. (Milford, MA) provided leucine encephalin, [Glu1]-fibrinopeptide (**GFP**), and myoglobin. The matrixes were purchased from Sigma Adrich except for 2,5-DHAP which was obtained from Fisher Scientific Inc. (Pittsburg, PA). Solvents used were purchased from Fisher Scientific Inc. (HPLC grade water, acetonitrile (**ACN**), methanol (**MeOH**), ethanol, acetic acid, and trifluoroacetic acid (**TFA**)). Purified water was purchased from Millipore (Billerica, MA) acetic acid and ammonium hydroxide from Mallinckdrodt Chemicals (Phillipsburg, NJ), and HPLC grade water and methanol from EMD Chemicals (Gibbstown, NJ). Microscopy glass slides used was from Gold Seal (about 80% transmission) Products (Portsmouth, NH).

Stock solutions of peptides and proteins were prepared as 1 mg mL^{-1} in water except for bovine insulin in 1:1 by volume methanol/water with 1% acetic acid. Lipids and drugs were prepared in either 100% ACN, methanol, or ethanol. Salts were dissolved

in water to make 1 M concentration. Peptides and proteins were diluted in 100% water or 1:1 ACN/water with or without 0.1% acid. Lipids and drugs were diluted in 100% water or 1:1 methanol/water or ACN/water. Most of the matrixes were dissolved in 1:1 ACN/water. For solvent-based matrix/analyte preparation, the dried droplet method [3] was used. Both the matrix and analyte were dissolved separately in a common solvent, mixed by vortexing, placed 1 μL of the matrix/analyte mixture on the microscope glass slide or target plate, and air dried or using a heat gun (low heat). A layer method was also used by placing 1 μL of the analyte on the glass slide, added 2 μL of the matrix solution and mixing before allowing to air dry or blow dry using a heat gun. The method for solvent-free sample preparation is described elsewhere.[72,73]

Mouse Brain Tissue - The mouse brain tissue sections were provided by Dr. Ken Mackie from Indiana University (Bloomington, IN). Twenty week old C57 Bl/6 mice were euthanized with CO_2 gas and perfused transcardially with ice-cold 1X phosphate-buffered saline (150 mM NaCl, 100 mM NaH_2PO_4, pH 7.4) for 5 min to remove red blood cells. The brains were frozen at -22 °C and sliced into 10 μm sections in sequence using a Leica CM1850 cryostat (Leica Microsystems Inc., Bannockburn, IL). The tissue sections were placed onto a pre-chilled plain or matrix pre-coated microscopy glass slides that were briefly warmed with the finger from behind to allow sections to relax and attach. Care was taken to avoid water condensation by storing at -20 °C. The tissue-mounted glass slides were placed in an airtight box containing desiccant and transported under dry ice.

For drug treated mouse brain, the mouse received 50 mg kg^{-1} of clozapine by intraperitoneal introduction for 90 min before it was sacrificed. For peptides and protein analysis, the mouse brain tissue sections mounted on the glass plate were washed to remove the lipids according to a published procedure.[74] Before washing the tissue twice with ethanol, the glass slide with the mounted mouse brain tissue was dried in the desiccator. In the first wash, the glass slide with the mounted tissue was immersed in a glass Petri dish filled with 70% ethanol, swirled for 30 s, and removed carefully. The glass slide was then tilted to remove the solvent for about 10 s and immediately washed with 95% ethanol in another Petri dish for an additional 30 s. After the second wash, the glass slide was allowed to dry in the desiccator for 20 min prior to analysis or stored at -20 °C until use or shipment under dry ice.

2.2 Laserspray Ionization *Inlet* (LSII)

Laserspray ionization *inlet* (**LSII**) operates at AP in FF-TG. The laser, a Spectra Physics, VSL-337ND-S nitrogen laser, is aligned at approximately 180° to the mass spectrometer inlet. The beam is focused using a focusing lens on to the matrix/analyte spot applied to a glass microscope at about 1-3 mm distance from the ion entrance (**Scheme 1.1.IA**). The laser fluence must be sufficient to ablate the matrix/analyte crystals from the surface. The fluence is substantially higher than that used with most MALDI experiments (typically on the order of 1-2 J cm^{-2}). The higher laser fluence does not result in detrimental effects on the observed mass spectra, including resolution. The LSII set up was used on an Orbitrap Exactive and LTQ Velos from Thermo Scientific

(**Scheme 2.1**) (Bremen, Germany) and SYNAPT G2 (**Scheme 2.2**) from Waters Co. (Manchester, UK).

Orbitrap Exactive - The Ion Max source was removed to have open access of the inlet of the mass spectrometer by overriding the interlocks. External voltages were set to zero and there were no external gas flow. ESI tuning condition was used for capillary voltage (typically 20-140 V) and the tube lens voltage (typically 80-150 V). Necessary precaution was exercised so that no potential hazardous exposure to the laser beam or hot surfaces near the ion entrance orifice. The ion transfer capillary was heated up to ~400°C. Resolution was set at 100,000 (*m/z* 200, full width at half height definition) and the maximum ion inject time was set at 500 ms. Positive ion mass spectra were obtained for 1 s giving 100,000 mass resolution.
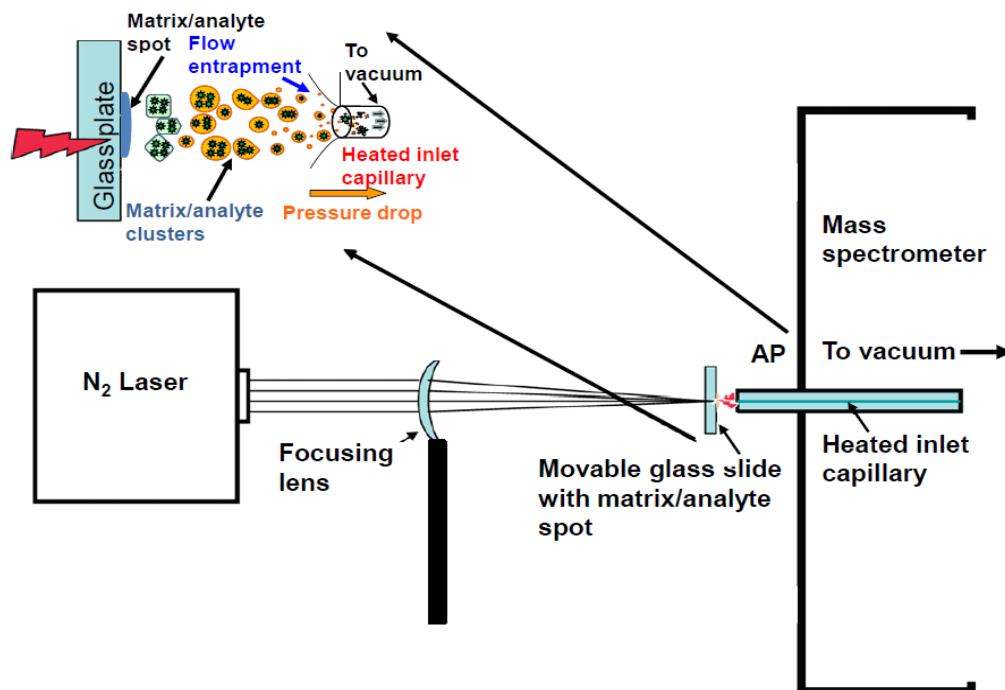
Scheme 2.1 Representation of FF-TG AP-MALDI (now called LSII) Source Design.[28]

LTQ Velos – Similar to the Orbitrap Exactive, the Ion Max source was removed and the interlocks were overridden to perform LSII, or with the Ion Max source with the removal of the front window for the laser beam to pass thru and aligned 180 °C to the mass spectrometer ion entrance. Also, the side window was removed so that the glass plate can be placed in front of the ion entrance. The temperature at the heated inlet ranged from 150-350 °C. Xcalibur 2.1.0 was used for data analysis.

LTQ Velos ETD - Fluoranthene was used as the electron transfer reagent and a mixture of ultrapure helium and nitrogen (25% helium and 75% nitrogen; purity, ~99.995%) was used as the reaction gas to perform the ETD experiments.

SYNAPT G2 – The Nanolockspray ion source of Waters SYNAP G2 was used to set up LSII.[49] This was achieved by removing the lockspray motor. In addition, the ion entrance orifice of the skimmer of the SYNAPT G2 mass spectrometer was modified since the source temperature can be heated only up to 150 °C. To have a source temperature above 150 °C, external heat was supplied to a fabricated external tube attached to the skimmer cone. A 1/8 in. outer diameter x 1/16 in. inner diameter x 1 in. length copper tubing was sanded on one end to fit through the cone gas nozzle (outer cone) and fitted on the ion entrance of the sample cone (inner cone) of the skimmer (**Scheme 2.2**). The copper tubing coated with Sauereisen cement (Insolute Adhesive Cement Powder no. P1), dried and 24 gauge nichrome wire (Science Kit and Boreal Laboratories, Division of Science Kit, Inc., Tonawanda, NY, USA) was coiled around the coated tube and again coated with a layer of Sauereisen cement and allowed to dry. The coated copper tubing was then attached to the skimmer and held to the cone gas nozzle

with a layer of Sauereisen cement. Both ends of the coiled nichrome wire were connected with alligator clips to the insulated copper wire from a variac (Powerstat Variable Transformer type 116). The copper desolvation device was heated by application of up to 12 V from the variac. The temperature measured on the outside of the device was > 200 °C. The nitrogen laser was placed 180 °C to the outer end of the attached copper tubing so that the laser beam fires at TG and focused on the sample. The x,y,z-stage of the Nanolockspray ion source was used to move the glass microscope slide with the matrix/analyte spot relative to the outer end of the copper tube and the laser beam.
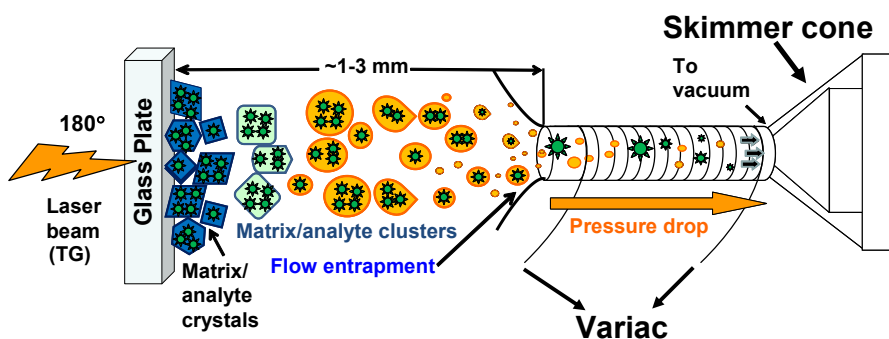
Scheme 2.2 Schematic representation of laserspray ionization *inlet* (**LSII**) with the fabricated desolvation device used on Waters SYNAPT G2 mass spectrometer.[49]

The SYNAPT G2 instrument was operated in positive and resolution modes. The sample cone was set at 40 V and the extraction cone at 4 V. The source temperature was set at 150 °C. The scan time was set for 1 s. All acquisitions were obtained up to 2 min at a scan time of 1 sec although sampling of the spot was frequently completed in a shorter time period. The gas used for the drift time (t_d) separation was nitrogen with a flow set at

22 mL min^{-1}. The IMS wave velocity was set at 650 m s^{-1} with a wave height of 40 V. The pressure in the drift cell of ~3.2 mbar was recorded. Acquisition was set in mobility-TOF mode on the SYNAPT G2 mass spectrometer to obtain both the *m/z* ratio and drift times. After acquisition, the mass spectrum was extracted using MassLynx 4.1 (Waters Corp., Manchester, UK) and 2-D plots of t$_d$ *vs.* *m/z* ratio using DriftScope ver. 2.1 (Waters Corp., Manchester, UK).

2.3 Laserspray Ionization *Vacuum* (LSIV)

A commercial intermediate pressure MALDI source of SYNAPT G2 mass spectrometer from Waters Co. (Manchester, UK) equipped with an IMS and operated using a Nd:YAG laser (355 nm) in reflection geometry mode (**Scheme 1.1.IIA**) was used in this study. Acquisition mode was set using mobility-TOF and operated in positive ion and sensitivity mode (also referred as V mode) with the following settings: 0 V sample plate, 10 V "extraction", 10 V "hexapole bias", and 5 V "aperture 0". LSI (ESI-like, 0 V sample plate) and/or MALDI (20 V sample plate) settings were used.[42,45] The laser fluence ranged from "50" to "500" (1.33 – 45.84 J cm^{-2}) [45] at a firing rate set at 200 Hz. The laser operates with an average power of 20 mW and a pulse energy of 100 μJ. The sample plate once loaded was under vacuum conditions of ~0.2 mbar (ca 0.16 Torr) [75]. Scan time was set at 1 sec and acquisitions were summed for 1 to 2 min. Nitrogen gas was used for the drift time separation with a flow set at 22 mL min$^{-1.}$ The IMS pressure in the drift cell was ~3.2 mbar. The wave velocity used ranges from 550 to 650 m s^{-1}, and the wave height was at 40 V. After acquisition, MassLynx 4.1 and DriftScope ver. 2.1 software were used for data processing.

2.4 Matrix Assisted Ionization *Vacuum* (MAIV)

MAIV was performed on an IP-MALDI vacuum and custom modified ESI sources. By simply mixing the analyte solution with the matrix, 3-NBN, and expose the matrix/analyte crystals to the vacuum of the mass spectrometer, molecular ions are formed.

MAIV on a Commercial Vacuum MALDI Source - The commercial IP-MALDI source of Waters SYNAPT G2 with IMS capability conventionally operated with an Nd:YAG laser (355 nm) was employed with the laser off (**Scheme 1.1.IIB**). Matrix/analyte sample was prepared using 3-NBN as matrix similar to MALDI sample preparation protocols [3] and spotted 1 µL on a sample plate. The source pressure when the sample plate was loaded was ~0.2 mbar. Ions are observed from the matrix and the analyte once the sample plate with the matrix/analyte spot is positioned near the extraction lens, a process that takes ca. 2 min (**Scheme 2.3**). The TOF mass analyzer was operated in positive or negative ion V mode (also referred to as sensitivity mode). "MALDI" or "LSI" settings [42,45] were used to perform MAIV-IMS-MS measurements. Acquisition times in MS and MS/MS ranged from 30 s to 2 min for standard samples and up to 4 min for the mouse brain tissue section sample, but single scan acquisitions were sufficient for most analytes. Mobility-TOF measurements were acquired with a drift cell pressure of ~3.2 mbar, wave velocity at 650 m s^{-1}, and wave height at 40 V.The nitrogen gas used for the drift time separation was set at 22 mL min^{-1}. MassLynx 4.1 and DriftScope ver. 2.1 software were used for data processing.
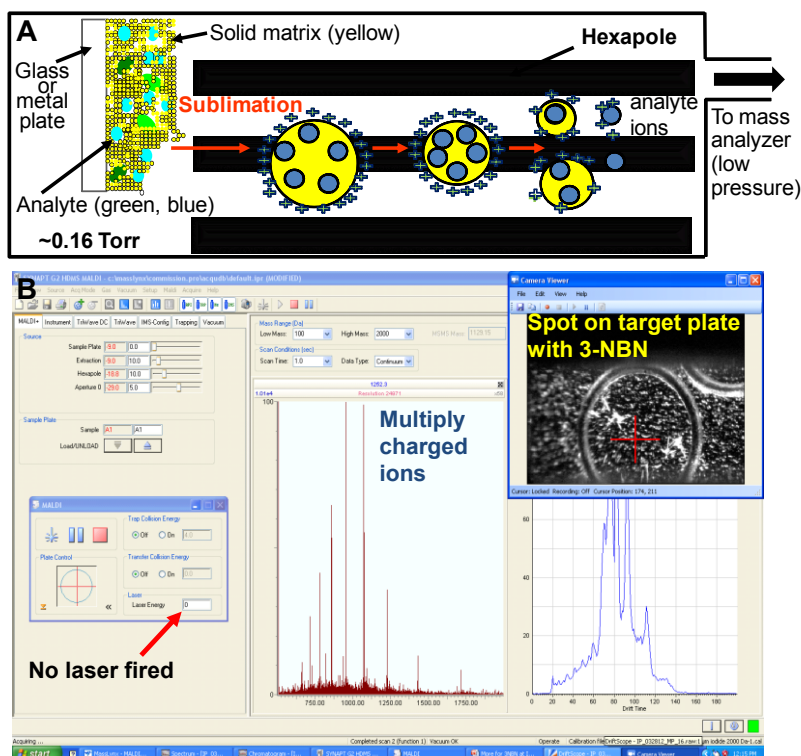
Scheme 2.3 (A) Representation on the ion formation of MAIV using an intermediate pressure vacuum MALDI source without the laser. (**B**) Screenshot during MAIV acquisition using the intermediate pressure vacuum MALDI source showing formation of multiply charged ions without the use of the laser.[47,71]

MAIV on Commercial Atmospheric Pressure ESI Source SYNAPT G2*-* MAIV on the ESI source of the SYNAPT G2 mass spectrometer was performed by modifying the skimmer cone of the z-spray. The outer cone aperture of the skimmer was widened to about ~4.5 mm to allow a metal ferrule to form a gas-tight seal with the inner skimmer cone (**Scheme 2.4**). Non-standard inner cone with ~3 mm inner diameter inlet aperture was used and assembled to the modified outer skimmer cone with the ferrule attached. The glass plate with the matrix/analyte spot was placed on the ferrule facing the source entrance, and once the vacuum isolation valve was opened, the glass plate was held to the

ferrule by the vacuum of the mass spectrometer. Ions were observed until the matrix was no longer visible. The ion source temperature for the experiments was set at 50 °C. The instrument was operated in mobility-TOF and sensitivity ('V') modes acquiring in both positive and negative ion detection. ESI default settings were used with 40 V sample cone and 4 V extraction cone voltages using mobility-TOF settings as described above. MassLynx 4.1 and DriftScope ver. 2.1 software were used for data processing.
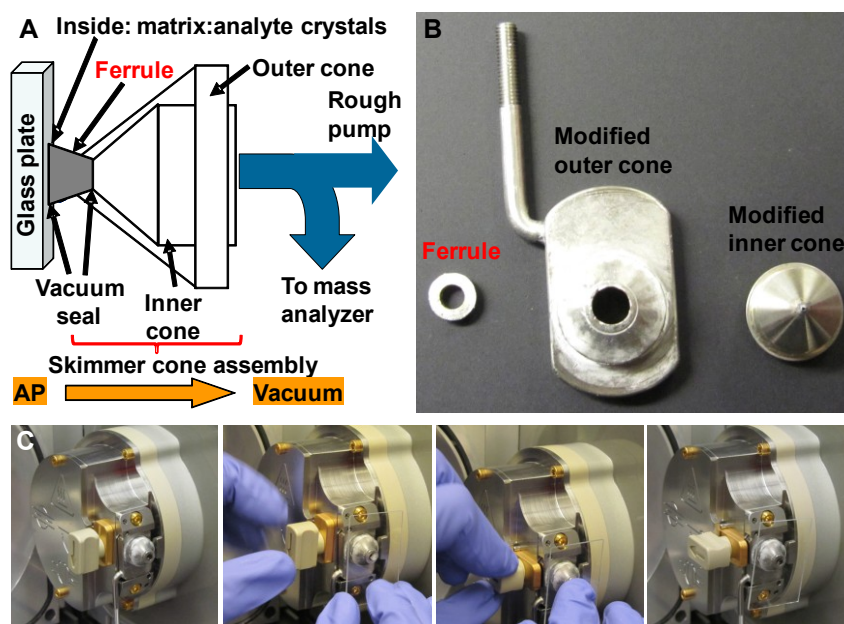
Scheme 2.4 MAIV on the ESI source of Waters SYNAPT G2: (**A**) Representation of the simple modification of the skimmer cone simply by inserting a ferrule, (**B**) picture of components of home-built modified skimmer cone (*left to right*): connecting ferrule, outer and inner skimmer cones, and (**C**) photographs of typical operation: (**1**) vacuum valve closed, (**2**) glass on, (**3**) vacuum valve open, (**4**) matrix/analyte sample enters readily mass spectrometer by vacuum forces.[46,47]

MAIV on Commercial Atmospheric Pressure ESI Source LTQ Velos - The Ion Max source was removed and the interlocks were overridden to have open access of the mass spectrometer inlet. The outer end of the transfer capillary was modified by inserting a

ferrule on the outer opening of the inlet tube to hold the glass plate. Nonstandard 750 μm inner diameter inlet capillary was used (**Scheme 2.5**). MAIV-ETD fragmentation for peptide sequencing used conditions similar to those described in a previous report [48]. Mass spectra were acquired using a maximum injection time of 50 ms and 2 microscans with an inlet capillary tube temperature of 150 °C. ETD acquisition was set at 1 *m/z* isolation width and 100 ms activation time. Xcalibur 2.1.0 was used for data analysis.
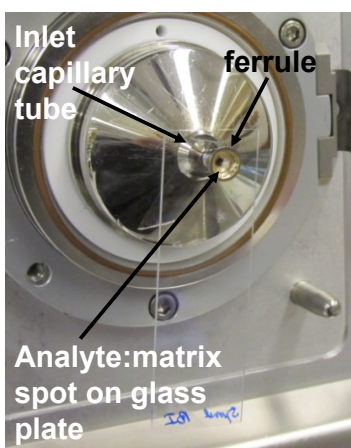
Scheme 2.5 MAIV on the ESI source of Thermo Scientific LTQ Velos. The outer end of the inlet capillary is inserted with the ferrule with wider opening. The sample plate with the matrix/analyte spot is held by the vacuum of the mass spectrometer thru the ferrule.

2.5 Microscopy Measurement

Optical microscopy (Nikon Eclipse LV100) was performed to obtain qualitative information on the ablated area of matrix/tissue ablated per laser shot after mass spectral analysis of the tissue using LSII. Various magnification conditions were used, ranging from 5x to 100x, providing detailed views to ~1 μm resolution.

CHAPTER 3

MATRIX-ASSISTED LASER DESORPTION/IONIZATION MASS SPECTROMETRY METHOD FOR SELECTIVELY PRODUCING EITHER SINGLY OR MULTIPLY CHARGED MOLECULAR IONS "Reprinted (adapted) with permission from (Trimpin, S.; Inutan, E.D.; Herath, T.N.; McEwen, C.N. *Anal. Chem.* **2010**, *82*, 11-15). Copyright (2010) American Chemical Society."

Introduction

Matrix-assisted laser desorption/ionization (**MALDI**) mass spectrometry (**MS**), along with electrospray ionization (**ESI**), has had an enormous impact on science because of the capability to ionize nonvolatile and high-mass compounds such as peptides and proteins.[2,3] MALDI is characterized by the production of low-charge state ions with singly charged ions being dominant, especially for compounds with molecular weights below 10-20 kDa, while ESI [1] is characterized by much higher charge states sometimes reaching hundreds of charges per molecule for larger proteins and polymers. The observation of mostly singly charged ions in MALDI reduces mass spectral complexity, which is especially useful for mixtures such as those found in polymer distributions, but they limit structural characterization because of the difficulty of producing fragment ions and requires a mass analyzer with a *m*/*z* range at least equal to the molecular weight of the compounds being analyzed.

Here, we report the ability to selectively produce either ESI-like multiply charged or MALDI-like singly charged ions using a MALDI process at atmospheric pressure

(**AP**). Thus, multiply charged molecular ions dominate the mass spectrum when the analyte along with the common MALDI matrix, 2,5-dihydroxybenzoic acid (**2,5-DHB**), is applied to a glass MALDI target plate using the standard dried droplet sample preparation method [3] and ablated using a nitrogen laser (337 nm). Under the same instrumental conditions, except that the sample preparation is by the solvent-free method [72,73] where analyte and matrix are ground together and placed on the MALDI target plate without the use of any solvent, MH+ singly charged molecular ions are dominant. The ability to produce, at will, multiply charged ions in a MALDI process is potentially analytically important as it extends the mass range of common atmospheric pressure ionization (**API**) mass spectrometers and provides enhanced user initiated fragmentation, similar to ESI.

AP-MALDI offers advantages over vacuum MALDI, including time and volatility constraints as well as the ability to analyze materials under more physiologically relevant conditions, which is especially important in the developing area of compound-specific tissue imaging. Vacuum MALDI which is more sensitive than AP-MALDI, and often more sensitive than ESI,[23] imposes analysis limitations with materials that are not compatible with vacuum and solvent conditions.[10] Thus, methods that offer improved sensitivity for AP-MALDI are needed. Some sensitivity improvement for AP-MALDI is achieved by the implementation of pulse dynamic focusing (PDF),[76] but part of the sensitivity gain is due to sampling a larger area. Thus, PDF only provides minimal sensitivity gain for imaging where spatial resolution (small sampled area) is important. A new AP-MALDI configuration based on theoretical studies

by Sheehan and Willoughby [24] and by laser ablation studies by Willis and Grosu [25] is reported here. Sheehan and Willoughby modeled AP ionization and reported that ~90% of the ions entering the AP to vacuum orifice are lost to the walls (so-called rim losses) if a high electric field is present in the AP region.[24] Forward momentum caused by the explosive expansion of materials irradiated in a transmission geometry (**TG**) laser ablation experiment in which the laser beam passes through the holder (glass or quartz) before striking the sample was demonstrated by Willis and Grosu.[25] Thus, combining these ideas into the configuration shown in **Scheme 1.1IA** with field-free (**FF**) conditions to minimize rim loses and placement of the sample in close proximity to the ion entrance orifice to enhance momentum transfer of material in the expanding gas jet is expected to ensure high transmission of ions into the mass analyzer. TG using glass microscope slides as the MALDI target plate is also ideal for such a source configuration as well as for tissue imaging microscopy.[77] The initial results from this ion source, with minimal optimization, demonstrate the FF-TG AP-MALDI concept by successfully obtaining mass spectra of lipids, carbohydrates, peptides, proteins, and polymers. The potential analytical utility of this new MALDI approach is discussed and representative examples presented.

Experimental Section

Materials and sample preparation are included in **Chapter 2.1**, and the LSI set-up using the Orbitrap Exactive mass spectrometer is described in **Chapter 2.2**. For solvent-based matrix/analyte preparation, lipids in 70:30 or peptides/proteins in 50:50 ACN/water was mixed with 2,5-DHB using dried droplet method.[3] One µL of the matrix/analyet

mixture (200/1 or 5000/1) was placed on the microscope slide and dried using a heat gun (low heat). Alternatively, the solvent-free sample preparation method was used as described elsewhere.[72,73] The ion transfer capillary was heated to 350 °C. Resolution could be set from 10,000 to 100,000 (m/z 200, full width at half height definition) and the maximum ion inject time was set to 50 ms.

Results and Discussion

The mass spectra obtained from laser ablation of the solution based matrix/analyte preparation dried on a glass microscope slide using FF-TG AP-MALDI are nearly identical to ESI mass spectra. Thus, singly charged ions are produced from compounds that do not have basic sites for attachment of more than one proton. Therefore, only singly charged ions are observed with FF-TG AP-MALDI using solvent-based sample preparation with 2,5- DHB, as well as with ESI using 50:50 acetonitrile/water, for lipids such as N-arachidonoylethanolamine (molecular weight [MW] 347.3), N-arachidonoyl glycine (MW 361.3), phospatidyl glycerol (MW 770.5), sphingomyelin (MW 812.7), and phospatidyl inositol (MW 886.6) as well as small peptides such as leucine enkephalin (MW 555.3) and β-amyloid 33-42 (MW 914.5) (**Appendix A Figures S1, S2 , S3**). However, for bradykinin antagonist (MW 1109.6), angiotensin I (MW 1295.7), angiotensin II (MW 1045.5), and adrenocorticotropic hormone (ACTH 18-39 human; MW 2464.2) using the same solvent-based sample preparation conditions with AP-MALDI or ESI, multiply charged ions dominated the mass spectrum while singly charged ions were either not observed or in very low abundance. Under these FF-TG AP-MALDI conditions, higher mass peptides, proteins, and synthetic polymers produce

higher charge states: insulin B chain oxidized, (MW 3536.7) < β-amyloid (1-42), (MW 4511.5) < porcine insulin (pancreas, MW 5772.6) < polyethylene glycol, (PEG) 6590 < ubiquitin, (bovine red blood cells, MW 8561) (**Figure 3.1A-F**).
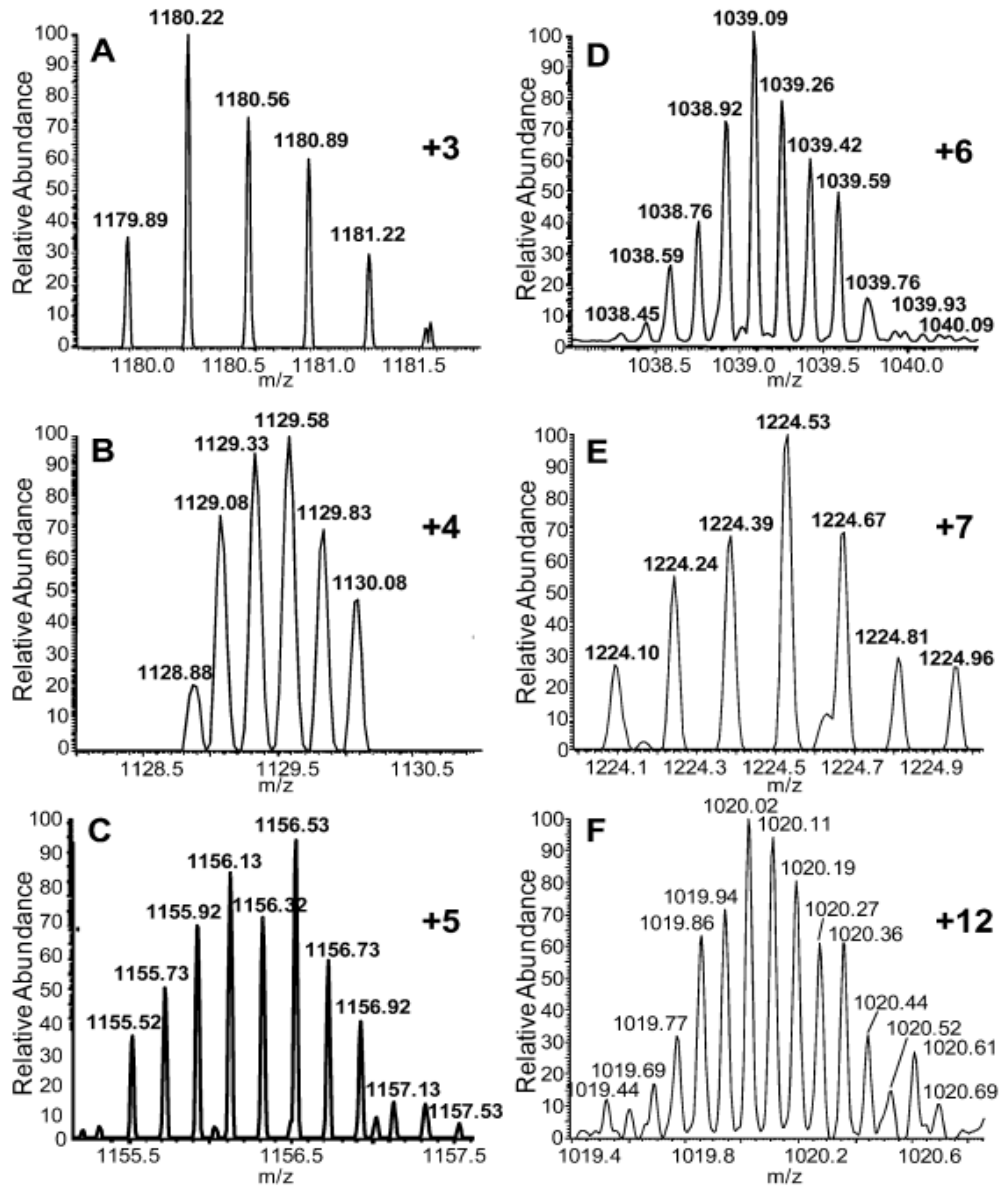
Figure 3.1. LSII inset mass spectra showing multiply charged molecular ions for (**A**) bovine insulin oxidized B chain (MW 3536.7, +3), (**B**) amyloid (1-42) (MW 4511.5, +4), (**C**) bovine pancreas insulin (MW 5772.6, +5), (**D**) PEG 6690 (+6), (**E**) ubiquitin (MW 8561, +7), and (**F**) cytochrome c (MW 12 224, +12).

Ubiquitin for example displayed ions from charge state +5 to +13. The mass spectrum

of cytochrome c (MW 12,224) obtained from a single 1 s acquisition of 4 pmol applied

to a microscope slide shows multiply charged ions from +8 to +15 in **Figure 3.2A**.
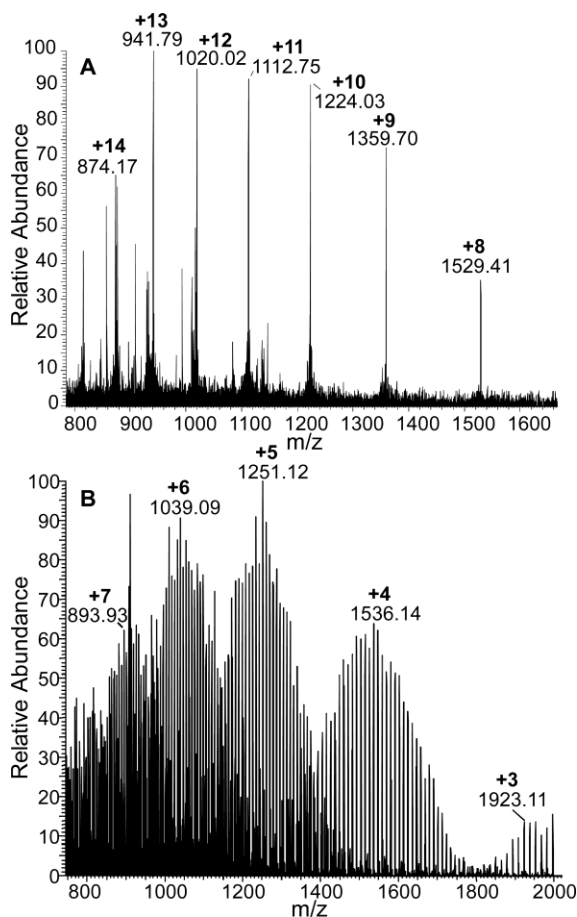
Figure 3.2. Full-range LSII-MS: (**A**) 4 pmol of cytochrome c applied to the microscope slide with 1- s acquisition at 100,000 resolution (MW 12,224) and (**B**) PEG 6690 in 2,5-DHB and NaCl prepared solvent-free and then dissolved in 70:30 ACN/water and 1 μL placed on the microscope slide using the dried droplet method.

As with ESI, the higher charge states allow MALDI mass spectra to be obtained for

compounds beyond the mass limitation (*m/z* 4000) of the mass spectrometer. Mass

spectra can be obtained from complex mixtures such a protein digests or polymers.

Multiply or singly charged mass spectra were obtained from narrow polydisperse PEG

samples with MWs below the 4000 *m/z* limit of the mass spectrometer using 2,5-DHB and a trace of NaCl employing solvent-based or solvent-free preparation, respectively. However, molecular ions of PEG 6590 were only observed with the solvent-based sample preparation as multiply charged ions that fall within the *m/z* range of the mass spectrometer (**Figure 3.2B**). Ionization with the singly or multiply charged mechanism was by Na+ adduction, showing that metal adduction is favored for this polymer when sodium salt is present.

The ability to produce multiply charged ions in a MALDI process has important advantages. It potentially enables production of enhanced fragmentation from processes such as collision induced dissociation (**CID**),[78] electron transfer dissociation (**ETD**),[58,79] and electron capture dissociation (**ECD**).[80,81] It also extends the mass range of mass spectrometers with limited *m/z* range, typically found with AP ionization instruments. Additionally, just as with nanospray ESI, the amount of sample necessary for an analysis can be reduced by minimizing the amount of matrix/analyte solution placed on the glass slide. Sufficient signal was obtained in a single laser shot to produce the isotope distribution of the doubly charged ions from 0.1 μL of a 400 amol solution (80 amol) of angiotensin II in 2,5-DHB placed on a glass slide (**Appendix A Figure S4**).

Singly charged molecular ions can be produced for the compounds discussed above that are within the *m/z* limit of the Orbitrap Exactive simply using the solvent-free sample preparation method with 2,5-DHB. The advantage of producing only singly charged ions is the simplified mass spectra obtained from complex mixtures such as found in plasma or even synthetic polymers (**Appendix A Figure S5**). The mechanism

for producing singly charged ions is distinct from that for producing multiply charged

ions and is shown to originate in the matrix choice or matrix/analyte preparation method.

This is shown in **Figure 3.3** for angiotensin I prepared using 2,5-DHB employing the

solvent-based (**Figure 3.3A**) and solvent-free (**Figure 3.3B**) methods. The mass spectra

obtained with the singly charged mechanism often displayed matrix or Na+ adduction,

especially for peptides (**Appendix A Figure S6**). These adductions were rarely observed

and then in low abundance with the multiply charged ionization mechanism.
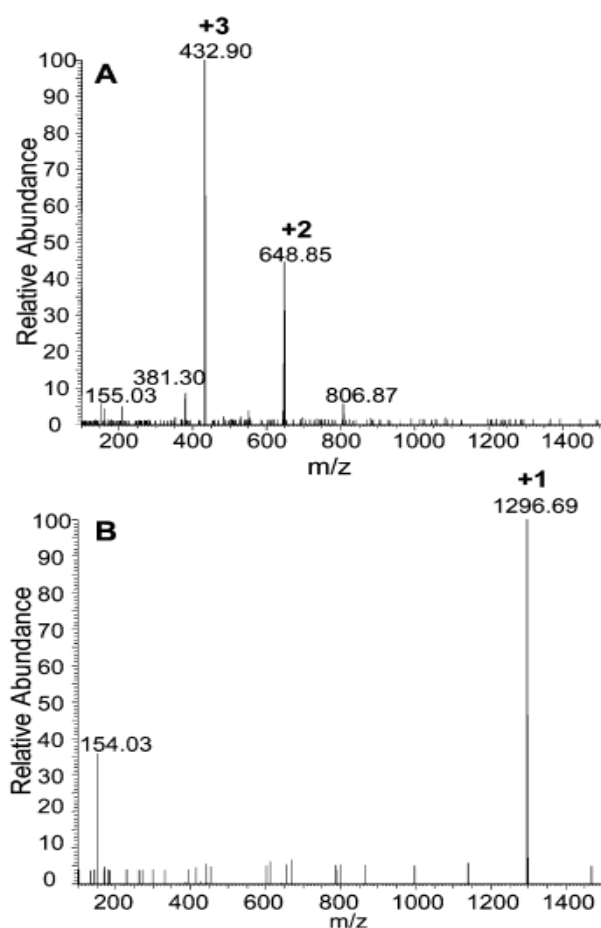
Figure 3.3. LSII mass spectrum of angiotensin I (MW 1295): (**A**) solvent-based dried droplet sample preparation using 2,5-DHB in 50:50 ACN/water and (**B**) solvent-free sample preparation using 2,5-DHB.

It was even possible with 2,5-DHB to produce a mixed mode of ionization with observation of singly and multiply charged ions by, for example, adding a drop of solvent onto the solvent-free prepared matrix analyte mixture on the glass plate. After solvent evaporation, the matrix/analyte mixture is only partially dissolved and the mixed mode ionization can be observed. The activation of the singly charged ion mechanism was also achieved using a thin layer experiment and increasingly non-incorporating conditions. Laser ablation of an aqueous solution of 2,5-DHB placed on angiotensin II which had been dried on the glass slide produced, after drying, exclusively doubly charged ions whereas an acetone solution of 2,5-DHB placed over the dried peptide produced mixed ionization and a dichloromethane 2,5-DHB solution produced only singly charged ions (**Appendix A Figure S7**).

With α-cyano-4-hydroxycinnamic acid (**CHCA**), even under solvent-based conditions, only singly charged ions are observed for angiotensin II (**Appendix A Figure S8**) and substance P. This observation is in line with previously described field-constrained TG AP-MALDI experiments.[26] Other compounds such as dithranol, ortho-chlorobenzoic acid, and benzoic acid were examined as matrixes for AP-MALDI. With angiotensin II, benzoic acid produced singly and no doubly charged ions while o-dichlorobenzoic acid produced low abundance doubly charged ions (**Appendix A Figure S9**). Dithranol, besides producing singly charged ions with angiotensin II, also produced notable matrix-adducted analyte molecular ions.

Previous studies have shown a moderate increase in multiple charging in MALDI using different sample preparations, high laser fluence, a metal-free sample stage, and

atmospheric pressure.[56,57] From the work presented here, it is clear that the MALDI process can generate analytically useful ion currents from mechanisms that produce multiply charged ions as well as singly charged ions. The ease and speed of the FF-TG AP-MALDI method for producing either singly or multiply charged ions from a wide variety of compound types with high sensitivity using a focused laser beam demonstrates analytical utility.

CHAPTER 4

LASERSPRAY IONIZATION – A NEW AP-MALDI METHOD FOR PRODUCING HIGHLY CHARGED GAS-PHASE IONS OF PEPTIDES AND PROTEINS DIRECTLY FROM SOLID SOLUTIONS "This research was originally published in Molecular and Cellular Proteomics (Trimpin, S.; Inutan, E.D.; Herath, T.N.; McEwen, C.N. *Mol. Cell. Proteomics* **2010**; 9:362-367) © the American Society for Biochemistry and Molecular Biology."

Introduction

Two primary differences between ESI and MALDI methods are the sample environment (solution *vs.* solid) and the observable charge state(s) (multiply *vs.* singly charged). The multiply charged ions observed in ESI mass spectrometry (**MS**) enhance the yields of fragment ions, a key benefit in structure characterization, and allow analysis of high molecular weight compounds on mass spectrometers with a limited *m/z* range. In contrast, MALDI-MS is ideal for the analysis of heterogeneous samples because it often requires less sample, and spectra of singly charged ions are easier to interpret. We report here the astonishing observation of highly charged molecular ions by laser ablation of a solid matrix/analyte mixture typically used in MALDI-MS analyses. The distribution and abundances of the observed ions are similar to those obtained by ESI. Importantly, the MALDI mechanism that produces singly charged ions can be "turned on" at the operator's will by changing only the matrix or matrix preparation conditions; this capability is not available with any other ionization method. These findings show for the

first time that singly charged ions as well as multiply charged ions are available in MALDI. Besides having important mechanistic implications relating to MALDI and ESI, our findings have enormous practical analytical utility.

ESI and MALDI combined with MS revolutionized the study of biological materials and earned the Nobel Prize in Chemistry for their ability to ionize proteins for analysis using MS. However, after two decades of extensive studies, the mechanism for ion formation in MALDI remains controversial [35,54,55,82-87]. At the heart of these debates lies the predominance of singly charged ions in MALDI mass spectra; the exception being very high mass compounds. A mechanism for the formation of multiply charged ions in MALDI has previously been proposed [54] based on molecular modeling studies [36,38] and glimpses of multiply charged ions have been observed in lower molecular weight compounds [56,57,88,89]. The formation of these multiply charged ions has been attributed to sample preparation, high laser fluence, a metal-free sample stage, use of an IR laser, and atmospheric pressure (AP) conditions. Multiply charged ions were also recently observed by laser ablation of a liquid surface in the presence of a high electric field [90]. The inability in that experiment to observe ions from a solid MALDI matrix/analyte sample or in the absence of an electric field suggests an ionization process involving liquid droplets in a high field similar to ESI [1] or other liquid based, field-induced ionization methods [91,92].

Here, we show analytically useful ESI-like MALDI mass spectra obtained using standard MALDI conditions but using a non-traditional source [27] mounted in place of the standard atmospheric pressure ionization source on a mass spectrometer most

commonly used with ESI. The utility of this MALDI-MS method for extending the mass range of mass spectrometers as well as the capability of peptide/protein sequencing using electron transfer dissociation (**ETD**) [58] is demonstrated. Because highly charged ions have not previously been observed with any MALDI ion source configuration, we briefly discuss the fundamental concepts that lead to their production. Key aspects of laserspray ionization (**LSI**) are laser ablation using a UV laser aligned in transmission geometry (**TG**) [26], field-free (**FF**) at AP [21], using a heated AP to vacuum ion transfer capillary. In order to emphasize the MALDI sample preparation but distinguish laserspray from conventional AP-MALDI, the new ionization method will here- after be referred to as FF-TG AP-MALDI.

Experimental Procedure

Materials and sample preparation are included in **Chapter 2.1**. An Orbitrap Exactive mass spectrometer was used for LSI experiments (see **Chapter 2.2)**. Peptides and proteins were further diluted in 30:70 ACN/water solution and premixed with 2,5-DHB, prepared as a concentrated solution in a room temperature 50:50 ACN/water solution using a standard solvent- based MALDI preparation method [3]. The premixed matrix/analyte solution was deposited on a glass microscope slide followed by evaporation of the solvent. The temperature of the ion transfer capillary was used to control the desolvation conditions for the temperature study with angiotensin I. For ESI, 1 µL of a 1 pmol µL^{-1} solution of lysozyme was injected into a 50:50 ACN/water solution infused at a flow rate of 2 µL min^{-1}. LSI-ETD experiments were obtained on a Thermo Fisher Scientific LTQ with ETD capabilities using the same LSI source configuration

described in **Chapter 2.2** as well as the ETD conditions as described elsewhere [58]. For intact sequencing of ubiquitin, ETD mass spectrum was obtained in single scan acquisition. Proton transfer reaction was applied to simplify the fragment ions.[93]

Results and Discussion

Lysozyme was chosen as a well-studied protein for initial experiments. A typical FF-TG AP-MALDI mass spectrum for lysozyme is shown in **Figure 4.1A** and can be compared with the ESI spectrum shown in **Figure 4.1B**, also acquired on the Orbitrap Exactive from the same 1 μM solution at 100,000 resolution and using 1-s acquisition. Observation of efficient production of such highly charged ions (up to 13+) in MALDI is unprecedented. As with ESI, the higher charge states allow AP-MALDI mass spectra to be obtained for compounds with molecular weights beyond the *m*/*z* limit of the instrument (4000). The capability to produce highly charged ions in high abundance in AP-MALDI and ESI strongly suggests that these ions are formed via related mechanisms.

Process for Producing Highly Charged Molecular Ions by MALDI - Here, we provide a brief description of mechanistic implications as well as the conditions that are necessary to observe highly charged ESI-like ions in MALDI-MS. In ESI, the ionization mechanism is thought to involve highly charged solvent/analyte droplets [51-53]. In MALDI, the most accepted model is a two-step ionization process that occurs in the expanding plume that is created by absorption of the laser energy by the MALDI matrix [82,86]. Primary photochemical ionization is followed by ion-molecule reactions similar to chemical ionization, leading primarily to singly charged analyte ions.
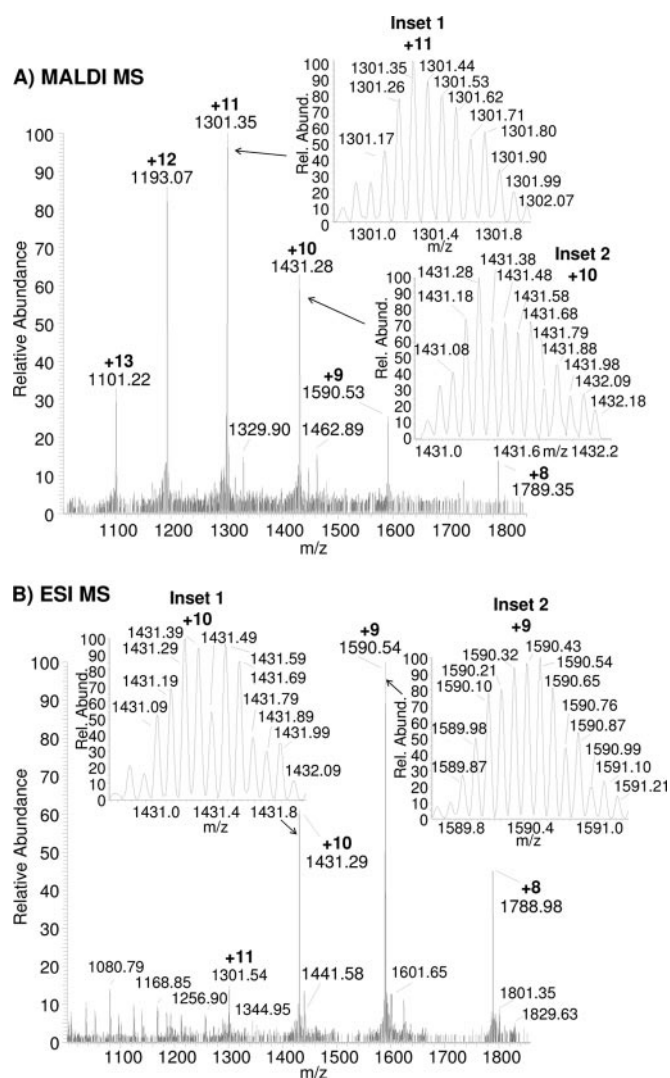
Figure 4.1. (**A**) LSII (1 pmol in 2,5-DHB loaded on a glass microscope slide) and (**B**) ESI mass spectra (1 pmol injected into 1:1 ACN/water infused at 2 µL min^{-1}) of a 1 pmol µL^{-1} solution of lysozyme (1-s acquisitions, 100,000 resolution (m/m, full-width half-height at *m/z* 200)). Insets show the isotope distributions for the most abundant peaks and charge 10 in each spectrum.

Alternatively, a cluster model has been proposed in which charged clusters produce multiply charged ions in a MALDI process by a mechanism similar to ESI [54,56,57]. To explain the dominant observation of singly charged ions, a "lucky survivor" mechanism was postulated in which highly charged positive ions, of e.g.

proteins, were reduced to singly charged ions, presumably by ion-electron recombination.[54] This mechanism was later modified to formation of singly charged ions directly from clusters.[55] Others have also suggested that clusters are a source of ions in MALDI, including background ions [85,87,94]. However, the validity of a cluster mechanism as a significant source of ions in MALDI MS has been questioned [35,82]. Given our observation of abundant, highly charged ions in FF-TG AP-MALDI, the potential mechanistic commonalities between ESI and MALDI must be reassessed.

In analogy to ESI [1,51-53] and the cluster (liquid droplet) model for MALDI [54,56,57], we propose a mechanism in which the laser-induced gas-phase clusters are highly charged. Similar to ESI, evaporation of solvent, but not charge, produces an unstable surface charge density, resulting in formation of smaller particles and eventually ion emission (**Scheme 1.1IA**). Unlike ESI in which an electric field induces excess positive or negative charges on solvent droplets, in the AP-MALDI experiments discussed here, cluster charging occurs in the absence of an electric field. Field-free production of charged clusters can occur at cluster birth by a statistical charge separation mechanism [53], photoionization, or electron loss from the cluster surface [35,55].

Provided a threshold laser fluence is achieved [56,57], cluster formation in MALDI is expected [36,38,54,82-87,94], and mechanisms exist for at least some of the clusters to become charged [35,53-55]. However, detection of higher charge state ions has remained elusive in MALDI until now. We propose that the highly charged clusters are initially produced during the explosive deposition of energy into the MALDI matrix in either AP- or vacuum MALDI at least with solvent-based matrix preparation using 2,5-

DHB. However, for field emission of multiply charged ions, it is necessary to evaporate sufficient matrix, but not charge, from the clusters to achieve a surface charge density > ~109 V m^{-1} [95]. One possibility for the absence of observable highly charged ions under vacuum conditions is that evaporative cooling quenches the initial rapid cluster evaporation process prior to achieving the necessary charge density.

In support of a requirement of desolvation for observation of multiply charged but not singly charged ions, the AP to vacuum ion transfer capillary (**Scheme 1.1IA**) temperature was varied for angiotensin I (molecular weight, 1295.7) using solvent-based and solvent-free 2,5-DHB sample preparation. Barely detectable 2+ and 3+ molecular ions were observed with the transfer capillary temperature set as low as 150 °C (no 1+ ions were observed). The 2+ and 3+ ion abundances increase rapidly above 275 °C, and at 350 °C they dominate the mass spectrum (**Figure 4.2**).
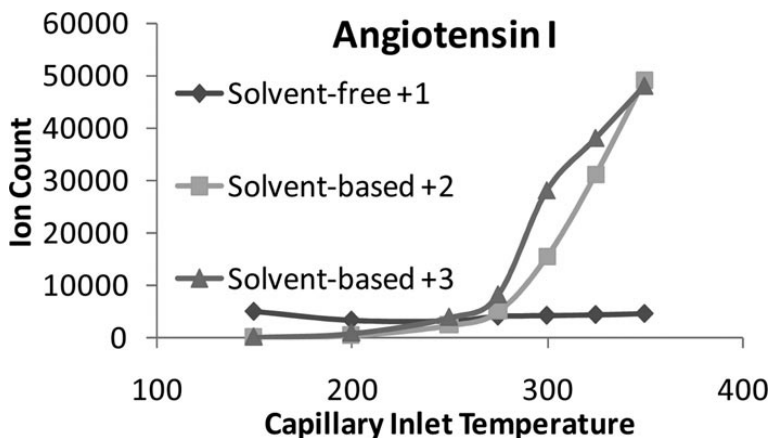
Figure 4.2. Ion count *vs.* ion transfer tube temperature plot for the 1 through 3 charge states of angiotensin I. The 2 and 3 ions are produced by the solvent-based and the 1 ions are produced by the solvent-free MALDI sample preparation methods. The plot suggests two distinctly different ionization mechanisms, one of which (multiply charged ion formation) is highly dependent on the ion transfer tube temperature.

Using the same matrix and analyte but prepared under solvent-free conditions [96,97], 1+ molecular ions are exclusively produced, and little change in ion abundance is observed over the same temperature range, strongly implying that an entirely different ion formation mechanism is being sampled. This and other evidence suggest that the singly charged ions produced using the solvent-free sample preparation method are formed near the sample surface by the two-step chemical ionization mechanism normally observed in MALDI but that the multiply charged ions are produced from clusters far downstream from the initial laser/matrix interaction (**Scheme 1.1IA**) and are enhanced by improved desolvation conditions (higher ion transfer tube temperature). Interestingly, **Figure 4.2** suggests that higher sensitivity will be achieved by increasing the ion transfer tube temperature beyond 350 °C.

The unique configuration of the FF-TG AP-MALDI arrangement (**Scheme 1.1IA**) may also provide improved ion sampling by the combination of the forward momentum of the laser-generated plume and the flow-dominated entrapment by gas diffusing from AP to vacuum through the instrument orifice. The absence of an electric field is expected to minimize loss of ions at the entrance to the ion transfer tube [24] and favor sampling of higher mass and thus higher momentum species such as clusters relative to free analyte ions created in the expanding plume region near the sample surface. Thus, the high efficiency of producing multiply charged ions may partially be the result of preferential sampling at the capillary inlet orifice.

As noted, either singly or multiply charged ions can be selected in FF-TG AP-MALDI by choice of matrix or matrix/analyte preparation conditions. Thus, using 2,5-

DHB and dried droplet solvent-based sample preparation, multiply charged mass spectra of peptides and proteins nearly identical to those in ESI are produced, whereas solvent-free sample preparation [96,97] produces MALDI-like singly charged mass spectra for peptides. One difference in these distinct MALDI sample preparation methods is that analyte incorporation in the matrix (solid solution) is believed to occur for solvent-based preparations [98] but not in the solvent-free case [72,99]. Consistent with this concept, the addition of a drop of ACN/water solution to the solvent-free prepared sample on the glass slide and evaporation of the solvent resulted in the mass spectrum changing from all singly charged with solvent-free preparation to dominantly multiply charged peptide ions after addition of solvent.

Further support for the importance of analyte incorporation into the matrix is derived from solvent-based experiments using Cyt. c and various DHB positional isomers. Highly charged ions of Cyt. c were observed only for the 2,5-DHB isomer. Previous work [98] reported quantitative incorporation of Cyt. c only into the 2,5-DHB isomer. Importantly, changes only in the matrix/analyte conditions alter the selected charge state population, thus assuring that the observed multiply charged ions are related only to the matrix and not instrument parameters. The ability to select different ionization pathways provides a unique opportunity to study fundamental processes related to formation of gas-phase ions from nonvolatile compounds as well as entire new applications.

Finally, it is unlikely that the multiply charged ions are a result of the ion source geometry because FF-TG MALDI has previously been used without such observations

[26]. This is demonstrated by changing the angle of the laser beam relative to the instrument orifice from 180° (**Scheme 1.1IA**) to 135°, making it possible to use FF reflective geometry so that the laser beam strikes the matrix/analyte mixture without passing through the glass plate. Multiply charged (2+) ions of angiotensin II were observed with FF reflective geometry AP-MALDI, thus demonstrating that TG alignment is not necessary for laser-generated multiply charged ion formation.

Analytical Applications of Highly Charged MALDI Ions - The ability to produce multiply charged ions by AP-MALDI has advantages relative to ease and speed of analysis, mass range enhancement, and fragmentation and potentially in tissue imaging studies [27]. The speed of the method is shown by the ability to obtain a complete high resolution mass spectrum of a peptide or protein in 1 s. Because in AP-MALDI ionization occurs at atmospheric pressure, the time requirement for loading samples is also greatly reduced relative to vacuum MALDI, making high throughput analyses a reality.

Sensitivity is also an important issue as it is commonly believed that AP-MALDI is significantly less sensitive than vacuum MALDI. As with any new technology, the optimum parameters for the FF-TG AP-MALDI method have likely not been achieved, and sensitivities much greater than reported here can be expected. Nevertheless, the limit of detection, defined here as the signal necessary to observe the triply charged molecular ion and its three ^{13}C isotope peaks for angiotensin I (molecular weight, 1295.7) using 2,5-DHB as matrix and the solvent-based sample preparation method, was determined to be ~0.3 fmol applied to the glass slide (data not shown). The actual amount of sample consumed is estimated to be a less than 50 amol. A more meaningful gauge of sensitivity

for most analyses is the amount of material required to produce a recognizable full-range

mass spectrum. The mass spectrum obtained from 40 fmol of insulin in 2,5-DHB applied

to the glass slide using the solvent-based dried droplet method is shown in **Figure 4.3**.
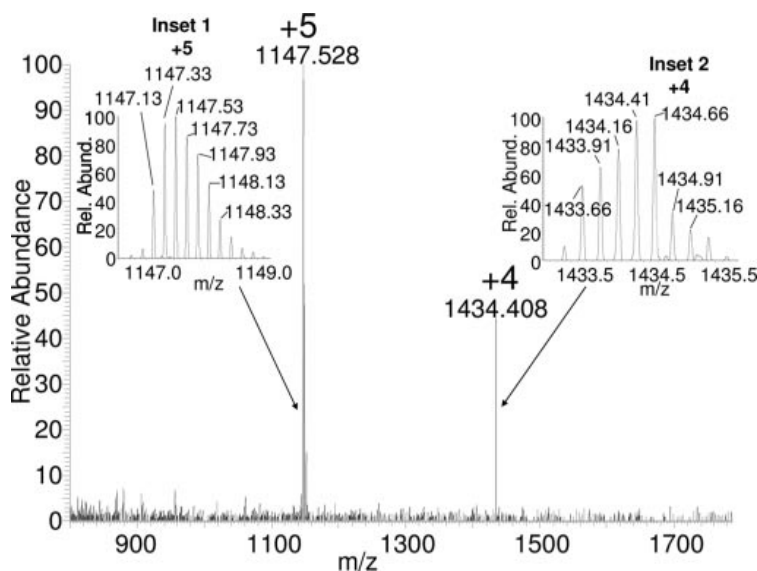
Figure 4.3. The FF-TG AP-MALDI mass spectrum obtained at 100,000 mass resolution from 40 fmol of bovine pancreas insulin loaded on the glass slide MALDI target plate in 2,5-DHB using the solvent-based dried droplet method. The insets show the ^{13}C isotopic distribution of the 4 and 5 charge state ions. *Rel. Abund., relative abundance.*

The ability to obtain enhanced fragmentation in a MALDI process is another

advantage of multiply charged ions. Important new fragmentation methods based on

either electron capture [80,81] or ETD [58] have been applied to sequence termination of

peptides and even proteins. Ubiquitin (molecular weight, 8561) was selected because it

had been previously sequenced using ETD fragmentation.[100] Fluoranthene was used as

the electron transfer reagent as described previously.[100] In initial experiments using

FF-TG AP-MALDI, 2,5-DHB, and solvent-based conditions, ~5 pmol of ubiquitin was

placed on the glass slide, and mass selecting the 11+ (*m/z* 779) charge state ion

produced the single scan mass spectrum shown in **Figure 4.4A**. The single acquisition

ETD spectrum is shown in **Figure 4.4B** and consists of numerous fragment ions of various charge states. Making use of the proton transfer reaction method [93] simplifies the fragment ion spectrum as previously demonstrated using ESI, thus allowing easier sequence interpretation (**Figure 4.4C**). These results represent the first MALDI-ETD mass spectra and provide sequence coverage of the protein as previously presented using ESI-ETD [93]. The capability to observe either multiply or singly charged molecular ions by a MALDI process allows new experimental information that fills a gap in the long standing controversy regarding ionization mechanisms in MALDI and additionally provides a unique opportunity to study such processes as laser-induced cluster formation, charging, and desolvation as well as charge reduction mechanisms [54]. The commonality with ESI also provides a means to probe the mechanisms by which analyte ions are released from highly charged droplets. Finally, these findings have significant analytical utility in areas such as high throughput analyses at high sensitivity, tissue imaging at AP using high resolution instrumentation, and identifying and characterizing proteins using fragmentation processes such as ETD.
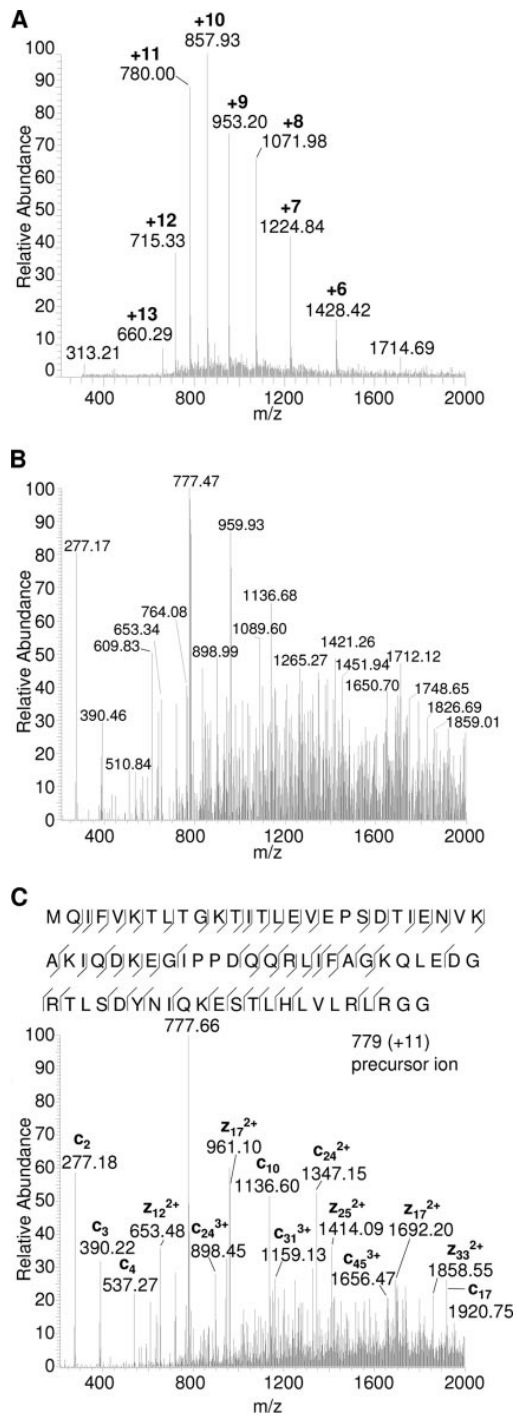
Figure 4.4. (**A**) The FF-TG AP-MALDI mass spectrum of a single scan acquisition from 5 pmol of ubiquitin in 2,5-DHB loaded onto the glass slide. (**B**) The single scan ETD acquisition from the mass-selected 11 charge state (*m/z* 779) ions. (**C**) The summed (40-s acquisition) proton transfer spectrum of the *m/z* 779 ion with the sequence coverage shown.

CHAPTER 5

LASERSPRAY IONIZATION (LSI) ION MOBILITY SPECTROMETRY (IMS)

MASS SPECTROMETRY (MS) "Springer and the original publisher (*J. Am. Soc.*
Mass Spectrom., 21, 2010, 1260-1264, Inutan, E.D., Trimpin, S.) is given to the
publication in which the material was originally published with kind permission from
Springer Science and Business Media."

Introduction

Laserspray ionization (**LSI**) mass spectrometry (**MS**) was recently introduced on
a Thermo Fisher Scientific Orbitrap Exactive [27-29]. The principle of this ionization
method is that the matrix/analyte sample is ablated by the use of a laser operating at
atmospheric pressure (**AP**) and ions are subsequently formed from highly charged
matrix/analyte clusters during a desolvation process. The free choice of charge state
selection demonstrates the utility of LSI for the analysis of complex mixtures. Singly
charged ions similar to those obtained with matrix-assisted laser desorption/ionization
(**MALDI**) or multiply charged ions similar to those produced by electrospray ionization
(**ESI**) [28] can be selected using LSI. Multiply charged ions are especially beneficial for
providing the ability to ionize by laser ablation larger molecules such as proteins and
synthetic polymers on high-performance but mass range limited mass spectrometers such
as the Orbitrap Exactive [28,29]. Full range mass spectra of bovine insulin were obtained
on as little as 40 fmol when applying ion transfer capillary temperatures of ~350 °C [29].

The unique feature of LSI to produce highly charged ions using direct laser

ablation of a solid surface enhances fragmentation as was demonstrated by obtaining nearly complete protein sequence coverage of ubiquitin using electron-transfer dissociation (**ETD**) technology on a LTQ mass spectrometer [29]. Initial laserspray applications demonstrated the ability to produce singly charged lipid ions from mouse brain tissue under ambient conditions [27]. Using transmission geometry, the matrix treated tissue sections were passed free-hand through the focused laser beam in front of the mass spectrometer orifice (Orbitrap Exactive) obtaining a spatial resolution of < 100 μm [27]. The objective is to observe proteins from tissue.

Ion mobility spectrometry (**IMS**) MS has many advantages compared with even high-resolution mass spectrometers because of its ability to extend the dynamic range and separate isomeric composition [64-67]. This is possible because ions are separated in the IMS dimension according to charge and cross-section (size and shape) [101-105]. One key benefit of this solvent-free gas-phase separation by IMS is that when combined with solvent-free sample preparation [96] achieves total solvent-free analysis by MS entirely decoupling ionization, separation, and mass analyses from the use of any solvent [10,27,30].

We rationalized that to produce LSI multiply charged ions from the proposed highly charged matrix/analyte clusters [29], a device is required that efficiently desolvates the 2,5-dihydroxybenzoic acid (**2,5-DHB**) matrix to produce the highly charged molecular ions. One function of the Waters Company (Manchester, UK) ESI z-spray source design used with the IMS-MS SYNAPT G2 is to reduce the background arising from cluster ions. However, this arrangement is not satisfactory as a means of

desolvating clusters in which the matrix (serving as solvent) is 2,5-DHB. We, therefore, fabricated a simple device that is mounted on the z-spray ESI source and provides the thermal conditions necessary for desolvation and multiply charged ion production using the LSI method. The benefits of IMS-MS in combination with direct LSI ambient ionization for the efficient separation and characterization of a protein mixture is demonstrated.

Experimental

Materials and sample preparation are included in **Chapter 2.1** and the LSI set-up using the SYANPT G2 mass spectrometer with the fabricated desolvation device is described in **Chapter 2.2**. Bovine insulin (50 pmol μL^{-1}) was used to test the fabricated desolvation device. For the protein mixture, ubiquitin and lysozyme were premixed using the stock solution in a 1:1 volume ratio. One μL was used to prepare the LSI sample on the microscope slide employing solvent-based sample preparation protocols using 2,5-DHB matrix [3], prepared in 50:50 ACN/water, and then dried to completeness. The dried LSI sample was placed in front of the desolvation device in a distance of about 1 to 3 mm (**Scheme 2.2**), similar to studies in which the dried sample was placed directly in front of the mass spectrometer orifice of the Orbitrap Excative [27-29]. LSI-IMS-MS was acquired using the Waters SYNAPT G2 as described in details in **Chapter 2**.

Results and Discussion

A maximum ion source temperature of 150 °C is available on the z-spray ESI source of the SYNAPT G2. This was insufficient to produce any meaningful ion current even for low molecular weight peptides such as angiotensin 1 (MW 1296) using 2,5-DHB

matrix and the identical laser and configuration used in previous work [27,28,29]. Applying the fabricated temperature device (**Scheme 2.2**), multiply charged ions of peptides and proteins are produced. A typical example is shown in **Figure 5.1** using bovine insulin (MW 5731). The total ion current (**Figure 5.1a**) shows the continuous ion production when moving the sample stage over unablated areas of the sample showing an increase when heat (1-84 s) and a decrease when no heat (850-115 s) were applied. The charge state distribution (**Figure 5.1b**) is similar to that previously observed using the commercially available heated transfer capillary of the Thermo Fisher Scientific Ion Max ESI source of the Orbitrap Exactive and the LTQ mass spectrometers [28,29].
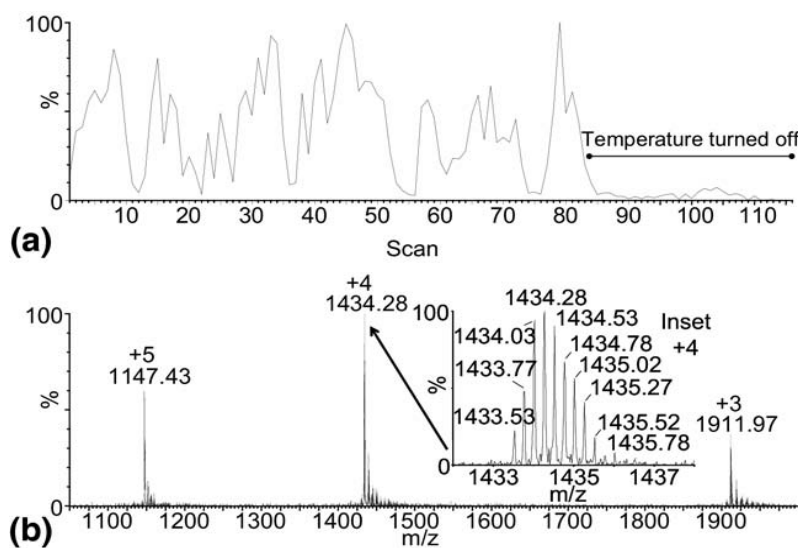
Figure 5.1. LSI-IMS-MS of bovine insulin (MW 5731): (**a**) The total ion current and (**b**) mass spectrum obtained using 2,5-DHB matrix incorporating the solvent-based sample preparation method.

Larger proteins such as ubiquitin (MW 8561) and lysozyme (MW 14,304) also produced multiply charged ions in good abundance (**Figure 5.2.1**) using the simple desolvation chamber. Myoglobin (MW 16,951), however, produced less abundant ions

ranging from charge state +10 to +16 possibly suggesting a mass range limit for this

particular desolvation device. All experiments incorporated ion mobility separation. In

ion mobility measurements, three-dimensional (3-D) information is acquired; t_d, m/z, and

signal intensity. Frequently, the intensity of a signal is embedded in a 2-D plot of t_d *vs.*

m/z (**Figure 5.2.2**) and visualized by the use of a color-code. The 2-D IMS-MS plots of

ubiquitin, lysozyme, and a mixture of ubiquitin and lysozyme are shown, respectively, in

Figure 5.2.2. LSI ions of proteins fall into families depending upon their sizes and charge

states as previously reported for biopolymers using ESI-IMS-MS [101]. Further, one can

readily observe the elongated features indicating con- formational differences within each

charge state of each protein. Similar observations have been reported, especially for

ubiquitin, using a homebuilt ESI-IMS-MS instrument [106-109].

Many features become noticeable in a 2-D plot. Without data extraction and

time-intensive analyses, the pictorial snapshot [66] determines readily the presence of

both proteins (**Figure 5.2.2c**). By selecting the specific part of the 2-D plot using the

DriftScope, it is possible to extract *m/z* and/or t_d information for any ion or inset region of

interest. This removes most of the background interference, especially those at lower

m/z. Most importantly, charge state families of different proteins can be extracted,

providing the respective mass spectrum for each protein.
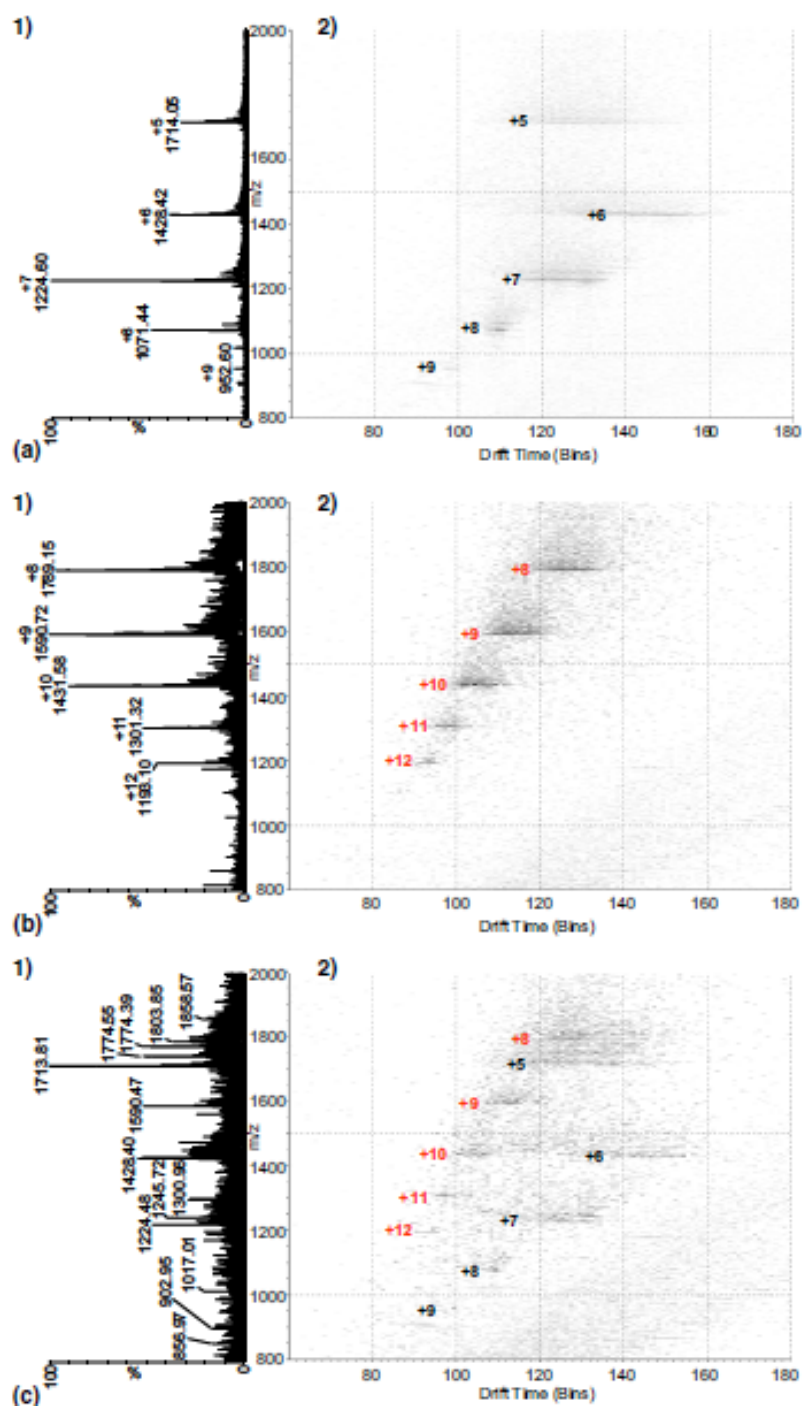
Figure 5.2. LSI-IMS-MS using 2,5-DHB matrix and the solvent-based sample preparation method of (**a**) ubiquitin (MW 8561), (**b**) lysozyme (MW 14,304), and (**c**) a mixture of ubiquitin and lysozyme. (**1**) Total mass spectra (as if no IMS dimension is employed) and (**2**) two-dimensional plots of t_d *vs.* m/z ratio.

An example of extracting easily interpretable data from lower abundant ions is shown in **Figure 5.3**. The mass spectrum of a mixture of ubiquitin and lysozyme, purposely designed to have a high signal to noise ratio and to be difficult to interpret, is shown. It is not obvious from the mass spectrum that lysozyme is present, and it could easily be overlooked. Because the mobility dimension provides clean separation of the multiply charged ions of these proteins (**Figure 5.2.2c**), mass spectra can be extracted for both proteins free of the other. The extracted mass spectrum of lysozyme in the protein mixture is shown in **Figure 5.3** and is similar to that of pure lysozyme (**Figure 5.2.1b**). The charge state distributions are essentially identical with the most abundant ions having charged state +9.
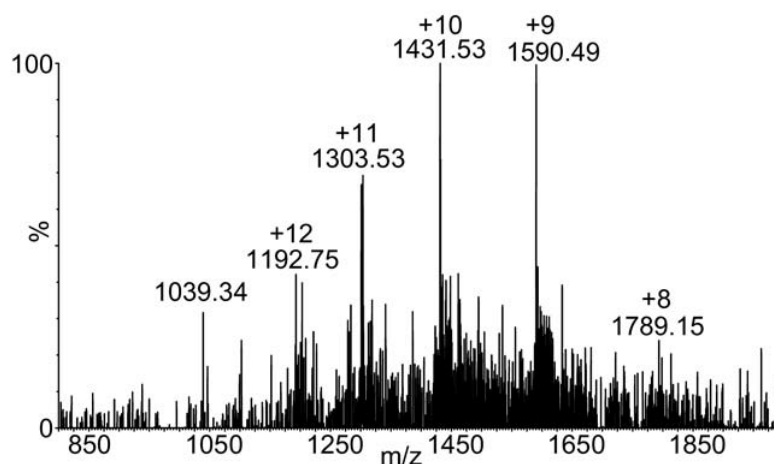
Figure 5.3. The LSI-IMS-MS mass spectrum of the extracted lysozyme component from the two-dimensional IMS-MS plot displayed in **Figure 5.2.2c**.

CHAPTER 6

LASERSPRAY IONIZATION-ION MOBILITY SPECTROMETRY-MASS SPECTROMETRY: BASELINE SEPARATION OF ISOMERIC AMYLOIDS WITHOUT THE USE OF SOLVENTS DESORBED AND IONIZED DIRECTLY FROM A SURFACE "Reprinted (adapted) with permission from (Inutan, E.D.; Trimpin, S. *J. Proteome Res.* **2010**, *9*, 6077-6081). Copyright (2010) American Chemical Society."

Introduction

No analytical method is available for detailed characterization of complex mixtures of closely related molecules present in tissue material. Challenges are related to many different factors associated with complexity including solubility, volatility, hydrophobicity, isobaric, and isomeric compositions. Mass spectrometry (**MS**), with benefits that include high sensitivity, specificity, mass resolution and the ability to simultaneously characterize many constituents of a mixture, is a promising technique. Unfortunately, MS methods are limited to the separation of ions measured and displayed by *m/z* ratios and ion intensities. Molecular structures, especially isomers, are inferred indirectly, if at all, through a combination of techniques such as liquid separation methods coupled with MS. Liquid based separation approaches perform poorly with solubility restricted materials [10,30] and can be inadequate for tissue analysis, especially if the need is to analyze the materials unadulterated and with a high spatial resolution.[110-113] Further issues include the ionization efficiency, especially of

compounds with limited solubility, frequently complicating or preventing analysis. [96] Ion mobility spectrometry (**IMS**) MS has been noted for the ability to separate ions in the gas-phase according to the number of charges and cross-section defined by size and shape.[59-67]

Laserspray ionization (**LSI**) shows advantages relative to other MS based methods, especially for tissue imaging, and include improved spatial and volume resolution, more relevant atmospheric pressure conditions, faster analyses, extended mass range for analysis of high-mass analytes that are beyond the mass range limitations of high performance **AP** ionization mass spectrometers, and improved fragmentation using electron transfer dissociation.[28-29,31,41] The desolvation conditions to obtain the highly charged protein ions from the charged matrix/analyte clusters are critical, especially for protein analysis, and are accomplished using 2,5-dihydroxybenzoic acid (**2,5-DHB**) matrix by heating the AP to vacuum ion transfer capillary to >400 °C for good sensitivity.[29] Unfortunately, most AP ionization mass spectrometers do not use a heated capillary for ion transfer from AP to vacuum.

Recently, LSI has been retrofitted to an IMS-MS instrument (SYNAPT G2) by constructing a heated desolvation device in front of the ion entrance orifice of the nanoelectrospray ionization (nano-ESI) source for evaporation of the matrix from the highly charged matrix/analyte cluster to give the multiply charged LSI ions.[49] This was, for example, shown for a mixture of ubiquitin and lysozyme.[49] The temperature capability of this home-built device is >250 °C. The necessity for proper desolvation conditions was exemplified by turning off the heat entirely. Without external heat

applied to the copper tube, the ion current was fully lost using 2,5-DHB as matrix even though the metal tube was connected to the inlet skimmer maintained at 150 °C.

Here, we introduce the ability for efficient desolvation of the highly charged matrix/protein clusters by lowering the thermal requirements of the matrix. This allows the operation at 150 °C cone temperature available with the SYNAPT G2 mass spectrometer without applying additional heat to the desolvation tube, and more importantly, under lower temperature conditions that retain the proteins' structure.

Experimental Procedure

Materials and sample preparation are included in **Chapter 2.1**, and the LSI set-up using the SYNAPT G2 mass spectrometer with the fabricated desolvation device is described in **Chapter 2.2**. For LSI-MS, 5 pmol μL^{-1} of ubiquitin, cytochrome C, and lysozyme were prepared individually in 50:50 ACN/water with 0.1% TFA, and insulin in 50:50 MeOH/water with 1% acetic acid. Solutions of 10 pmol μL^{-1} each of β-amyloid (1-42), β-amyloid (42-1), and the mixture of β-amyloid peptides (1-42) and (42-1) were made in 50:50 ACN/water with 0.1% TFA to obtain the LSI-IMS-MS. One μL sample solution was placed on top of the microscopy glass slide after which 1 μL of 2,5-DHAP matrix prepared in 50:50 ACN/water was added on top, and briefly mixed with the tip of the pipet. Three more times, 1 μL of matrix solution was added but without further mixing. The matrix/analyte spot was then blow dried with warm air. For ESI-IMS-MS, a 10 pmol μL^{-1} solution of the isomeric mixture in 50:50 ACN/water with 0.1% TFA was used and infused at a flow rate of 1 $\mu L\ min^{-1}$. The capillary voltage was set at 3 kV, sampling cone at 40 V, and extraction cone at 4 V. The ion source temperature was set to

150 °C to mimic conditions with LSI. Desolvation gas flow was set at 500 L h^{-1} at a temperature of 150 °C.

Results and Discussion

LSI produces mass spectra from proteins that are nearly identical to those produced by ESI but has the advantages of fast analyses at high spatial resolution directly from surfaces. Thus, the method is potentially a powerful new approach to imaging. While the mass spectra seem very similar to ESI in charge state and relative charge state abundances, the method is considerable different in the approach to ion formation leaving questions relative to the softness of this ionization method. Concerns relate to possible destruction of the protein structure by the deposited laser energy and the applied heat for desolvation of the matrix/analyte cluster [29,31,49] which is necessary to obtain the ESI-like multiply charged ions by laser ablation.[27] A new LSI matrix, 2,5-dihydroxyacetophenone (**2,5- DHAP**), was shown to produce multiply charged ions using only the 150 °C provided by the source heater supplied with the SYNAPT G2 Z-spray ion source. Typical mass spectra obtained for proteins using 2,5-DHAP and only the energy from the 150 °C ion source temperature are shown in **Figure 6.1**. As noted above, the mass spectra appear very similar to ESI mass spectra. Multiply charged ions as high as +17 for cytochrome C (**Figure 6.1C**) are produced without the high temperature applied to the desolvation region that was required when using 2,5-DHB as an LSI matrix.[28] Further, when the desolvation device is removed entirely and the experiment performed with only the 150 °C skimmer cone temperature, similar results related to ion abundance and charge state distribution of these proteins are obtained (**Appendix A**

Figure S10); however, significant low mass chemical background and contamination of the source are then observed.
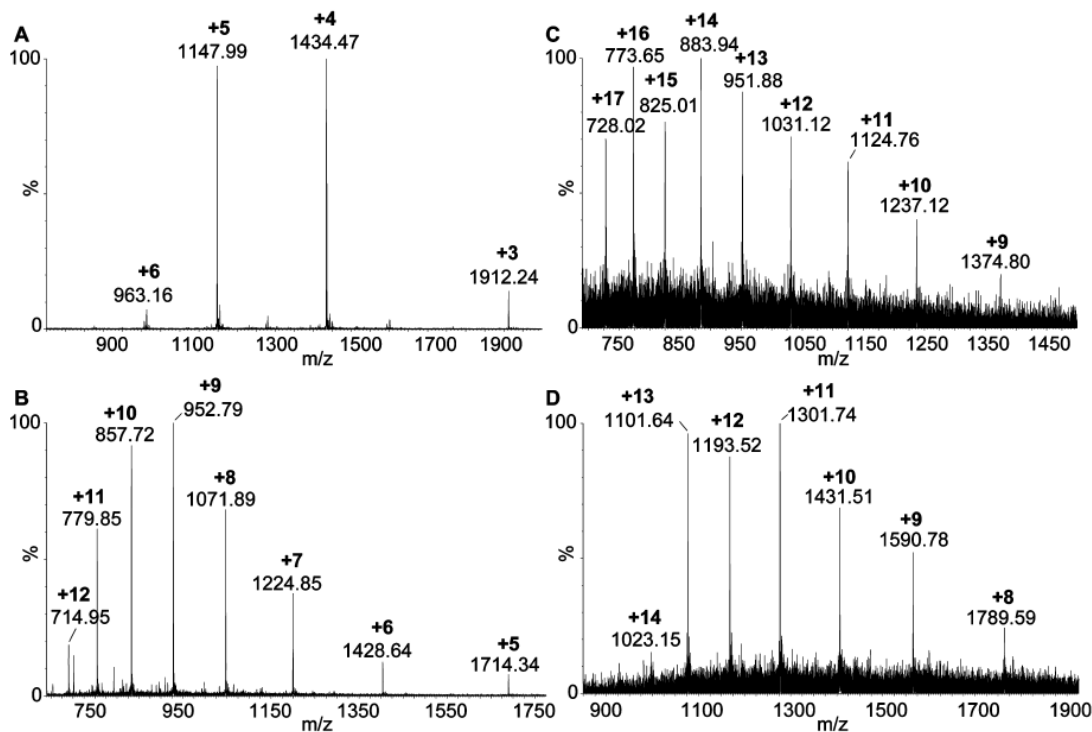
Figure 6.1. LSI-MS mass spectra of (**A**) insulin (MW 5731) in 50:50 MeOH/water with 1% acetic acid, (**B**) ubiquitin (MW 8561), (**C**) cytochrome C (MW 12361), and (**D**) lysozyme (MW 14300) prepared in 50:50 ACN/water with 0.1% TFA using 2,5-DHAP matrix in 50:50 ACN/water with ion source temperature of 150 °C.

The importance of a soft LSI ionization relates to the desire to obtain structural conformation information directly from the solid state from proteins as in tissue imaging experiments. An advantage of the lower heat application is that mass spectra obtained under similar thermal conditions using ESI and LSI can be compared to determine the relative softness of the ionization methods. LSI using 2,5-DHAP generally produces lower charge states than ESI of the same proteins. The lower charge states have been shown to relate to more compact protein structures while higher charge states are

frequently elongated by Coulombic repulsion of the ions subject to conditions used for mass spectral acquisition such as sample preparation, the choice of solvent, skimmer voltage, and trapping times.[106,114,115] The lower thermal conditions used with 2,5-DHAP are expected to be beneficial in retaining the proteins' structure. To examine the validity of intact protein structure and the practical utility by LSI-IMS-MS, we studied β-amyloid (1-42),[10,96,116-118] reversed β-amyloid (42-1), and the isomeric mixture of β-amyloid (1-42) and (42-1). β-Amyloid (1-42) is known to have low solubility in common ESI solvents.

Figure 6.2 shows the mass spectra (*left panel*) and the 2-D plots (*right panel*) of drift time *vs. m/z* for isomeric mixture (**A**) and the pure β-amyloids (B, C) obtained by the LSI method using 2,5-DHAP matrix prepared in 50:50 ACN/water and spotted on a glass microscope slide as described above and dried to completeness before laser ablation. The mass spectrum alone cannot distinguish one isomer from the other because of the same charge states and similar abundances (**Figure 6.2.1**), but the IMS-MS pictorial 'snapshot'14 readily shows separation and identification of the charge states from the isomeric mixture (**Figure 6.2A2**). The separation of the two isomers was then verified by analyzing the individual isomer samples (**Figure 6.2B2 and C2**). Thus, solvent-free IMS-MS gas-phase separation successfully separated and clearly showed both components of the isomeric mixture. From the drift times shown in **Figure 6.2.2**, the β-amyloid (1-42) reveals a much more compact structure than the reversed β-amyloid (42-1) as one would expect from the aggregation tendency.[119]

63
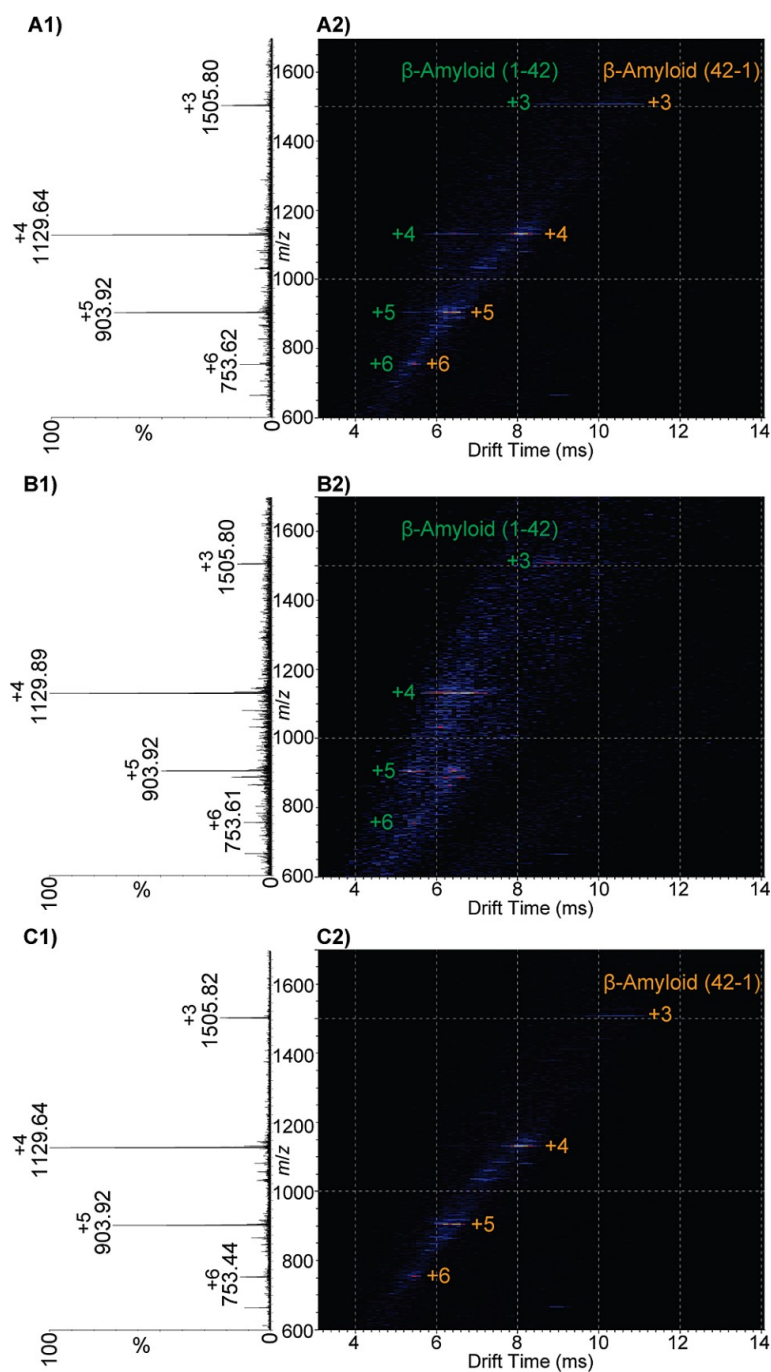
Figure 6.2. LSI-IMS-MS of (**A**) an isomeric mixture of β–amyloid (1-42) and reversed β-amyloid (42-1), (**B**) β-amyloid (1-42), and (**C**) β-amyloid (42-1) prepared in 50:50 ACN/water with 0.1% TFA acquired using 2,5-DHAP matrix in 50:50 ACN/water. The (**1**) mass spectrum does not distinguish one isomer from the other, but the (**2**) 2-D plot of drift time *vs.* mass-to-charge (*m/z*) ratio snapshot clearly shows separation of the two components.

Using the DriftScope, it is possible to extract *m/z* and drift time information for any ion or inset region of interest and give a much better insight to drift time separation. The extracted drift time distributions for the individual charge states +3 to +5 are shown in **Figure 6.3A**. Charge state +3, the lowest charge state and most compact structure of β-amyloid (1-42) and (42-1), shows the least difference in shape as can be seen by some degree of overlapping drift time distributions for ions. Baseline separation without the use of any solvent is achieved for charge states +4 and +5 of this isomeric, solubility restricted protein mixture. Using 2,5-DHAP as matrix and the ion source temperature set to 150 °C allows very similar instrumental conditions for LSI- and ESI-IMS-MS of the
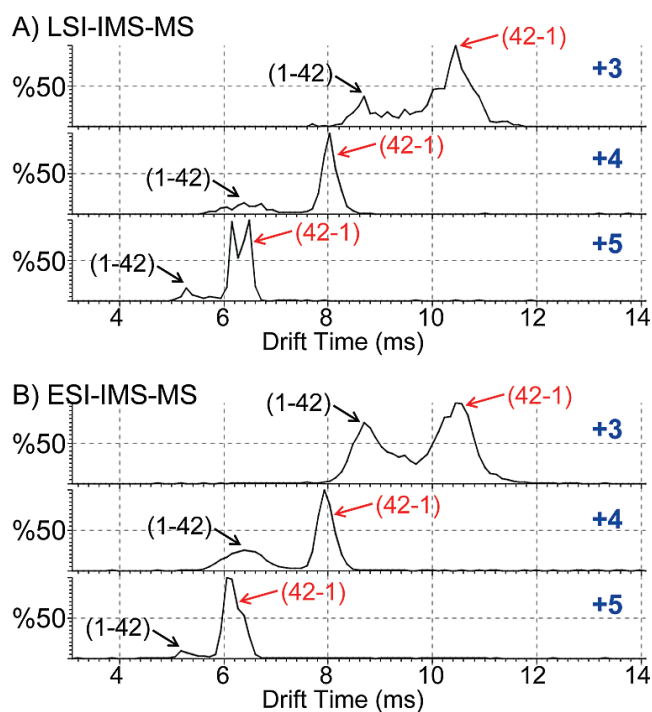
Figure 6.3. Extracted drift times of an isomeric mixture of β-amyloid peptides (1-42) and (42-1) prepared in 50:50 ACN/water with 0.1% TFA acquired with the ion source temperature set to 150 °C by (**A**) LSI using 2,5-DHAP matrix in 50:50 ACN/water, and (**B**) by ESI obtained at a flow rate of 1 μL min^{-1}. The drift times in (**A**) and (**B**) are nearly identical demonstrating similar or identical gas phase ion structures by the two ionization methods.

isomeric β-amyloid mixture. The results of such a comparison between ESI and LSI is shown in **Figure 6.3** where the drift times for each charge states of the protein mixture were extracted and compared. The drift times of the ions for the isomeric mixture are essentially identical between LSI (**Figure 6.3A**) and ESI (**Figure 6.3B**) with the minor exception that the LSI drift distributions are frequently sharper and therefore produce improved baseline separation of the different isomeric structures. This is evidence that both ESI and LSI are energetically similar and temperature effects observed for ion structures studied by ESI might occur after the ions are released into the gas phase and not in the charged droplets.

Although ESI is the MS technique predominately used for amyloid peptide detection, for investigating cleavage sites for specific amyloid peptide interaction,[117] and to study mechanisms of initial oligomerization reactions,[118] the solubility issues [116] make LSI an alternative method to ESI. Hyphenated with IMS-MS, LSI is a suitable analytical method for characterizing complex mixtures and possible molecular conformations present in tissue material. In case of isomeric composition, IMS separation is reduced from separation according to the number of charges, size, and shape to the sole separation according to shape. The baseline separation achieved for the isomeric protein composition by solvent-free gas-phase separation using IMS-MS demonstrates the utility of soft desorption directly from a surface combined with soft desolvation for ion production by LSI in retaining the protein structure (shape).

CHAPTER 7

LASERSPRAY IONIZATION - A NEW METHOD FOR PROTEIN ANALYSIS DIRECTLY FROM TISSUE AT ATMOSPHERIC PRESSURE AND WITH ULTRA-HIGH MASS RESOLUTION AND ELECTRON TRANSFER DISSOCIATION SEQUENCING "This research was originally published in Molecular and Cellular Proteomics (Inutan, E.D.; Richards, A.L.; Wager-Miller, J.; Mackie, K.; McEwen, C.N.; Trimpin, S. *Mol. Cell. Proteomics* **2011**; *10*:1-8) © the American Society for Biochemistry and Molecular Biology."

Introduction

Tissue imaging by mass spectrometry (**MS**) is proving useful in areas such as detecting tumor margins, determining sites of high drug uptake, and mapping signaling molecules in brain tissue [111,120-,121,122,123,124,125,126]. Imaging using secondary ion mass spectrometry is well established but is only marginally useful with intact molecular mass measurements from biological tissue [127-129]. Matrix-assisted laser desorption/ionization (**MALDI**)-MS operating under vacuum conditions has been used for tissue imaging with success, especially for abundant components such as membrane lipids, drug metabolites, and proteins [113,130,131]. Spatial resolution of ~20 μm has been achieved [132], and the MALDI-MS method has been applied in an attempt to shed light on Parkinson disease [13,15], muscular dystrophy [133], obesity, and cancer [130,134].

Unfortunately, there are disadvantages in using vacuum-based MS for tissue

imaging in relation to analysis of unadulterated tissue. Also, the mass spectrometers used in these studies frequently have much lower mass resolution and mass accuracy than are available with atmospheric pressure ionization (**API**) instruments and are not as widely available. Because the vacuum ionization methods produce singly charged ions, mass-selected fragmentation methods provide only limited information, especially for proteins. In addition, no advanced fragmentation such as electron transfer dissociation (**ETD**) [58,100,135] is available for confident protein confirmation or identification. Atmospheric pressure (**AP) MALDI** can be coupled to high performance mass spectrometers but suffers from sensitivity issues for tissue imaging where high spatial resolution is desired [136]. AP MALDI also primarily produces singly charged ions [2,3]. Thus, mass and cross-section analysis of intact proteins has yet to be accomplished using AP MALDI because of intrinsic mass range limitations of API instruments, which frequently have a m/z limit of < 4000. Thus, new improved methods of mass-specific tissue imaging, especially at AP, are needed.

The potential of laserspray ionization (**LSI**) (**Scheme 1.1.IA**) [27-31,41,49,50,137,138] for protein tissue analysis is reported here. LSI has advantages relative to other MS-based methods, including speed of analysis, laser ablation of small volumes, more relevant AP conditions, extended mass range and improved fragmentation through multiple charging, and the ability to obtain cross-section data for proteins on appropriate instrumentation. The applicability of LSI for high mass compounds on high performance API mass spectrometers (Orbitrap Exactive and SYNAPT G2) has been demonstrated producing ESI-like multiply protonated ions [28,29,49]. The first

experiments showing sequence analysis by ETD using the LSI method were successfully carried out on a Thermo Fisher Scientific (San Jose, CA) LTQ-ETD mass spectrometer [29]. Nearly complete sequence coverage was obtained for ubiquitin, an important regulatory protein. Applying ETD fragmentation to LSI-MS analyses potentially provides a new method for studying biological processes, including the mapping of phosphorylation, glycosylation, and ubiquitination sites from intact proteins and directly from tissue.

Furthermore, unlike ESI and related ESI-based methods such as desorption-ESI [139], the LSI method has been shown to allow analysis of lipids in tissue from ablated areas < 80 μm [27]. In comparison with literature reports for AP MALDI at the same stage of development [140], LSI is more than an order of magnitude more sensitive and is capable of analyzing proteins on high resolution mass spectrometers as was demonstrated by obtaining full-acquisition mass spectra at 100,000 mass resolution (FWHH, m/z 200) after application of only 20 fmol of bovine pancreas insulin in the matrix 2,5-dihydroxyacetophenone (2,5-DHAP) onto a glass microscope slide [31]. The analysis speed of LSI was demonstrated by obtaining mass spectra of five samples in 8 s [137]. Here, we show the utility of LSI for intact peptide and protein analyses directly from mouse brain tissue. The ability to obtain a protein mass spectrum directly from mouse brain tissue in a single laser shot at 100,000 mass resolution and with ETD fragmentation is demonstrated.

Experimental Procedure

Analysis of Aged and Fresh Tissue Samples - The mouse brain tissue sections used in

this study were shipped in dry ice before being delipified according to published procedure [74] and then again shipped overnight in dry ice. The aged, delipified tissue sample was stored for approximately 2 months at -5 °C. The delipification was initially obtained on the aged tissue sample and verified by MALDI-TOF-MS analysis. The optimized delipification conditions were used for further study comparing results obtained from MALDI- and LSI-MS analysis. A second set of mouse brain tissue samples were cut, frozen, and immediately shipped overnight. Each microscopy glass slide, plain and gold-coated, was mounted with four to five tissue sections. On receipt of the frozen samples, delipification of the tissue on glass slides was performed as described below, and again the samples were immediately frozen and shipped overnight for prompt LSI-MS analysis on an Orbitrap Exactive mass spectrometer. These samples were again frozen and shipped overnight for microscopy and subsequent MALDI-MS and LSI LTQ Velos analysis.

LSI-MS of Mouse Brain Tissue - The glass microscope slide mounted with mouse brain tissue was prepared with the LSI matrix (5 mg mL^{-1} of 2,5-DHB or 2,5-DHAP, saturated solution) dissolved in 50:50 ACN/water by placing a number of 0.2-µL drops on top of the tissue material and allowing them to air dry. After solvent evaporation, the glass slide containing LSI matrix applied to mouse brain tissue was placed 2-3 mm in front of the mass spectrometer ion transfer tube entrance, moved manually through the laser beam, and aligned 180° relative to the ion entrance orifice (transmission geometry) (**Scheme 1.1IA**). The AP to vacuum ion transfer capillary was heated to 375 °C for 2,5-DHB and 300 °C for 2,5-DHAP, and the laser fluence per pulse was about 0.5-1 J cm^{-2}. Multiply

charged ions were observed in the absence of an electric field in the ion source region. Both plain and gold-coated glass slides were used.

LSI-ETD – An LTQ Velos mass spectrometer with ETD capabilities was used as described in **Chapter 2**. The reaction time was set at 120 ms using an isolation width of 3 amu. The activation time ranged from 25 to 50 ms for the precursor ions' 917.5 (2+), 1491 (12+), and 1789 (10+). A supplemental activation of 20 V was used for the 2+ precursor ion. A single 0.33-s acquisition was selected to obtain the ETD fragment ion mass spectra for peptide identification; the total ETD acquisition time was set for 1 min.

LSI Tissue Imaging - Mouse brain tissue mounted on a glass microscope slide and coated with a saturated solution of 2,5-DHAP in 50:50 ACN/water using 0.2-μL drops was controllably moved through the laser beam with ablation in transmission geometry (**Scheme 1.1IA**) using an eTrack series xy-stage (Newmark Systems, Mission Viejo, CA). Lanes were at 100-μm intervals, and each lane was 10 mm long from which 22 s of data were acquired. For these studies, three mass spectral acquisitions were obtained per second with the laser operating at ~12 Hz. The ablated diameter for each laser shot after microscopy was ~15 μm (neglecting the stray beam commonly observed), which converts to an area of about $4(15)$ x 15 $μm^2$ ablated per MS acquisition.

MALDI-MS of Mouse Brain Tissue - A MALDI-TOF Bruker Ultraflex mass spectrometer (Bruker, Bremen, Germany) equipped with a nitrogen laser (337 nm) was used to monitor the success of the tissue delipification and for comparison with LSI results. The MALDI sample preparation was performed according to published work [74]. After washing the tissue and drying in the desiccator, the tissue was spotted with

0.2-µL of either sinapinic acid matrix dissolved in 50:50 ACN/water in 0.1% TFA or 2,5-DHAP in 50:50 ACN/water. The mass spectrum was acquired using the linear positive ion mode with an accelerating voltage of 20.16 kV, extraction voltage of 18.48 kV, lens voltage of 7.06 kV, and pulsed ion extraction of 360 ns. Delayed extraction parameters were optimized to have the optimal resolution and sensitivity for the MALDI range was 12-kDa. An increment of 30 laser shots was used, and shots were positioned and moved within a single matrix spot to obtain a mass spectrum having a total of 120 laser shots. The mass spectrum was processed and base line-corrected using the Flex Analysis software. Both plain and gold-coated microscopy slides were used; only gold-coated microscopy slides are expected to provide the correct mass calibration.

Data Analysis - MASCOT Distiller version 2.3.2.0 (Matrix Science, London, UK) [141] was used to interpret ETD mass spectra for peptide and protein identification obtained from the LTQ-ETD Velos. The Mass Spectrometry protein sequence DataBase (MSDB) was searched using the no enzyme setting to obtain the sequence analyses directly from mouse tissue. Parameters were set to include acetylation, deamination, oxidation, methylation, and phosphorylation. The peptide and protein masses had to be within the mass tolerance characteristic of the mass spectrometer used for data acquisition. Searches within 1-Da mass error were performed, but to consider a peptide as well matched, it had to be within < 5 ppm of the mass obtained from the Orbitrap Exactive.

Results and Discussion

Evaluation of Experimental Conditions on Aged Tissue Sample - Tissue fixation or washing with solvents to extract lipids enhances the signal quality of peptides and

proteins and slows enzymatic processes, thus extending the useful life prior to analysis [142]. The washing solvent was selected based on previously reported studies [74,143] as well as from results we obtained from MALDI-MS analyses of tissue extracted with recommended solvents, ethanol and isopropanol. Here, the ethanol wash was selected because it gave higher intensity protein MALDI-MS signals using SA as the matrix. The guidelines developed by Schwartz et al. [144] for the proper handling of tissue sections (tissue storage, sectioning, and mounting) for peptide and protein analyses were applied. The choice of matrix and its deposition onto the tissue have been shown to be important in determining the subset of proteins extracted from the tissue and detected using MALDI [143]. For the MALDI analysis of the delipified mouse brain tissue, peptide and protein signals were detected using SA as matrix from m/z 5000 to 19,000 (**Appendix A Figure S11**) which is within the range that Seeley et al. [74] presented; the mass calibration is expected to be somewhat off for results in which plain microscopy glass slides without conductive coating were used. Only a few of the proteins detected give significant signal intensity similar to previous studies [130].

Once a satisfactory procedure for handling and delipifying mouse brain tissue was established for MALDI analysis, that method was applied for LSI-MS. Using 2,5-DHB as matrix, only lipids were observed even with the delipified tissue, similar to a previous report [27]. However, for the delipified tissue using 2,5-DHAP, lipids were observed in low abundance if at all, and signals for multiply charged ions having masses as high as 5–19 kDa (at ZS1) were detected. A mass spectrum obtained from the Orbitrap Exactive at 100,000 (FWHH, m/z 200) mass resolution by summing 15 1-s acquisitions is shown in

Figure 7.1 and represents ablation of most of the tissue covered by a 0.2-μL solution of 2,5-DHAP. Because the mass resolution of the Orbitrap Exactive provides ^{13}C isotope separation even for proteins, a single ^{13}C isotope distribution is all that is necessary to determine the monoisotopic protein molecular weight with high mass accuracy (**Figure 7.1, insets**). Ions observed just above noise, for which the monoisotopic peak cannot be reliably identified, provide a more accurate average mass than obtained with linear MALDI-TOF instruments. **Figure 7.1B** is the inset region from **Figure 7.1A** with the mass range displayed between *m/z* 650 and 1000. The multiply charged ions range from 3+ to 8+, representing ions having molecular masses from approximately 650 to 5000 Da. For this data set, most ions were from compounds below 10 kDa. Because of the long storage time for the aged sample, it is possible that some of the observed multiply charged ions are from post-mortem enzymatic digestion of proteins [74,130]. The use of gold-coated and plain microscopy glass slides provides comparable abundance LSI mass spectra of the delipified tissue. As expected, no mass shift was observed in the AP LSI results using conductive or non- conductive glass slides; matrix placed below the tissue increased the ion abundance at the expense of a larger ablated area. Experiments without the addition of the LSI matrix did not provide any useful analytical results. Microscopy images of the aged mouse brain tissue after LSI analysis showed a variety of ablated areas, including numerous areas where the laser beam did not appear to penetrate the tissue (**Appendix A Figure S12**).
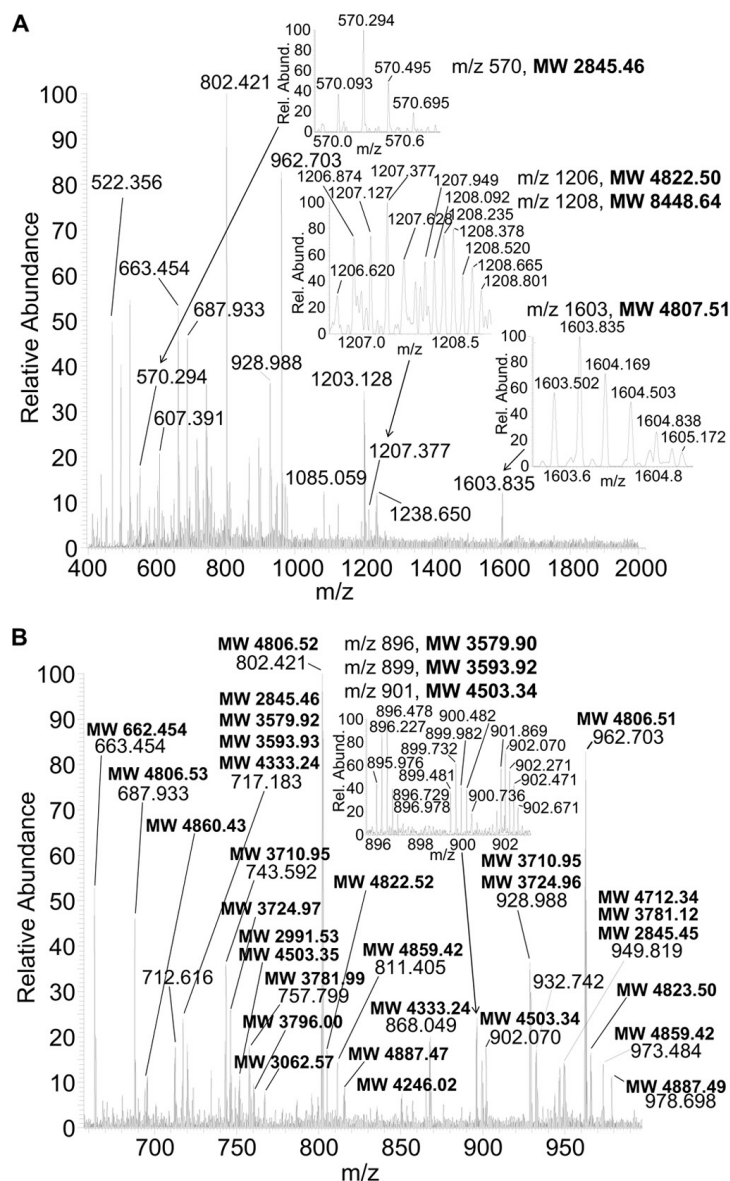
Figure 7.1. LSI mass spectra from aged mouse brain tissue washed with ethanol and spotted with 2,5-DHAP matrix in 50:50 ACN/ water using an Orbitrap Exactive mass spectrometer. **A**, full mass spectrum with insets showing multiple charged protein and peptide ions. **B**, limited mass range between *m/z* 650 and 1000 is displayed with monoisotopic molecular weights of the various multiply charged ions presented. Rel. Abund., relative abundance.

The areas in which the tissue was completely ablated ranged in dimensions from ~3 to 9

μm x ~5 to 25 μm. Because the laser was fired at several hertz as the tissue was

constantly moved through the laser beam, each 1-s acquisition was the sum of several laser shots. The elongated features observed in the microscopy image may be the result of multiple laser shots producing continuous ablation as the tissue was moved slowly through the beam. Holes in the tissue that appear to be from a single laser shot were typically < 30 μm^2 (**Appendix A Figure S13**). For the 10-μm tissue thickness used in this study, these microscopy data suggest that the tissue volume below the ablated area represents ~300 μm^3 for a single laser shot. However, to achieve this spatial resolution will minimally require matrix preparation methods that result in no diffusion of compounds outside the boundary area and improved mass spectral sensitivity.

Comparison of LSI-MS and MALDI-MS Analysis on Fresh Tissue Samples - Successful results with the aged tissue samples prompted us to examine fresh tissue sections that were maintained at or below -20 °C except for short times required for mounting the tissue to the glass slide, delipification, mass spectral analysis, and microscopy. The fresh delipified samples using 2,5-DHAP matrix and acquired on the Orbitrap Exactive showed an abundant doubly charged LSI ion at *m/z* 917.50 (molecular weight 1833.0) and numerous other multiply charged ions at higher *m/z* values (**Figure 7.2**). The highest mass protein with at least two observed charge state distributions had a molecular mass (monoisotopic) of 17,882 Da, although a single low abundance isotope distribution was observed for an ion having an average molecular mass of ~19,665 Da. Some of the lower molecular weight proteins observed in the aged tissue sample (**Figure 7.1**) were also observed in the fresh sample but in lower abundance, whereas the higher mass proteins were significantly more abundant in the fresh tissue sample. **Appendix A**

Figure S14 shows that in a single laser shot the most abundant proteins were observed from the fresh tissue using the 100,000 mass resolution set- ting of the Orbitrap Exactive. The mass spectra for the single laser shot, the sum of seven laser shots, and the sum of the full acquisition for a 0.2-μL matrix deposition are shown in **Appendix A Figure S14B**. Notable differences between gold-coated (**Appendix A Figure S15**) and plain glass slides (**Figure 7.2**) were again not observed. **Appendix A Figure S15** shows three isotope distributions each for multiply charge ions representing proteins having molecular masses of 9908, 11,788, and 12,369 Da (monoisotopic mass).
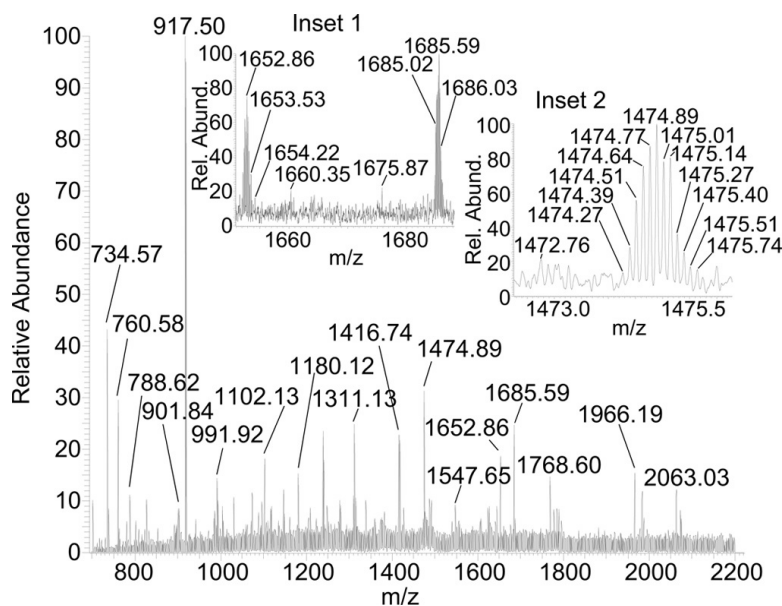
Figure 7.2. LSI-MS summed full and inset mass spectra of delipified fresh tissue on plain glass slide spotted with 2,5-DHAP matrix in 50:50 ACN/water showing multiple charged protein ions using Orbitrap Exactive mass spectrometer. Rel. Abund., relative abundance.

A fresh tissue section from the same mouse was delipified and immediately mass-measured on an LTQ Velos instrument. The multiply charged ions described above for fresh tissue were observed. The mass spectrum from summing multiple acquisitions on

the tissue slice is provided in **Figure 7.3A**. The distribution of multiple charged ions of

the protein having molecular weight 11,788, however, could be observed in a single

acquisition representing one laser shot (**Figure 7.3B1**). Single laser shots in different

areas of the mouse brain tissue gave different results. For example, **Figure 7.3B2**, also

from a single laser shot, shows the protein at molecular weight 17,882 in lower

abundance than the first protein of molecular weight 11,788, and a peptide having a

molecular weight of 1833 was observed more in the center than the edges of the tissue.

The ability to acquire a mass spectrum from a single laser shot using a relatively

inexpensive nitrogen laser suggests the potential for high speed tissue imaging.

Potential of Tissue Imaging Using LSI - To evaluate the potential for tissue

imaging using LSI, a crude experiment was performed using a glass slide with mounted

mouse brain tissue that was coated with the matrix 2,5-DHAP by depositing 0.2-µL

droplets of a saturated solution of 50:50 ACN/water over the tissue surface and allowed

to air dry. This matrix deposition method is not suitable for tissue imaging because

delocalization of compounds in the tissue and uneven matrix deposition are expected with

this approach. An attempt at spray applying the matrix from solution, which is a more

appropriate matrix deposition method, resulted in very low abundances of peptide and

protein   ions   (**Appendix A Figure S16**). Clearly, improved matrix preparation

conditions for LSI imaging are needed. Nevertheless, attaching the glass microscope slide
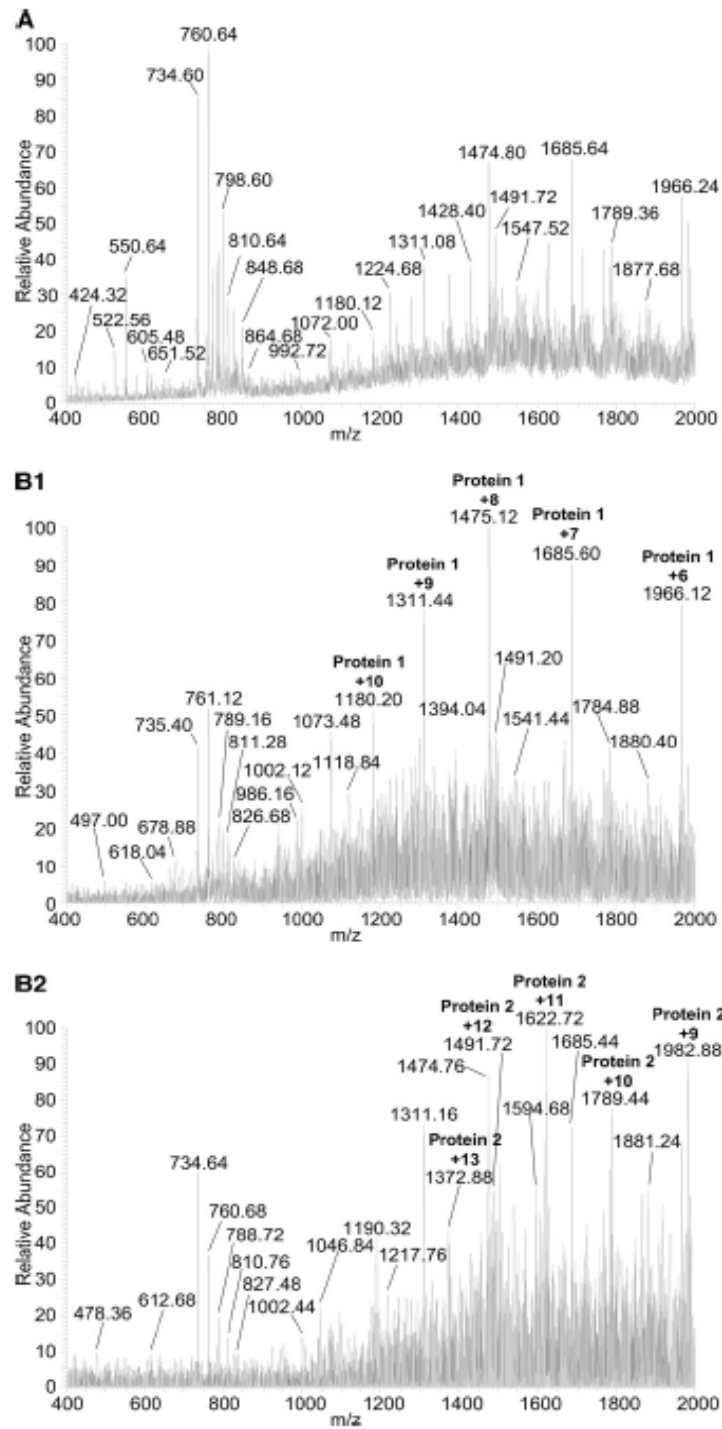
Figure 7.3. LSI-MS spectra of delipified fresh tissue on plain glass slide spotted with 2,5-DHAP matrix in 50:50 ACN/water using LTQ Velos. *A*, sum of the full acquisition. *B1* and **B2**, single acquisitions at different tissue locations showing different protein abundances. The ions observed around *m/z* 760 are from lipids.

to a computer controlled xy-stage allowed a crude image of mouse brain tissue to be obtained. Mass-specific imaging for two charge states of the protein with MW 11,788 and one charge state of the protein with MW 12,369 is shown in **Appendix A Figure S17**. Several other peptides and proteins gave sufficient signal intensities in single acquisitions to produce crude images. Obtaining higher shot-to-shot reproducibility and increased analyte ion abundances are areas that require further research.

Microscopy images of the laser-ablated tissue after the imaging analysis are shown in **Figure 7.4**. Rows spaced at 100-µm intervals of single laser shots are readily seen. The individual laser-ablated areas in this experiment, as determined by optical microscopy, are ~15 µm in diameter.
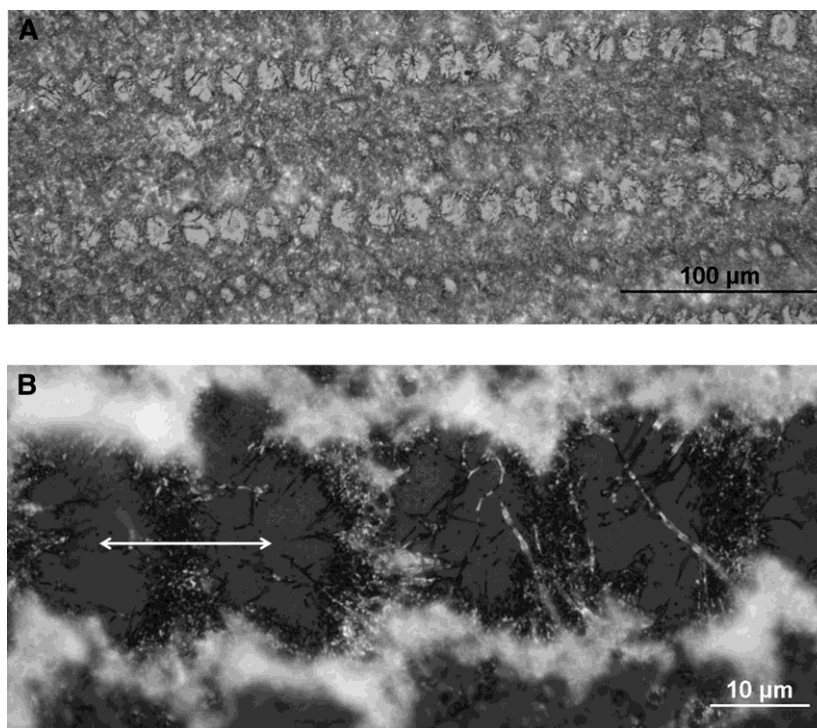
Figure 7.4. Optical images of laser-ablated areas obtained in im- aging experiment. A, 20x magnification. B, 100x magnification. Arrow denotes 15 µm.

The mass spectrum shown in **Appendix A Figure S18** is of a single MS acquisition during which time four laser shots impacted the tissue in adjacent positions. Thus, each mass spectral acquisition was of a visibly ablated area of approximately 15 x 4 x 15 μm^2. It is clear from these images that the laser beam frequently completely ablates the tissue and matrix producing sufficient ions to be detected. The 10-μm-thick tissue slices likely absorb a fraction of the laser energy before it is absorbed by the matrix.

The LSI method introduces remarkable speed and simplicity of analysis compared with reflective geometry MALDI where frequently >100 laser shots are summed to provide each data point in the image [145,146]. For tissue imaging experiments, high repetition and therefore expensive lasers are required to keep the analysis time reasonable (hours *vs*. days). The ability to obtain mass spectra of proteins directly from tissue in a single or even a few summed laser shots using the LSI approach suggests the potential for using less expensive lasers to achieve comparable analysis speed relative to high repetition laser MALDI. For the crude imaging experiment reported here, the laser repetition rate was ~12 Hz, and each lane received 89 laser shots in 22 s. With 100-μm spacing between rows, 80 rows were required to image the mouse brain tissue. Thus, actual acquisition time was only about 30 min. This work demonstrates the potential speed of this method for tissue analysis or imaging.

The ability to obtain mass spectra of proteins directly from tissue using LSI offers considerable potential in tissue analysis. However, difficulties that need to be addressed before tissue imaging becomes a reality using LSI are increased ion abundances from single acquisitions and higher shot-to-shot reproducibility. We expect reproducibility is

related to uneven tissue thickness, the condition of the tissue, matrix application, and the laser flux per unit area. Just as in MALDI imaging, matrix application in LSI is a crucial step. The dried droplet method of spotting matrix that was used in the present study is inappropriate for tissue imaging studies. We are currently beginning research aimed at improving solvent-based and solvent-free matrix preparation methods for tissue imaging using LSI. Future advances also need to incorporate solvent-free gas-phase separation for efficient simplification of complexity of the produced gas-phase ions [10,30,49].

For comparison purposes, sequential tissue sections from the same mouse brain used for the fresh tissue studies mounted on gold-coated and plain glass slides were used for vacuum MALDI-MS analysis. One-half of each delipified tissue section was coated with 2,5-DHAP, and the other half was coated with SA applying several 0.2-µL matrix solutions. Interestingly, none of the observed molecular weights are common between LSI using 2,5-DHAP and MALDI using either 2,5-DHAP or SA. MALDI with the 2,5-DHAP matrix gave poor results, which may help explain the different proteins observed between vacuum MALDI and LSI.

ETD Fragmentation of Peptides Directly from Tissue - Because LSI produces ESI-like multiply charged mass spectra directly from tissue, it becomes possible to achieve ETD fragmentation of these ions. This is demonstrated for the doubly charged peptide ion that was observed at *m/z* 917.5 (molecular weight 1833) for a single ETD acquisition representing four single laser shots, each on fresh spots of the tissue obtained on the LTQ-ETD Velos mass spectrometer (**Figure 7.5**). **Table I** shows the result of the MASCOT search obtained from the single acquisition data. A MASCOT score of 73 (67

is considered to be significant) was achieved for the peptide having the sequence Ac-ASQKRPSQRSKYLATA that also is well within the 5-ppm mass tolerance for this peptide acquired on the Orbitrap Exactive.
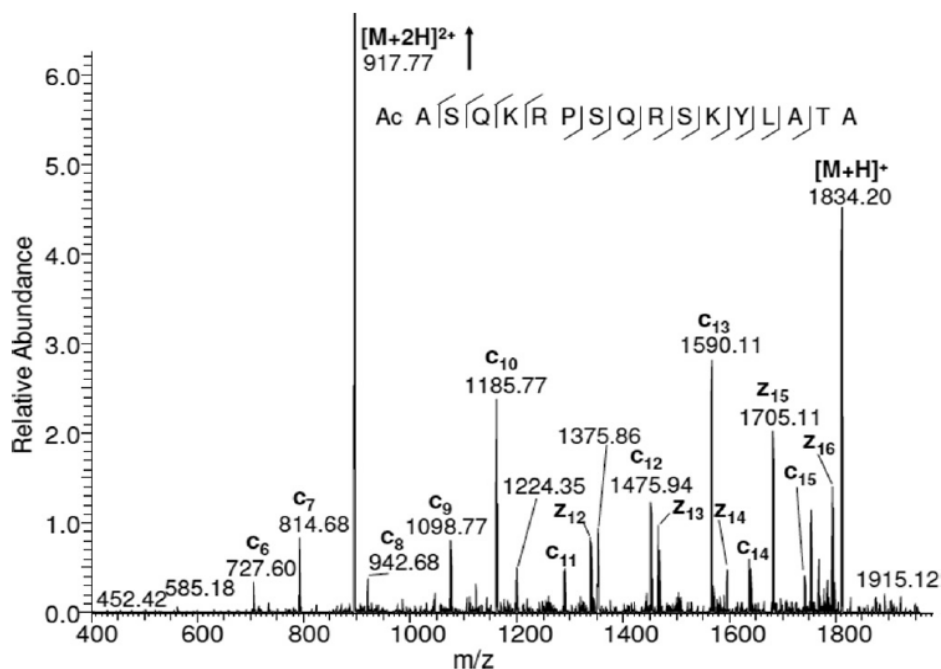
Figure 7.5. LSI-ETD single scan acquisition mass spectrum at precursor ion 917.5 (+2) of delipified fresh mouse brain tissue on plain glass slide spotted with 2,5-DHAP matrix in 50:50 ACN/water using LTQ Velos.

This sequence encodes for the myelin basic protein *N*-terminal fragment that is known to occur in mouse brain. The labeled masses in **Figure 7.5** are the predicted "c" and "z" fragments expected from ETD fragmentation of this peptide. The only missing sequence ions are related to the proline residue. It is clear that synergy exists between accurate mass measurement and ETD for reducing the number of hits obtained by database searching. ETD fragment ions and accurate mass measurement were also obtained for *m/z* 1491 and *m/z* 1789, which are the 12+ and 10+ charge states, respectively, for the protein of molecular weight 17,889 (**Appendix A Figure S19**). We

are in the process of attempting to identify this protein. These first results demonstrate the potential of LSI for protein identification directly from tissue and are a significant advance over current methods in which the identity of the ions observed are made only from an approximate average mass value of the proteins known to be in the tissue.

Table 7.1 LSI-ETD MASCOT scores for *m/z* 917.5. The Delta value is the difference between the calculated mass for the sequence shown and the accurate mass measurement obtained from the Orbitrap at 100,000 mass resolution. Only sequences with a Delta 0.005 were within the mass tolerance of the mass.

Table 7.1 LSI-ETD MASCOT scores for *m/z* 917.5.

Score	M_r (calculated)	Delta	Sequence
73.1	1832.9856	−0.0002	ASQKRPSQRSKYLATA
65.1	1832.9856	−0.0002	ASQKRPSQRSKYLATA
41.0	1832.7539	0.2315	ADLTSCSSLKEEVYH
41.0	1832.7539	0.2315	ADLTSCSSLKEEVYH
40.5	1832.8686	0.1168	ADEMKEIQERQRDK
40.5	1832.6936	0.2918	SVLYQYQTHSKR
40.3	1832.8370	0.1485	AEWIFGGVKYQYGGNQ
40.3	1832.8791	0.1063	ANIYKNKKSHEQLSA
40.2	1832.9631	0.0223	ANLKYNQQLEKKKNA
40.2	1832.9631	0.0223	ANLKYNQQLEKKKNA

CHAPTER 8

COMMERCIAL INTERMEDIATE PRESSURE MALDI ION MOBILITY SPECTROMETRY MASS SPECTROMETER CAPABLE OF PRODUCING HIGHLY CHARGED LASERSPRAY IONIZATION IONS "Reprinted (adapted) with permission from (Inutan, E.D.; Wang, B.; Trimpin, S. *Anal. Chem.* **2011**, *83*, 678-684). Copyright (2011) American Chemical Society."

Introduction

Matrix-assisted laser desorption/ionization (**MALDI**) mass spectrometry (**MS**), for over 20 years, has been an important analytical method for a variety of fields, especially those related to analysis of synthetic and biopolymers.[2,3,10,147-150] The method has been extended from a vacuum technique in which time-of-flight (**TOF**) mass analyzers provided nearly unlimited mass range to intermediate pressure (IP; ~0.2 Torr) and atmospheric pressure (**AP**) techniques interfaced to mass analyzers having limited mass-to-charge (*m/z*) range.[21,75,136] Production of singly charged ions on these *m/z* limited instruments eliminates the ability to mass analyze the singly charged ions of high-mass compounds. Further, the most accepted ionization mechanism for MALDI involves ion molecule reactions occurring in the laser plume similar to atmospheric pressure chemical ionization (**APCI**).[82] An undefined fraction of the analyte is available for ionization by this mechanism because a substantial fraction is ablated as matrix/analyte droplets or clusters.[31,36,37,94,151] Some reports have speculated that the singly

charged ions produced by MALDI originate from these clusters.[54,85,152] Several mechanisms by which the clusters become charged have been suggested.[35,54,55,82]

Laserspray ionization (**LSI**) was the first example of laser ablated matrix/analyte producing electrospray ionization (**ESI**)-like multiply charged ions.[27-31,41,48-50,137,138] Defining features of LSI are AP conditions, the absence of applied ionizing voltage, the necessity of a heated region in the AP to vacuum interface, and the use of lasers and matrix compounds commonly employed in ultraviolet (UV)-MALDI (e.g., 2,5-dihydroxyacetophenone, **2,5-DHAP** and 2,5-dihydroxybenzoic acid, **2,5-DHB**) [153,154]. Thus, LSI has the attributes of MALDI related to analysis of compounds directly from surfaces with high spatial resolution and the attributes of extended mass range and improved fragmentation associated with multiply charged ions in ESI. LSI is most commonly applied using transmission geometry (**TG**) where the laser beam strikes the matrix/analyte from the backside relative to the ion entrance orifice of the mass analyzer. While TG is not a requirement for LSI,[41] it is of practical importance for simplicity of alignment, reproducibility, speed of acquisition, and especially the potential of high spatial resolution imaging.[27,48] MALDI, especially in vacuum, uses a laser fluence near the ionization threshold to achieve ions with a low energy spread and, thus, improved mass resolution. Therefore, numerous laser shots are typically acquired and summed to produce a mass spectrum, while LSI can achieve ultrahigh resolution even at high laser fluence, often providing good results from a single laser shot.[48,138] Nevertheless, vacuum MALDI has been shown to be more sensitive than either AP-MALDI or AP-LSI.

Here, we report the first example of producing highly charged LSI ions using vacuum conditions (ca. 0.16 Torr). The results were achieved on a commercial intermediate pressure (**IP**)-MALDI ion source interfaced to a Waters SYNAPT G2 ion mobility spectrometry (**IMS**) MS instrument using conditions common with AP-LSI. Multiply charged ions are also produced in MALDI under vacuum conditions, but the average mass-to-charge ratio is much higher than reported here. To our knowledge, the only similar charge state distribution achieved under vacuum conditions two orders of magnitude higher (~30 Torr) than here was with ESI operated under special conditions for the purpose of the use of ion funnel technology for ion focusing.[94] Besides the fundamental implications of this work, an important potential analytical advantage of IP-LSI, other than use of a commercial instrument, is the potential for high sensitivity equivalent or better than AP-LSI and vacuum MALDI. We demonstrate that analysis of peptides directly from tissue produces nearly identical mass spectra and drift time distribution appearance observed with AP-LSI and from solution using ESI.

Experimental Section

Analyte solutions were prepared individually in 50:50 ACN/water with 0.1% TFA (ACTH), 50:50 ACN/water with 0.1% FA (N-acyl MBP fragment), 50:50 MeOH/water with 1% acetic acid (Ang I, GFP, BI), and 49:49:2 ACN/water/acetic acid (ubiquitin). The matrix solutions were prepared saturated (20 mg of 2,5-DHB in 100 μL of 50:50 ACN/water with 0.1% TFA, 10 mg of CHCA in 2 mL of MeOH/ACN, and 5 mg of 2,5-DHAP in 150 μL ACN, vortexed for a few minutes, then 150 μL water was added and vortexed again until a darker yellow solution is obtained). The matrix/analyte mixture

was prepared in 1:1 volume ratio to make the final concentration of the analyte 1 pmol μL^{-1} before deposition on the target plates. One microliter of the matrix/analtyte mixture was used and deposited on metal and glass plates using the dried droplet method.[3] The model mixture composed of 1 pmol Ang I, 2 pmol GFP, 2 pmol BI, and 2 pmol SM was prepared in 50:50 MeOH/water with 1% acetic acid. For the tissue sample, an aged delipified tissue slice prepared as described in a previous study,[48] was spotted with 0.2 μL of the 2,5- DHAP matrix solution and allowed to air-dry prior to analysis.

LSI at IP using the MALDI source of SYNAPT G2 - An IMS-MS SYNAPT G2 (Waters Corporation) with an IP-MALDI source operating using a Nd:YAG laser (355 nm) was employed in this study. Instrument parameters and acquisition conditions are included in **Chapter 2.3**.

LSI at AP using the NanoESI source of SYNAPT G2 – The description of the set-up is included in **Chapter 2.2**. The LSI sample holder was slowly moved through the focused laser beam using the xy-direction of the stage.

ESI-IMS-MS - The Waters SYNAPT G2 instrument was operated in mobility-TOF using positive ion sensitivity mode. A 1 pmol μL^{-1} solution of MBP in 50:50 ACN/water with 0.1% TFA was infused at a flow rate of 1 μL min^{-1}. The capillary voltage was set at 3 kV, sampling cone at 50 V, and extraction cone at 4.4 V. Desolvation gas flow was at 800 L h-1 and at a temperature of 150 °C.

MALDI-TOF-MS - A MALDI-TOF Bruker Ultraflex mass spectrometer (Bruker, Bremen, Germany) equipped with a nitrogen laser (337 nm) was used to acquire the mass spectrum of the same mixture/analyte used in IP studies on the IMS-MS SYNAPT G2

mass spectrometer. The mass spectra were acquired using the reflectron positive-ion mode with a reflectron voltage of 20.30 kV and an ion source lens voltage of 8.85 kV. Laser repetition rate was set at 20 Hz and increments of 20 laser shots were used to acquire the mass spectrum with a total of 100 shots. The laser attenuation was set at 45%, 55%, and 70% (highest laser fluence) for CHCA, 2,5-DHB, and 2,5-DHAP, respectively. Flex Analysis software was used to process the data and obtain the mass spectrum.

Results

The mass spectra obtained at IP on a commercial MALDI-IMS-MS (SYNAPT G2) are nearly identical in charge state to mass spectra obtained using ESI and LSI on the same instrument at AP. A number of parameters were explored for their influence to provide multiply charged peptide and protein ions with high abundance and good reproducibility. These include the sample support (glass and metal), matrixes (2,5-DHAP, 2,5-DHB, CHCA), solvent (MeOH, water, ACN, and combinations thereof), laser fluence (relative values, with settings: low "50" to highest "500"), and pressure (IP and high vacuum MALDI instruments). Typical IP results are shown in **Figure 8.1** for Ang I, BI, and ubiquitin, though with increasing molecular weight, the ion abundance decreases notably. As is the case in LSI at AP using laser alignment in reflective geometry,[41] both glass and metal plates can be used at IP (**Appendix B Figure S1**). The glass plate provided higher abundance than a metal target plate for multiply charged ions and less chemical background, a well-known issue in MALDI.[94]
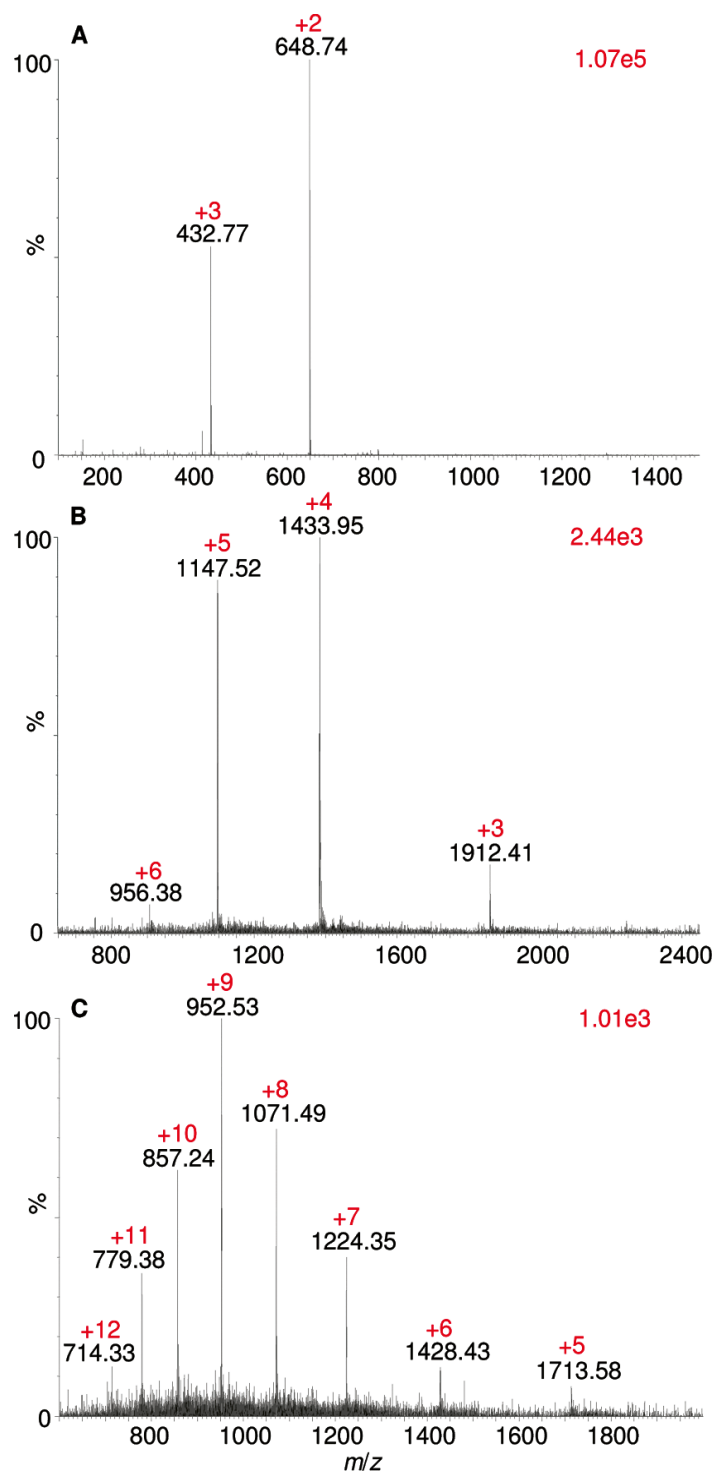
Figure 8.1. IP-LSI-IMS-MS mass spectra using a glass plate, 2,5-DHAP matrix (50:50ACN/water), "200" laser power: (**A**) angiotensin I (methanol/water with 1% acetic acid), (**B**) BI (methanol/water with 1% acetic acid), (**C**) ubiquitin (49:49:2% acetic acid).

As with AP-LSI, the best results were obtained with 2,5-DHAP (*vs.* CHCA and 2,5-DHB, **Appendix B Figure S2**). Also similar to previous studies [41] on a commercial AP-MALDI source on an Orbitrap XL using 2,5-DHAP and reflection geometry, irreproducibility is encountered at relative low threshold laser fluence by the inability to observe ions after a couple of laser shots at the same location. Moving to the next spot and increasing the laser fluence improved the reproducibility. We relate this issue to the laser aligned in reflection geometry and not to IP conditions; in transmission geometry, this is not observed because the sample in the path of the laser beam is completely ablated in a single shot. [48,138] In MALDI, first shot phenomena have been reported for the analysis of molecular complexes.[155,156]

Another interesting phenomena affecting the relative abundances of singly and multiply charged ions produced by IP is the sample preparation and morphology as determined for 2,5-DHAP using microscopy. The crystallized LSI matrix/analyte sample showed a flat film-like appearance around the edge and a center with a fluffy crystalline appearance (**Appendix B Figure S3**). Mass spectral results showed that the center provided more abundant multiply charged ions (**Appendix B Figure S4**) while the outer film produced more singly charged ions. The similarity to results obtained using AP-LSI, suggests that a similar ionization mechanism is active at IP, and thus, we refer to this new method as IP-LSI.

The commercial MALDI source at IP allows for the first time a precise assessment of the laser fluence on the production of highly charged LSI ions. The effect of laser fluence on the formation of multiply charged ions is notable for any of the

matrixes. Results are summarized in **Appendix B Figure S5** for Ang I and **Appendix B Figure S6** for MBP, a neuropeptide, using in both cases 2,5-DHAP matrix. At very low laser fluence of "50" and "100" low abundant MBP ions are detected barely above the baseline. At "150", highly charged ions are observed but in relative low abundance and with essentially no chemical background. At "200", the ion abundances of the highly charged ions increase by a factor of 3 *vs.* "150", also with essentially no chemical background signals. With increasing laser fluence up to "500", matrix signals start to show up and the relative intensity of the multiply charged ions increases for the lower charge states and formation of singly charged ions become much more evident. At the highest laser fluence of "500", the doubly charged ions are the base peak for both compounds but the triply charged ions are significantly reduced in abundance. Further, the ion abundance of the background increases to the point of overwhelming the ion intensity of both the multiply and the singly charged ions present in the mass spectra. Increasing the laser fluence to "500" provided only highly charged but no singly charged ions of BI (**Appendix B Figure S7**).

Only singly charged ions (Ang I, GFP, ACTH, BI) are observed using the same matrix/analyte samples on a high vacuum commercial MALDI instrument (**Appendix B Figure S8**) with glass or metal sample plates using 55% and 70% laser fluence for CHCA and 2,5-DHAP matrixes, respectively. Higher laser fluence was necessary for 2,5-DHAP in comparison to CHCA and 2,5-DHB for the detection of singly charged analyte ions. 2,5-DHAP produced low abundant doubly charged ions for ACTH and BI at high laser fluence under vacuum MALDI conditions, whereas the other matrixes only produced

singly charged ions. These results suggest that matrix/analyte clusters are formed under vacuum conditions, similar to suggestions by Karas, Tabet, and others,[54,85,152] but multiply charged ions are only observed with proper desolvation conditions, which in this case are produced primarily by the choice of matrix and laser fluence.

The evaluation of parameters under our control on the SYNAPT G2 allowed extension of the mass range at IP to proteins as large as ubiquitin with charge states to +12 (**Figure 1C, laser "200", and Appendix B Figure S9, laser "500"**). There are no provisions to provide heat in the pressure drop region between the IP source and the high vacuum of the mass analyzer. Previous AP-LSI studies on a LTQ Velos (Thermo Fisher Scientific) with the capability of heating the ion inlet capillary to 450 °C produced highly charged ions of carbonic anhydrase (~29 kDa) with charge states up to +27.[138] Interestingly, with the SYNAPT G2, it appears that the helium gas associated with the IMS region is of critical importance. Only singly charged ions are observed, as expected from a MALDI process without added helium gas, but the addition helium gas results in observation of multiply charged ions (**Appendix B Figure S10**). We assume this is a result of desolvation of charged clusters and are currently developing methods to apply heat within the IP region with the expectation that similar sensitivity [29] and mass range [138] enhancements observed with AP-LSI will be observed at IP-LSI.

The practical utility of this novel ionization method is shown for analysis of a mixture composed of a lipid (SM), peptides (Ang I, GFP), and a small protein (BI) using the common LSI matrix 2,5-DHAP, a glass plate sample holder, and the maximum laser fluence provided by the manufacturer settings (**Figures 2 and S11, Appendix B)** metal

plate of mixture; **Figures S12 and S13 (Appendix B)** pure samples with low and high

laser fluence). Interestingly, the lipid and small peptide showed metal adducted singly

charged ions especially with high laser fluence. Collision-induced dissociation can be

used to characterize lipid compositions directly from tissue (**Appendix B Figure S14**).
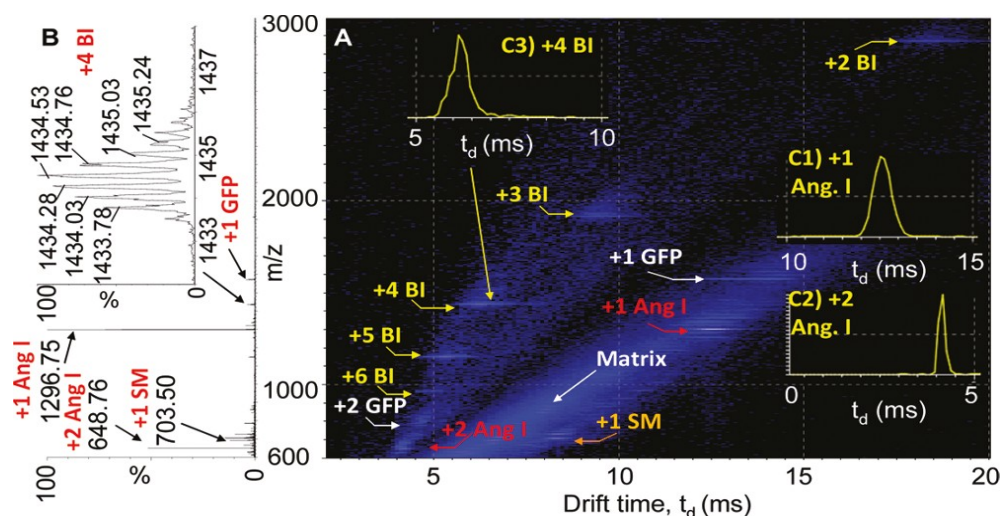
Figure 8.2. IP-LSI-IMS-MS of a model mixture of angiotensin I (Ang I), sphingomyolin (SM), [Glu1]-fibrinopeptide B (GFP), and bovine insulin (BI) using a glass plate, 2,5-DHAP matrix (50:50 ACN/water), and "500" relative laser power: (**A**) 2-D plot of drift time *vs.* *m/z* and extracted drift time for +4 BI, +2 and +1 Ang I ions; (**B**) total mass spectrum and inset spectrum of +4 BI ion.

Figure 2A shows the 2D data set of drift time *vs.* *m/z* separations of the IP-LSI-

IMS-MS measurement of this model mixture at a laser fluence of "500". In the total mass

spectrum (**Figure 2B**), the most abundant signal is from Ang I observed with charge

states +1 and +2. The other components of the model mixture, especially the higher

charge states of the protein, are not very noticeable because of the low signal intensity as

compared to the higher abundant Ang I. Because of the exquisite sensitivity for the entire

sample composition, the IMS-MS 2-D display allows these ions to be readily visualized

(**Figure 2A**).

Singly charged ions of lipids and peptides fall nearly on the same diagonal indicating little separation in the IMS dimension. However, the charge states +1, +2, and +3 are well separated from each other and readily observed individually. The highly charged bovine insulin ions +4, +5, and +6 fall on a diagonal line that is well separated from lower charge states +3, +2, and +1. The relative drift times of the diagonal lines drawn through the different components in the sample are highly charged protein ions +6, +5, and +4 < multiply charged peptide and protein ions +3 and +2 < singly charged matrix ions < singly charged peptide and lipid ions. The separation trend is in accord with previous studies using vacuum MALDI-IMS-MS.[157-162] Here, the extent of separation between the highly charged and the singly charged ions is of notable analytical utility.

Comparison of the results obtained with IP-LSI to those obtained with AP-LSI (**Appendix B Figure S15**) shows that, at IP using low laser fluence of "200", the results closely resemble those obtained with unattenuated laser fluence at AP. Increasing the laser fluence at IP to "300" increases the abundance of the singly charged lipid and peptide ions at the expense of a notable increase in matrix background and decrease of the abundance of higher charged ions.

A second set of comparison experiments was applied to obtain data directly from mouse brain tissue using IP-LSI-IMS-MS (**Figure 3**). This same tissue section was previously analyzed using AP-LSI-MS in combination with ultrahigh mass resolution and electron transfer dissociation (**ETD**) enabling identification of an endogenous

neuropeptide directly from its native and complex environment.[48] At IP, charge state families similar to the model mixture in **Figure 2** were observed ranging from charge state +1 to +3. Extracting diagonal slices through the 2D data set in **Figure 3** provide mass spectra that deconvolute the different charges states, as is exemplified by the extracted mass spectrum and inset mass spectra for charge state +2 shown in **Figure 8.4A**.
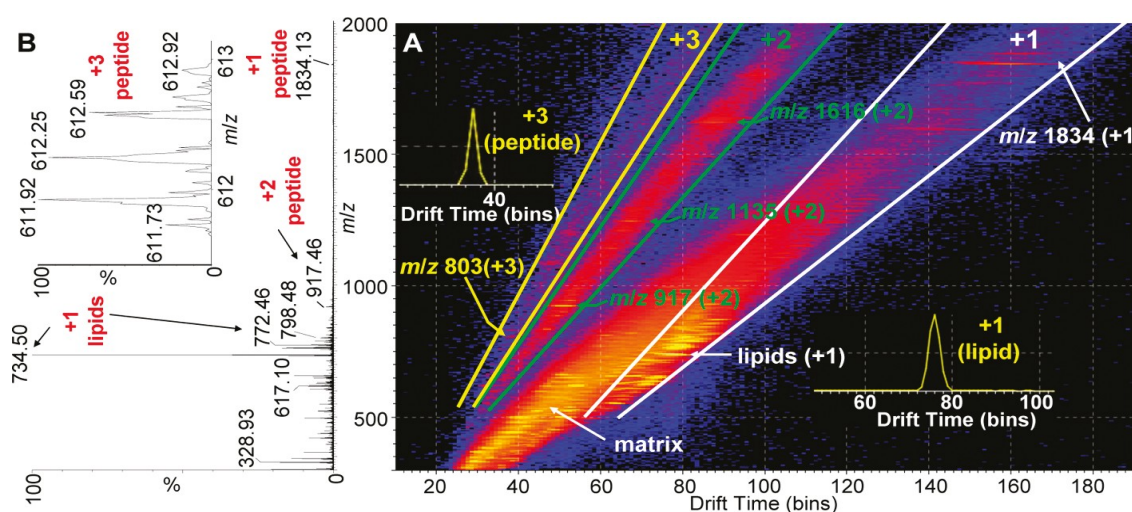
Figure 8.3. IP-LSI-IMS-MS of a delipified mouse brain tissue (analyzed previously,[31]) using a glass plate, 2,5-DHAP matrix (50:50 ACN/water), and "500" relative laser power: (**A**) 2-D plot of drift time *vs. m/z* and extracted drift time for +3 peptide and +1 lipid ions; (**B**) total mass spectrum and inset spectrum of +3 ion and the ion (+2) with the largest MW 3216.

The highest molecular weight peptide observed is 3216 Da. Previous studies of the same tissue using AP-LSI-MS on LTQ Velos and Orbitrap mass spectrometers showed low abundant protein ions up to MW ca. 19,665 Da.[48] The extracted slices from the 2-D data set permit examining in detail the different charge-state distributions (+2, **Figure 8.4A**) and drift time distributions (**Figure 8.4B; Figures S16 and S17, Appendix B**, for lipids and peptides) even of low-abundant ions that would otherwise be

diffcult to extract (e.g., charge state +2 *vs.* charge states +1 or +3).
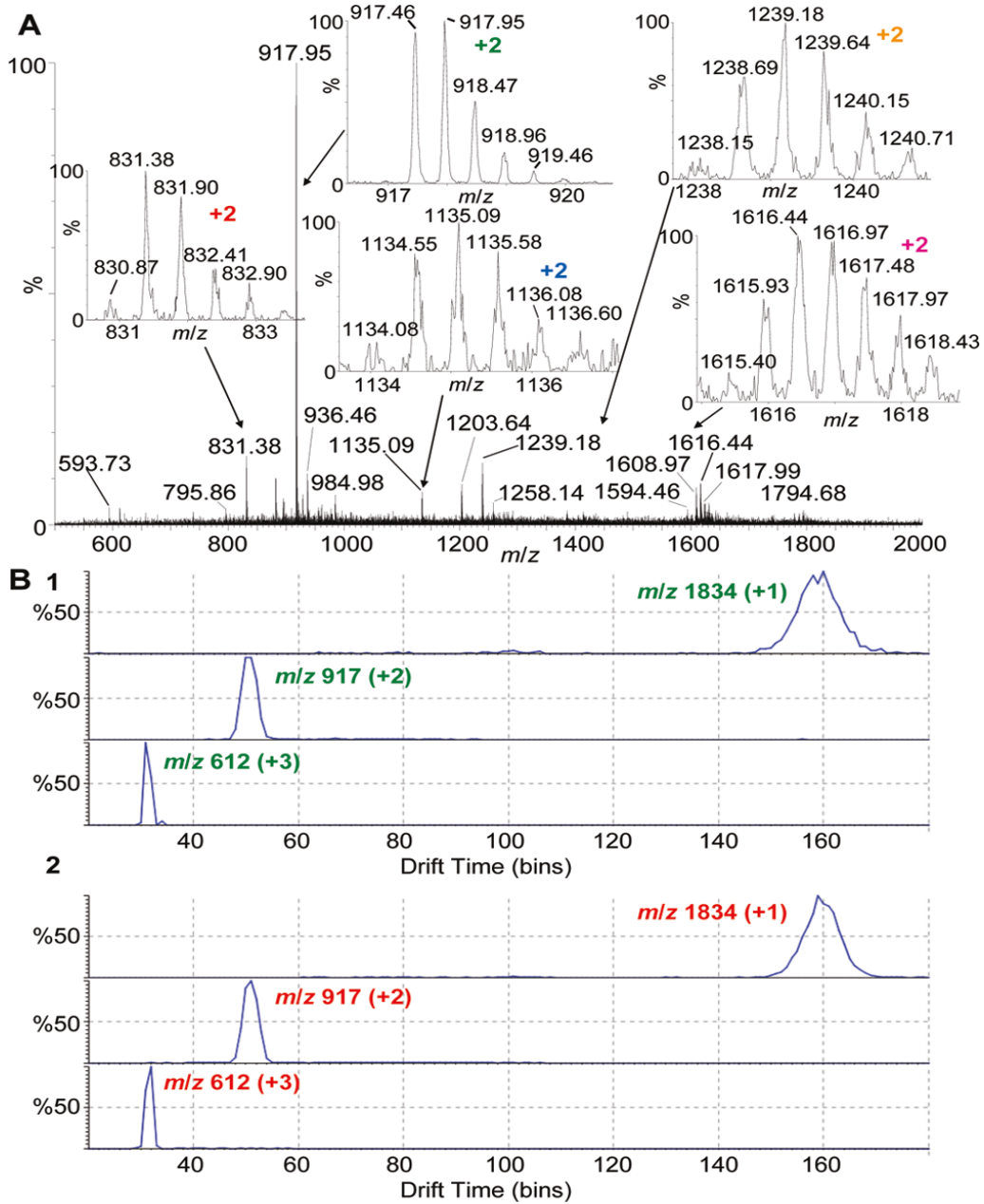
Figure 8.4. Extracted data from **Figure 3**: (**A**) mass spectrum of chargestate family +2 and respective inset mass spectra; (**B**) drift time distributions of charge states +1 to +3: (**1**) *N*-acetylated fragment of myelin basic protein (characterized previously by ETD,[8]) and (2) from the synthesized neuropeptide (+1, +2, and +3, MW 1833).

Drift time distributions can be extracted for specific *m/z* values from which cross sections can be determined using a calibration approach.[163] These values can give insight into structures when combined with computer modeling approaches [164-176] or aid identification when standards are available.[50,66] For example, **Figure 8.4B** shows the drift time distributions obtained for +1, +2, and +3 charge states for the *N*-acetylated fragment of myelin basic protein with a MW of 1833 Da. Narrower drift time distributions are observed with increasing charge state. The drift time distributions of the singly charged ions are, however, unexpectedly broad, as is the case for any of the peptides that showed singly and doubly charged ions (**Appendix B Figure S16**). The singly charged ions obtained from the defined lipid, peptides, and protein mixture analysis (**Appendix B Figure S17**) also showed notably broader drift time distributions relative to the multiply charged ions. The width of the drift time distributions may indicate more than one ionization mechanism for singly charged ion production.

For further insight, we obtained the custom synthesized neuropeptide that was previously identified directly from tissue by a MASCOT search of LSI data from a LTQ-ETD and Orbitrap Exactive.[48] The extraction of the drift times of the IP-LSI-IMS-MS measurements of singly charged ions (**Figure 8.4B**) again showed the unusual broad drift time distributions as compared to the multiply charged ions. Importantly, the endogenous neuropeptide and the standard sample provide identical drift time distributions for charge states +1 to +3 obtained by IP-LSI-IMS giving further confirmation of the structure present in the tissue. We noted earlier that the charge state and drift time distribution appearance is nearly identical for the synthetic neuropeptide sample to that observed in

AP-LSI or ESI IMS-MS (**Appendix B Figures S18-S19**) but with the important difference that singly charged ions are not present under AP conditions even though AP-LSI uses significantly higher laser fluence than those used with IP-LSI. Previous investigations of isomeric beta amyloid peptide mixtures showed baseline separation using a LSI-IMS-MS (SYNAPT G2) approach,[50] strongly suggesting that even rather small differences in the structures of the peptides would be observed using the IMS-MS approach.

Discussion

The production of highly charged ions using a commercial IP-MALDI source has important analytical implications but is also of fundamental interest. As noted previously, a number of authors have suggested ion formation in MALDI occurs from charged matrix/analyte clusters or droplets.[54,55,85,94,152] Garrison and co-workers first modeled formation of matrix droplets by vacuum laser ablation of a solid matrix.[36,38] Tabet and co-workers postulated on the basis of Karas's lucky survivor model [152] that two energy-dependent processes exist for ion formation from matrix/analyte clusters: hard desolvation leading to low charge states (+1) by emission of charged matrix molecules and soft desolvation leading to multiply charged ions (+2) by emission of neutral matrix molecules in a process similar to the mechanism proposed for ESI. This study was based primarily on relative abundances of +1 and +2 ions produced at different laser fluences. If, in fact, MALDI ions are produced from charged clusters, then the results presented here are the logical extension of this process as would be the case with AP-LSI. However, both AP-LSI and the work presented here have almost

identical outcomes for various matrix compounds tested and, thus, we refer to the methods as AP-LSI and IP-LSI rather than MALDI methods. Not only do these methods produce highly charged ions not previously observed with MALDI but also the out- come of all experiments to date is nearly identical to matrix assisted ionization *inlet* (**MAII**) results.[39] MAII requires no laser and, thus, is outside the definition of MALDI. However, it is not clear yet if ions can be produced at IP with MAII, at least without a source of thermal energy. The laser fluence in IP-LSI may provide the energy that the heated inlet provides in AP-LSI and MAII for the initial ionization. The ability to extend the LSI/MAII methods to vacuum conditions also poses new questions relating to the MALDI mechanism and has the potential to even shed new light on the ionization mechanism in ESI.

CHAPTER 9

LASERSPRAY IONIZATION IMAGING OF MULTIPLY CHARGED IONS USING A COMMERCIAL VACUUM MALDI ION SOURCE "Reprinted (adapted) with permission from (Inutan, E. D.; Wager-Miller, J.; Mackie, K.; Trimpin, S. *Anal. Chem.* **2012**, *84*, 9079–9084). Copyright (2012) American Chemical Society."

Introduction

Matrix-assisted laser desorption/ionization (**MALDI**) mass spectrometry (**MS**) produces abundant singly charged ions of peptides from the solid state under low pressure, intermediate pressure, and atmospheric pressure conditions.[3,21,75] Time-of-flight (**TOF**) is the common mass analyzer used with low-pressure MALDI and in principle provides unlimited mass range for detection of large molecules.[177] A limitation of the production of primarily singly charged ions is that high-mass compounds cannot be analyzed using high-performance instruments with only a limited mass range such as Fourier transform ion cyclotron resonance, Orbitrap, or ion mobility spectrometry (IMS) (SYNAPT G2) mass spectrometers. MALDI imaging mass spectrometry has provided information on spatial distributions of lipids,[162,178] peptides,[179] and proteins [180] directly from biological tissue sections, and MALDI-IMS-MS imaging has been applied for lipids [113,162] and peptides [162] as well as studying protein changes related to several diseases such as Alzheimer's and Parkinson's [13,15,16] as well as cancer.[124,181,182] Secondary ion mass spectrometry (**SIMS**) has also been used to map the distribution of cancer

chemotherapeutic agents in tissues and cells,[183,184] lipids,[185-187] and later, matrix-enhanced SIMS to enhanced subcellular imaging of tissue samples.[188-190] Desorption electrospray ionization is promising for imaging living tissue without sample preparation.[191-193]

Laserspray ionization *inlet* (**LSII**) [27-31,41,48-50,137,138] and matrix assisted ionization *inlet* (**MAII**) [39,194] are two new ionization methods in MS operating from atmospheric pressure to produce highly charged ions similar to electrospray ionization (**ESI**). Both LSII and MAII have attributes in common with MALDI allowing analysis of compounds directly from the solid state by using a solid matrix material composed of a small organic compound.[40] The application of heat and the presence of an atmospheric pressure to vacuum pressure drop region are two important factors in producing abundant highly charged ions in the inlet of the mass spectrometer.[29,31,45] In LSII, the laser alignment is not important because multiply charged ions are formed without the use of a laser,[39,40,44] as well as with the use of a laser aligned in transmission [27-31,48-50,138] or reflection geometry.[41] For example, a commercial atmospheric pressure MALDI source with the laser aligned in reflection geometry produced abundant highly charged protein (e.g., lysozyme) ions on a Thermo Orbitrap mass spectrometer.[41] Critical is that sufficient heat is provided to the inlet of the mass spectrometer which directly depends on the matrix used.[29,40] Multiply charged ions produced by LSII and MAII using 2-nitrophologlucinol (**2- NPG**) matrix extend the mass range of detection to at least bovine serum albumin (~66 kDa).[194] LSII was also shown to produce sufficient ion abundance directly from tissue to identify an endogenous

peptide, a fragment of *N*-acetylated myelin basic protein (**MBP**) (amino acid (**aa**) 1−16), using electron transfer dissociation (**ETD**) and high-accuracy mass measurement [48] and has been successfully introduced on a mass spectrometer with a heated inlet to perform imaging of lipids.[50,138] The laser aligned in transmission geometry provides ease of operation [27-31,48-50,138] and offers the potential for high spatial resolution imaging. [48,195,196].

Initial studies on matrixes [138] enabled us to introduce LSI technology operating from vacuum, LSIV, using a commercial intermediate pressure MALDI ion source interfaced to a Waters IMS-MS SYNAPT G2 mass spectrometer.[42] In the absence of a heated inlet region, abundant multiply charged analyte ions are formed by laser ablation using a matrix that efficiently evaporates.[40] 2-NPG matrix is the first matrix to produce highly charged ions at atmospheric pressure, intermediate pressure, and low pressure.[44,45,194] The mechanism proposed [45] for the LSI inlet and vacuum ionization process is laser ablation producing highly charged matrix/analyte droplets which upon matrix evaporation releases ions by a similar process to that proposed for ESI.[51,52] The impact of a laser has been experimentally and theoretically shown to form molten droplets of matrix/analyte, and the existence of clusters was verified recently for LSII.[31,36,197] 2,5-Dihydroxyacetophenone (**2,5-DHAP**),[48,50] a matrix that requires a lower inlet temperature than, for example, 2,5-dihydroxybenzoic acid (**2,5-DHB**), produces abundant multiply charged ions at intermediate pressure under LSI tuning conditions.[39,42] However, the use of higher laser power [42] and voltages [45] increase the abundance of singly charged ions. Using a higher laser power makes

only minor contribution to the production of singly charged ions. It is primarily the higher voltages of the MALDI settings that allow switching from multiply charged using ESI-like settings to singly charged ions either at atmospheric pressure [41] or intermediate pressure.[45] The practical utility of LSIV on a commercial vacuum MALDI source in combination with IMS-MS was demonstrated using 2,5-DHAP as matrix for the mixture analysis of lipids, peptides, and proteins.[42] Various families of compounds are well-separated from each other. Imaging applications are an extension to these tissue analysis developments. Here, we show the applicability of LSIV using a commercially available vacuum MALDI source operating at intermediate pressure (~0.16 Torr) for tissue imaging of multiply charged peptide ions achieved without any physical instrument modifications.

Experimental Section

2,5-DHAP and 2-NPG matrix solutions were prepared by dissolving 5 mg in 150 μL of 50:50 ACN/water (warmed), and 100 and 300 μL of 50:50 ACN/water (with and without 0.1% FA), respectively. The matrix:analyte mixture was prepared in 1:1 volume ratio before depositing 1 μL of the analyte/matrix mixture on a glass plate using the dried droplet method.[42] Mouse brain tissue sections were obtained as previously described [48,113,195,196] and included in **Chapter 2.1**. The tissue sections were mounted on plain and precoated glass plates with CHCA matrix using a tissue box [195] and delipified with ethanol as previously described.[48] The delipified tissue slices were spotted separately with several 0.5 μL of 100% 2,5-DHAP and 100% 2-NPG matrix in 50:50 ACN/water for direct analysis and spray-coated with 2-NPG for imaging. A binary

mixture of 10% 2-NPG and 90% 2,5-DHAP by volume composition matrix solutions was also used for tissue imaging.

Laserspray Ionization Vacuum (LSIV) – A commercial IP-MALDI source of SYNAPT G2 mass spectrometer was employed in this study as described in **Chapter 2.3**. In the analysis of standards (MBP, galanin, bovine insulin), the laser power used ranged from 4.2 to 7.3 J cm^{-2} as previously reported,[45] at a firing rate of 200 Hz and a scan rate of 1 scan s^{-1} acquiring a sum mass spectrum of 1-2 min. For tissue imaging, the instrument's MALDI imaging pattern creator software was used as one would use for MALDI imaging. The sampling resolution was set at 100 μm × 100 μm x,y laser step size, similar to MALDI imaging. Acquisition was set at a scan time of 2 s, laser power of 12.5 J cm^{-2} at a firing rate of 200 Hz, and 1 scan time per pixel. The total imaging acquisition time was ~5 h to image the entire tissue section. *Laserspray Ionization Inlet (LSII)* - A Nanolockspray source of the SYNAPT G2 was used LSII comparison as described in **Chapter 2.2** using a home-built skimmer cone with a fabricated copper inlet tube attached, and the laser was aligned at 180° to the inlet tube, focused onto the matrix/analyte sample on a glass plate, and ablated in transmission geometry (**Scheme 2.1**) relative to the inlet of the mass spectrometer. The source temperature was set at 150 °C, and acquisition was obtained in resolution mode using 100 and 4 V sample cone and extraction cone voltages, respectively, with a scan time of 1 s for 2 min.

Data Processing - MassLynx version 4.1 was used to process the mass spectra, DriftScope version 2.2 was used to extract the two-dimensional (**2-D**) plot of drift time *vs.* mass-to-charge (*m/z*) ratio, and mobility extractor was used to obtain the drift time *vs.*

m/z selected data set and convert into an MSI file using the MALDI imaging converter. BioMAP 3.8.0.1 was used from Novartis Institutes for Biomedical Research, Basel, Switzerland, to extract from the MSI file the images of the peptides.

Results and Discussion

The endogenous *N*-acetylated MBP peptide (Ac-ASQKRPSQRSKYLATA), previously sequenced by LSII (**Scheme 1.1IA**) using high-performance fragmentation,[48] was the initial focus for obtaining MS images of multiply charged ions using LSIV (**Scheme 1.1IIA**) on a commercial IP-MALDI source of the SYNAPT G2 mass spectrometer. The use of a suitable matrix material and appropriate settings and acquisition conditions such as laser power and voltages for ion acceleration and transmission are important factors influencing the formation of the highly charge ions at intermediate pressure.[40,42,45] The direct analysis of MBP peptide from delipified mouse brain tissue was first achieved by spotting 2,5-DHAP matrix onto the tissue. Multiply charged peptide ions up to charge state +3 were detected with the largest MW of ~3.2 kDa (**Appendix B Figure S20**). Exceptional ion abundance is obtained for the MBP peptide with *m/z* 917.39 using 2,5-DHAP, but only when the matrix is directly spotted on the tissue (**Appendix B Figure S20A**). With LSII, spotting 2,5-DHAP matrix on nondelipified mouse brain tissue allowed detection of lipids as well as multiply charged ions of the *N*-acetylated MBP fragment peptide (**Appendix B Figure S21**). However, spray-coating of the matrix, necessary for good spatial resolution in tissue imaging, provided poor ion abundance using 2,5-DHAP operated from atmospheric pressure or vacuum.

2-NPG, a more volatile matrix than 2,5-DHAP, produced abundant multiply charged ions of up to charge state +4 from a synthesized MBP peptide standard (**Figure 9.1I.A**) at low laser power applying "LSI settings" [42,45] on the commercial IP-MALDI source without any physical instrument modifications. The analyte ion intensity increased as did the chemical noise background with increasing laser power (**Figure 9.1I.B**). The chemical background could be removed using the IMS dimension, especially because the different charge state ions are well-separated in the IMS dimension, identical to ESI-IMS-MS.[59-63,67] Only singly charged ions are produced when the default "MALDI settings" [45] are applied (**Figure 9.1II**). The ion abundances observed are similar for the multiply charged ions ("LSI settings") (**Figure 9.1I**) and the singly charged ion ("MALDI settings").[45] For a number of peptide and small-protein standards using "LSI settings" [42,45] (**Appendix B Figure S22**): (A) MBP, MW 1833 Da; (B) galanin, MW 3150 Da; and (C) bovine insulin, MW 5731 Da), 2-NPG matrix allows detection of higher charge states than 2,5-DHAP matrix. 2-NPG requires less laser power (ca. 4.2 J cm^{-2}) than 2,5-DHAP (ca. 7.3 J cm^{-2}) to obtain good ion abundance while maintaining higher charge states (**Appendix B Figure S23**). However, the ion abundance near the respective threshold for ion formation is then slightly lower with 2-NPG relative to 2,5-DHAP (**Appendix B Figure S22**). The laser power dependence is in agreement with a previous study that found a higher laser power induces lower charge states using 2,5-DHAP matrix.[42]
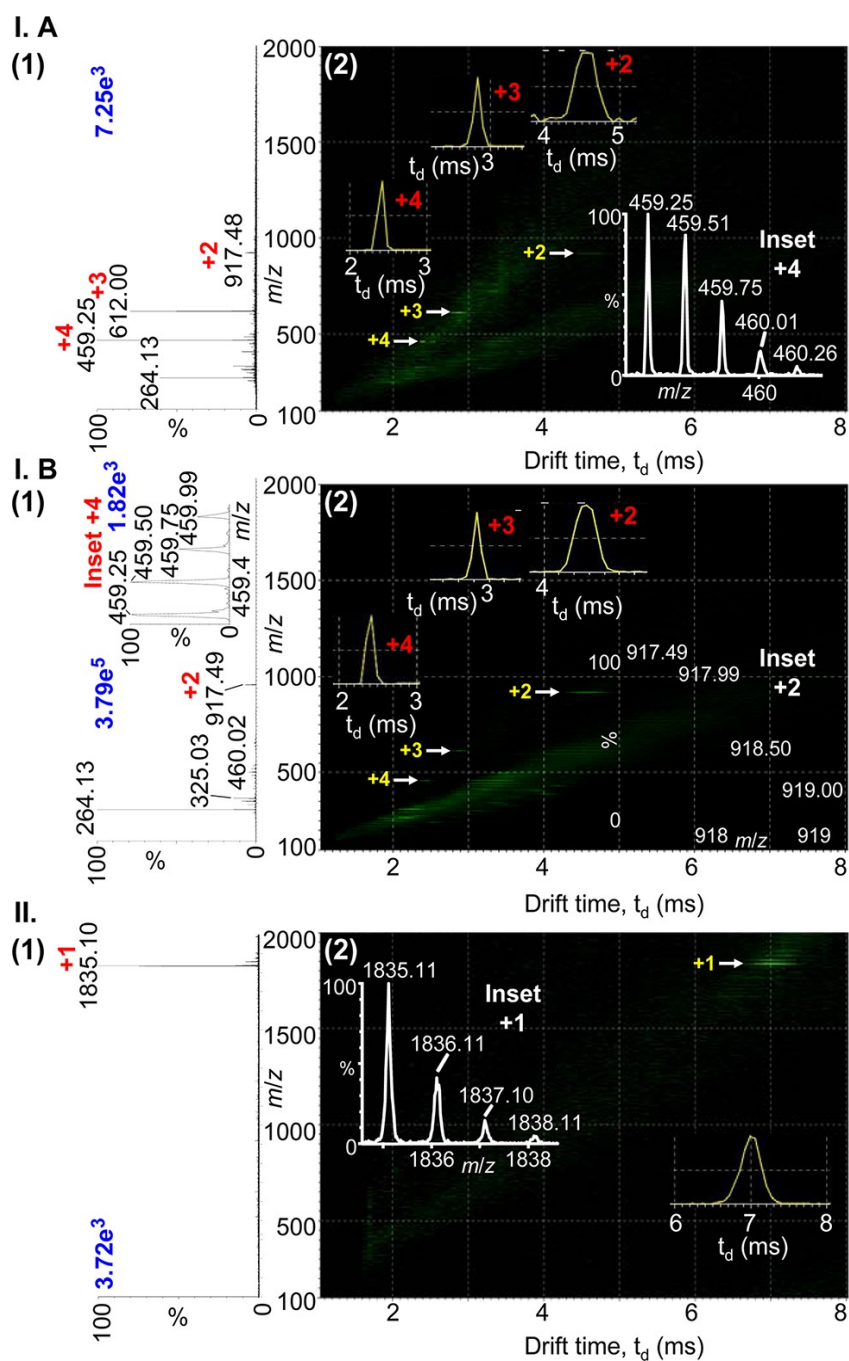
Figure 9.1. LSIV-IMS-MS (**1**) total mass spectra and (**2**) two dimensional plot of drift time vs *m/z* of *N*-acetylated MBP peptide (MW ~1833 Da) with 2-NPG matrix acquired using (I) "LSI settings" [42,45] at (**A**) low "4.2 J cm^{-2}" and (**B**) higher "7.3 J cm^{-2}" laser power with an inset of the isotopic distribution of +4 ion and (**II**) commercial "MALDI settings" [45] on a Waters SYNAPT G2 MALDI source. Insets in parts 1 and 2 show isotopic distributions and drift times of MBP ion.

Figure 9.2 shows the LSIV analysis of delipified mouse brain tissue using "LSI settings" with 2-NPG matrix applied to the tissue by different deposition methods. By directly spotting 100% 2-NPG matrix on the tissue and the use of a relatively high laser power (12.5 J cm^{-2}), abundant multiply charged ions from peptides and proteins are obtained (**Figure 9.2I.A**) and are well-separated by IMS from the singly charged lipid ions (**Figure 9.2I.B**). Ions are observed from proteins that are present in the tissue having molecular weights up to ~8.6 kDa (**Appendix B Figure S24**) on a high-performance mass spectrometer with a mass range of 8000. As noted above, spotting the tissue with 100% 2,5-DHAP matrix only detected up to ~3.2 kDa (**Appendix B Figure S20**). Unfortunately, 100% 2-NPG matrix spray-coated on a mouse brain tissue section required the application of a laser power of 12.5 J cm^{-2} to obtain sufficient ion abundance (**Figure 9.2II**) for good images. Using "LSI settings", as described above, under these higher laser fluence conditions, only +2 and +1 ions are detected (**Figure 9.2II.A**) from mouse brain tissue. However, the IMS dimension separating +2 from the +1 charge state allows extraction of the +2 peptide ions with good ion abundance (**Figure 9.2II.B**).

Just as in MALDI imaging, sample preparation is important with LSI imaging. Thus, a number of sample preparation protocols were explored. For example, mouse brain tissue sections mounted on a CHCA precoated glass slide, similar to previous protein studies,[31] and spray-coated with a binary mixture of 90% 2,5-DHAP and 10% 2-NPG allowed observation of higher molecular weight peptides and proteins ions (**Appendix B Figure S25**) but with notably less ion abundance relative to 100% 2-NPG (**Figure 9.2I**). Thus, in the absence of the heated inlet,[27−40] the volatility of the

matrix composition in vacuum defines the outcome of the tissue analysis and is especially restrictive to imaging for which direct matrix spotting cannot be employed because of delocalization of the tissue composition, as is also the case with MALDI. Clearly, further developments in sample preparation will be necessary to advance LSIV imaging just as it was for MALDI.
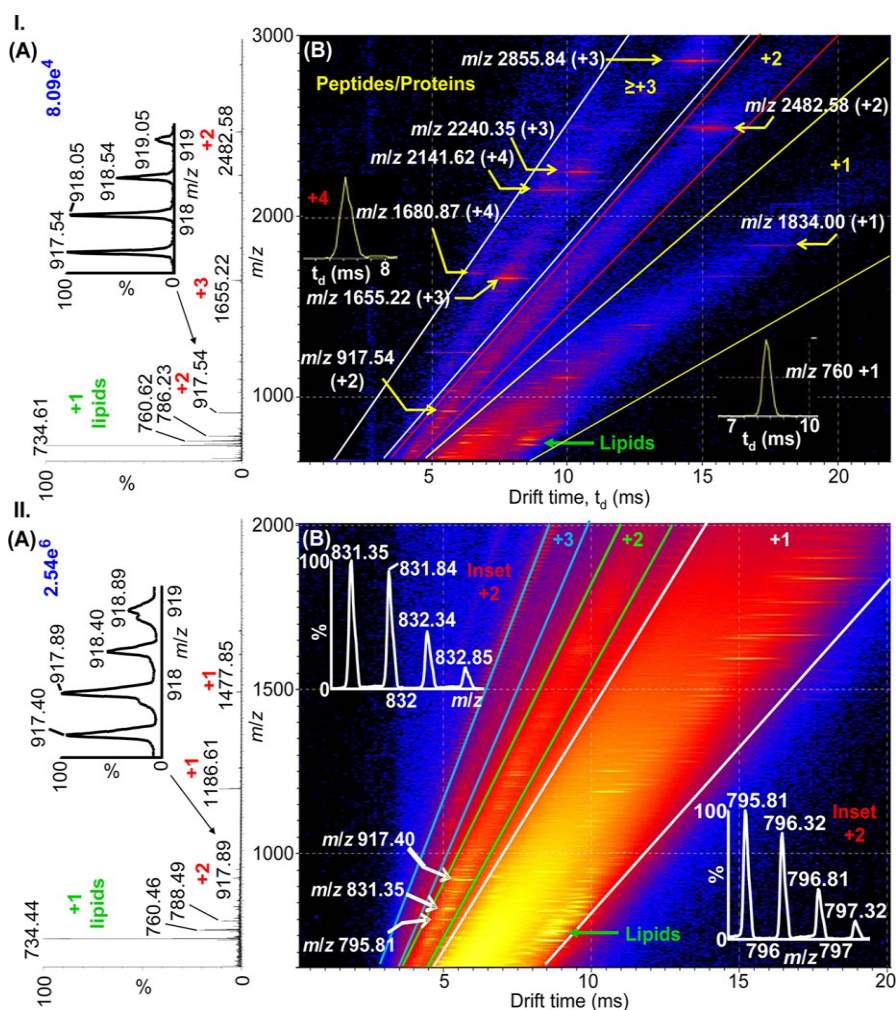

Figure 9.2. LSIV-IMS-MS (**A**) total mass spectra and (**B**) two-dimensional plot of drift time vs. *m/z* of delipified mouse brain tissue (**I**) spotted and (**II**) spray-coated with 100% 2-NPG matrix. Insets show (**A**) isotopic distributions of +2 charge state ion of the identified peptide *N*-acetylated MBP fragment, (I.B) drift times of charge state +4 and +1 ions, and (**II.B**) isotopic distribution of the +2 ions. Insets of higher charge states in part I are included in Supporting Information **Figure S24**.

The drift time and *m/z* values of an area of choice can be selected in the 2-D IMS-MS plot, which becomes possible because of the two dimensionality of the data set,[66,67] allowing investigation of any ion of interest, while disregarding others. Here, using the ion mobility embedded mass spectral data set from the 100% 2-NPG spray-coating approach in **Figure 9.2II.B**, images were created for three peptides. This ion at *m/z* 917.40 had previously been sequenced using ETD fragmentation of the doubly charged *N*-acetylated MBP peptide (1−16) ion.[48] The image (**Figure 9.3A**) relates well with the known location of the myelin basic protein (**Figure 9.3D**),[54] validating our tissue imaging MS approach of multiply charged ions at vacuum. Using similar procedures, images of two additional doubly charged peptide ions are obtained, *m/z* 831.35 and 795.81 (**Figure 9.3, parts B and C**), respectively. All three peptide images have the same location as the myelin basic protein in the mouse brain tissue (**Figure 9.3D**).[198] Using the amino acid sequence information obtained from the identified peptide MBP fragment with a MW of 1832.8 Da [48] (aa residues (1−16), **Figure 9.3A**), images of MWs 1660.7 Da (aa residues (1−14), **Figure 9.3B**), and 1589.6 Da (aa residues (1−13), **Figure 9.3C**), then correspond to MBP peptides with two and three amino acid truncations (**Figure 9.3, parts B and C**) of the C-terminal end.
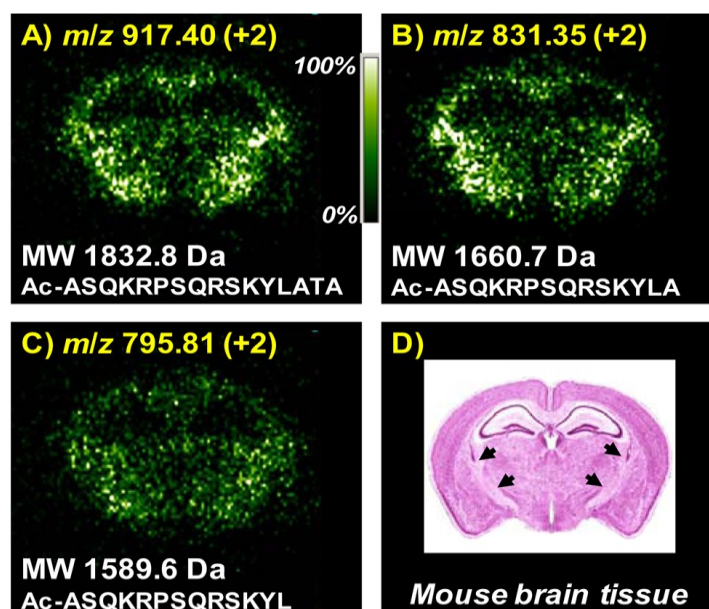
111

Figure 9.3. LSIV at intermediate pressure images of endogenous peptides from delipified mouse brain tissue spray-coated with 100% 2-NPG matrix: (**A**) *m/z* 917.40 (+2) MW 1832.8, (**B**) *m/z* 831.35 (+2) MW 1660.7, and (**C**) *m/z* 795.81 (+2) MW 1589.6. (**D**) Coronal section of the mouse brain [198] at a level similar to those analyzed in panels **A−C**. Arrowheads in panel **D** indicate heavily myelinated fiber tracts. Insets show molecular weight and amino acid sequence of the images relative to the identified peptide N-acetylated MBP fragment. The highest ion intensities are *m/z* 917 = 1.02 e^4, *m/z* 831 =1.27 e^4, and *m/z* 795 = 1.06 e^4, respectively.

CHAPTER 10

MATRIX ASSISTED IONIZATION *VACUUM*, A NEW IONIZATION METHOD FOR BIOLOGICAL MATERIALS ANALYSIS USING MASS SPECTROMETRY

"This research was originally published in Molecular and Cellular Proteomics (Inutan, E.D.; Trimpin, S. *Mol. Cell. Proteomics* **2013**; 12:792-796) © the American Society for Biochemistry and Molecular Biology."

Introduction

The conversion of large and nonvolatile compounds such as proteins into gas-phase ions is of immense fundamental and practical importance. The 2002 Nobel Prize in Chemistry was awarded for the accomplishment of this conversion via electrospray ionization (**ESI**) [1] and matrix-assisted laser desorption/ionization (**MALDI**) [2] interfaced with mass spectrometry (MS) to obtain the molecular weights of proteins with high accuracy. These methods employ high voltage or a laser to form gaseous analyte ions from a wide variety of compounds in solution or a solid matrix, respectively.

MALDI interfaced with a time-of-flight (**TOF**) mass spectrometer produces gas-phase analyte ions in vacuum and is the method of choice for the molecular imaging of biological surfaces. Ionization in vacuum provides excellent ion transmission [23], as well as good spatial resolution achieved using a focused laser beam. However, the analysis of protein complexes is very challenging with MALDI, requiring strategies such as first-shot phenomena [199] and chemical crosslinking [200]. The necessity of a laser

also makes MALDI less soft than ESI and produces background ions, which can hinder the analysis of small molecules [94,201]. MALDI is also of limited utility on high performance mass-to-charge (*m/z*) analyzers because of mass range issues related to the formation of singly charged ions, which also produce few fragment ions for structural characterization [202].

Multiple charged ions produced directly from solution in ESI bring the *m/z* ratio within the range of high performance mass spectrometers, allowing the analysis of high-mass compounds. These instruments have advanced features for structural characterization, such as ion mobility spectrometry (**IMS**) for gas-phase separations [42,45,50], ultra-high mass resolution and mass accuracy [27-29,48], and advanced fragmentation such as electron transfer dissociation (**ETD**) [29,48]. However, ESI is limited for surface characterization, requiring approaches such as desorption-ESI [139] and laser ablation ESI [203], ionization methods that produce multiply charged ions but are not compatible with analyses of larger proteins or fragile complexes.

A softer ionization approach is needed in order to observe fragile molecules and molecular complexes in living organisms at low levels directly from tissue and cell cultures, without extensive sample preparation, while retaining spatial information. Ideally, this approach would be compatible with mass spectrometers having advanced capabilities to aid structural characterization directly from surfaces. The new ionization method described here, in which molecules are transferred from solid-phase to gas-phase ions through the simple exposure of a material of interest in a suitable matrix to vacuum, is an advance toward this goal and is of fundamental interest.

Experimental Procedures

Analyte solutions were diluted with water to make concentrations ranging from 1 to 5 pmol uL^{-1}, 20 pmol uL^{-1} for BSA, and 50 fmol uL^{-1} for ubiquitin. For the noncovalent complex, stock solutions of lysozyme and penta-*N*-acetylchitopentaose were individually diluted in 25 mMol ammonium acetate buffer with 10% methanol according to published procedures [204]. The molar ratio of the protein-ligand mixture was optimized, and a premixed noncovalent complex mixture of 1:285 protein:ligand molar ratio was used. The blood sample was diluted in water at a 1:10 volume ratio. 3-NBN was dissolved in 50 uL of 100% ACN with 0.1% formic acid and 150 uL of 50:50 ACN/water with 0.1% formic acid (positive mode measurements), and 150 uL of 50:50 ACN/water was mixed with 0.1% NH$_4$OH for peptides and 1% NH$_4$OH for proteins (negative mode measurements). The matrix/analyte solution was prepared at 1:3 and 1:1 volume ratios for positive and negative mode measurements, respectively, and 1 uL was spotted on the target plate. Mouse brain tissue, obtained using a protocol described elsewhere [48,195,196], was donated by Professor Ken Mackie (Indiana University). The delipified mouse brain tissue [48] was coated with several 0.5-uL spots of 3-NBN matrix in 50:50 ACN/water with 0.1% formic acid. The matrix deposition on brain tissue sections from mouse brain tissue was miniaturized by spotting, on the same area, a total of 1 uL in five increments of 0.2 uL, covering a ~400 μm x 150 μm area on the tissue. Blood was extracted from Band-Aid using water. After solvent evaporation of the matrix/analyte spot, the target plate was introduced into the vacuum of the mass spectrometer.

Matrix Assisted Ionization Vacuum (MAIV) on a Commercial Vacuum MALDI Source – IMS-MS SYNAPT G2 (Waters Co., Milford, MA) with a commercial intermediate-pressure MALDI source conventionally operated with an Nd:YAG laser (355 nm) was employed with the laser off as described in **Chapter 2.4**. Analyte ions were observed with as little as 1 V applied between the sample plate and the extraction lens. Some voltage is necessary to accelerate ions into the hexapole ion guides and to the mass analyzer.

MAIV on Commercial Atmospheric Pressure ESI Source of Waters Co. SYNAPT G2 – The skimmer cone of the z-spray was modified as described in **Chapter 2.4** using a wider outer (~4.5 mm) and inner (~3 mm) cones.

MAIV on Commercial Atmospheric Pressure ESI Source of Thermo Scientific LTQ Velos – The transfer capillary was modified by inserting a ferrule on the outer opening of the inlet tube to hold the glass plate as described in **Chapter 2.4**.

Results and Discussion

The MAIV method described here, using 3-NBN as matrix, produces ions when placed in vacuum. Similar to ESI [204], multiple charging, even of protein complexes, is observed, but it occurs directly from the solid state. For example, the MAIV mass spectrum of the 14.3 kDa lysozyme protein using the vacuum MALDI source of the SYNAPT G2 is shown in **Figure 10.1A**, and its complex with penta-*N*-acetylchitopentaose, separated from both the lysozyme and the peptide ions via IMS, is shown in **Figure 10.1B**. A challenge in analyzing molecular complexes via any MS approach is that the sample preparation must keep the complex intact under conditions

suitable for ionization. These mass spectra are obtained simply by placing the matrix/analyte sample in vacuum. Ions are continuously formed until the matrix completely sublimes, which, depending on the applied conditions, can take a few seconds to tens of minutes (**Figure 10.1C**). No laser, voltage, or heat is used to initiate the ionization process. The "hot spot phenomenon" [205-207], an intrinsic limitation for quantitation in MALDI, is not an issue because the entire matrix/analyte sample is analyzed by simply summing mass spectra acquired during complete matrix sublimation.
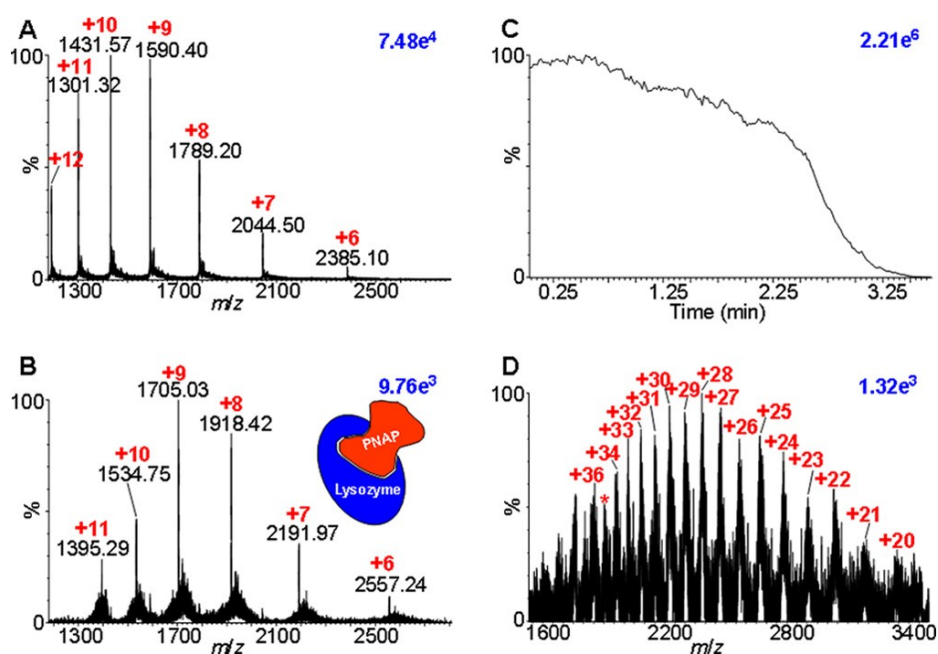
Figure 10.1. MAIV mass spectra of (**A**) lysozyme, 14.3 kDa, (**B**) noncovalent complex of lysozyme/penta-*N*-acetylchitopentaose (PNAP) extracted from the IMS-MS two-dimensional dataset, (**C**) total ion current of **A**, (**D**) bovine serum albumin, 66 kDa. Red numbers indicate the charge states, and blue numbers in the upper right corner of each spectrum provide relative ion abundances.

3-NBN has no acidic protons needed for ionization, so the protons must be supplied by the solvent, analyte, or acid during sample preparation. Typically, the matrix is dissolved in organic or water-organic solvents, with or without 0.1% formic acid, and the analyte in water/organic solvent or, for complexes, water buffered with ammonium acetate. The matrix and analyte solutions are mixed in the same way as the sample preparation used in MALDI, dried, and placed in vacuum or, for labile compounds, immediately placed in vacuum without drying. Astonishingly, MAIV produces ions from proteins at least as large as BSA (~66 kDa) (**Figure 10.1D**).

As with ESI, small molecules are detected as singly charged with little matrix-related chemical background (e.g. leucine enkaphelin; **Figure 10.2IA**), and larger peptides (e.g. acetylated N-terminal fragment peptide of myelin basic protein; **Figure 10.2IB**) as multiply charged ions. Mass spectra are obtained using the SYNAPT G2 mass spectrometer vacuum MALDI source, consuming low femtomoles of small proteins such as ubiquitin (50 fmol) (**Figure 10.2IC**). Good negative ion abundances of, for example, ubiquitin (**Figure 10.2IIA**), the hirudin (55– 65) peptide (**Figure 10.2IIB**), and the phosphorylated peptide cholecystokinin (10 –20) (**Figure 10.2IIC**) are also observed with MAIV.

Peptides and proteins are detected by applying 3-NBN in an appropriate solvent onto the surface of a mouse brain tissue section (**Figure 10.3A**) and subjecting the sample to the vacuum of the mass spectrometer (**Figure 10.3B**). Selected areas of interest of a tissue can be exposed to matrix, and even if the entire tissue section is placed in vacuum, only molecular ions from compounds in those specific areas are observed

(**Figure 10.3C**). Miniaturizing the matrix deposition area to ca. 150 μm x 400 μm using a micropipette enables enhanced spatial resolution analyses without the need for a laser, as is required with MALDI [208]. The high signal-to-noise obtained for this analysis suggests that much smaller spot sizes can be analyzed with appropriate matrix deposition methods and faster introduction of the sample into vacuum. The multiple charging in
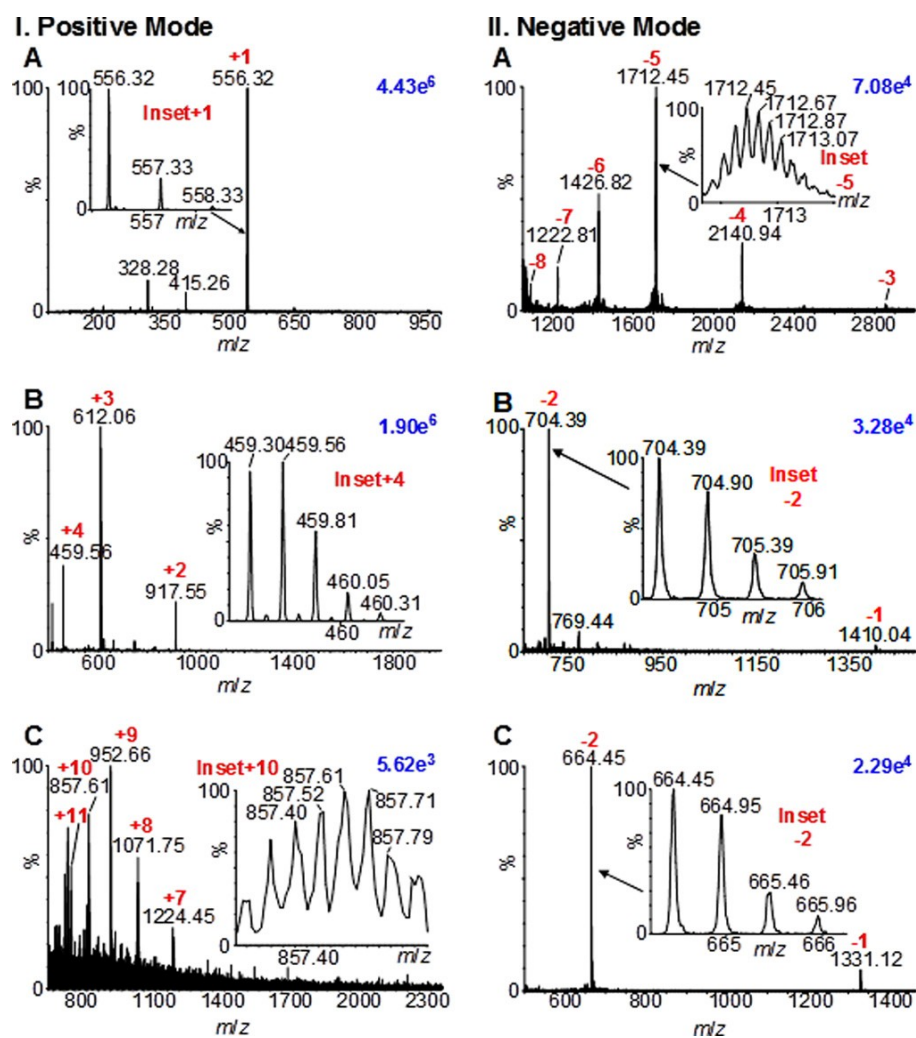

Figure 10.2. MAIV mass spectra acquired in (**I**) Positive ion mode: (**A**) 1 pmol leucine enkephalin (molecular weight (MW) 555 Da), (**B**) 1 pmol MBP peptide (MW 1833 Da), and (**C**) 50 fmol ubiquitin (MW 8559 Da) and (**II**) Negative ion mode: (**A**) ubiquitin, (**B**) phosphorylated peptide cholecystokinin (10 –20) (MW 1332 Da), and (**C**) hirudin (55–65) peptide (MW 1411 Da).

MAIV aids the separation of the compound classes (proteins, peptides, and lipids) by size, shape, number of charges, and *m/z* using IMS-MS.
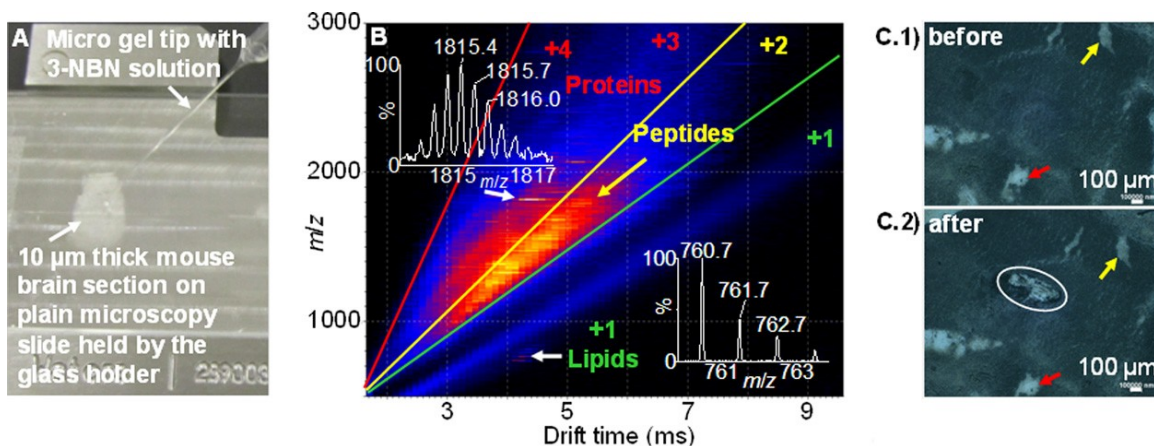

Figure 10.3. MAIV-IMS-MS of a mouse brain tissue section using a commercial vacuum MALDI source with the laser off: (**A**) photograph of application of matrix solution to a section of mouse brain on a glass microscope slide, (**B**) two-dimensional IMS-MS plot of drift time *vs. m/z* of ions showing separation of compound classes by charge, size, and shape of lipids, peptides, and proteins. Insets show isotopic distributions of lipid and protein ions, and (**C**) microscopy photograph of the mouse brain tissue before and after ionization. Circled area shows the area on the tissue analyzed in **B**, and small arrows are included to guide the eye for a better relative comparison of the photographs.

Mass spectrometers with vacuum MALDI sources are not a requirement for MAIV, as ESI sources can be reversibly modified for MAIV operation. **Figure 10.4A** shows a glass microscope slide (**Appendix C Figure S1**) onto which a microliter of blood, diluted 1 part in 10 of water, mixed with 3-NBN matrix in ACN:water, and dried, is held against the inlet of a modified ESI source of the SYNAPT G2 mass spectrometer by the atmospheric-pressure-to-vacuum differential. Unlike with ESI, which detects predominantly the α-subunit of hemoglobin [209], both the α- and β-subunits are detected in good ion abundance from the blood spot using MAIV. **Figure 10.4B** shows the IMS-MS plot of the gas-phase drift-time separated α- and β-subunit multiply charged

molecular ions. The extracted mass spectrum of the β-subunit is shown in **Figure 10.4C**.

These results correlate well with blood spot results obtained with MAIV using the

SYNAPT G2 vacuum MALDI source, indicating the universal utility of this ionization

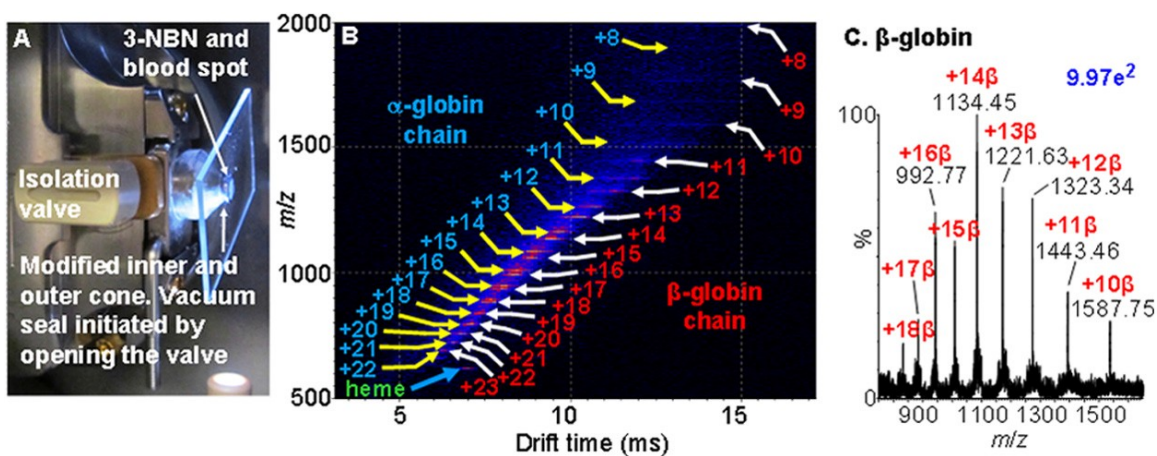method with vacuum and atmospheric pressure ion sources.

Figure 10.4. MAIV-IMS-MS of a solvent-extracted blood spot from a Band-Aid using a commercial atmospheric pressure ESI source with a modified skimmer cone to provide a larger inlet aperture. (**A**) photograph of the device showing the isolation valve in the open position with a glass microscope slide held by the pressure differential against the skimmer opening, with the matrix– blood spot sample exposed to the vacuum initiating ionization; more details on source modifications are provided in supplemental Appendix C **Figure S1.** (**B**) two-dimensional IMS-MS plot of drift time *vs. m/z* of ions showing separation of compound classes by charge, size, and shape: α-globin (MW 15,126 Da) and β-globin (MW 15,866 Da) chains of hemoglobin. Both and chains of hemoglobin are detected with MAIV in good ion abundance (mass spectral details in supplemental **Appendix C Figure S2**), something that has been reported [209] to be problematic with ESI (**1**). Extraction of the mass spectral information from the two-dimensional display in B provides the individual mass spectra of the proteins, and (**C**) extracted full range mass spectrum of the β-globin chain.

Using MAIV, sufficient ion abundance is obtained with the modified ESI source

to perform sequence characterization. ETD fragmentation of the quadruply charged

molecular ions of the acetylated *N*-terminal peptide fragment of myelin basic protein

provides complete sequence coverage (**Figure 10.5**) using the modified ESI source,

identical to the principle shown in **Figure 10.4A**, of a linear ion trap LTQ Velos. An expansion of the region between *m/z* 450 and 900 is shown in the inset, graphically demonstrating the degree of fragmentation obtained with this method. ETD is more applicable to the fragmentation of peptides and proteins than collision-induced dissociation, but only with ionization methods that produce abundant multiply charged ions [13, 14].

The similarity of the charge states of ions produced via MAIV and ESI suggests similar mechanisms for their formation. A requirement for producing bare ions in ESI is solvent evaporation from highly charged droplets, and MAIV may require matrix sublimation from highly charged particles. A special property of 3-NBN, beside its ability to sublime at ambient temperature when placed in vacuum [68], is triboluminescence [69,70] producing unusually strong dinitrogen discharge emission under conditions in which crystal fracturing occurs. This discharge is believed to result from a high electric field created between fractured crystal surfaces having opposite charge [26]. In vacuum, the fracturing would be driven by sublimation of the matrix or residual solvent, producing charged particles that, upon sublimation of matrix, release analyte ions. 3-NBN matrix particles are observed leaving the surface in vacuum. Other matrices have been found to produce ions via MAIV, but none as well as 3-NBN.

This contribution represents the first example of a new ionization phenomenon demonstrating that small and large molecules are transferred as ions from the solid phase to the gas phase under vacuum conditions, without the application of external energy or
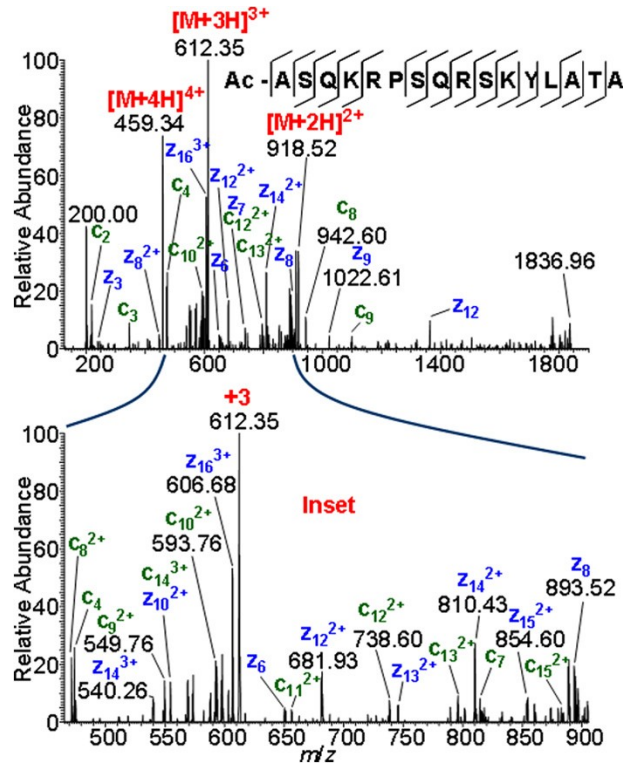
Figure 10.5. MAIV using the LTQ Velos ESI source to perform ETD fragmentation of the MBP peptide +4 charge state ion (*m/z* 459). Top, total fragment spectrum; bottom, inset *m/z* 400–900. Sequence coverage is increased relative to previous ETD studies of this peptide [48]. Red numbers indicate the charge state, and blue numbers the ion abundance. Sequence coverage is provided (top).

fields, apparently via a sublimation-driven process. Multiply charged ions are produced from the solid state with high sensitivity, giving MAIV advantages of both ESI and MALDI. Analyses of surfaces of biological tissue, thin layer chromatography plates, and one- and two-dimensional gels are logical applications. MAIV, requiring only the vacuum necessary for the proper functioning of the mass spectrometer, might be applicable with common electron/chemical ionization mass spectrometers, with the filament used for ionization turned off. The simplicity and wide applicability of MAIV also might prove useful in clinical settings and in field portable instruments.

CHAPTER 11

MATRIX ASSISTED IONIZATION IN VACUUM, A SENSITIVE AND WIDELY APPLICABLE IONIZATION METHOD FOR MASS SPECTROMETRY "Springer and the original publisher (*J. Am. Soc. Mass Spectrom.*, 24, 2013, 722-732, Trimpin, S., Inutan, E.D.) is given to the publication in which the material was originally published with kind permission from Springer Science and Business Media."

Introduction

Vacuum ionization coupled to mass spectrometry (**MS**) is highly sensitive and has enormous potential [23], but relative to ambient ionization methods, progress in this area has been relatively slow since the introduction of matrix-assisted laser desorption/ionization (**MALDI**) [2,3]. Important developments include intermediate pressure vacuum MALDI [75,136], solvent-free MALDI [30,72], surface enhanced LDI [210], the application of MALDI in imaging [111,146], soft laser desorption [211-213], and cluster beam methods [214-217], all of which produce singly or low charge state ions. However, the ability to produce high charge state ions under vacuum conditions would expand analytical capabilities to high performance mass spectrometers that have limited mass ranges, would enable advanced fragmentation technology for improved characterization, and would have the potential to maximize signal-to-noise in complex samples [23,202]. Vacuum ionization approaches are promising in terms of applications because ion transmission losses inherent with atmospheric pressure ion sources are eliminated [24], thus, potentially enhancing sensitivity [23].

Highly charged quasi-molecular ions have been observed under sub-ambient pressure using electrospray ionization (**ESI**) [218], and in low abundance, using an explosive matrix with plasma desorption MS [219,220]. Inlet ionization was described, in which multiply charged ions were produced under sub-ambient conditions inside a heated inlet tube connecting the atmospheric pressure ionization region and the first vacuum region of a mass spectrometer. Mass spectra nearly identical to those produced in ESI were obtained by laser ablation of matrices common to MALDI [28,29], or by using physical forces to dislodge the matrix/analyte into the inlet from a surface [39,194]. Introduction of solubilized analyte into the heated inlet also produced multiply charged ions [221,222]. Concepts learned from these inlet ionization methods enabled discovery of methods for producing highly charged ions of peptides, proteins, and polymers at intermediate [42] and low pressure [44] using laser ablation of certain matrix compounds.

Here, we report the rather astonishing discovery [46] of matrix compounds that produce positive or negative analyte ions simply by placing the matrix/analyte sample directly in vacuum in the absence of a laser, high voltage, or even added heat. We have termed this method matrix assisted ionization *vacuum* (**MAIV**). MAIV has been shown to operate in the positive and negative ion modes and to produce ions from a variety of compound classes including drugs, lipids, peptides, and proteins with high sensitivity. Besides the analytical utility of MAIV, this work demonstrates that a laser is not a requirement for ion formation in vacuum, just as it was not required for inlet ionization using matrices common with MALDI [40,45].

Experimental Procedure

Analyte solutions were diluted with water, with the following exceptions: lysozyme was diluted using 25 mM ammonium acetate in 10 % MeOH, 50:50 ACN/water with 0.1 % TFA was used with β-amyloid (1-42) for positive mode measurements and 50:50 MeOH/water was used for negative mode measurements. Final concentrations of all analyte solutions ranged from 1 to 10 pmol μL^{-1}. PEG-DME 2000 was doped with LiCl (10 % by volume from a 1 M LiCl solution). The small molecule model mixture composed of 5 pmol μL^{-1} each of clozapine, Leu-enkephalin, sphingomyelin, angiotensin II, ACTH, and bovine insulin was prepared in water. The large molecule model mixture in addition contained Leu-enkephalin, sphingomyelin, galanin, bovine insulin, and ubiquitin. The higher mass protein mixture contained 5 pmol μL^{-1} each of lysozyme (added from 25 mM ammonium acetate in 10 % MeOH) and ubiquitin, and 10 pmol μL^{-1} of myoglobin.

For testing the different compounds for use as MAIV matrix, solutions were prepared by dissolving 5 mg of the matrix compound in 100 μL of 50:50 ACN/water. The 3-nitrobenzonitrile (**3-NBN**) matrix was also dissolved in 150 μL of 50:50 ACN/water with 0.1 % formic acid and 50 μL 100 % ACN with 0.1 % formic acid. For positive mode measurements, the matrix/analyte mixture was prepared (1:3 v:v) using 3-NBN in 100 % ACN with 0.1 % formic acid; for negative mode, the ratio was 1:1 v:v using 3-NBN in 50:50 ACN/water with 1 % ammonium hydroxide. Coumarin was also prepared by dissolving 5 mg in 50 μL of 50:50 ACN/water with 0.1 % formic acid and 2,5-DHAP in 150 μL of 50:50 ACN/water with 0.1 % formic acid (warmed).

From a given matrix/analyte mixture, 1 μL was typically spotted on the target plate using the dried droplet method. For matrix assisted ionization *inlet* (**MAII**) and MAIV using a custom modified ESI source, 1 μL of the analyte was spotted on a glass plate and 2 μL of 3-NBN matrix was added and air-dried, as previously described [40]. A similar procedure was used with 2,5-DHAP and coumarin. For the glass capillary experiments, the capillaries were partially filled with acidified 3-NBN matrix containing an equal volume of analyte solution. The sample was allowed to dry before taping the capillary to a modified MALDI sample plate.

A number of surfaces were analyzed by taping different materials (e.g., currency, filter paper, KimWipe (Kimberly-Clark Professional, Roswell, GA USA) tissue, plastic, aluminum foil, and thin layer chromatography (TLC) plates) onto a MALDI modified plate; each surface was spotted with 1 μL of matrix/analyte. Solvent-free sample preparation was employed as previously described using angiotensin I [223]. In brief, metal beads (1.3 mm, BioSpec Products, Inc., Bartlesville, OK, USA) and matrix powder were combined in a vial in which analyte had been added in solution and completely dried. Homogenization/transfer of the matrix/analyte to the glass plate was accomplished using a TissueLyser II (Qiagen Inc., Valencia, CA, USA) with a 30 Hz frequency and a duration of 10 minutes. Binary matrices were prepared according to published procedures [40,44] using 3-NBN and α-cyanohydroxycinnamic acid (**CHCA**). Partially dry and wet samples were introduced to the vacuum of the mass spectrometer in a glass capillary and on a metal plate. Some 3-NBN/analyte samples were frozen in the wet state on the MALDI plate at -80 °C and immediately placed in vacuum for analysis.

Matrix Assisted Ionization Vacuum (MAIV) - MAIV-MS was performed on IMS-MS SYNAPT G2 mass spectrometer (Waters Co.) operated in the positive, negative and sensitivity (V) modes. For MAIV using the commercial vacuum MALDI source, the source was operated without firing the laser (**Scheme 1.1.IIB and 2.3**) as described in details in **Chapter 2.4**. The dried and in some cases slightly wet matrix/analyte mixtures were individually loaded into the source vacuum (0.226 mbar) requiring ∼2 min to load. Glass tubes and other surfaces, such as a currency bill, were introduced to the vacuum source using the commercial MALDI plate holder and moving stage. Ionization from the cold (from -80 °C) and glass tube experiments lasted for 10 and 30 min, respectively. For MAIV using the commercial ESI source, the skimmer cone of the z-spray was first modified by inserting a small ferrule to the normal outer cone of the skimmer. The glass plate with the matrix/analyte spot was placed tight to the ferrule facing the source entrance. The matrix/analyte crystals were drawn by the pressure differential between the atmospheric pressure and the instrument vacuum. Ions were observed once the matrix/analyte crystals were drawn by the vacuum of the mass spectrometer. The ESI source block temperature was set to 80 °C and was operated with default ESI settings. In the second version as described in **Chapter 2.4**, the inner cone opening was widened to about ~3 mm and the outer cone was widened to about ~4.5 mm with a ferrule inserted forming vacuum seal between the glass plate and the inner cone; in this case, the vacuum was protected by keeping the isolation valve closed until the sample was loaded (**Scheme 2.4**). For sensitivity comparison between MAIV and ESI, 5 fmol clozapine in 50:50

MeOH/water was used depositing 1 μL in 3-NBN for MAIV and for ESI using an infusion flow rate of 1 μL min^{-1} for 1 min.

Matrix Assisted Ionization Inlet (MAII) - MAII-MS was performed on a LTQ Velos mass spectrometer (Thermo Fisher Scientific, Bremen, Germany) with commercially available inlet temperature control using inlet temperatures of 50 to 450 °C as previously reported (**Scheme 1.1.IB**).[40]

Results and Discussion

Introduction of analyte, incorporated in the matrix 3-NBN into the vacuum of the mass spectrometer produces ions from small molecules as well as proteins without the need of a laser voltage, other than that necessary for ion transmission, or heating the sample. A typical example using the SYNAPT G2 vacuum MALDI source is shown in **Figure 11.1a** where multiply and singly charged ions, similar to ESI, are observed with good resolution and abundance from a mixture containing the lipid sphingomyelin, peptides Leu-enkaphelin, and galanin, and small proteins insulin and ubiquitin. This example demonstrates the breadth of the MAIV method to ionize differing compound classes over a wide mass range. Ions were produced until the matrix was no longer observed on the commercial sample plate. The MAIV mass spectrum of lysozyme is shown in **Figure 11.1b**, but using a binary matrix mixture containing only 20% 3-NBN in CHCA matrix solution, corresponding to a molar ratio of 1.6:1 molar ratio of 3-NBN:CHCA. By incorporating a less volatile matrix with the more volatile 3-NBN, the time over which ions are observed was increased. Snapshots of the plate taken about 2 and 3 min after introduction to vacuum shows loss of matrix from the surface with

increasing time (**Appendix C Figure S4**). A video of the ionization process is provided online as **Supplemental ('MAIV on MALDI source video I')**.
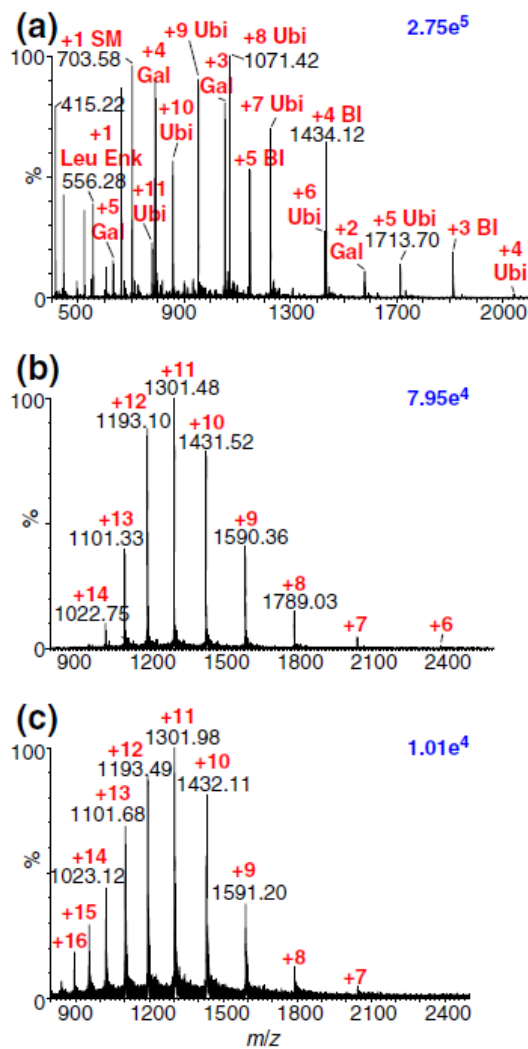
Figure 11.1. MAIV mass spectra using the vacuum MALDI source of: (**a**) a mixture of sphingomyelin (molecular weight, MW 703 Da), leu-enkephalin (MW 555 Da), galanin (MW 3156 Da), bovine insulin (MW 5731 Da), and ubiquitin (MW 8561 Da), (**b**) lysozyme (MW 14.3 kDa) using binary matrix mixture of 3-NBN and CHCA in 1.6:1 molar ratio using the SYNAPT G2 intermediate pressure MALDI source, and (**c**) is the same sample obtained on the SYNAPT G2 modified ESI source. Isotopic distributions are shown in **Appendix C Figure S3**. Blue numbers in upper right corner of each spectrum provide relative ion abundance and red numbers the charge states.

The MAIV matrix, 3-NBN, was discovered while testing compounds having characteristics similar to 2-nitrophloroglucinol (**2-NPG**), the best matrix found to produce multiply charged analyte ions using MAII [40,194], and one that requires a relatively low inlet temperature for ion production [45]. Importantly, 2-NPG was also shown to produce multiply charged ions using laser ablation under vacuum conditions [44,45]. Of the compounds tested (**Table S1.I, Scheme 1.1.IB**), 3-NBN was found to produce highly charged ions of acidified insulin by MAII at an inlet temperature of 50 °C and with maximum abundance at ca. 100 °C (**Appendix C Figure S5**). This is contrary to other matrix compounds (>100) useful for inlet ionization for which good ion abundance is only obtained at much higher inlet temperature [40] using the same mass spectrometer. Thus, the thermal requirement for 3-NBN matrix to produce abundant analyte ions from atmospheric pressure is low.

This matrix was therefore deemed to be a potential matrix for producing highly charged ions on atmospheric pressure ionization mass spectrometers lacking a heated inlet as well as with vacuum MALDI ion sources which are postulated to need matrix volatility to produce multiply charged ions through desolvation of charged matrix droplets/clusters that are produced by laser ablation [45]. 3-NBN was therefore employed with a homebuilt modification to the SYNAPT G2 skimmer cone inlet, which allowed rapid testing of matrices using laser ablation of the sample under vacuum conditions. In this approach, a connecting ferrule was constructed at the inlet skimmer cone of the ESI source (**Scheme 2.4**), which made a sufficient vacuum seal to hold a glass microscope slide. Matrix/analyte was placed on the vacuum side of the glass slide with the intention

of ablating the sample using a focused beam from a nitrogen laser fired in transmission geometry.

Surprisingly, a mass spectrum of insulin was obtained without the laser. A larger inner and outer cone opening was subsequently shown to provide improved vacuum when sealed using the glass slide, as judged by the force with which the slide is held to the modified mass spectrometer entrance (**Appendix C Figure S6**). The larger opening also achieves substantially improved ion abundance (**Figure 11.1c**) and more rapidly (a few seconds, **Appendix C Figure S6**) than the smaller opening. A video of the process is provided online in the Supplemental ('MAIV on ESI source video II'). Introducing the same matrix/analyte sample composition into the intermediate pressure vacuum MALDI source of the SYNAPT G2 produced very similar mass spectra to those observed with the sealed atmospheric pressure inlet but requires longer introduction time and sublimation/evaporation of the matrix/analyte sample is slower. This, to our knowledge, is the first example of matrix assisted ionization requiring only vacuum conditions, which are available with any mass spectrometer.

A number of compounds similar to 3-NBN were also examined for their potential as MAIV matrices to ionize insulin and ubiquitin. Using the same acquisition settings and insertion of the matrix/analyte into a vacuum MALDI source without the use of a laser, 3-NBN performed exceptionally well, 2-NBN showed reasonable analyte ion abundance, and 4-NBN produced no ions (**Appendix C Figure S7**). A visually apparent difference is that 3-NBN sublimes quickly in the SYNAPT G2 MALDI source and is completely removed from the sample plate after roughly 5 min followed by 2-NBN, and then 4-

NBN, which could still be observed on the plate with no visual differences after 1 h. Even with laser ablation, 4-NBN does not produce the desired analyte ions. Of the isomers of NBN and nitrobenzaldehyde, 3-NBN and 4-nitrobenzaldehyde are reported to sublime under vacuum conditions [68]. Of the nitrobenzaldehyde isomers (**Appendix C Figure S8**), only 1,3-nitrobenzaldehyde produces ions of angiotensin I under the conditions employed, but with low ion abundance. The best results with this matrix were obtained when the matrix:analyte was prepared solvent-free. Morphology changes during the prolonged grinding of matrix/analyte in the solvent-free preparation [223] may be related to matrix melting aiding incorporation of analyte.

With 3-NBN matrix containing insulin on the MALDI sample plate, multiply charged quasi-molecular analyte ions are detected with the mass spectrometer while simultaneously observing the matrix through the optical microscope camera display available with the SYNAPT G2 MALDI source. The footprint of the matrix decreases with time due to sublimation and the detected ion abundance similarly decreases. No ions are observed once there is no visible matrix. The ability of the matrix to sublime or evaporate is apparently critical for producing ions of nonvolatile analyte molecules, but can also be a hindrance because the matrix must not sublime/evaporate too rapidly or it will not survive the ca. 2 min introduction period from atmospheric pressure to vacuum of the commercial MALDI source. There are a number of ways to partially circumvent the rapid sublimation besides use of binary matrix mixtures (**Figure 11.1b**), including cooling the sample plate to -80 °C before insertion to vacuum (main ion abundance postponed to ~2.5 min, **Appendix C Figure S9b**), and placing the sample in capillaries

which restricts the rate of sublimation by reducing the matrix surface exposed to vacuum (ion abundance extended to ~30 min, **Appendix C Figure S10**). A problem with current vacuum MALDI sources is that, because of sublimation, only one sample can be placed into vacuum at a time. However, a modified atmospheric pressure ionization source (**Scheme 2.4**) allows rapid analysis of samples by MAIV (**Figure 11.1c**).

Mechanistic Considerations

Under vacuum conditions, the matrix, as noted above, appears to sublime from the surface until it is no longer observed. However, placing a glass plate near 3-NBN under low pressure conditions does not result in a thin even layer of matrix collecting on the surface as would be expected for sublimation, but in numerous small particles, which can be observed using an optical microscope at 50× magnification. One possibility for the observed ejection of particles is the cooling of the surface in vacuum due to the latent heat of sublimation causing surface splintering, and may be similar to charged ice particles observed to be ejected from freezing water droplets [224]. Alternatively, sublimation/evaporation of the matrix, or trapped solvent, under vacuum conditions may contribute to ejection of matrix particles from the surface.

Charged solvent droplets in ESI and solvent assisted ionization inlet (**SAII**) [221,222] and charged matrix droplets/particles in MAII are proposed to be responsible for producing similar charge state distributions to those observed with MAIV. Producing charged droplets or particles is common in nature. For water droplets and ice crystals, it has been shown that a cold subliming/evaporating surface has an excess of positive charge and a warm condensing surface an excess negative charge [224]. The dislodging

of the surface of ice crystals [225] carrying excess surface charge is believed to be the source of electrification of thunderclouds [224]. Thus, the observed 3-NBN particles, by a similar mechanism may be ejected having an excess of the surface charge. Such a charging mechanism occurring from the surface rather than individual particle is problematic for explaining continuous ionization and observation of both positive and negative ions.

Another characteristic of 3-NBN that could lead to charging of the ejected particles is dinitrogen discharge emission (triboluminescence) during crystal fracturing [69,70]. Triboluminescence [226,227] is known to occur when 3-NBN undergoes a fracturing process [69,70]. The emitted light, referred to as lightening, is caused by electric charge of opposite sign being produced on opposing surfaces of a crack in the crystal. The electric field caused by these charges is sufficiently high to initiate a discharge at atmospheric pressure, and thus it seems reasonable that the process of splintering matrix particles from the 3-NBN surface could create charges. The particles ejected from the matrix surface could also splinter, creating smaller charged particles. In the case of 3-NBN, once the charged particles are formed, matrix sublimation, similar to solvent evaporation in ESI, would also be required to release the bare analyte ions. Sublimation/evaporation of the charged solid particles could release analyte ions by the charge residue mechanism [51], or possibly a modified ion evaporation mechanism [52]. However, without addition of thermal energy, it seems unlikely that the matrix could convert to molten droplets [31] or molten clusters [197] as previously observed for LSII

and modeled for vacuum MALDI [36,37]. Thus, multiply charged ions must be produced directly from the solid state.

Sublimation/evaporation of the charged particles appears to be rapid based on similar ion abundances with and without the use of the IMS TriWave Technology of the SYNAPT G2 mass spectrometer (**Appendix C Figure S11**). Thus, with 3-NBN, the bare ions are already formed before they reach the TriWave device. This was not the case for laser ablation of 2,5-DHAP matrix, where desolvation appears to occur as late as the IMS region [42].

According to the above scenario, a successful MAIV matrix requires both a fracturing mechanism that produces charged particles and either sublimation or evaporation to release bare ions. Conditions of pressure and temperature will affect both charge generation and ion release. Therefore, the number of successful MAIV matrices may be restricted in the absence of heat and proper vacuum conditions. A means of supplying thermal energy under vacuum conditions may increase analyte ion abundance and expand the compounds that act as MAIV matrices. This hypothesis is based on the fact that heating the mass spectrometer inlet tube in MAII to 450 °C produced multiply charged ions for peptides and proteins with well over 100 small molecules tested as matrices [40].

A number of compounds tested show sublimation (**Table S1.I**) but no analyte ions are formed using MAIV conditions. Several compounds that triboluminescence were also examined, but did not sublime visually from the surface of the sample holder and produce no ions by MAIV (**Table S1.II**). However, like 3-NBN, coumarin is a

triboluminescence compound [228] that sublimes [229] in vacuum and produces multiply charged analyte ions in the SYNAPT G2 MALDI source and ESI source (**Appendix C Figure S12**) similar to 3-NBN. On the other hand, 2,5-dihydroxyacetophenone (2,5-DHAP) matrix does not produce ions in the intermediate pressure vacuum MALDI source without laser ablation and requires added heat to produce analyte ions using the modified ESI source (**Appendix C Figure S13**). Based on these results, we hypothesize that MAIV is a sublimation/evaporation-driven triboluminescence process leading to analyte ionization.

Fundamentally interesting is that larger proteins are efficiently ionized with MAIV, with and without acidifying the matrix or analyte solutions, and, because of multiple charging, can be analyzed on a mass range limited mass spectrometer having a commercial MALDI source. Higher charge state ions are obtained when the matrix:analyte sample is introduced to the vacuum source with some solvent still present. Myoglobin (**Figure 11.2a**) is found to produce up to +22 charges and carbonic anhydrase (**Figure 11.2b**) up to +31 charges. Observation of multiply charged ions of proteins using matrix assisted laser ablation in a vacuum MALDI source (**Scheme 1.1.IIA)** was limited at high mass to ionization of ubiquitin using 2,5-DHAP as matrix [42]. However, the MAIV results for carbonic anhydrase are similar to those obtained with MAII [194] or LSII [138] (**Scheme 1.1.I**). This seems to indicate a similar ionization mechanism, but in MAII and LSII ionization occurs in a heated inlet to the mass spectrometer, whereas in MAIV ions are produced under cold vacuum sublimation conditions. ESI and SAII also

produce similar mass spectra of proteins [221] demonstrating that ion formation from charged droplets and charged particles produce similar results.
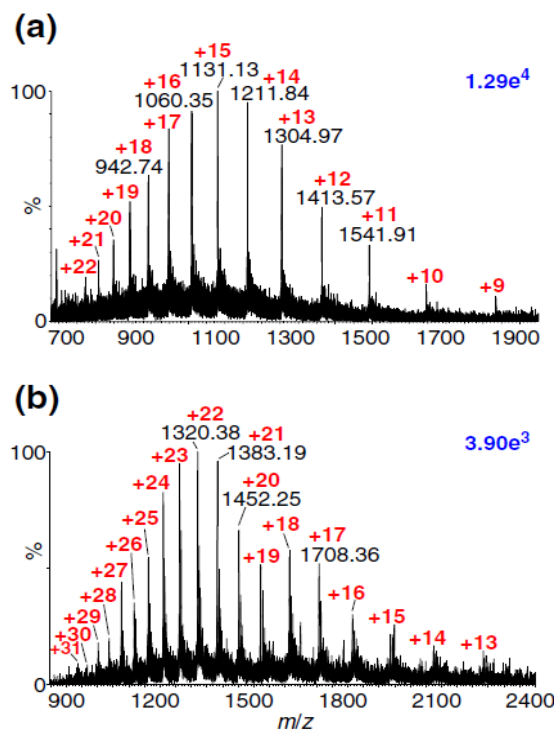
Figure 11.2. MAIV-IMS-MS of (**a**) myoglobin (MW ~17 kDa) and (**b**) carbonic anhydrase (MW ~29 kDa) with 3-NBN matrix using the intermediate pressure vacuum SYNAPT G2 MALDI source. Blue numbers in upper right corner of each spectrum provide an indication of ion abundance and red numbers the charge states.

Applications

The sensitivity of MAIV is demonstrated by a comparison using ESI and MAIV of 5 fmol consumed of clozapine, a schizophrenia drug (**Figure 11.3**). The isotopic distribution is readily discerned for MAIV but not ESI because of the chemical background observed with ESI. Cooling the plate slows matrix loss during the ca. 2 min sample plate introduction period allowing observation of sub-fmol of clozapine using MAIV on the vacuum MALDI source (**Appendix C Figure S14**).
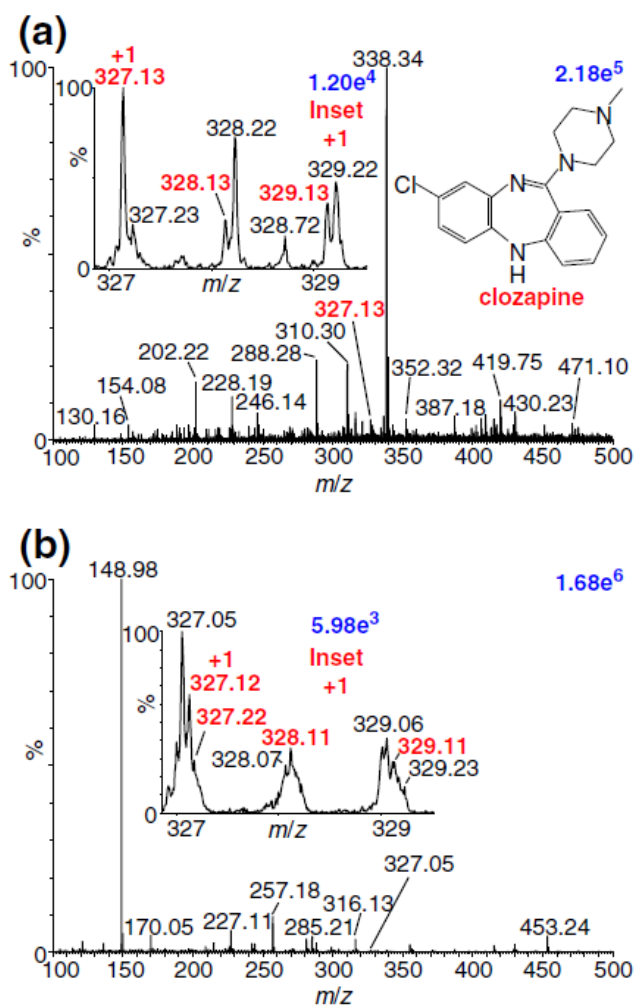
Figure 11.3. Mass spectra of 5 fmol clozapine (MW 326 Da) using: (**a**) MAIV on an intermediate pressure vacuum MALDI source with 3-NBN matrix and (**b**) an ESI source in 50:50 MeOH:water. Insets show isotopic distribution of clozapine and its chemical structure. Numbers in red are clozapine ions reflecting the expected chlorine isotopic distribution. Blue numbers in upper right corner of each spectrum provide an indication of ion abundance and red numbers indicate the isotopic distribution.

MAIV is also broadly applicable to a wide range of compounds. Because of multiply charging, MAIV works well with advanced methods such as IMS. The two-dimensional dataset of drift time *vs.* mass-to-charge (*m/z*) separations for the MAIV-IMS-MS measurement of a mixture of compounds is shown in **Figure 11.4Ia**.
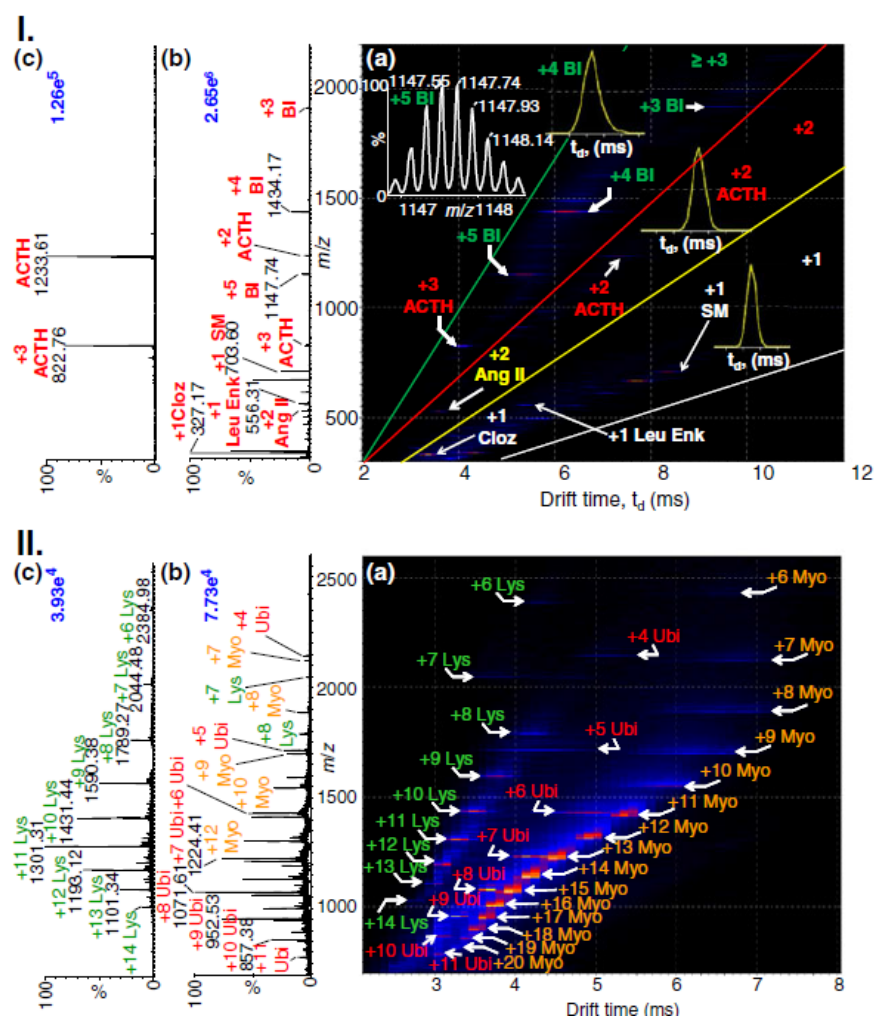
Figure 11.4. MAIV-IMS-MS of a mixture of (**I**) clozapine (MW 326 Da), sphingomyelin (MW 702 Da), leu-enkephalin (MW 555 Da), angiotensin II (MW 1040 DA), ACTH (MW 2465 Da), and bovine insulin (MW 5731 Da), and (**II**) ubiquitin (MW 8561 Da), lysozyme (MW ~14.3 kDa), and myoglobin (MW ~17 kDa) in 3-NBN matrix using the SYNAPT G2 intermediate pressure vacuum MALDI source: (**a**) two-dimensional plot (2-D) of drift time *vs. m/z*, (**b**) total mass spectrum, and (**c**) extracted mass spectrum from the 2-D plot of the least abundant component from (**b**). Other extracted mass spectra are displayed in **Appendix C Figure S15**. Blue numbers of each spectrum provide an indication of ion abundance; other colors indicate the charge states.

The charge states +1 (clozapine MW 326, sphingomyelin MW 702, Leu-enkephalin MW 555), +2 (ACTH MW 2465, angiotensin II MW 1040), and +3 (ACTH, insulin MW 5731) are well separated from each other and from the higher charge states (+4 and +5)

from bovine insulin. The mass spectrum of this mixture (**Figure 11.4Ib**) show exceptional quality both in terms of ion intensity across the mass range for all mixture components and low chemical background. Making use of the two-dimensionality of the dataset allows clean mass spectra to be extracted for any of the component of the mixture (e.g., ACTH, **Figure 11.4Ic**). IMS-MS can also be used to separate proteins that are beyond the *m/z* range of the instrument. **Figure 11.4II** demonstrates this capability with a mixture containing the proteins ubiquitin (~8.5 kDa), lysozyme (~14.3 kDa), and myoglobin (~17 kDa). The cleanly extracted mass spectrum for the least abundant component, lysozyme, is shown in **Figure 11.4IIc**.

A variety of other compounds have been analyzed using the MAIV method on the commercial vacuum MALDI source of the SYNAPT G2 without the use of the laser. For example, the low solubility β-amyloid (1-42) peptide produces abundant multiply charged ions using MAIV in the positive (most abundant charge state +4, **Figure 11.5a**) and negative (most abundant charge state -3) modes (**Figure 11.5b**). Arachidonic acid produces abundant negative singly charged ions (**Figure 11.5c**). PEG-DME 2000 doped with LiCl produces multiply cationized molecular ions (**Figure 11.5d**). Similar to ESI, small molecules such as the illicit drug cocaine (**Appendix C Figure S16a**), the pesticide foramsulfuran (**Appendix C Figure S16b**), and the D-mannopyranose derivative (**Appendix C Figure S16c**), produce singly charged ions with MAIV from the solid state in vacuum and with relative little chemical background ions. The background ions observed in MALDI-MS at every mass has been shown to be related to charged matrix clusters [94]. The low background in MAIV-MS may be related to the absence of laser

ablation. Ions related to the matrix and, possibly, matrix and solution impurities are observed in MAIV, but only at a relatively few masses (e.g, m/z 328 and 415).
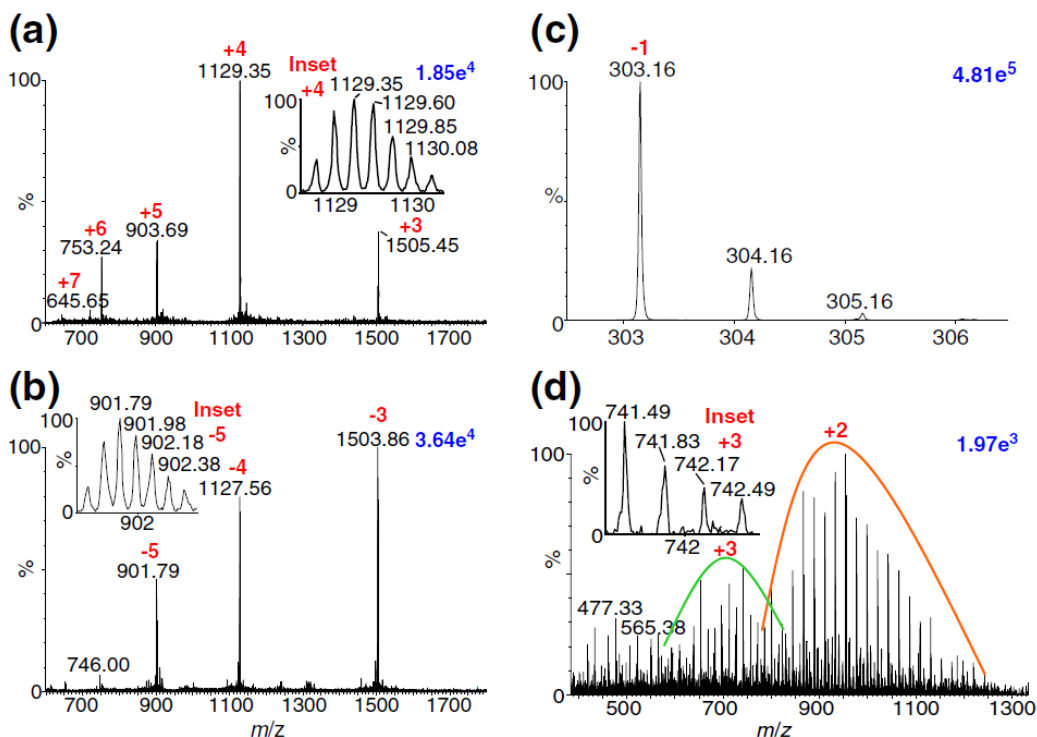
Figure 11.5. MAIV-IMS-MS of beta-amyloid (1-42) (MW 4511 Da) (**a**) positive and (**b**) negative mode measurements, (**c**) arachidonic acid (MW 304 Da) in negative mode, and (**d**) PEG DME 2000 doped with 10 % 1 M LiCl in positive mode using the intermediate pressure vacuum SYNAPT G2 MALDI source. Insets show isotopic distributions. Red numbers indicate the charge states of the negatively and positively charged analyte ions.

Other applications show MAIV to be useful for the analysis of molecules from native surfaces such as mouse brain tissue [46]. Synthetic surfaces can also be sampled in this manner (e.g., TLC plate, tissue, and filter paper, **Appendix C Figure S17**). Characterization of cocaine from paper currency using MS (**Figure 11.6a**), IMS (**Figure 11.6b**), and MS/MS (**Figure 11.6c**) was achieved by application of 2 μL of matrix solution on the eye of President Jackson and introducing the $20 bill folded and

attached to the sample plate into the intermediate pressure vacuum MALDI source of a

SYNAPT G2 mass spectrometer.
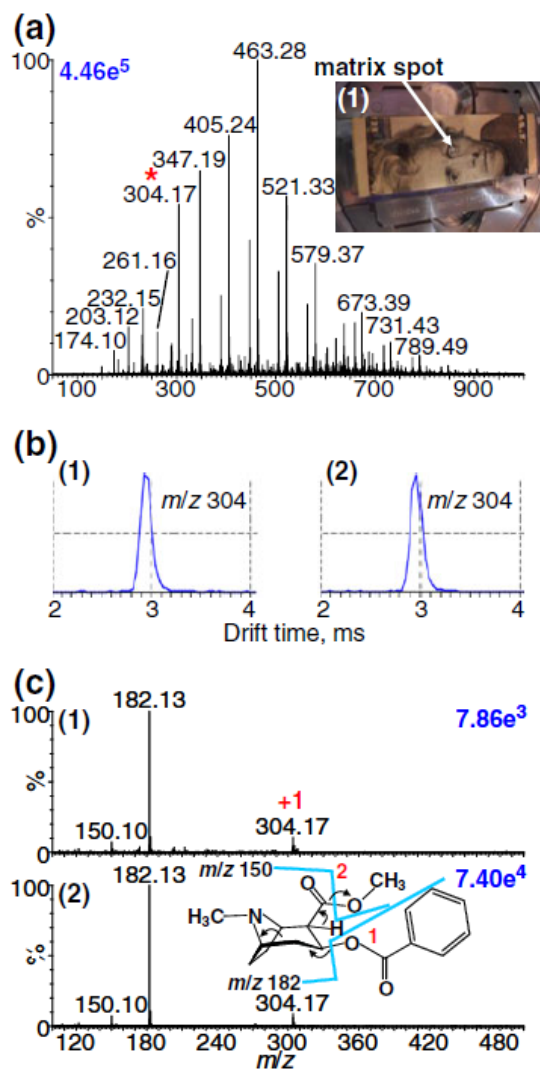
Figure 11.6. Surface analysis by MAIV (**a**) MAIV mass spectrum from a $20 bill spotted with 3-NBN matrix and acquired using the intermediate pressure vacuum SYNAPT G2 MALDI source, (**b**) extracted drift time, and (**c**) collision-induced dissociation mass spectra of illicit drug cocaine (MW 303 Da) detected from (**1**) $20 bill and (**2**) standard cocaine. MS/MS fragmentation pattern is essentially identical to [298]. The other major component detected from the surface of the bill with a repeat unit of 58 indicates polypropylene glycol. Blue numbers of each spectrum provide an indication of ion abundance and red numbers the charge state.

The results were compared with those obtained from a cocaine standard prepared on a glass slide and with MS/MS results described in the literature [230]. Cocaine has been analyzed directly from currency by a number of ambient ionization methods [231,232], but with MAIV, the location sampled is readily defined by the matrix application.

CHAPTER 12

THE POTENTIAL FOR CLINICAL APPLICATIONS USING A NEW IONIZATION METHOD COMBINED WITH ION MOBILITY SPECTROMETRY-MASS SPECTROMETRY "Springer and the original publisher (*Int. J. Ion Mobility Spectrom.*, 16, **2013**, 145-159, Inutan, E.D.; Wager-Miller, J.; Narayan, S.; Mackie, K.; Trimpin, S.) is given to the publication in which the material was originally published with kind permission from Springer Science and Business Media."

Introduction

Identifying clinically relevant health and disease biomarkers is often like searching for the proverbial needle in a haystack. Mass spectrometric approaches are well suited for such a search because they can interrogate complex biological matrices at the molecular level with superb sensitivity, mass resolution, and mass accuracy. However, improved sensitivity and dynamic range, as well as reproducibility from sample to sample, are required for many clinically relevant applications. The extreme complexity that comes with clinical samples combined with the pressure of accuracy, time and cost constraints requires that operator involvement be limited as much as possible. While tandem mass spectrometry (**MS**) targeted screening has been very successful, it requires expertise in operation, data interpretation, and is time consuming because it is usually preceded by liquid chromatography (**LC**) or gas chromatography (**GC**), methods that can be prone to column fouling, and additionally the targeted approach does not detect non-

targeted molecules. LC-MS has significantly impacted analyses of complex biological materials such as tissue, plasma, and urine [233-246]. However, this technology has had only limited success in clinical applications. It is generally accepted that clinical MS analysis needs more efficient and simple ionization, and ideally, real time separation orthogonal to MS for additional specificity. Ion mobility spectrometry (**IMS**), especially combined with MS, has emerged as a powerful method for separating ions, without the use of a solvent, according to number of charge, size, and shape. Near real time separation is achieved and molecular shape information is available using cross-section analysis [61,64,67,247-262]. Additional characterization technologies can be applied such as MS/MS using collision induced dissociation (**CID**) or electron transfer dissociation (**ETD**) [58,100,263,264].

MS ionization methods are powerful, but problematic for many clinical applications for reasons including cost, robustness, degree of difficulty, and interference from the generation of high background ions. In the past decade, numerous 'ambient ionization' sampling strategies have been implemented using established ionization methods to circumvent some of these issues [139,232,265-267]. Heretofore unknown ionization methods for MS have recently been discovered and fundamental studies are starting to define physical underlying processes [29,31,40,45,197]. These new ionization methods encompass inlet ionization with a laser, laserspray ionization *inlet* (**LSII**) [28,49], and without a laser, matrix assisted ionization *inlet* (**MAII**) [39,194], or with a solvent, solvent assisted ionization *inlet* (**SAII**) [221,222,268,269], as well as the vacuum ionization methods of laserspray ionization *vacuum* (**LSIV**) [42-44], and

matrix assisted ionization *vacuum* (**MAIV**) [46,47,]. These methods are sensitive, operate from atmospheric pressure or vacuum, and are applicable for low and high mass analytes in the solid phase or in solution. Charge states similar to electrospray ionization (ESI) are produced, and on high performance mass spectrometers yield high resolution, accurate mass measurement, charge state resolved IMS-MS, and/or advanced fragmentation for structural characterization. Of these new ionization methods, MAIV stands out as being exceptionally simple, requiring no high voltage or laser, and operates at room temperature or with heat, ionizing a variety of different compounds from fatty acids to a protein complex [46,47]. We previously hypothesized that the underlying mechanism of MAIV may be a sublimation driven triboluminescence like process [46,47]. Four different MAIV matrix compounds have been discovered, 3-nitrobenzonitrile (3-NBN), 2-nitrobenzonitrile, 3-nitrobenzaldehyde, and coumarin [47], but none work nearly as well as 3-NBN. Here we show initial results to analytical utility using MAIV in conjunction with real-time separation by IMS, MS, and MS/MS, which suggests a future of this methodology in clinical applications.

Experimental Methods

Materials and sample preparation are included in **Chapter 2.1**. Nicotine and its metabolite standards and the smoker's urine were provided by DMC (Detroit, MI). Cetirizine, an allergy medication, was purchased as tablets from a pharmacy and taken orally (human) and subsequently used for urine analysis. Dilutions from stock solutions were made in water for most of the analytes, in 50:50 methanol/water for clozapine, and in 25 mM ammonium acetate in 10 % methanol for lysozyme to make 1 to 5 pmol μL^{-1}

concentrations. The analyte concentrations in the model mixture of lipids, peptide, and proteins ranged from 1 pmol μL^{-1} (sphingomyelin, leucine enkephalin, angiotensin II) to 5 pmol μL^{-1} (galanin, bovine insulin, ubiquitin) and the small molecule mixture ranged from 1 to 8 pmol μL^{-1}. The protein mixture contained 5 pmol μL^{-1} lysozyme and 10 pmol μL^{-1} myoglobin. The mixture for negative mode measurements contained bovine insulin (2 pmol μL^{-1}), beta amyloid (1–42) (5 pmol μL^{-1}) and ubiquitin (10 pmol μL^{-1}). Clozapine, angiotensin I, and ubiquitin were diluted in 1 M NaCl for the salt studies. Clozapine was diluted in water and 50:50 methanol/water for solvent and pH studies of small and large molecules with 3-NBN added with and without formic acid. 3-NBN matrix was prepared by dissolving 5 mg in 50 μL 100 % ACN with and without 0.1 % formic acid, 150 μL 50:50 ACN/water with 0.1 % formic acid (mixing and deposition on tissue), and 50 μL 50:50 ACN/methanol with 0.1 % formic acid (small molecule mixture) for positive mode measurements, and 150 μL 50:50 ACN/water with 1 % NH_4OH (MAIV and ESI comparison) and 50:50 ACN/methanol with 1 % NH_4OH for negative mode measurements.

The dried droplet method was used to prepare 1 μL spots of analyte:matrix mixture in 3:1 and 2:1 volume ratio for positive and negative measurements, respectively. For tissue analysis, sections of a non-drug and drug treated mouse brain tissue were collected and mounted on a glass microscope slide as previously described in **Chapter 2.1** and in previous studies.[48,195] The mouse received clozapine (50 mg kg^{-1}, intraperitoneal) 90 min before it was sacrificed. Clozapine plasma was obtained by centrifugation of heparinized blood collected by cardiac puncture from treated mouse

after euthanasia. A 25 μL volume of the plasma was concentrated by evaporation in the biodryer without heat and redissolved in 10 μL water. A total of 1 μL of 3-NBN matrix in 50:50 ACN:water with 0.1 % formic acid was spotted in 0.2 μL increments. Small sections of tissue removed from the glass plate were also dipped in 3-NBN matrix solution and spotted directly on the sample target plate. For the human body fluids analysis, separately 10 μL of the drug dosed urine and blood (extracted with water from an adhesive bandage) was diluted to 100 μL with water. The smoker's urine (5 μL) was directly combined with the 3-NBN solution. Isomeric mixture of 5 pmol μL^{-1} beta-amyloid (1–42) and 2 pmol μL^{-1} (42–1) was prepared in 50:50 ACN/water with 0.1 % TFA. For the matrix assisted laser/desorption ionization (**MALDI**) comparison, 5 mg of CHCA was dissolved in 1 mL of 50:50 ACN/water with 0.1 % formic acid and mixed with the analyte in 1:1 volume ratio. For ESI comparison, 10 pmol μL^{-1} of beta-amyloid (1–42) in 50:50 MeOH/water was used at an infusion flow rate of 4 μL min^{-1} for 30 s.

Ion mobility spectrometry (IMS)-MS - An IMS-MS (SYNAPT G2) mass spectrometer (Waters Co., Manchester, UK) was used in this study. The mass spectrometer was operated in the positive, negative and sensitivity ('V' optics of the time-of-flight mass analyzer) modes. The IMS drift cell pressure was set at ~3.7 mbar. Argon was used as the collision gas for MS/MS in the transfer region. MassLynx 4.1 software was used to extract the mass spectrum and DriftScope version 2.2 for the IMS 2-dimensional (2-D) display of drift time (t_d) *vs.* mass-to-charge (*m/z*) using a color background of hot metal or emerald forest and square root display. Nested datasets of drift(flight)time in units of t_d(*m/z*) were used as previously defined [67,270]. BayesSpray

from MaxEnt methods [271] was used to deconvolute the multiply charged ions to mass values.

Matrix assisted ionization vacuum (MAIV) -

MALDI source SYNAPT G2 - The IP-MALDI source of SYNAPT G2 was used to perform MAIV using a vacuum source as described in **Chapter 2.4**. Unless otherwise noted, the data were acquired using 'LSI settings' as previously reported [42,45] similar to those used with ESI with the extraction lens at a lower voltage than used with the default 'MALDI settings'. The default 'MALDI settings' [45] of the vacuum MALDI source were used to obtain comparison mass spectra and proteins from tissue. In both operation modes, no laser was used and acquisition times were set at a scan time of one second for a period of 1 to 2 min. *ESI source SYNAPT G2* - The interlocks of the ESI source of SYNAPT G2 were overridden using the connecting flange available with the MALDI source of the instrument to allow open access to the Z-spray skimmer cone; however, MAIV acquisition can also be obtained using the nano-ESI source as previously described for LSI [49,50]. The Z-spray skimmer cone was modified as described in **Chapter 2.4** to perform MAIV on an ESI source. The source temperature was set at 50 °C with a sample cone voltage of 40 V and extraction cone voltage of 4 V, similar to ESI source settings.

Conventional ionization methods

MALDI - The intermediate pressure MALDI source of SYNAPT G2 was operated using a Nd:YAG laser (355 nm, 200 Hz). Default 'MALDI settings' [45] were used in sensitivity mode with 20 V on sample plate holder and a laser power of setting of

'225' or ca. ~12.5 J cm^{-2}. **ESI** - Acquisition conditions were set similar to MAIV using the MALDI source but with capillary voltage of 2.5 kV, desolvation gas flow of 500 L hr−1, and 80 °C source temperature.

Results and Discussion

The MAIV method depends only on an appropriate matrix and the vacuum conditions common to mass analyzers. Thus, this method is applicable on either a commercial intermediate pressure MALDI source (**Appendix C Figure S18.I**) or an ESI source with minor modifications (**Appendix C Figure S18.II**). MAIV sample preparation can be the same as MALDI but produces multiply charged ions essentially identical to ESI. The MAIV procedure to generate a mass spectrum is amazingly simple. A solution of the MAIV matrix compound, e.g. 3-NBN, is pipetted onto the sample in a manner that is identical to MALDI sample preparation protocols. The matrix:analyte sample is then exposed to the vacuum of the mass spectrometer (**Appendix C Figure S18.Ia**). The total ion current (TIC) exemplifies the ion production during the time required for the matix:analyte to be removed from the sample plate surface, which is approximately 2 min for sample introduction and an additional 1 to 5 min, depending on the sample preparation, during which time analyte ions are observed (**Appendix C Figure S18.Ib**). Matrix apparently sublimes when exposed to vacuum. As long as the matrix is on the sample plate (**Appendix C Figure S18.Ia, Inset**), analyte ions are observed even for proteins (**Appendix C Figure S18.Ic**). Similarly, the nicotine standard and its diagnostic metabolite cotinine, which is predictive of recent tobacco smoking, are readily observed with MAIV using an ESI source (**Appendix C Figure S18.IIa**). Analyte

ions are observed in high abundance with little chemical background (**Appendix C Figure S18.IIc**). The ion formation in MAIV is continuous until the sample is depleted. Using the ESI source (**Appendix C Figure S18.IIb**) the analysis time is considerably compressed relative to MAIV operated on the intermediate pressure vacuum MALDI source (**Appendix C Figure S18.Ib**). From visual observations at atmospheric pressure, the matrix:analyte sample under favorable conditions is entirely removed within a few seconds, which accounts for the more rapid ionization process. Samples can be completely dry or still in solution when presented to the vacuum (**Appendix C Figure S19**) because the vacuum assists in drying the sample. The ready sublimation of 3-NBN under vacuum conditions is expected to eliminate instrument contamination by this matrix.

The MAIV method is sensitive as is demonstrated by the mass spectra of 50 fmol of levofloxacin, an antibiotic drug, and bovine insulin shown in **Appendix C Figure S20**. MALDI mass spectra (**Appendix C Figure S20.I**) were acquired with the same levofloxacin sample (50 fmol applied) using the common matrix CHCA. The abundant chemical background observed with MALDI dominates the mass spectrum, and is likely related to photoionization of the matrix [94]. MAIV also fairs better than MALDI because without the use of a laser, 'hotspot' issues are not observed. Only 5 fmol of clozapine in the presence of 20 pmol of bovine insulin allow identification of clozapine using the extracted mass spectrum (**Appendix C Figure S20.III**). This is accomplished through the use of the IMS real time separation, which increases the dynamic range of the experiment, allowing minor components to be detected in the presence of abundant

components. Previous studies on pure clozapine standard showed mass spectra consuming only 5 fmoles in MS, and in MS/MS only 900 attomoles [47]. The use and application of IMS are discussed below.

MAIV is also tolerant of salts which often add difficulty when directly analyzing biological samples using MS. High levels of salt (1 M NaCl, **Appendix C Figure S21**) added to samples had minimal deleterious effects as is demonstrated for clozapine, angiotensin I, and ubiquitin, all of which are detected as protonated ions. Only with increasing size of the protein is sodium adduction detected. Initial experiments suggest that pH has little influence on the charge state distribution. The ion abundance is best near neutral pH conditions for small and large molecules (**Appendix C Figure S22**), however, different solvents systems show different degrees of chemical background (**Appendix C Figure S22.I).** For smaller molecules, more volatile solvents seem to aid in ionization; visual observations suggest that crystal formation of matrix:analyte is more favorable. Although MAIV is a soft ionization method, fragmentation can be induced by, for example, increasing the extraction voltage in the intermediate pressure MALDI source. Using the low extraction voltage of LSI settings the drug clozapine is detected intact or with little fragmentation (*m/z* 270) (**Appendix C Figure S23a**), however, using the higher extraction voltage of the default MALDI settings with the same matrix:clozapine sample, abundant fragment ions are observed (**Appendix C Figure S23b**). Interestingly, the softer MAIV ionization conditions using LSI settings provide simplicity of data interpretation (**Appendix C Figure S24.I**) whereas MAIV using commercial MALDI settings (**Appendix C Figure S24.II**), but without the use of a laser,

form gas-phase dimers of lipid aggregates commonly observed in MALDI [272] and ESI analysis [273], especially when using laser irradiation or increased concentrations. These aggregates are readily visualized incorporating IMS [67,157,166], as is the case here (**Appendix C Figure S24.IIB**). All compounds tested to date have produced less chemical background, fragmentation, or aggregation, and improved ion abundance of the multiply charged ions using 'LSI settings'. In the following examples, LSI settings were therefore used for analyte ionization with the exception for proteins from tissue. These ionization trends of high salt and pH tolerance allow direct analysis of small and large molecules from their native and complex environments by simply exposing the analyte or just the area of interest to 3-NBN and the vacuum of the mass spectrometer. Small and large molecule analyses using MAIV in combination with IMS real time separation technologies are discussed for potential use as a direct analysis platform in clinical applications using MS.

Small molecules

Drugs such as clozapine (MW 326), and levofloxacin (MW 361) as well as commonly abused drugs (cocaine MW 303, fentanyl MW 336, benzoylecgonine MW 289) (**Figure 12.1.Ia**) can rapidly be analyzed using MAIV on an ESI source without the low-mass matrix background ions common at every mass with MALDI [274,275]. The 2-dimensional (2-D) plot of drift time *vs. m/z* (**Figure 12.1.Ib**) shows separation in the ion mobility dimension of the singly charged MAIV ions produced for each of the compounds in the mixture. Singly charged ions are detected with no fragmentation and little chemical background (**Figure 12.1.I**). The extracted drift times (**Figure 12.1.Ib**,

Insets) display well-resolved peaks, and the isotopic distributions (**Appendix C Figure S25.I**) and accurate mass assignments help in identifying the drugs in the mixture. Nested t_d(*m/z*) data information [67,270] from IMS and MS can be extracted and used for identification, e.g. levofloxacin 4.28(337). An example of this approach with direct ionization from a mouse brain tissue sample is provided below. For additional specificity and confirmation, MS/MS without precursor ion selection (**Figure 12.1.Ia**) is performed with IMS similar to MSe but without the alternating low and high collision energy [276], or LC separations [277-288]. In other words, the entire set of ions, both directly ionized by MAIV as well as separated by IMS, are fragmented in the transfer region without precursor selection of the ions. **Figure 12.1.Ib** shows the 2-D plot display of drift time *vs. m/z* of the fragment ions obtained for each of the analyte molecules in the mixture. With the IMS dataset, each of the MS/MS mass spectra can be extracted based on the drift time information. This is shown for cocaine in **Figure 12.1.Ic** and **Appendix C Figure S25.II**. The validity of the method is shown by comparison with conventional IMS-MS/MS using precursor selection in the quadrupole, as demonstrated for cocaine in **Figure 12.1.III**. Identical results were obtained for all mixture components without (**Appendix C Figure S25.II**) and with (**Appendix C Figure S25.III**) precursor selection so that nested data information applies for IMS-MS/MS, e.g., t_d(*m/z→m/z*) 3.25(304→182). Obtaining specificity for all mixture components without the precursor selection has the advantage of potentially being a fast non-targeted approach. The collective IMS-MS and IMS-MS/MS dataset should be sufficiently specific for automated data interpretation of large datasets, even if molecular ions are not completely

baseline separated by IMS or MS, and without LC, which is important for robust, direct, and surface analyses methods.

The direct characterization of drugs from tissue is illustrated for clozapine using IMS and MS (**Appendix C Figure S26**). The first dimension information, the drift time distribution, is identical to the synthesized standard (**Appendix C Figure S16b**, **Insets bottom right**). The second dimension information, the mass measurement and isotopic distribution, readily identifies the drug because of the uniqueness of the chlorine pattern and superimposes over the standard sample (**Appendix C Figure S26b, Insets top left**). Therefore the nested dataset, 3.26(327) for clozapine, is sufficiently distinctive for identifying a small drug molecule directly from complex biological matrix such as tissue, at least if a standard is available. However, MS/MS can be employed if improved specificity is desired (**Appendix C Figure S27**). This may require an additional minute of data acquisition and perhaps more user expertise to enable interpretation. As long as the fragmentation patterns are known, the procedures are similar to those employed for targeted analysis using triple quadrupole technology, but includes a MS profile of the sample composition.

Ions are only observed from the section of the tissue (**Figures 12.2** and **S26, Appendix C**) where matrix is applied, which can be substantially smaller than 1 mm2. Matrix solution added to minute amounts of tissue is shown in **Figure 12.2c**. Contary to
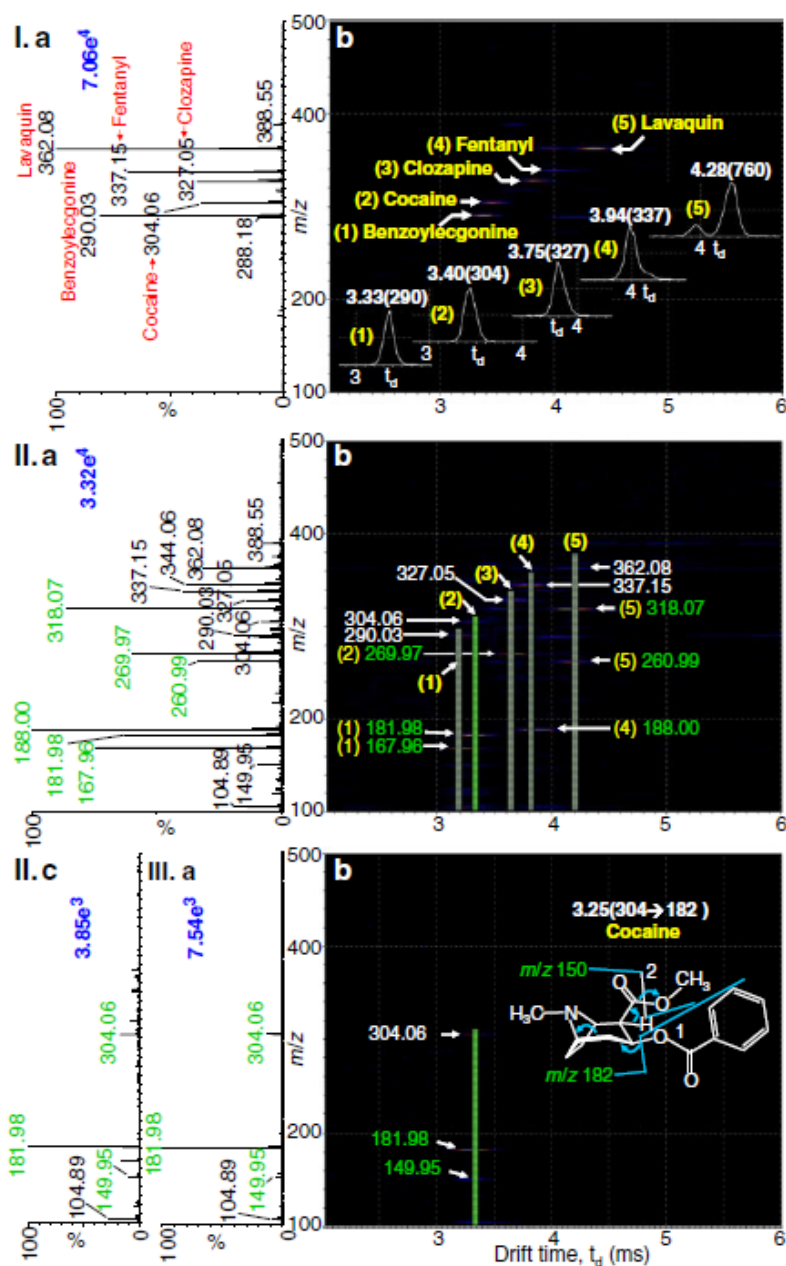
Figure 12.1. MAIV-IMS of small molecule mixture of clozapine (MW 326 Da), lavaquin (MW 361 Da), and common abused drugs cocaine (MW 303 Da), fentanyl (MW 336 Da), and benzoylecgonine (MW 289 Da) with 3-NBN matrix using the custom modified ESI source of SYNAPT G2 mass spectrometer: (**I**) MS, (**II**) MS/MS without precursor ion selection, and (**III**) MS/MS with *m/z* 304 precursor selection (cocaine). **a** Total mass spectra, **b** 2-D plot of drift time (t$_d$) *vs. m/z*. Insets in **I.b** show extracted drift times labeled in a nested fashion as t$_d$ (*m/z*) as described previously [67,270]. **II.c** show the extracted MS/MS mass spectrum of cocaine from **II.b**

established technology, location is frozen in time as only the tissue exposed to the 3-NBN is ionized (**Figure 12.2a**). A spatial analyses of about 500 μm diamater is readily obtained without the use of a laser or a (micro) dissecting knife. Using this approach, mouse brain tissue was readily analyzed only 30 min after receiving 50 mg kg^{-1} of clozapine (**Figure 12.b**). This approach is therefore sensitive enough for low abundance drug detection. The protocol can be repeated until the tissue has been consumed by the ionization event. Using a similar approach, a tissue piece dipped into the matrix solution and subsequently inserted into the mass spectrometer for analysis is shown in **Appendix C Figure S28.I**.
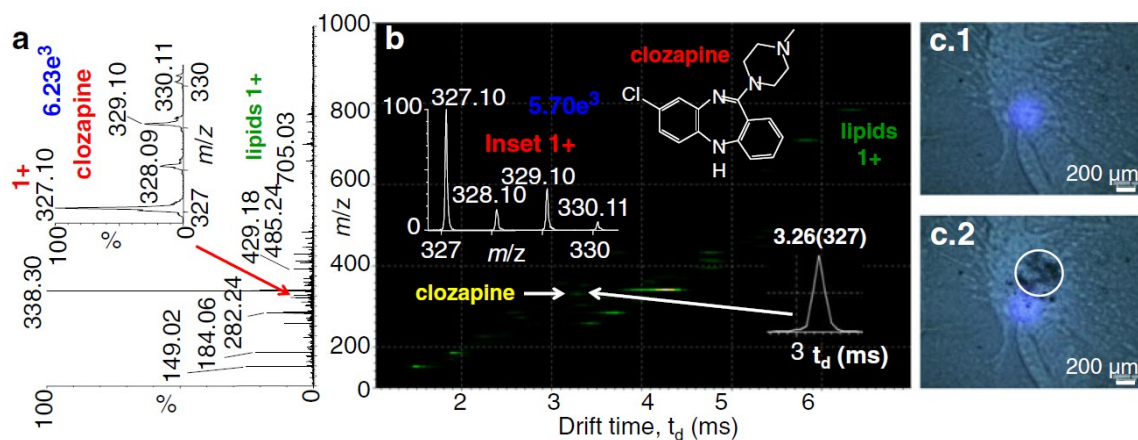
Figure 12.2. MAIV-IMS-MS of clozapine treated mouse brain tissue spotted with 3-NBN matrix: **a** total mass spectra, **b** 2-D plot display of drift time *vs. m/z*, and **c** microscopy photographs of the tissue (**1**) before and (**2**) after matrix deposition. Insets show (**a**) isotopic distribution fromthe total mass spectrum, (**b**) isotopic distribution extracted from the 2-D plot, and extracted drift times labeled in a nested fashion for clozapine. Data was acquired using LSI settings without the use of a laser on the intermediate pressure MALDI source of SYNAPT G2 mass spectrometer.

This simple method holds great potential as a rapid means for (e.g.) biopsy assays. Further, blood taken from a mouse 30 min after receiving 50 mg kg^{-1} of clozapine was also analyzed in a straightforward manner (**Appendix C Figure S28.II**). Despite the

complexity of the sample composition, clozapine at *m/z* 327 is readily observed. Because no laser is used and hot spot issues are avoided, quantitation studies might be possible.

Using MAIV-IMS-MS, diluted urine can be analyzed without sample desalting. Ample ion abundance to characterize the drug cetirizine hydrochloride (**Figure 12.3.I**) from the urine of an individual taking allergy medication is produced by simply diluting the urine 1:10 in water and mixing it with the 3-NBN matrix before placing in vacuum. Again, the nested dataset is sufficiently distinctive. Specificity gained through MS/MS data for the drug cetirizine confirms its presence in the urine sample (**Appendix C Figure S29.I**). Similarly, the diagnostic nicotine metabolites, cotinine and nornicotine, can be observed simultaneously from the urine sample from a smoker using MAIV-IMS-MS (**Figure 12.3.II**). Interestingly, the isobaric compounds (*Inset right*) of nornicotine (accurate molecular weight 148.0995 Da), one of the metabolites of nicotine, and 3-NBN (accurate molecular weight 148.0267 Da) are baseline separated in the IMS dimension (Inset left). Nornicotinine (*Inset top*), present in relatively low abundance, is matched with its nested data against the pure standards discussed above (**Appendix C Figure S18.IIc**). Using the notably different drift times and MS/MS fragmentation in the transfer fragmentation region of the mass spectrometer verified the identities of the two different isobaric small molecules (**Appendix C Figure S29.IIa**). Both urine solutions and plasma samples have been directly analyzed from glass microscope slides requiring only dilution with water before mixing with the matrix and required no sample clean up. Typically, such complex mixtures can result in column fouling in LC/MS and GC/MS, but with MAIV nonvolatile, un-ionized compounds remain on the sample plate, while compounds

that are volatile under the vacuum, including the matrix, are pumped from the instrument, potentially reducing or eliminating instrument contamination. IMS-MS and, if need be, MS/MS provide a instantaneous means for separation, profiling and characterization with very little operator expertise needed for sample preparation and analyses. Unlike targeted
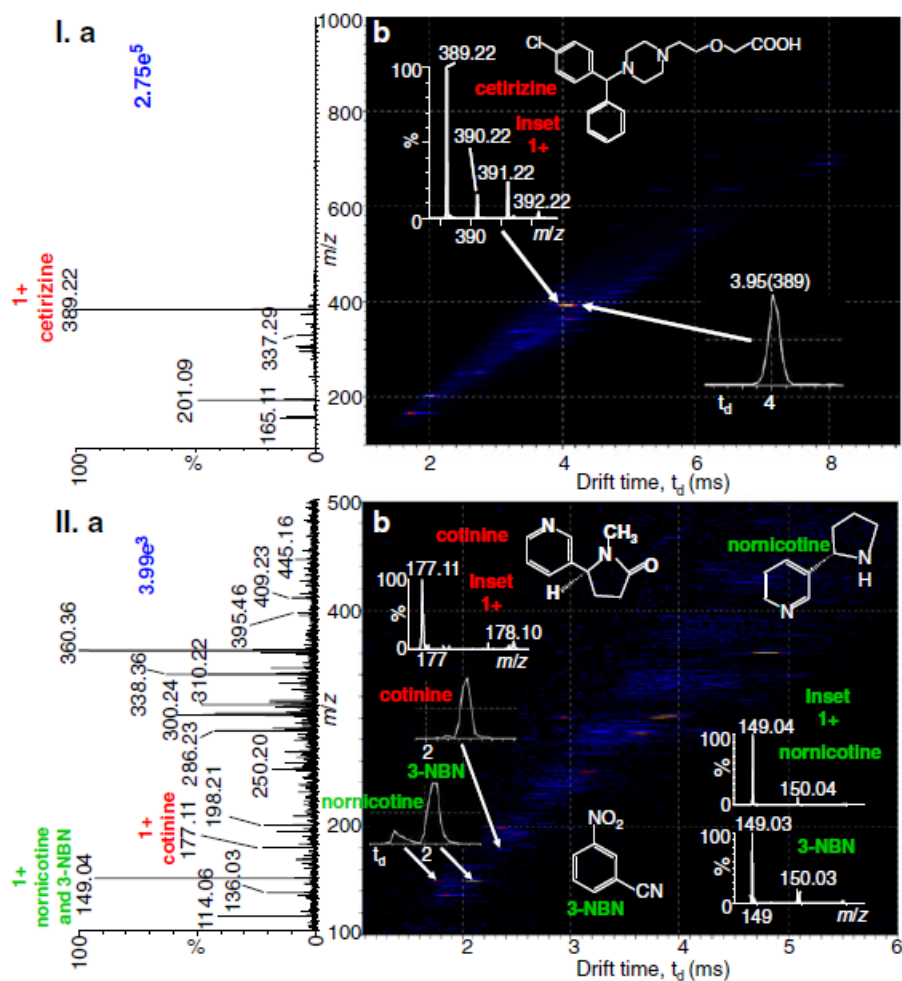
Figure 12.3. MAIV-IMS-MS using 3-NBN matrix of (**I**) urine from drug dosed individual taking cetirizine, an allergy medication and (**II**) smoker's urine: (**a**) total mass spectra and (**b**) 2-D plot display of drift time *vs. m/z*. Insets in b show extracted drift times labeled in a nested fashion and isotopic distributions. Data was acquired using LSI settings without the use of a laser on the intermediate pressure MALDI source of SYNAPT G2 mass spectrometer.

analysis, the entire material is profiled. An intrinsic limitation of targeted analyses using traditional clinical assays is that one can only interrogate analytes for which assays are established and must run many samples, if need be, until the 'hit' is determined.

Large molecules

An example of a MAIV mass spectrum of the peptide beta amyloid (1–42) (molecular weight 4511 Da) using 3-NBN on the intermediate pressure Waters SYNAPT G2 MALDI source with the laser 'off' (**Appendix C Figure S18.Ia**) is shown for both positive (Fig. 4.I) and negative (**Figure 12.4.II**) mode detection. For comparison, the same sample was analyzed using ESI (**Figure 12.4.III**) on the same mass spectrometer. The negative mode mass spectra are nearly identical in charge state and sensitivity to ESI as shown in **Figure 12.4.II** and **III** but the charge states are slightly lower relative to the positive mode (**Figure 12.4.I**). The successful ionization in the negative mode is in support of the triboluminescence particle charging hypothesis [46,47]. With the IMS dataset, the drift times of the multiply charged ions of beta amyloid (1–42) (**Figure 12.4.b**, **Insets**) can be extracted. The extracted drift time information using the MALDI source with MAIV in the negative mode measurements (**Figure 12.4IIb**, **Insets**) is essentially identical to the extracted drift time using traditional ESI (**Figure 12.4IIIb**, **Insets**) additionally to the same charge state distributions. This is of fundamental interest because two different methods and acquisition conditions are used; MAIV operates from the solid state and ESI from solution. This indicates that cross-section analyses are applicable for MAIV using conditions and methods established for ESI. Previous studies
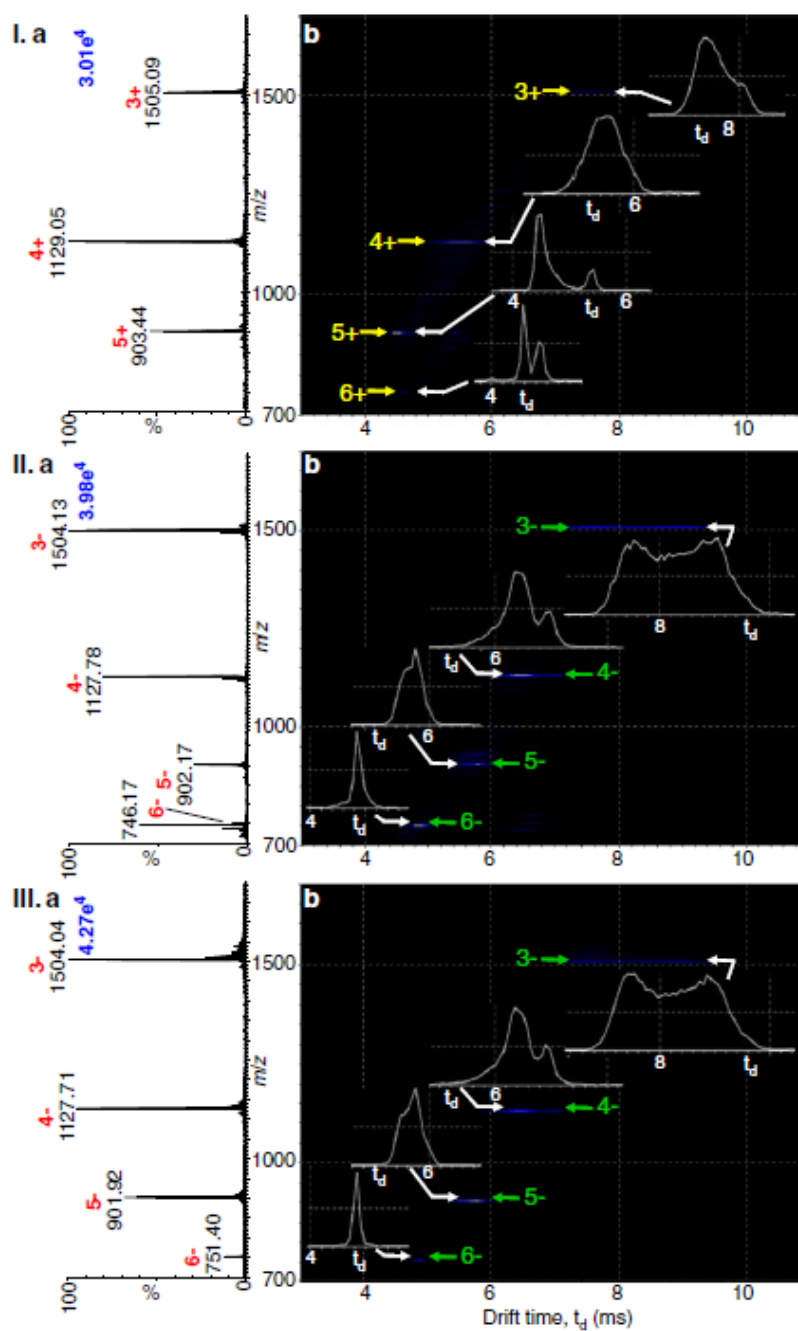
Figure 12.4. IMS-MS (**a**) mass spectra and (**b**) 2-D plot display of drift time *vs. m/z* of beta-amyloid (1–42) (MW 4511 Da) using MAIV with 3-NBN matrix in (**I**) positive mode and (**II**) negative mode on the intermediate pressure vacuum MALDI source, and (**III**) ESI comparison in negative mode of the SYNAPT G2 mass spectrometer. Insets show extracted drift times.

using ESI-IMS-MS suggested that negative mode measurements for amyloid β-protein are more reliable than positive mode measurements relative to cross-section analyses [118]. The drift time distributions may give additional information to the relative structures of these analyte ions directly from their native surfaces in the future.

Figure 12.5 shows the MAIV data obtained from a mixture of beta amyloid (1–42) (molecular weight 4511 Da), bovine insulin (molecular weight 5730 Da), and ubiquitin (molecular weight 8560 Da) in 2.5:1:5 molar ratio, respectively, using 3-NBN as matrix in the negative mode on the custom modified ESI source. Good ion abundance is observed from this mixture. However, ubiquitin ions are observed in lower ion abundance in the total mass spectrum (**Figure 12.5a1**) compared to bovine insulin, which is in the lowest concentration in the mixture. Using the drift time dimension provided by IMS (**Figure 12.5b**), the mass spectrum of each protein can be extracted (**Appendix C Figure S30**). The cleanly separated mass spectrum for ubiquitin is exemplified in **Figure 12.5a2**.

The ability of MAIV to analyze a variety of samples is demonstrated for a model mixture containing a lipid (sphingomyelin molecular weight 702 Da), peptides (leucine enkephalin molecular weight 555 Da, angiotensin II molecular weight 1045 Da), small proteins (galanin molecular weight 3156 Da, bovine insulin molecular weight 5730 Da) and ubiquitin (molecular weight 8560 Da) in the positive detection mode using the SYNAPT G2 MALDI source (**Appendix C Figure S31**). MAIV ionizes all the individual components of the mixture from lipids to proteins with good ion abundance and essentially no chemical background (**Appendix C Figure S31a**). The multiply charged
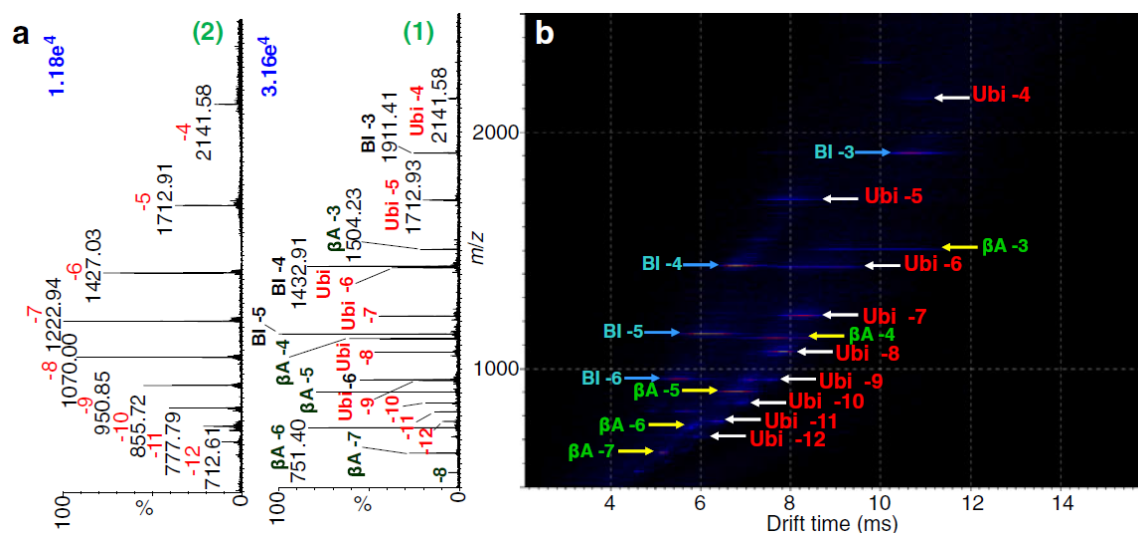
Figure 12.5. MAIV-IMS-MS a mass spectra: (**1**) total and (**2**) extracted from **b** 2-D plot display of drift time *vs. m/z* of model mixture of beta amyloid (1–42) (MW 4511 Da), bovine insulin (MW 5730 Da), and ubiquitin (MW 8560 Da) in negative mode using the custom modified ESI source of SYNAPT G2 mass spectrometer.

peptide and protein ions are well separated from the singly charged ions in the IMS dimension (**Appendix C Figure S31b**) allowing extraction of the mass spectra for the individual components (**Appendix C Figure S31c**).

A mixture of higher mass proteins comprising lysozyme (MW ~14.3 kDa) and myoglobin (MW ~17 kDa) using MAIV with the MALDI source is shown in **Appendix C Figure S32a**. Lysozyme is present in low abundance compared to myoglobin, and therefore its signal is not readily observed in the total mass spectrum. However, the multiply charged ions of lysozyme are well separated from myoglobin as can be seen in the 2-D plot (**Appendix C Figure S32b**) making it possible to extract the cleanly separated protein mass spectra (**Appendix C Figure S33c**). Without the inclusion of IMS, lysozyme could have been overlooked in the total mass spectrum (**Appendix C**

Figure S32a). The multiply charged ions allow this dataset to be observed using a MALDI source (**Appendix C Figure S18.I and II**) on an instrument that is limited to *m/z* 8000. Thus, the multiply charged ions produced by MAIV have the advantage that protein analysis can be implemented on mass range limited IMS-MS mass spectrometers. Programs previously introduced for ESI analyses [271] are available to convert mass spectra of multiply charged ions to the molecular weight, as demonstrated using MAIV-IMS-MS in **Appendix C Figure S33** for the total mass spectrum of the mixture compositions discussed above (Figures S14 and S15). This is also applicable to proteins directly analyzed from whole blood (**Appendix C Figure S33c and S34**).

A mixture of beta amyloid (1–42), of biological significance in Alzheimer Disease [289,290], and the reversed peptide (42–1) is efficiently ionized using the 3-NBN matrix (**Appendix C Figure S35a**). The two isoforms are baseline separated as is shown for charge state +4 (**Appendix C Figure S35b**); the achieved separation is identical to LSII-IMS-MS [50]. Using MS/MS in the transfer region, as is shown in **Figure 12.6**, and thus after the isomers are cleanly baseline separated according to their apparent shape difference using IMS, provides good fragmentation yield and sequence information content as is shown for the *m/z* selected charge state +5. The fragmentation pattern is different for the two peptides as might be expected considering that the hydrophobic end of (1–42) is at the C-terminus and at the N-terminus for (42–1). Although the charge mostly resides on the hydrophilic amino acids of both peptides, the highest sequence coverage is from the hydrophobic end.

DAEFRHDSGYEVHHQKLVFFAEDVGSNKGAIIGLMVGGVVIA

AIVVGGVMLGIIAGKNSGVDEAFFVLKQHHVEYGSDHRFEAD

b₃₃³⁺

[M+5H]⁵⁺ β-amyloid (1-42)
903.47 b₂₃³⁺ b₃₄³⁺
b₃₁³⁺
1162.89 b₃₅³⁺
b₃₀³⁺ 1300.61 b₃₈³⁺
1372.03

y₂⁺
203.16

y₃⁺
302.22

185.15 400 800 1200 1600
b₂⁺ b₃⁺
284.22

y₁₇²⁺
1034.00 β-amyloid (42-1)
y₃₉⁴⁺y₃₃³⁺
1225.62
[M+5H]⁵⁺ y₃₁³⁺ y₃₄³⁺
903.45 y₁₈²⁺ y₃₅³⁺ y₃₈³⁺
1378.03
b₄⁺ y₆⁺ y₂₇²⁺
1568.21

400 800 m/z 1200 1600

m/z

4 6 Drift time (ms) 10 12

Figure 12.6. The 2-D display of an isomeric mixture of beta-amyloid (1–42) (in red) and (42–1) (in yellow) using MAIV-IMS-MS/MSwith 3-NBN acquired on the intermediate pressure vacuum MALDI source of SYNAPT G2 mass spectrometer shows the IMS separated ions fragmented in the transfer region of the IMS TriWave using CID fragmentation. The charge state 5+ precursor ion was selected in the quadruple. The fragment ion mass spectra and sequence coverage of both isomers are overlaid on the 2-D plot. MAIV-IMS-MS results are provided in **Appendix C Figure S35** and, for comparison, the same characterization approach was obtained using MAIV on the ESI source (**Appendix C Figure S36**).

The fragmentation of the (1–42) peptide has previously been reported [291,292]. The MAIV-MS/MS of beta-amyloid (1–42) relates well with those observed with ESI-MS/MS [292]. Another interesting observation is that MAIV on the vacuum MALDI source provided the better sequence coverage for both isoforms relative to those obtained with MAIV on the ESI source using the same matrix:analyte sample (**Appendix C Figure S36**). The apparent difference is better ion abundance of the parent ion using MAIV on the vacuum MALDI source. Expectedly, traditional ESI was cumbersome with the solubility restricted (1–42) relative to capillary clogging and MALDI only provides

singly charged ions with less resolved IMS separation and poorer fragmentation. MAIV combines the positive attributes of ESI and MALDI ionization methods for efficient ionization and characterization using high performance technology such as IMS and MS/MS.

Application of 3-NBN to tissue is not limited to determining the location of small molecules. An example is shown in **Figure 12.7** in which a specific area of a delipified mouse brain tissue ($\sim 500 \times 600$ μm) was exposed with 3-NBN matrix and analyzed (**Figure 12.7a,b**). The spatially resolved area depends on the matrix deposition; a delipification procedure is currently needed to observe proteins from tissue similar to MALDI-MS [74]. Information is obtained more rapidly without the laser by simply exposing the area of interest to matrix solution and placing the tissue into the vacuum of the mass spectrometer (**Figure 12.7c**). Proteins are detected with a molecular weight of 5440 Da [46] and 16788 Da (**Figure 12.7b**). The deconvoluted masses for the extracted higher molecular weight are shown (**Figure 12.7d**). A literature search failed to confirm the identity of this protein and we found no report of it being observed in mouse brain tissue using MALDI of the higher abundant proteins such as myelin basic protein (**MBP**) [293]. This suggests that this novel ionization method may be complementary with MALDI as well as LSI [43,48]. Complementary information using laserspray ionization and MALDI was previously reported [48]. At the current development stage, sufficient ion abundance from tissue is obtained using MAIV on the vacuum MALDI source, but not on the ESI source. Therefore, ETD fragmentation, which is currently only available

on the ESI source, is not available to characterize these proteins directly from tissue as was achieved for laserspray ionization of peptides from tissue [48].
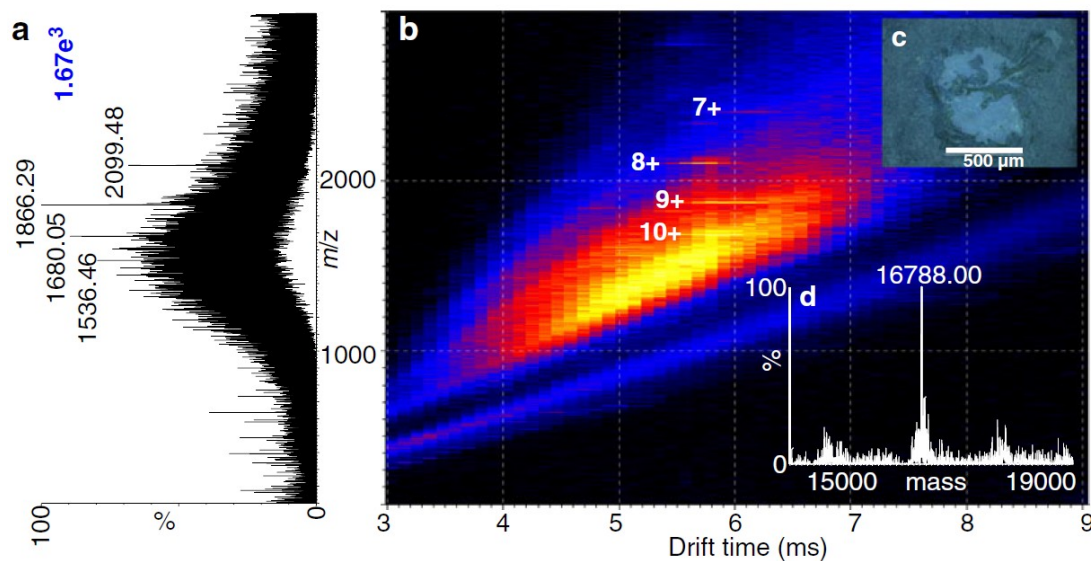
Figure 12.7. MAIV-IMS-MS of delipified mouse brain tissue spotted with 3-NBN matrix: (**a**) total mass spectrum, (**b**) 2-D plot display of drift time *vs. m/z*, (**c**) microscopy photograph on the tissue after poking, and (**d**) deconvolved mass spectrum of protein. Data was acquired using the intermediate pressure vacuum MALDI source of SYNAPT G2 mass spectrometer.

CHAPTER 13

CONCLUSIONS AND PROSPECTUS

The novel ionization methods presented at AP and vacuum produces multiply charged ions similar to ESI in a MALDI-like sample preparation. The production of multiply charged ions extends the mass range of high performance mass spectrometers that have limited mass-to-charge (m/z) range and enhances fragmentation. The incorporation of IMS to these new ionization methods provides separation of ions according to charge, size and shape or cross section. Further compounds are ionized directly from surfaces. The laser-based ionization method at AP (LSII) has the speed of analysis beneficial for tissue imaging, and the TG approach produces smaller ablated areas to improve spatial resolution provided sufficient ion intensity is obtained. Single scan acquisition by LSII using a high performance mass spectrometer is sufficient to obtain good quality mass spectra with sensitivity as low as attomole amounts of the analyte. The observation of clusters and liquid droplets from the microscopy study of the collected ablated material and the heated inlet temperature study suggest that the multiply charged ions are formed by heating the inlet to desolvate the matrix in the clusters in a field-free environment. The use of high performance mass spectrometer provides isotopic resolution and accurate mass measurement even for proteins and allows the characterization and identification of endogenous peptide directly from mouse brain tissue using advanced fragmentation such as ETD. The coupling of LSII with IMS-MS separates mixtures, including isomers directly from surfaces. LSII shows identical drift

times to ESI suggesting ion structure information occurs after formation of the gas phase ions.

LSII extended its application using a vacuum MALDI source. In the absence of a heated inlet, multiply charged ions are formed by using a matrix that has low thermal requirements for evaporation or sublimation. The multiply charged ions observed are similar to LSI and is thus termed LSIV. No external energy is supplied except for the laser energy absorbed by the matrix and the pressure drop from IP to vacuum. The use of a suitable matrix, laser power, and proper acquisition and instrument settings are important factors in producing multiply charged ions using LSIV in a vacuum MALDI source. With IMS, drift time analysis directly from mouse brain tissue is achieved, and are identical to the drift times from the synthesized standard using LSII and ESI indicating similar structures are detected from the tissue. LSIV with IMS for tissue analysis improves the separation of singly charged lipids from multiply charged peptides and proteins. With the use of a suitable matrix, the proper sample preparation, and incorporation of IMS for tissue imaging, images of multiply charged endogenous peptide are obtained from the mouse brain tissue. These compounds were characterized and identified previously by LSII.

The fundamental understandings gained from LSII, the production of ions by tapping matrix:analyte into the inlet tube without the use of laser (MAII), and the observation of multiply charged ions in a vacuum MALDI source (LSIV) emboldened us to continue the search for matrixes that can produce multiply charged ions with very low thermal requirements. The aromaticity and/or functionality, as well as absorption of the

laser wavelength by the matrix, is not a requirement to produce multiply charged ions either with (LSII) or without the use of a laser (MAII). Astonishingly, one of these matrixes, 3-NBN has the highest ion abundance of multiply charged ions at very low temperature and produces ions in an IP-MALDI vacuum source without the use of a laser and was thus termed MAIV in analogy to MAII. MAIV using 3-NBN produces gas phase ions directly from the matrix/analyte crystals through a sublimation process, a characteristic property of 3-NBN. Both positive and negative ions are detected. A property of 3-NBN that may explain the production of charges is triboluminscence. MAIV produces ions from small and large molecules with little or no chemical background. Large molecules are observed as multiply charged ions in a vacuum MALDI source. Without the use of a laser, MAIV is applicable to fragile molecules and protein complexes. Biological fluids or tissue are ionized efficiently by just incorporating 3-NBN matrix into the sample and exposing the sample to the vacuum of the mass spectrometer. The sublimation process in the formation of ions makes it possible to miniaturize the matrix deposition on the tissue which is potentially useful for spatial and drug target analyses. The use of 3-NBN as the matrix and formation of the ions by exposing the matrix/analyte crystals to the vacuum of the mass spectrometer can be extended to ESI sources. This ionization process is rapid, robust, sensitive, and fast, making it potentially useful for clinical applications. The instantaneous ionization by MAIV, and the real time separation and characterization by IMS enhances the dynamic range, provides rapid analysis, separation of isomers and isobars, and cross section analysis directly from the surface important for biological applications. The laser based ionization methods LSII

improves spatial resolution and the vacuum condition LSIV enhances sensitivity useful
for tissue imaging.

APPENDIX A

Laserspray Ionization *Inlet* Supplementary information
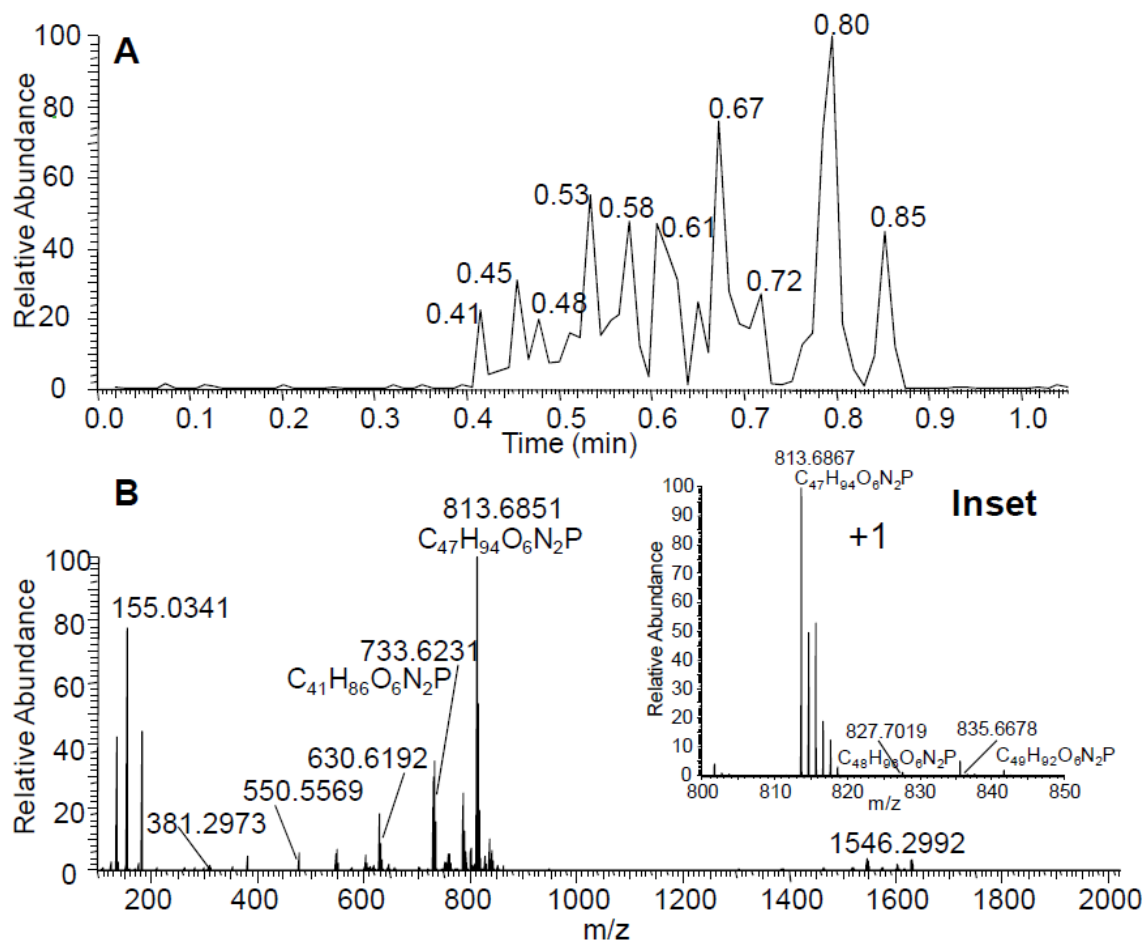
Figure S1: Chemical analysis of sphingomyelin (molecular weight [**MW**] 812.7): **A)** Total ion current: Ions are produced in a continuous fashion obtained by moving the sample holder through the focused laser beam. **B)** TG AP-MALDI mass spectrum with Inset region. Additionally, the [M2+H]$^+$ dimers at > *m/z* 1500 are observed in accordance with previous studies (*Trimpin, S., Tan, B., Bohrer, B.C., O'Dell, D.K., Merenbloom, S.I., Pazos, M.X., Clemmer, D.E., Walker, J.M. Profiling of Phospholipids and Related Lipid Structures usingMultidimensional Ion Mobility Spectrometry-Mass Spectrometry* **2009**, *287*, 58-69.
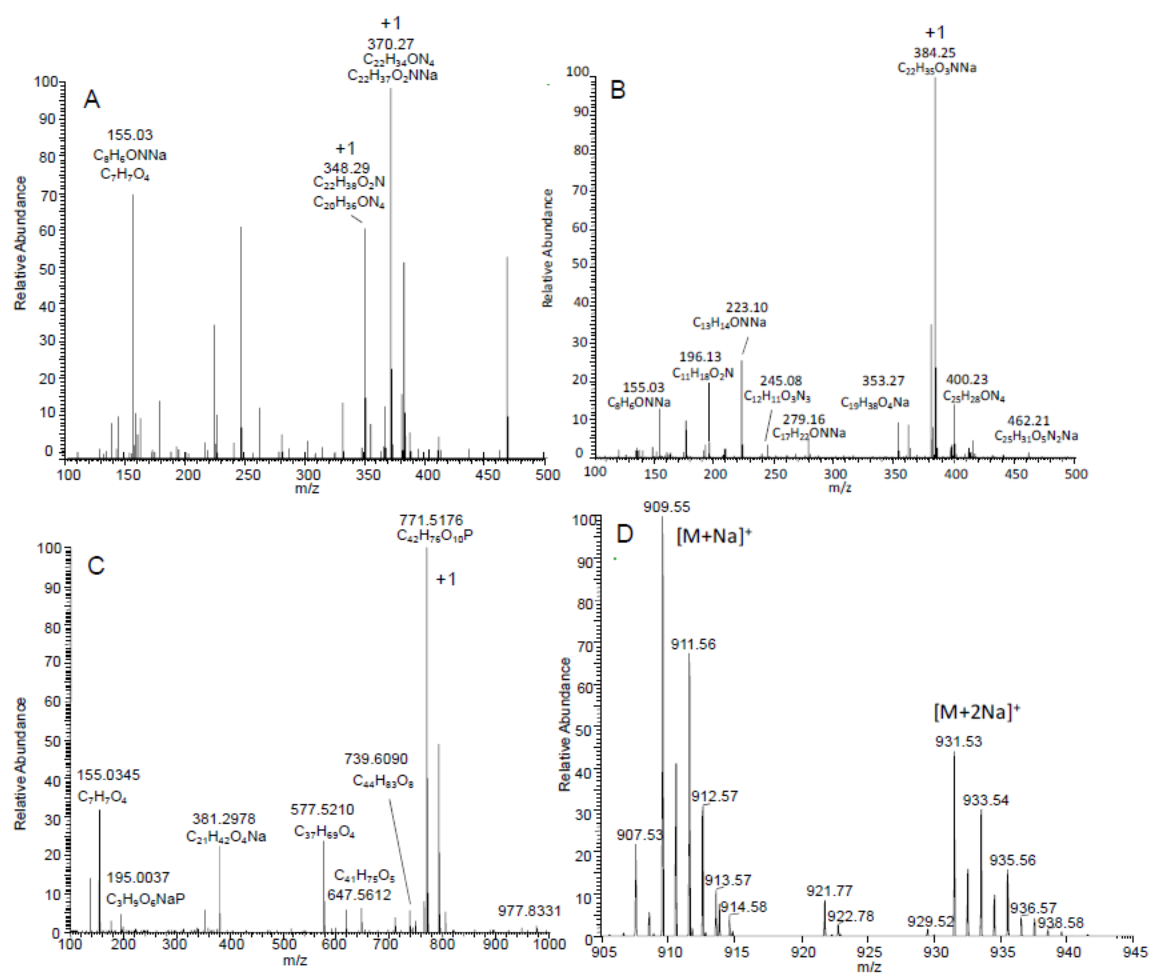
Figure S2: TG AP-MALDI mass spectra using 2,5-DHB: **A**) anandamide (MW 347.3); **B**) NAGly (MW 361.3); **C**) phosphatidyl glycerol (MW 770.5); **D**) phosphatidyl inositol (MW 886.6).
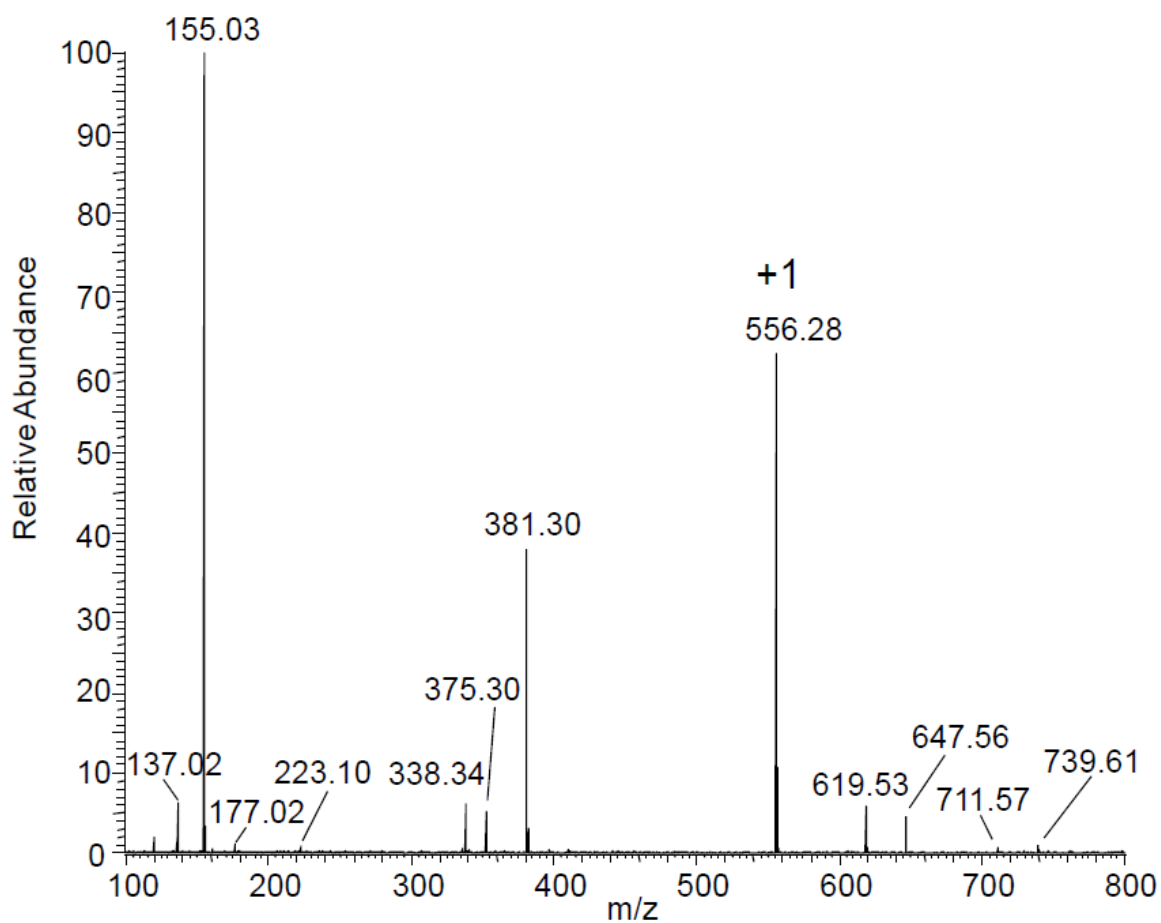
Figure S3: Solvent-based TG AP-MALDI mass spectrum of Leu-Enkaphelin (MW 555.3) and 2,5-DHB.
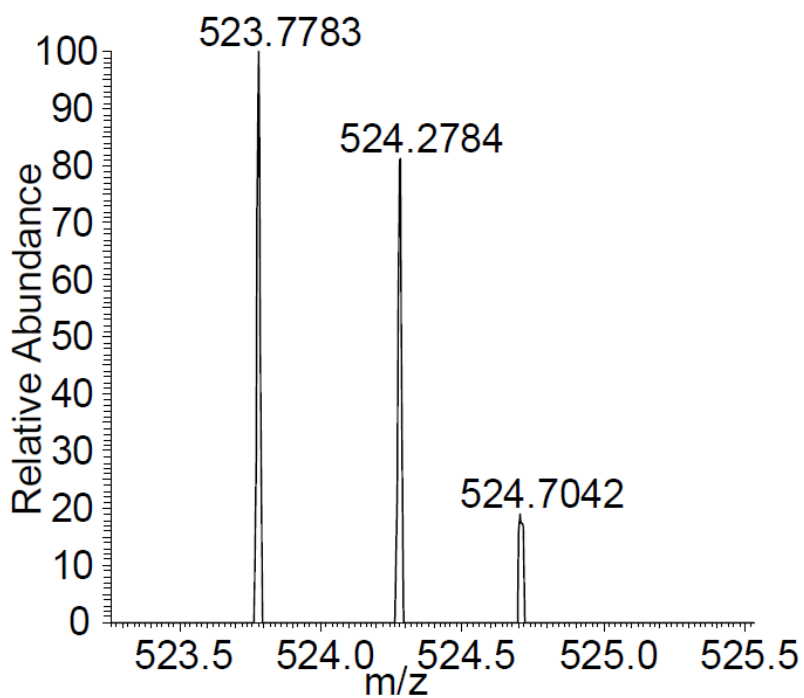
Figure S4: TG AP-MALDI mass spectrum of angiotensin II (MW 1045.5) with a resolution 100,000 (solvent-based 2,5-DHB). The inset shows the doubly charged ion for a single laser shot obtained from the application to the glass slide of 0.1 μL of 400 attomoles of angiotensin II solution.
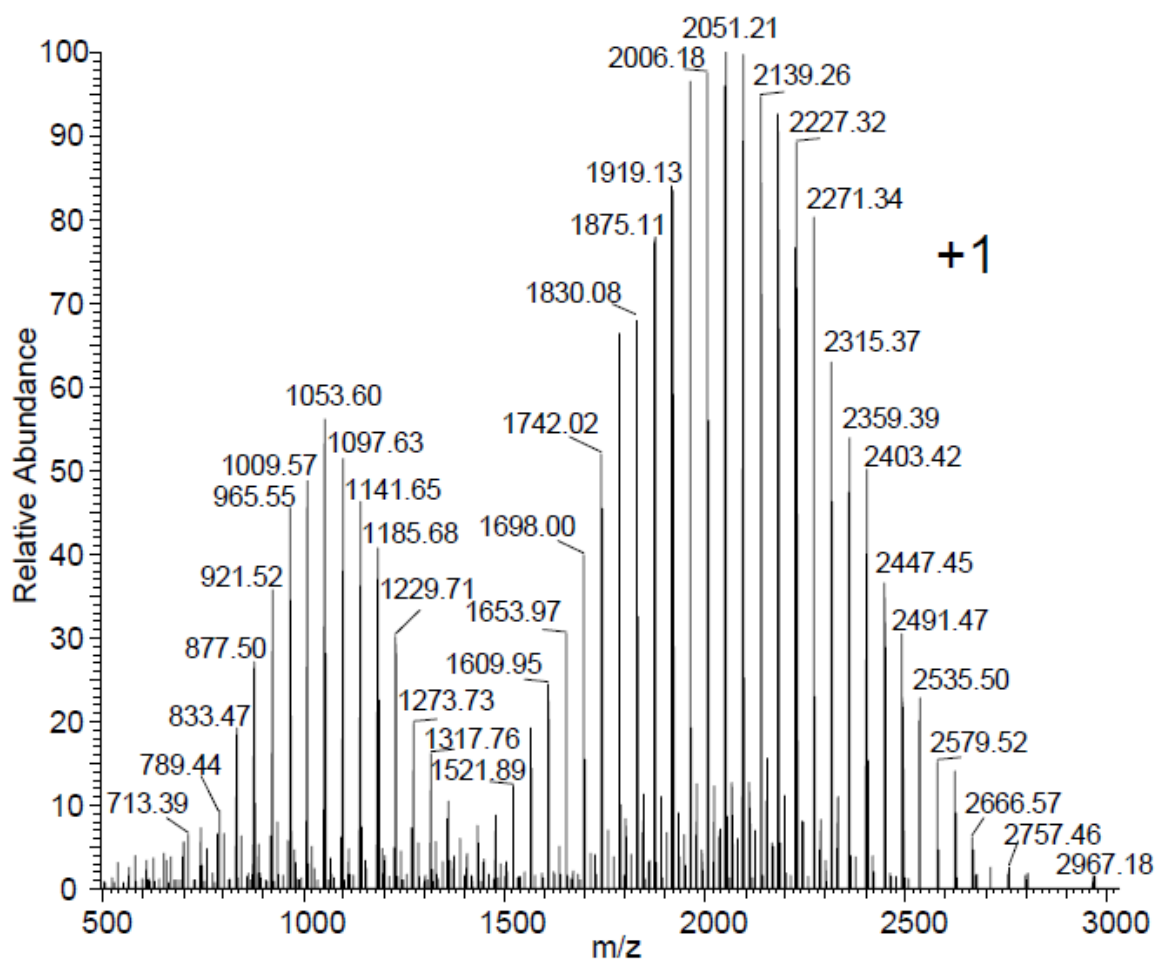
Figure S5. TG AP-MALDI mass spectrum of a mixture of PEG 970 and PEG DME 2160 in dithranol and NaCl prepared solvent-free.
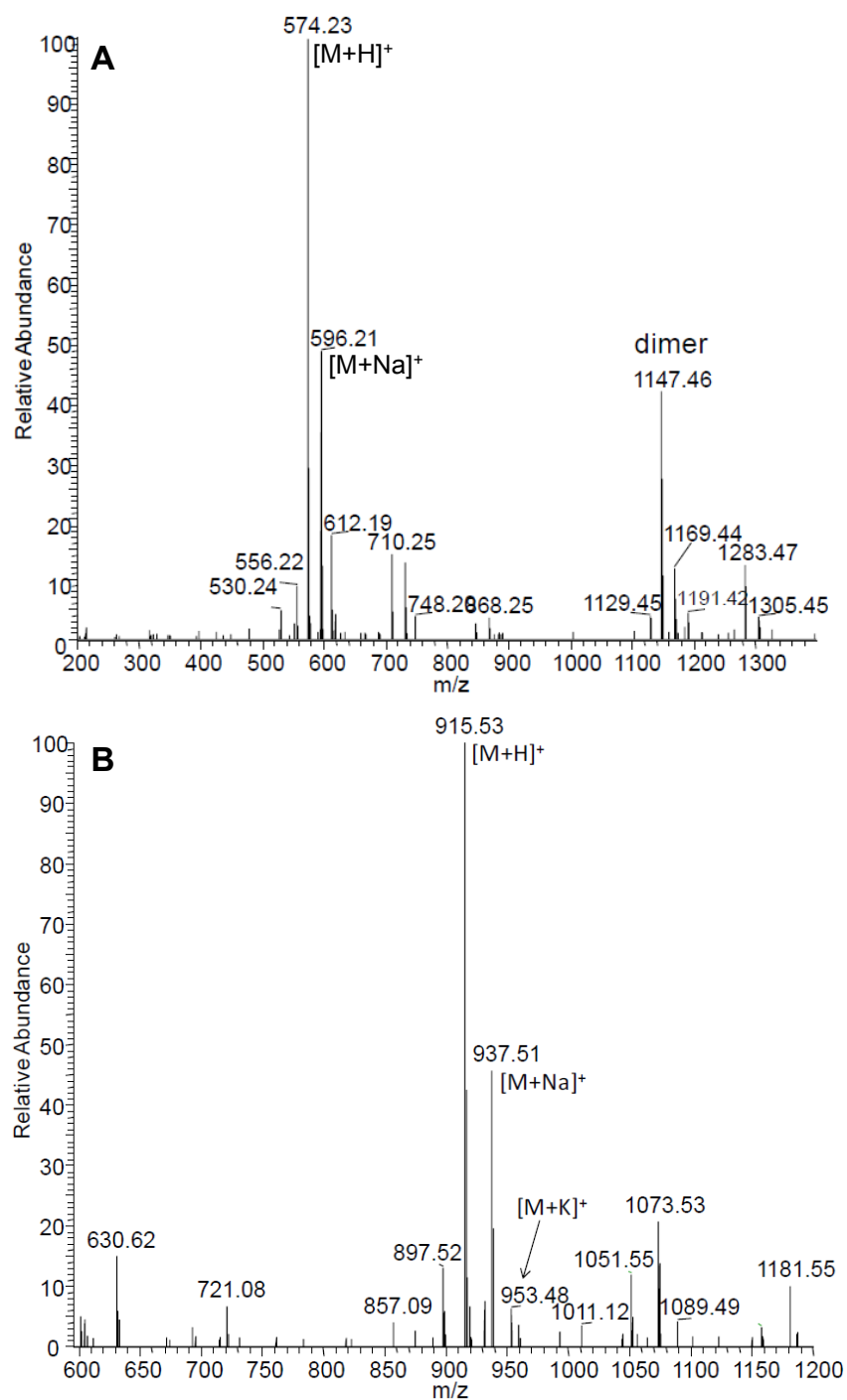
Figure S6: TG AP-MALDI mass spectrum of (**A**) Met-Enkephalin (MW 573.2) and (**B**) beta-amyloid (33-42) (MW 914.5) in 2,5-DHB prepared solvent-free.
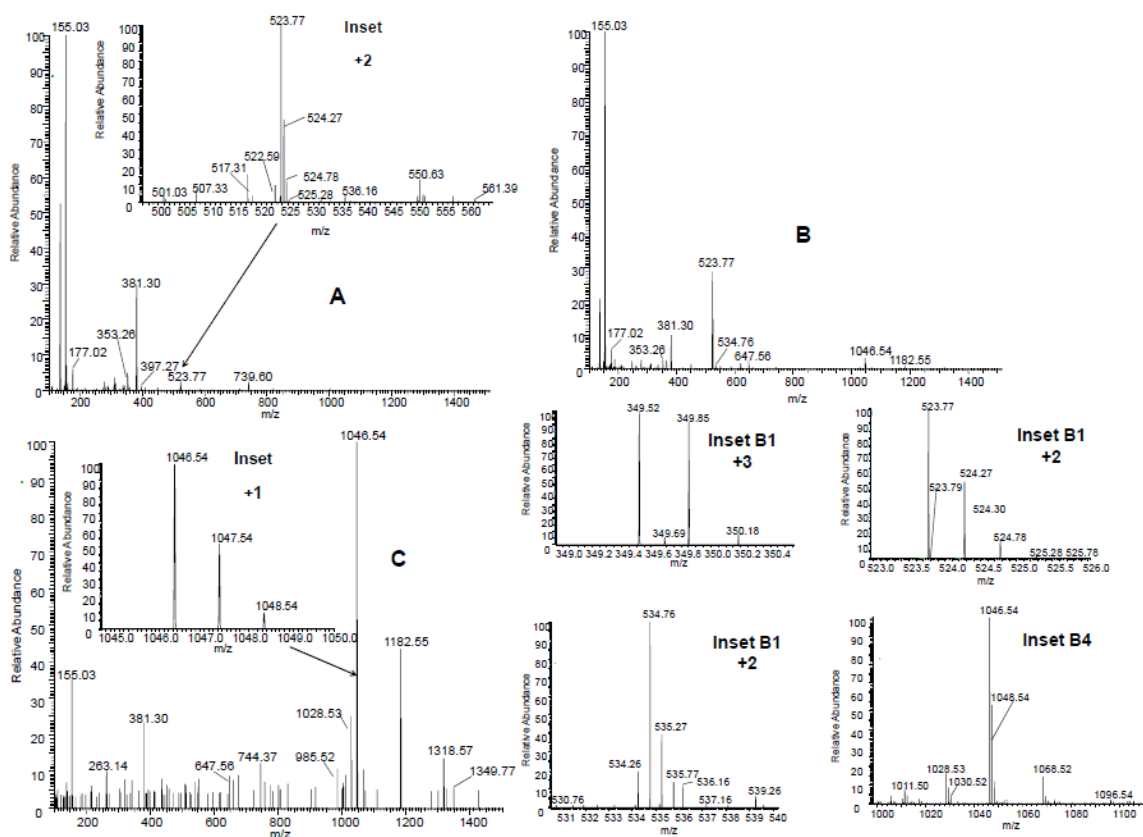
Figure S7: TG AP-MALDI mass spectra (with Inset regions) of angiotensin II (MW 1046.2) in a layered experiment by placing the analyte (1 μg) on the glass substrate, drying to completeness, and adding the 2,5-DHB matrix on top of the analyte using increasingly non-incorporating analyte/matrix conditions: **A)** aqueous, **B)** acetone, **C)** dichloromethane solution.
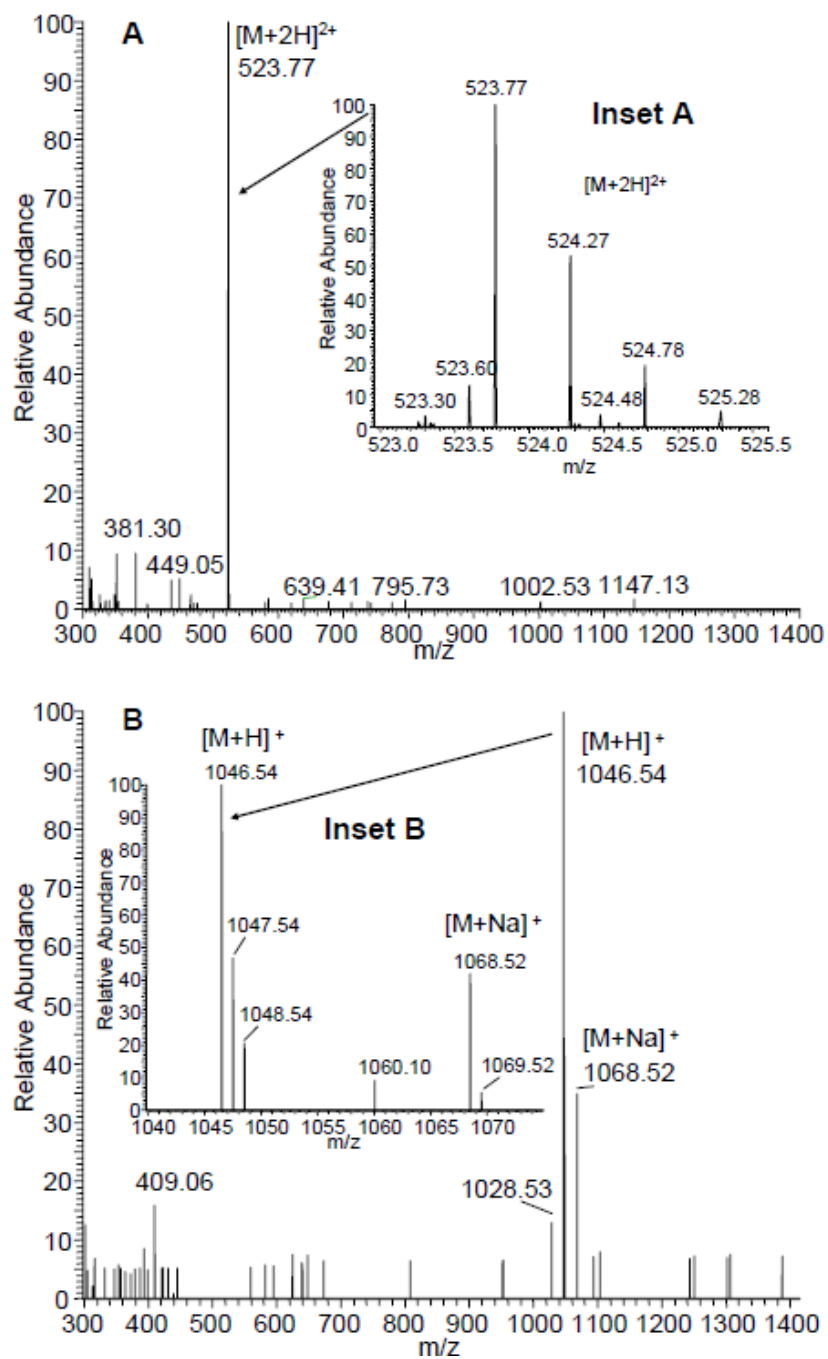
Figure S8: TG AP-MALDI mass spectrum of angiotensin II with **A)** 2,5-DHB: full mass: 30 pmol μL⁻¹; 50,000 resolution; 100,000 resolution. **B)** CHCA: 100,000 resolution with Inset regions.
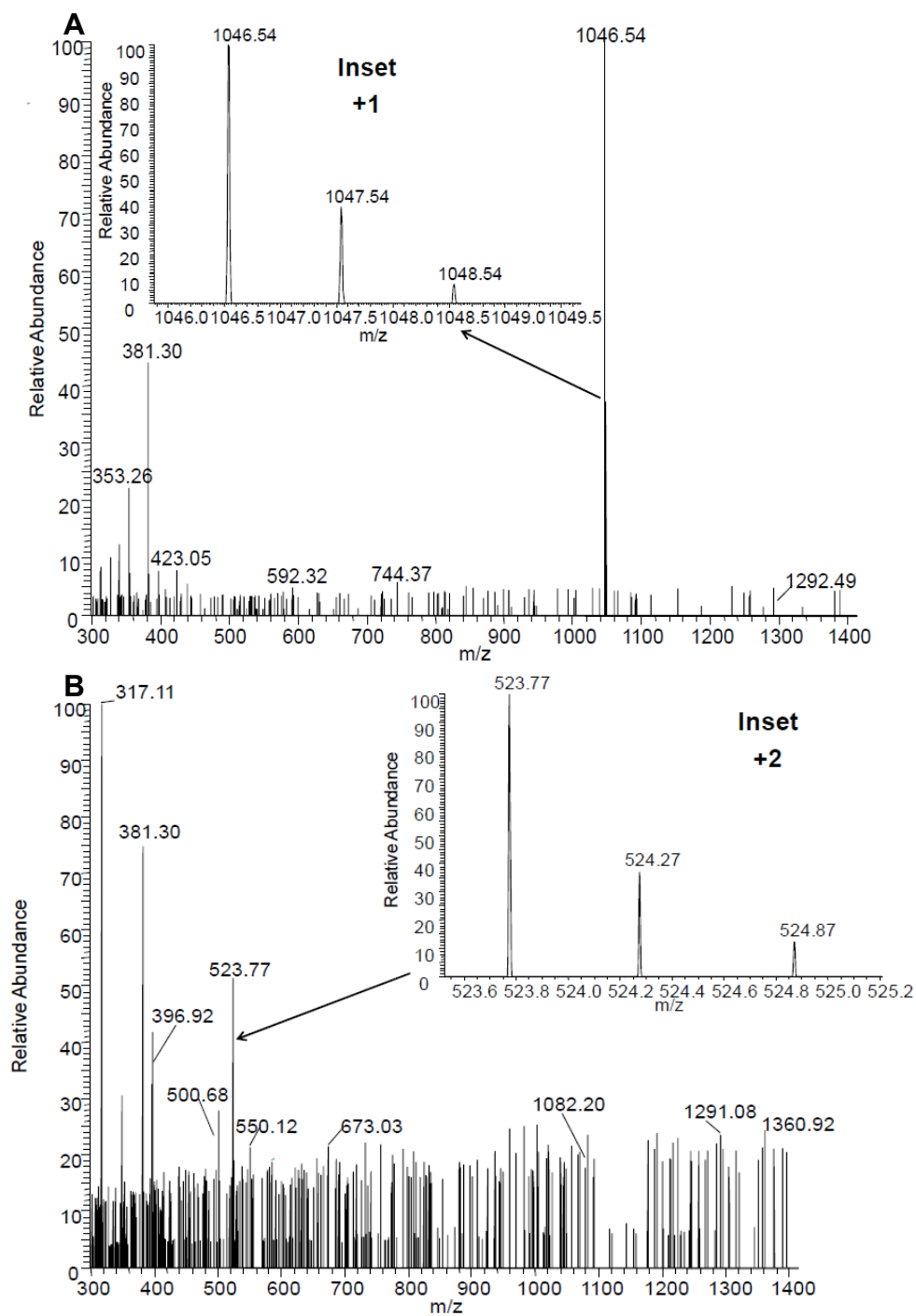
Figure S9: TG AP-MALDI mass spectra (single shot) of angiotensin II (MW 1045.5; 30 pmol μL^{-1}) in (**A**) benzoic acid matrix and (**B**) *o*-chlorobenzoic acid matrix; resolution 100,000; with Inset region.
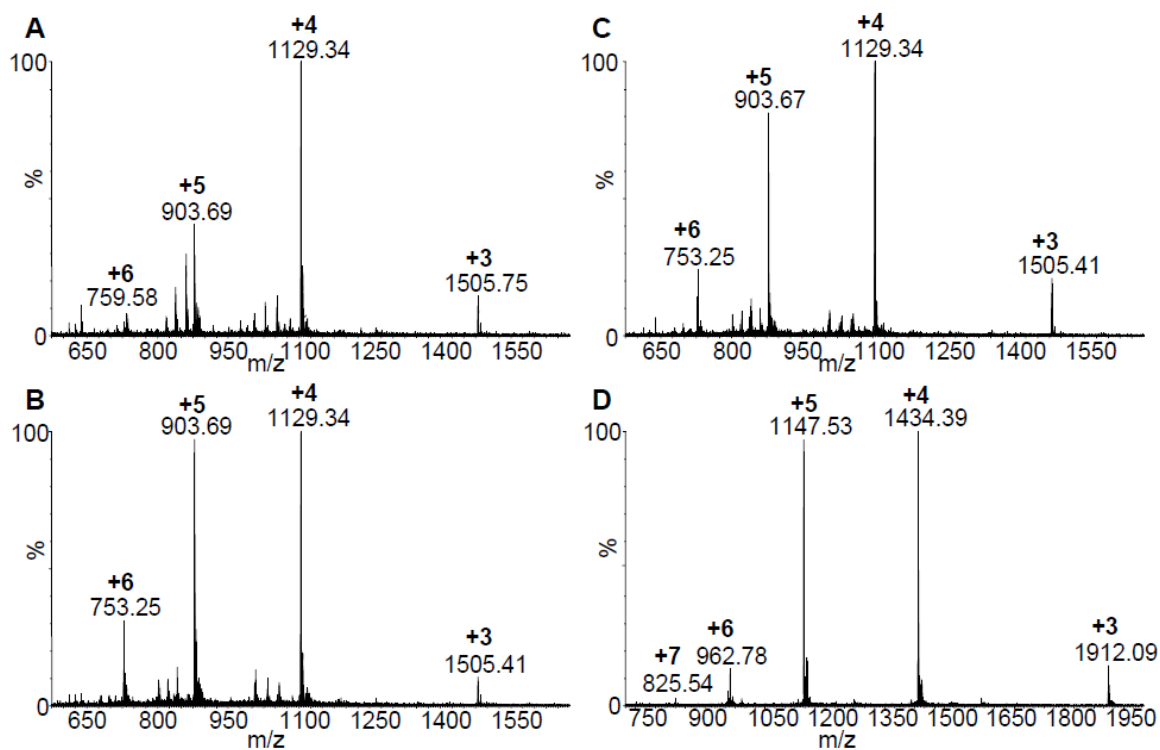
Figure S10: LSI-IMS-MS total mass spectra of (**A**) β-amyloid (1-42), (**B**) β-amyloid (42-1), (**C**) an isomeric mixture of β-amyloid (1-42) and (42-1) prepared in 50:50 ACN:water with 0.1% TFA and (**D**) insulin in 50:50 MeOH/water with 1 % acetic acid obtained without the use of the desolvation device but with the source temperature set at 150 °C using 2,5-DHAP matrix in 50:50 ACN:water employing the thin layer sample preparation.
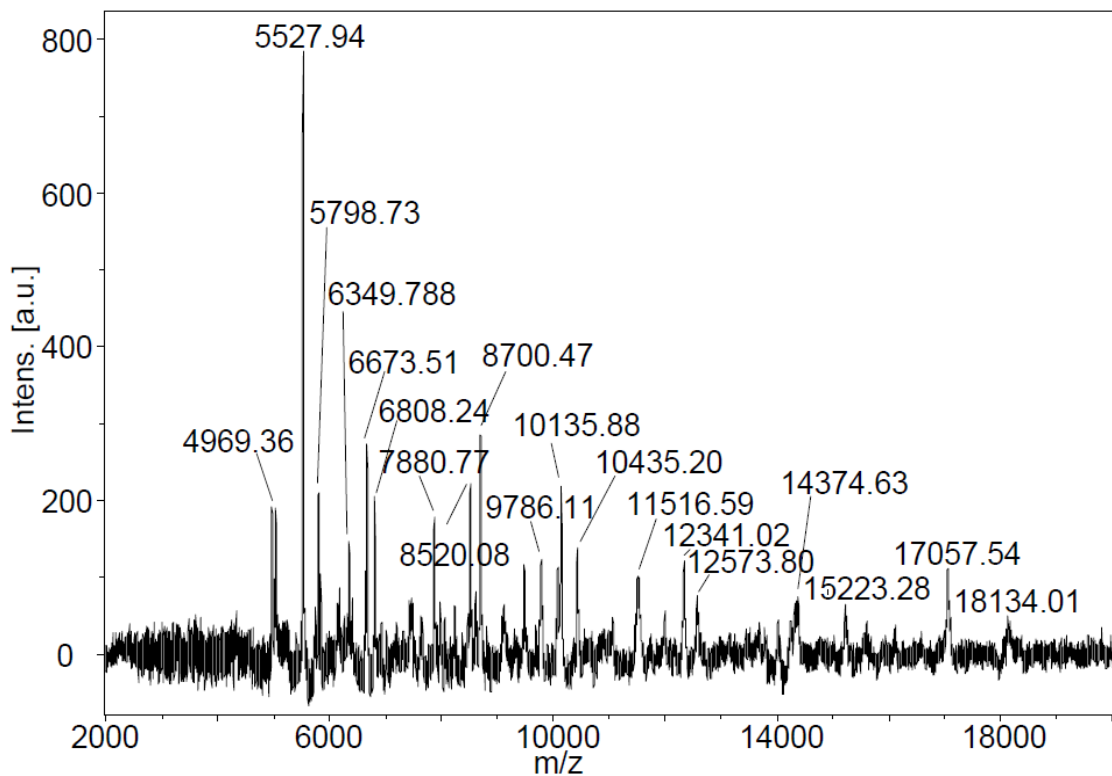
Figure S11: MALDI mass spectrum of delipified aged tissue on a plain glass slide using sinapinic acid as the matrix desolved in 50:50 ACN:water in 0.1% TFA.
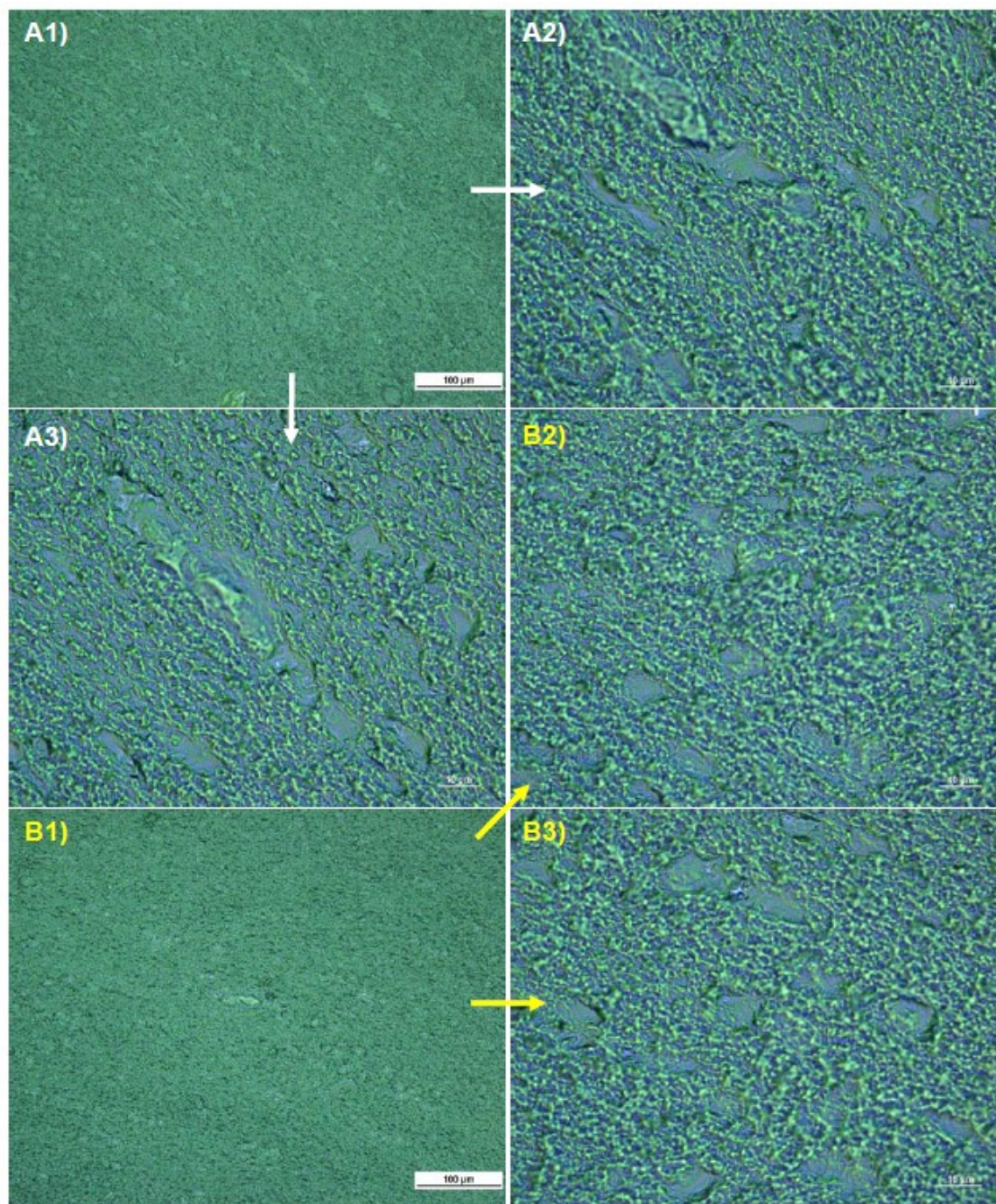
Figure S12: Microscopy after laser ablation using LSI-IMS of delipified aged tissue on a plain glass slide spotted with 2,5-DHAP matrix in 50:50 ACN:water. (**A1**) and (**B1**) 20x magnification and (**A2**), (**A3**), (**B2**), (**B3**) 100x magnification.
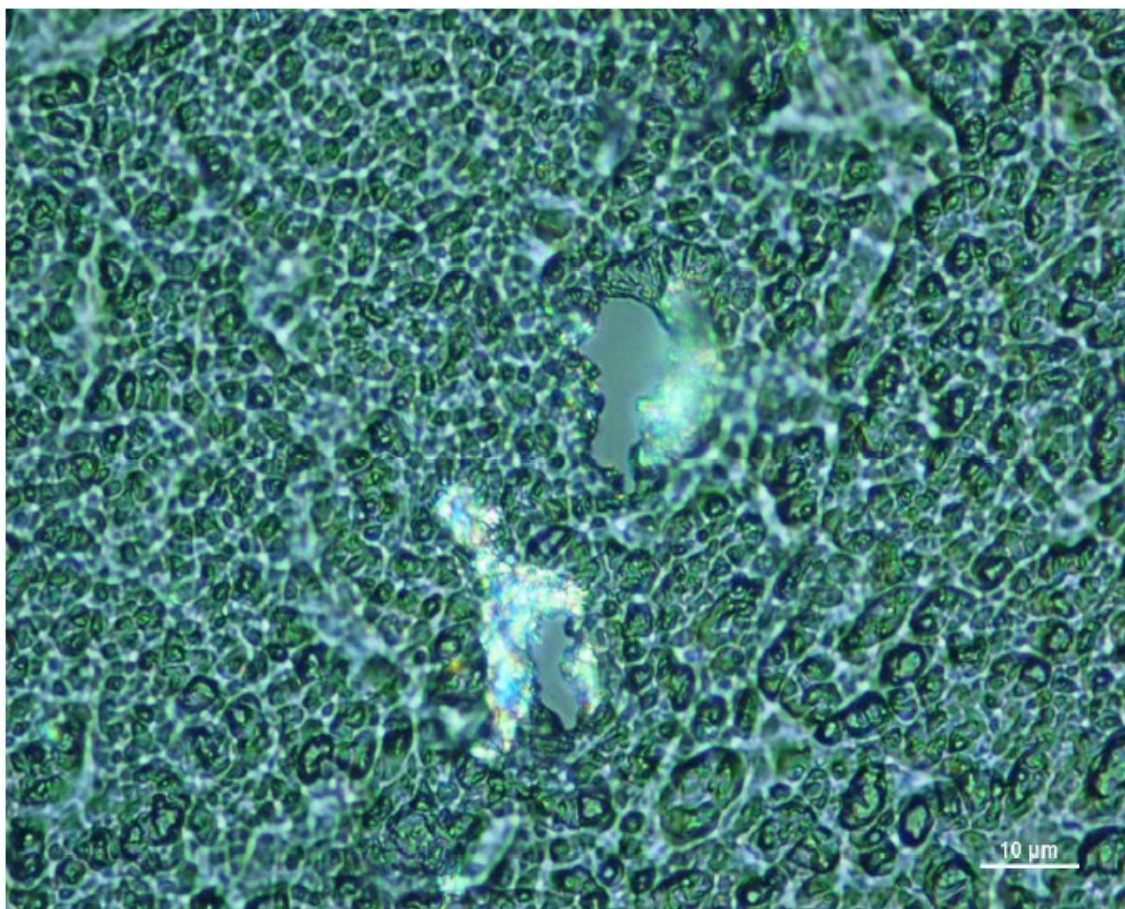
Figure S13: Optical microscopy image from delipified aged mouse brain tissue after LSI-MS analysis showing two ablated areas. The spatial resolution scale is shown in the lower right corner.
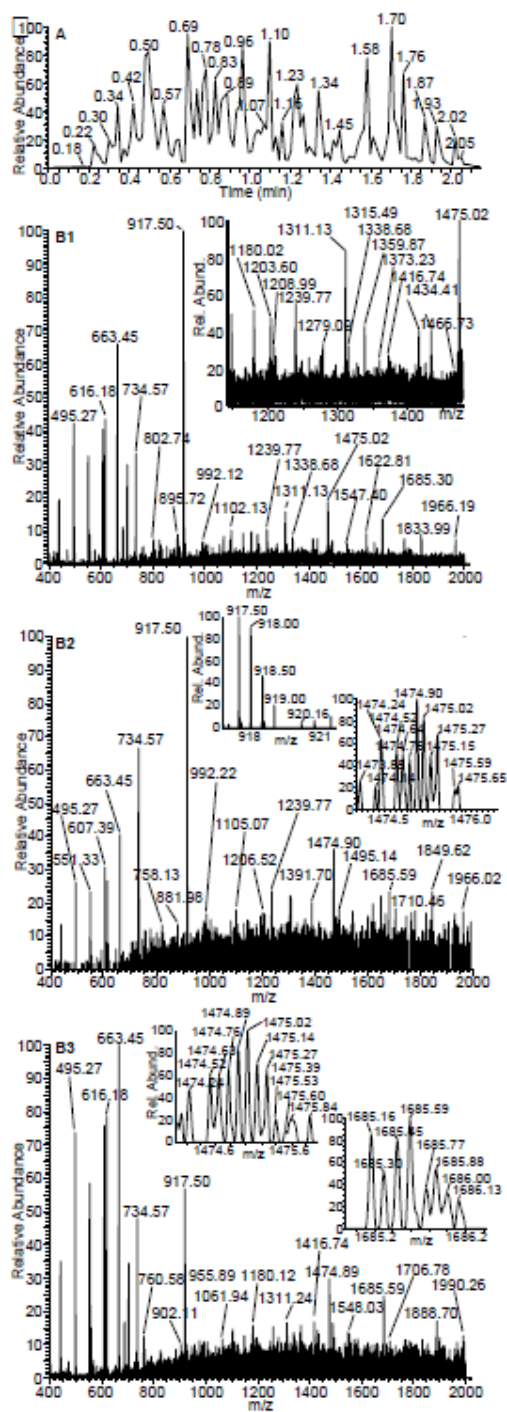
Figure S14: LSI mass spectra of delipified fresh tissue on gold coated glass slide spotted with 2,5- DHAP in 50:50 ACN:water using the Orbitrap Exactive. **A)** Total ion current; **B1)** Sum of 120 acquisitions; **B2)** single shot acquisition; **B3)** sum of 7 laser shot acquisitions.
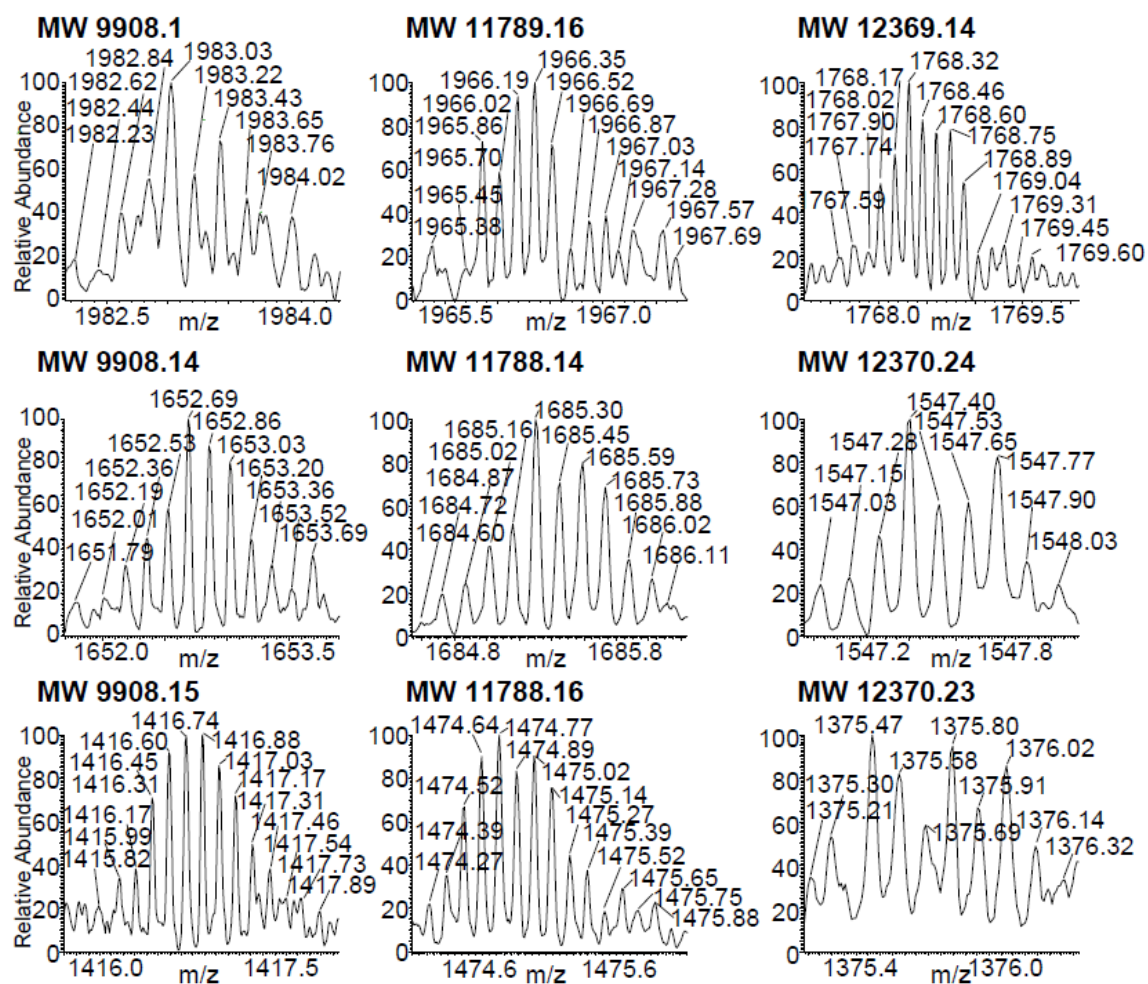
Figure S15: Insets of LSI mass spectra: Isotopic distributions of the proteins detected from delipified fresh tissue on a gold-coated glass slide spotted with 2,5-DHAP matrix in 50:50 ACN:water using the Orbitrap Exactive.
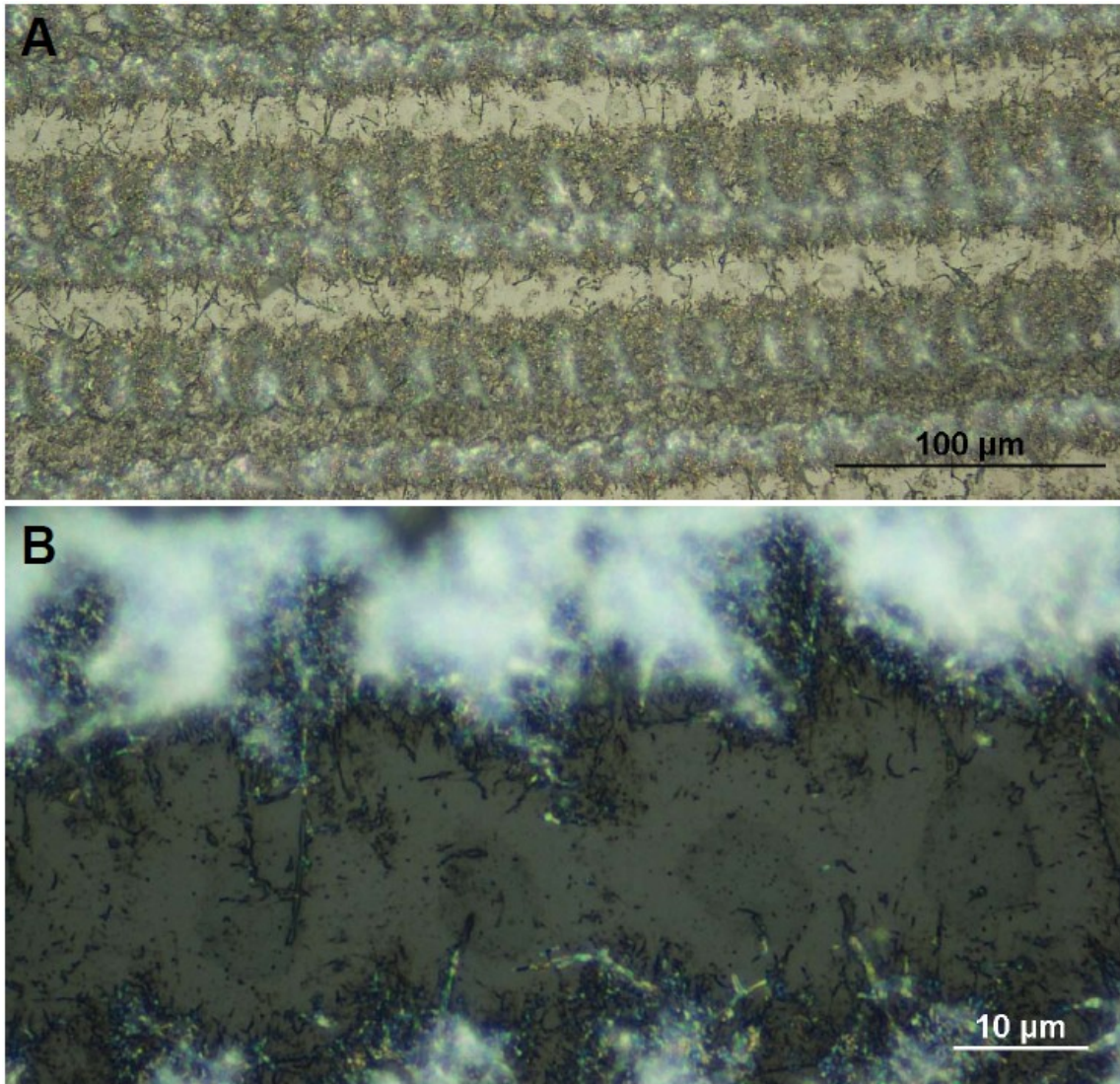
Figure S16: Optical images of laser ablated areas obtained in an imaging experiment on mouse brain tissue spray-coated with matrix using an airbrush: **A)** 20 X magnification and **B)** 100X magnification
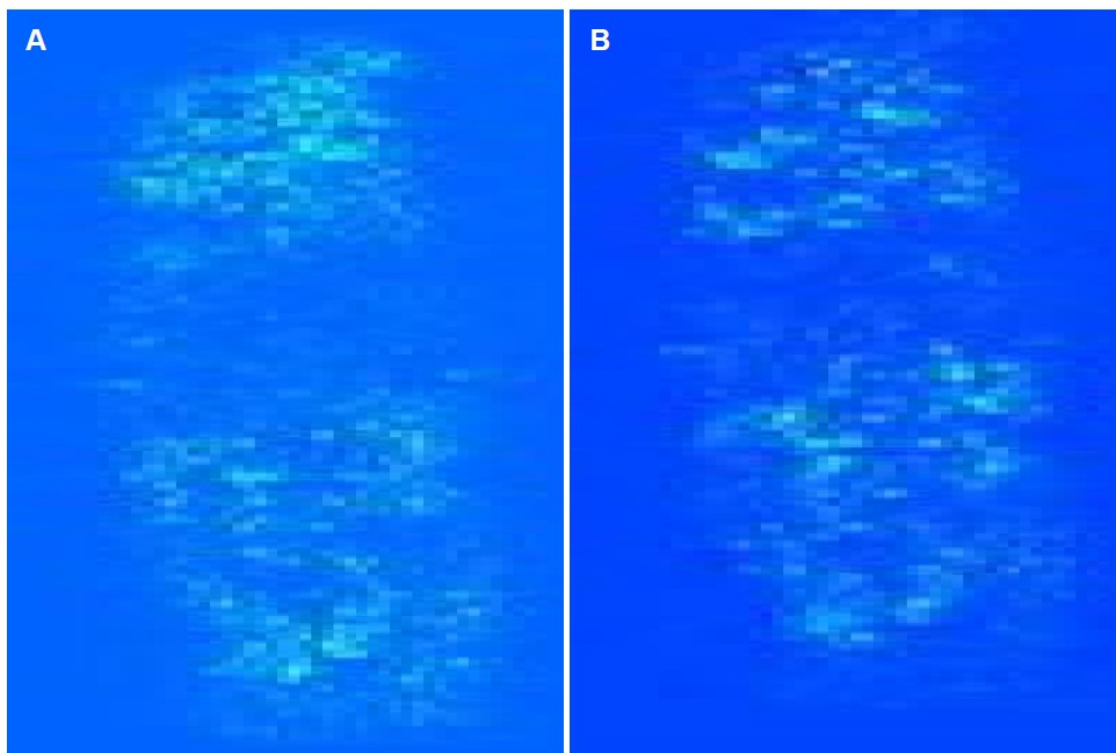
Figure S17: Mass specific images for the same charge state +8 of two different proteins: **A**) MW 11788 and **B**) MW 12369.
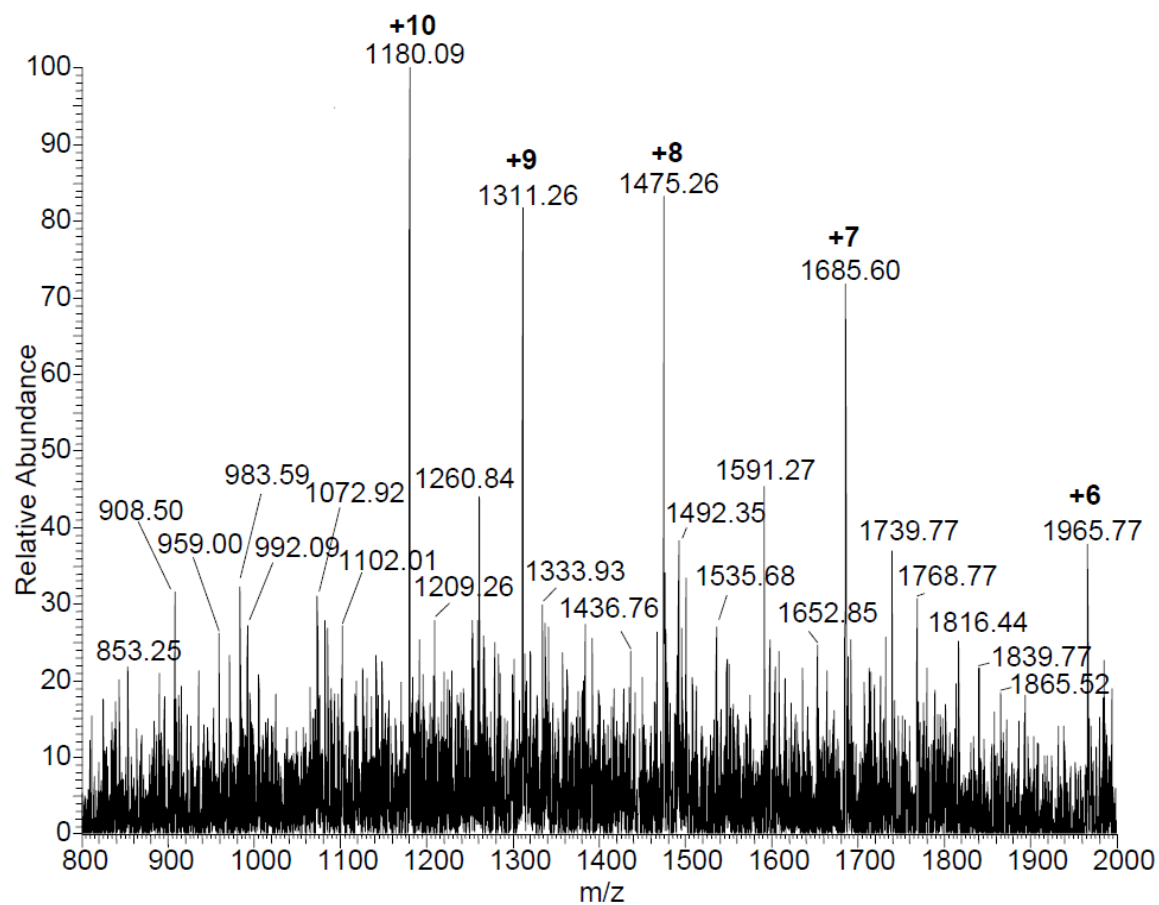
Figure S18: Single scan acquisition on the LTQ Velos obtained in imaging experiment. The protein with monoisotopic mass 11788 Da as determined on the Orbitrap Exactive is labeled with +6 to +10 charges.
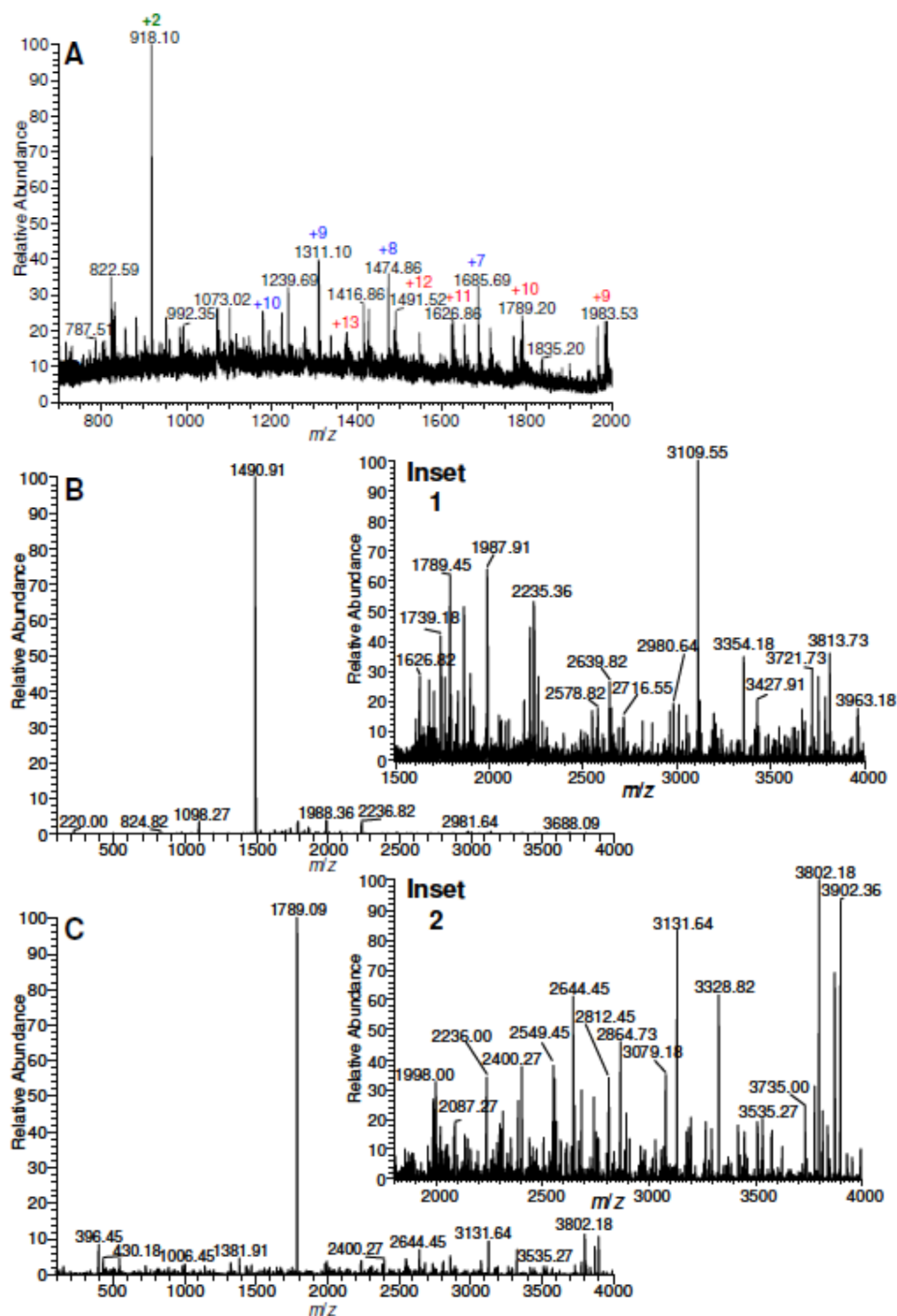
Figure S19: LSI-MS and MS/MS mass spectra using ETD obtained from delipified tissue spotted with 2,5-DHAP in 50:50 ACN:water. **A)** Full mass spectrum and ETD fragment ion mass spectra of **B)** *m/z* 1491 (+12) and **C)** *m/z* 1789 (+10) with Insets displaying the *m/z* range above the selected parent ions of (**1**) 1491 and (**2**) 1789.

APPENDIX B

Laserspray Ionization *Vacuum* Supplementary information
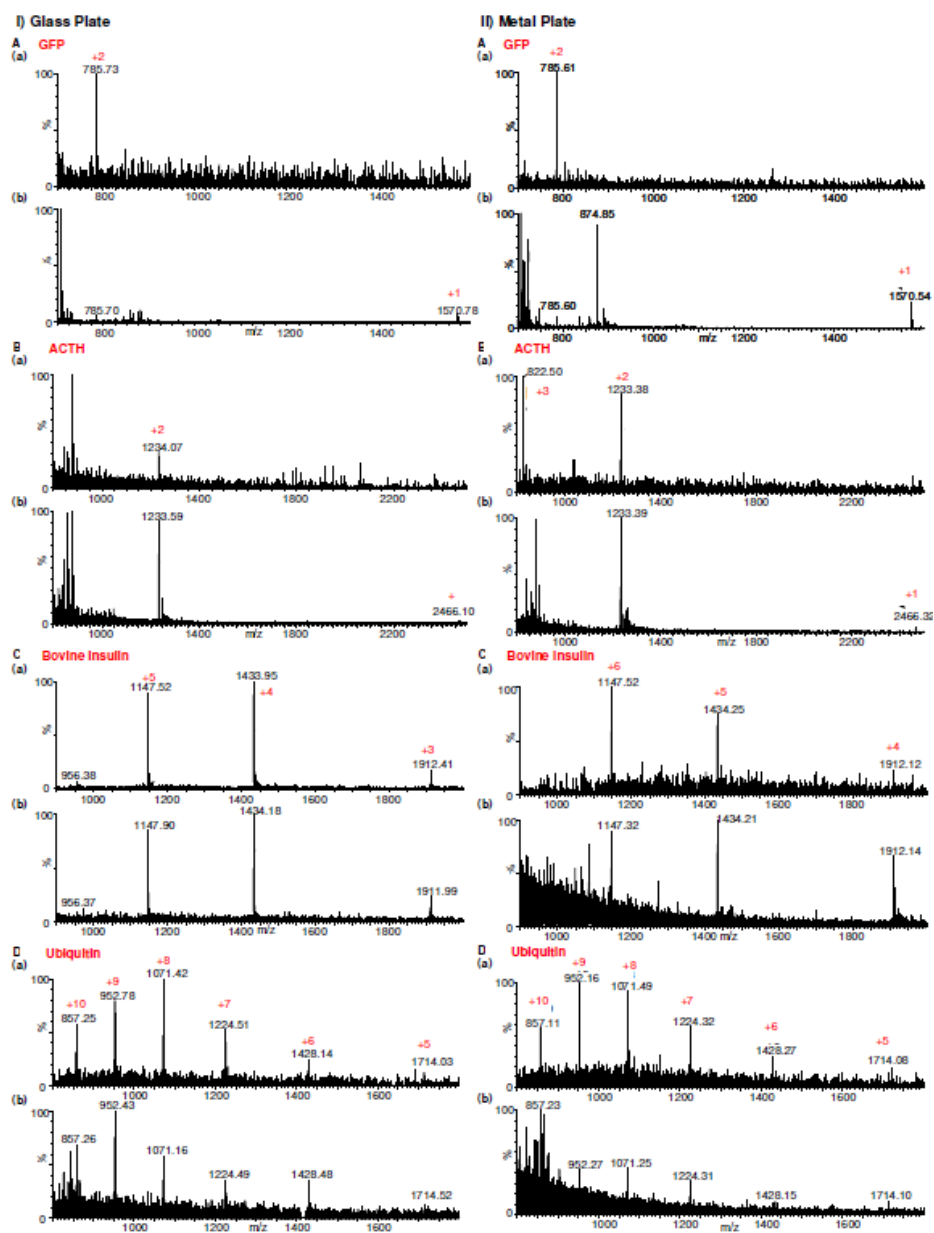
Figure S1. IP-LSI-MS mass spectra of peptides and proteins: (**A**) GFP, (**B**) ACTH, (**C**) insulin and (**D**) ubiquitin acquired using 2,5-DHAP matrix prepared in 50:50 ACN:water using laser energy of (**a**) "200" and (**b**) "500" on different target plates: (**I**) glass plate and (**II**) metal plate.
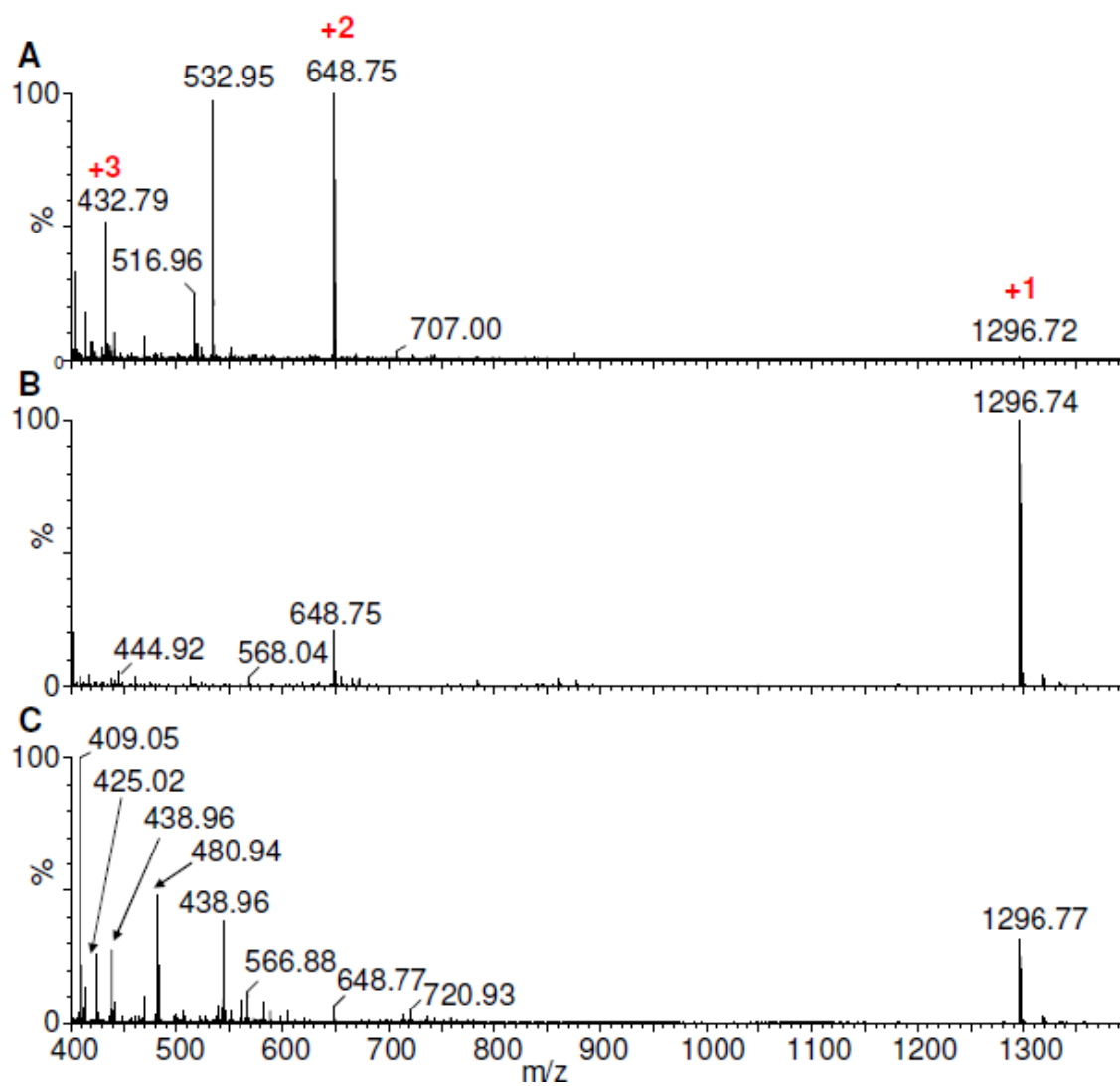
Figure S2. IP-LSI-MS mass spectra of angiotensin I (MW 1295) acquired from different matrixes: (**A**) 2,5-DHAP in 50:50 ACN:water, (**B**) CHCA, and (**C**) 2,5-DHB both in 50:50 ACN:water with 0.1% TFA using laser energy of "500".
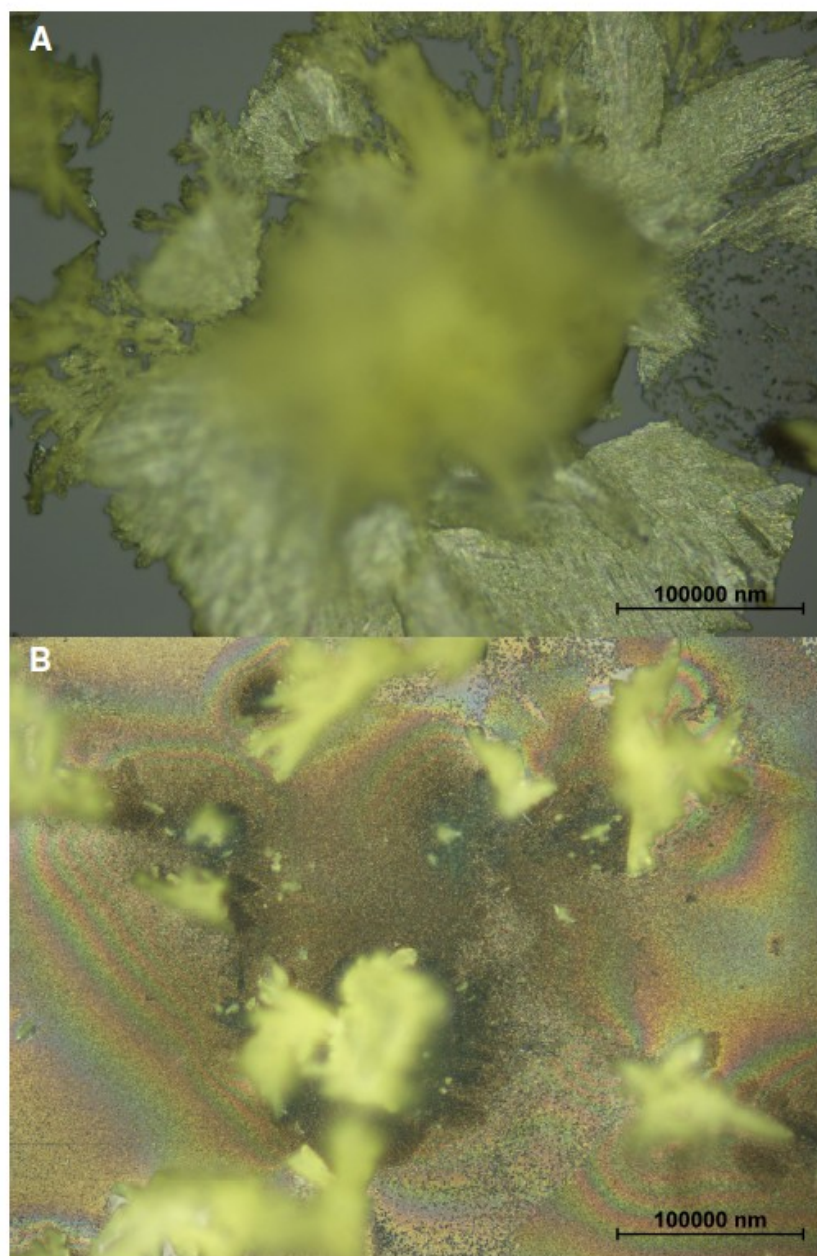
Figure S3. Photographs of the microscopy of the analyte/matrix mixture spot of angiotensin 1 (**A**) before ablation and (**B**) after ablation using 200 laser energy. Analyte/matrix mixture prepared in 1:1 volume ratio using 2,5-DHAP matrix in 50:50 ACN:water. The center spot (**A**) provides preferentially the multiply charged ions **(Figure S4)**.
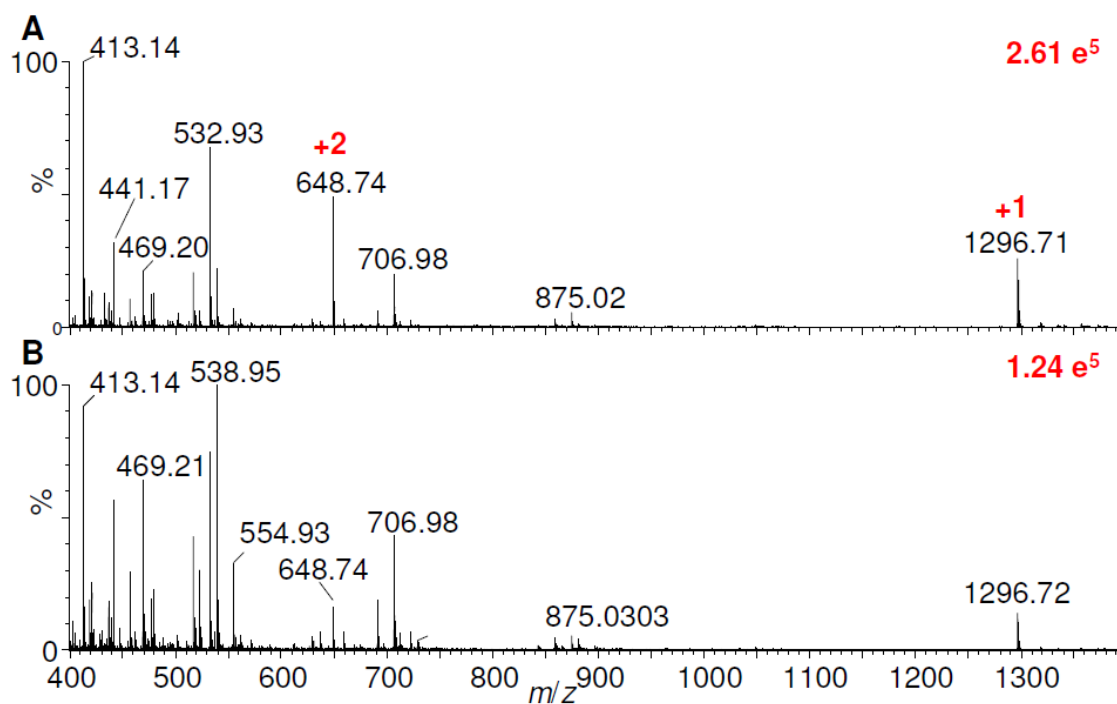
Figure S4. Comparison of the IP-LSI-MS mass spectra of angiotensin 1 (MW 1295) acquired using 2,5-DHAP matrix prepared in 50:50 ACN:water between (**A**) large and (**B**) needle-like crystals after deposition of analyte/matrix mixture (**Figure S3**). Laser energy used was "500".
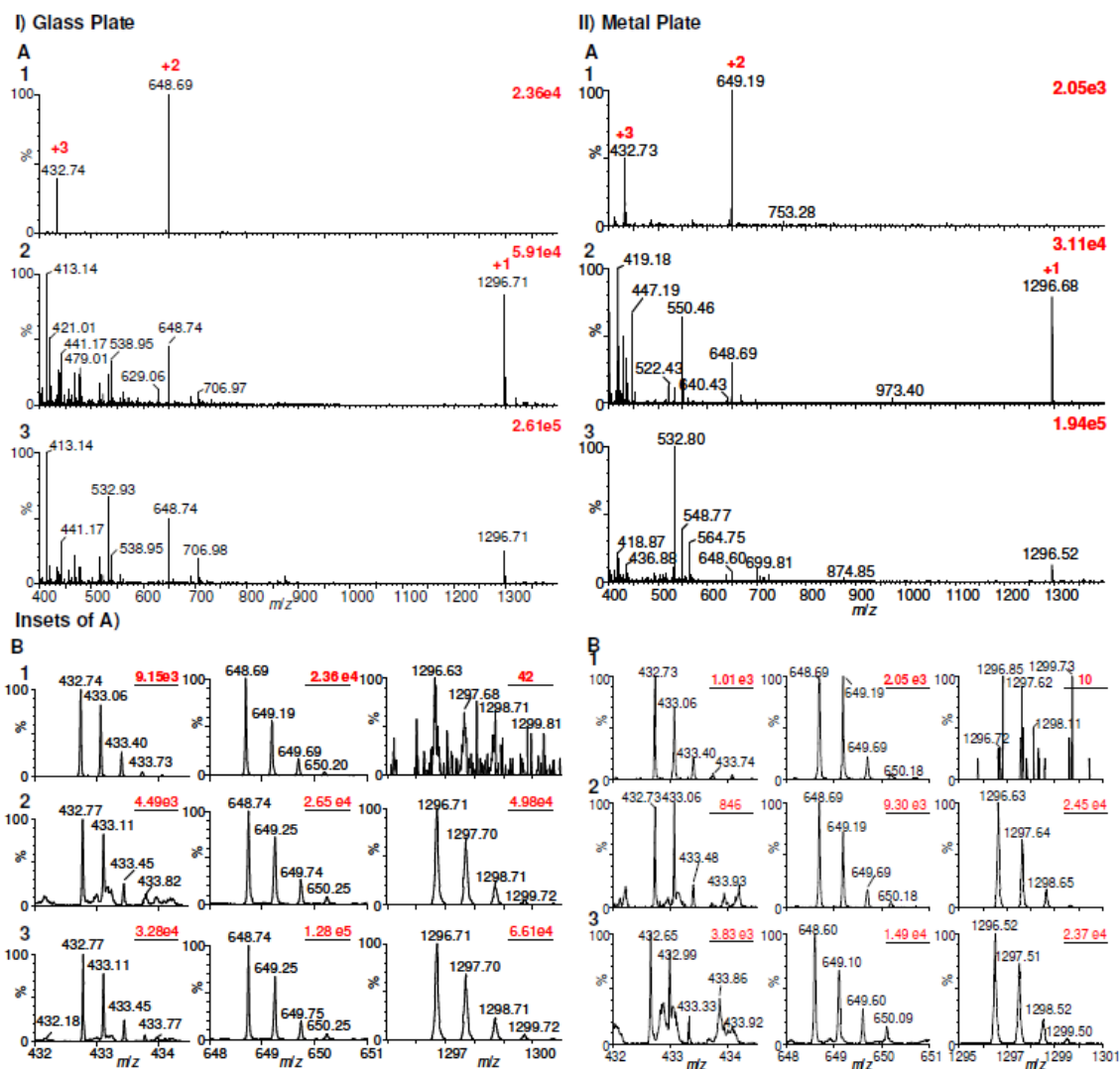
Figure S5. IP-LSI-MS mass spectra of angiotensin I (MW 1295) acquired using 2,5-DHAP matrix prepared in 50:50 ACN:water from (I) glass plate and (II) metal plate with different laser fluence: (**1**) "200", (**2**) "300", and (**3**) "500". (**A**) Full mass spectra and (**B**) insets of +3, +2, and +1.
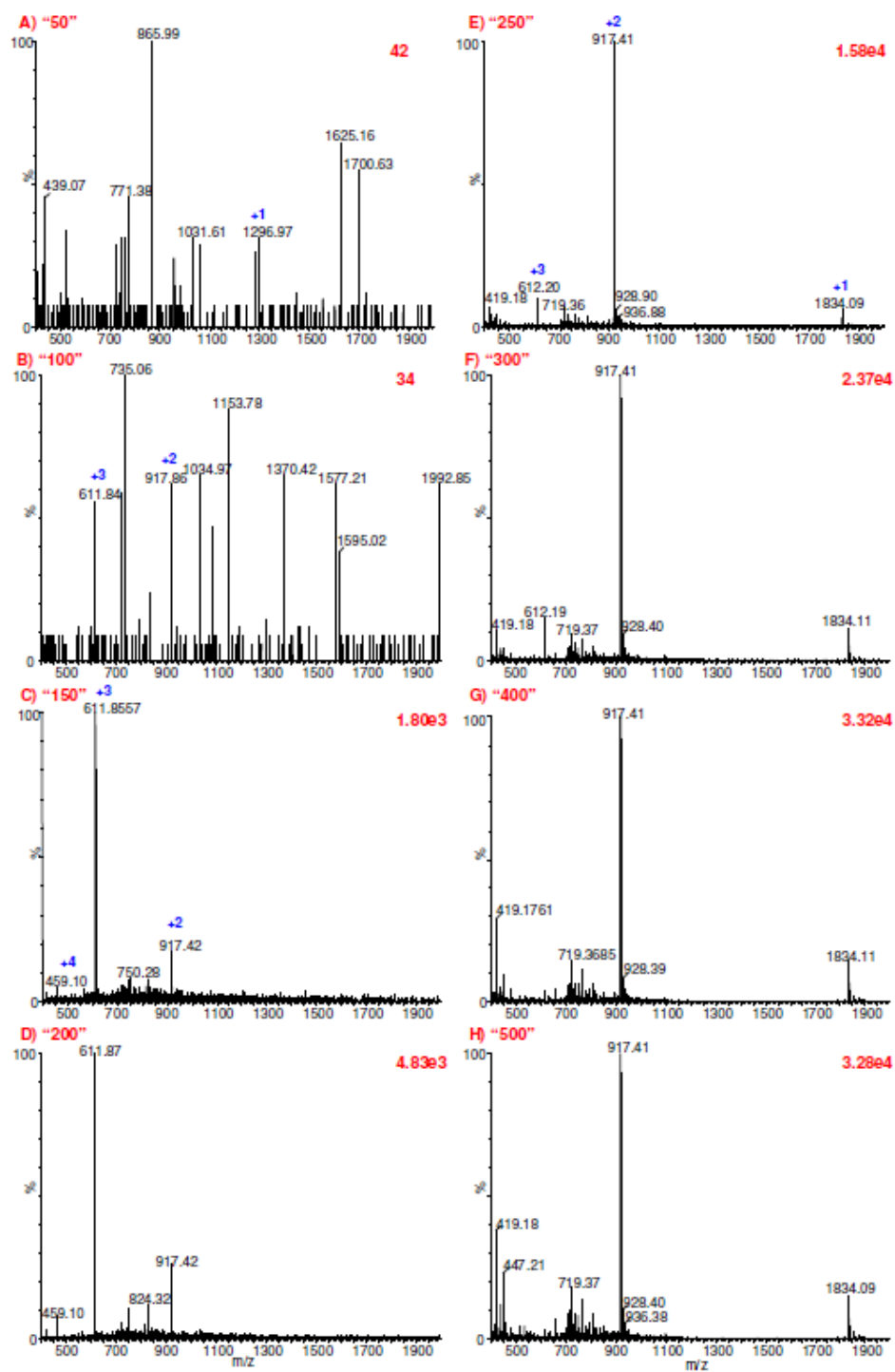
Figure S6. IP-LSI-MS mass spectra of *N*-acetylated fragment of MBP (MW 1833) acquired using 2,5-DHAP matrix prepared in 50:50 ACN:water at different laser fluence from **A)** "50" to **H)** "500".
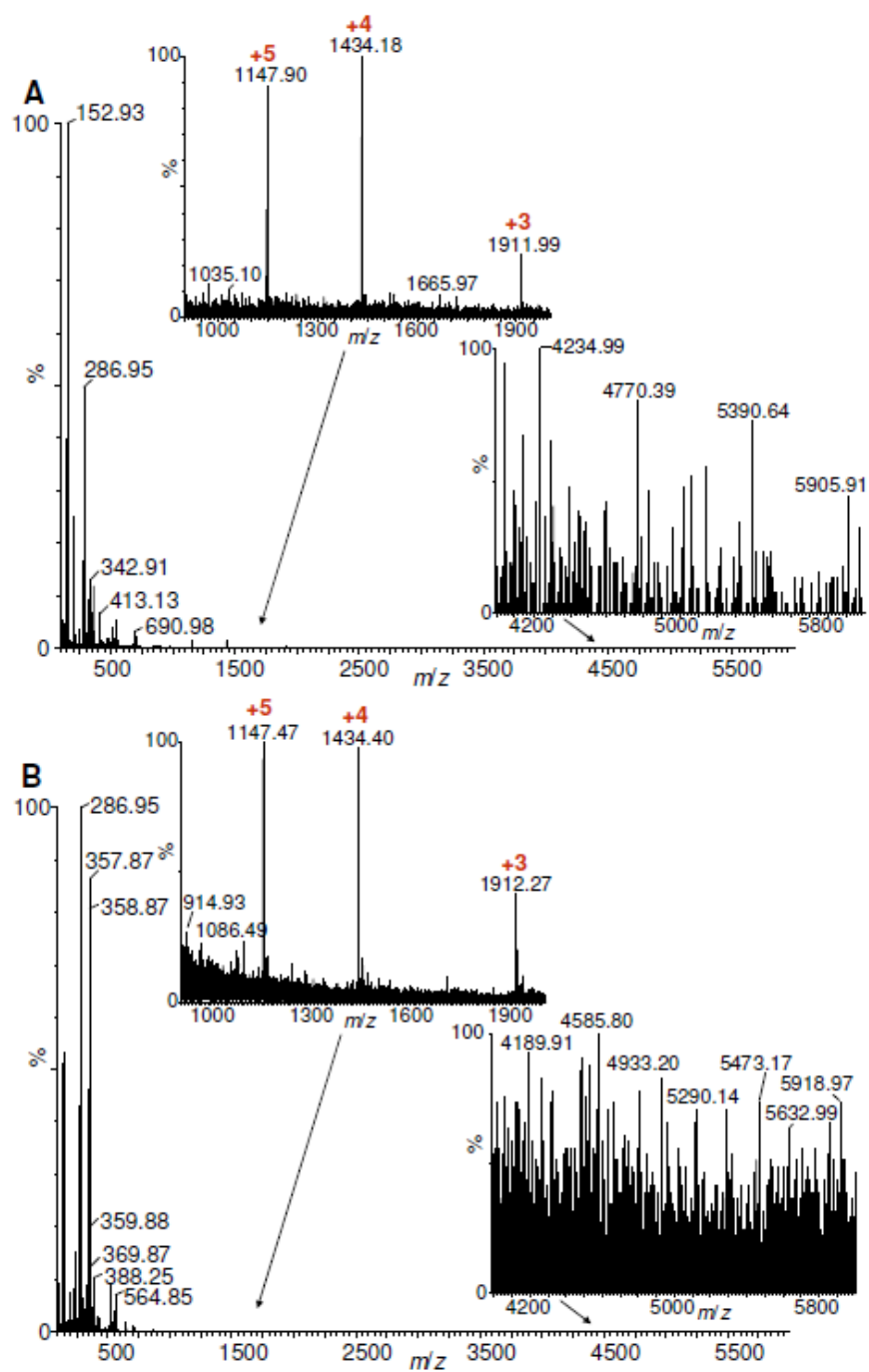
Figure S7. IP-LSI-MS of bovine insulin using 2,5-DHAP matrix in 50:50 ACN:water acquired in full mass range. (**A**) Glass Plate and (**B**) Metal Plate.
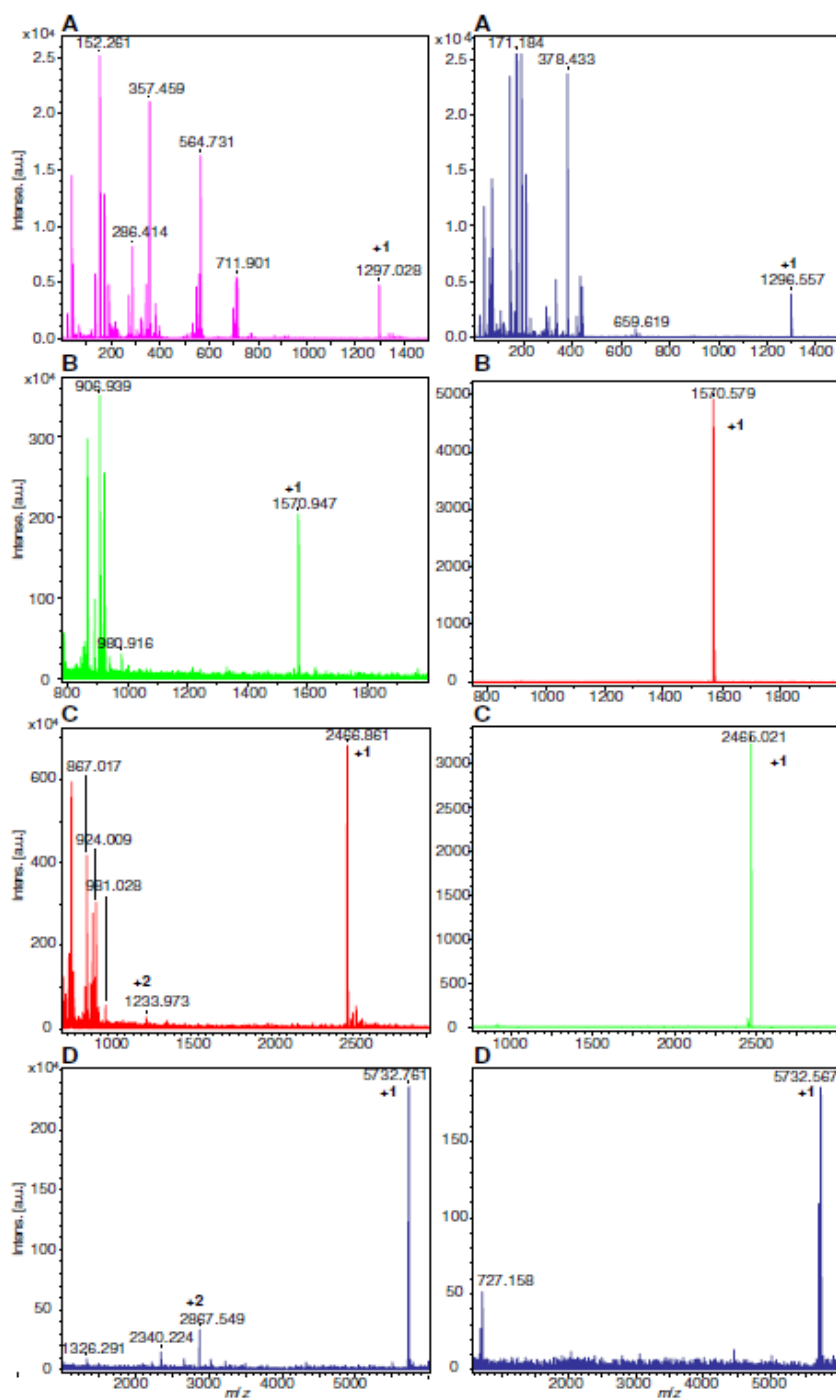
Figure S8. MALDI-TOF-MS mass spectra of (**A**) Angiotensin I (MW 1295), (**B**) [Glu-1]-fibrinopeptide B (MW 1569), (**C**) adrenocorticotropic hormone fragment (MW 2465), and (**D**) bovine insulin (MW 5731) acquired under high vacuum conditions using the same analyte/matrix mixture used to obtain the mass of spectra of IP-LSI-IMS-MS using 2,5-DHAP matrix prepared in 50:50 ACN:water.
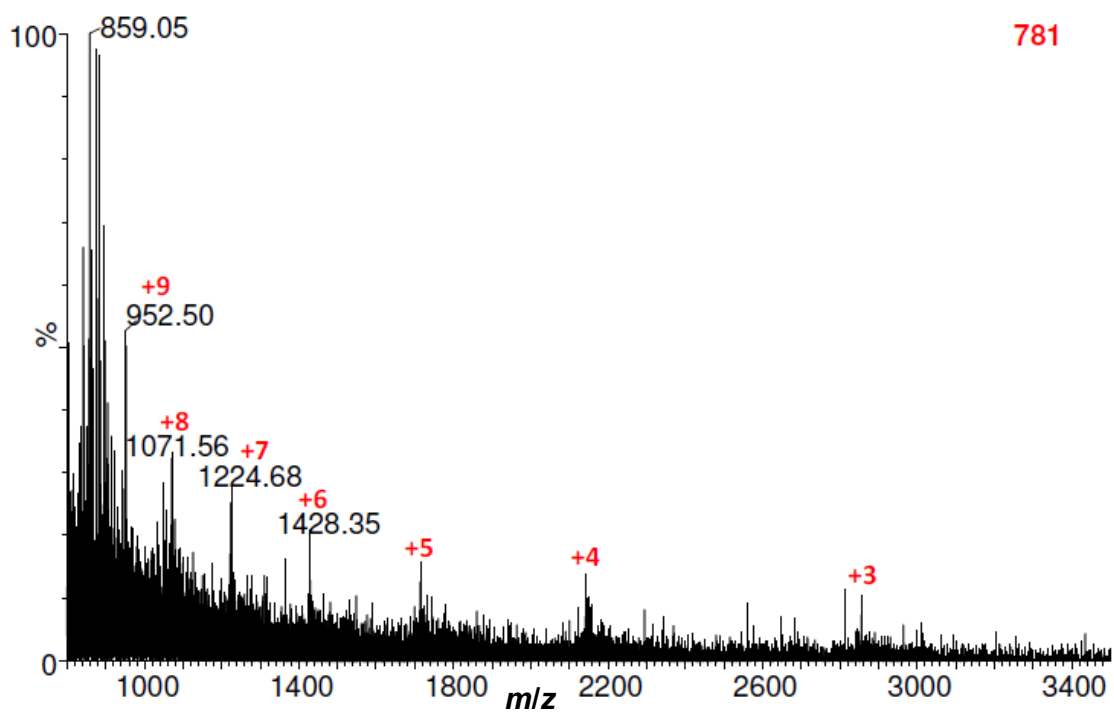
Figure S9. IP-LSI-MS mass spectrum of ubiquitin (MW 8561) acquired using 2,5-DHAP matrix prepared in 50:50 ACN:water using laser energy of "500".
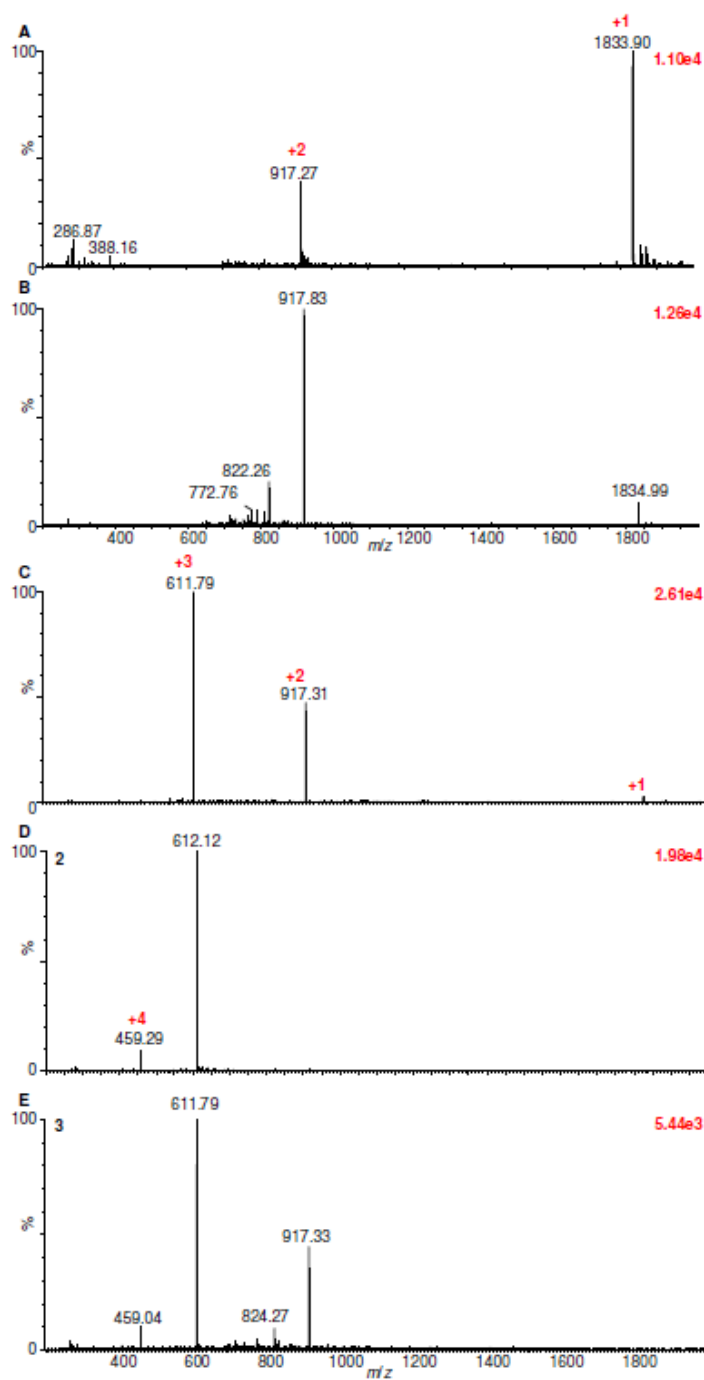
Figure S10. IP-LSI mass spectra of synthesized N-acetylated terminal fragment of myelin basic protein acquired using 2,5-DHAP matrix prepared in 50:50 ACN:water using low laser fluence: **A)** TOF (cooling gas 10 mL min-1 and trap gas flow (2.5 mL min^{-1}) and **B)** IMS-TOF modes with He cell and IMS gas flow at 24 mL min^{-1}; **C)** He cell (180 mL min^{-1}), **D)** IMS cell (90 mL min^{-1}) and **E)** both gas flows increased.
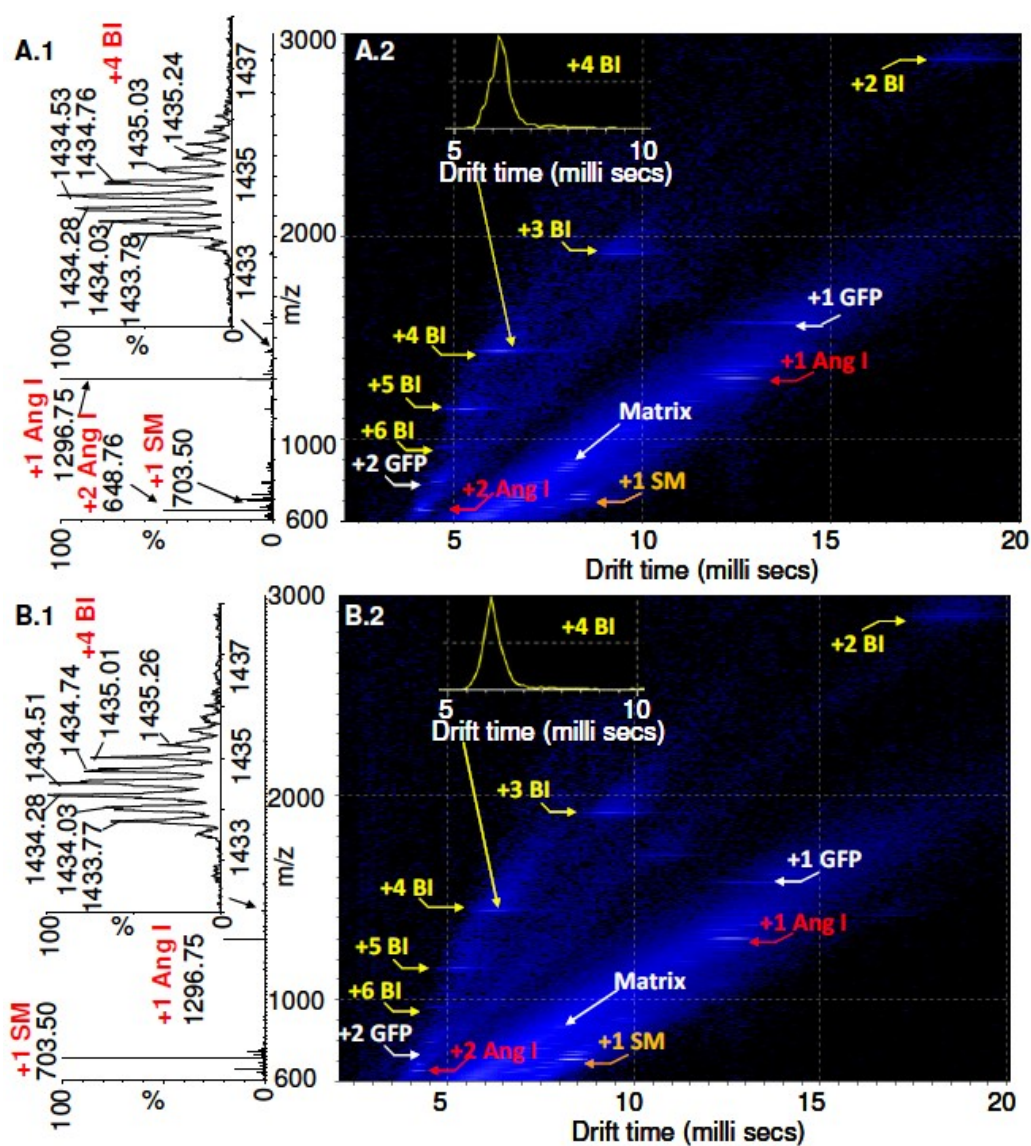
Figure S11. IP-LSI-IMS-MS of the model mixture (SM, Ang I, GFP, and BI) acquired using 2,5-DHAP matrix prepared in 50:50 ACN:water from (**A**) glass plate and (**B**) metal plate. (**1**) Total mass spectrum with an inset +4 charged state distribution of BI and (**2**) 2-D plot of drift time *vs. m/z* and drift time distribution of +4 for BI.
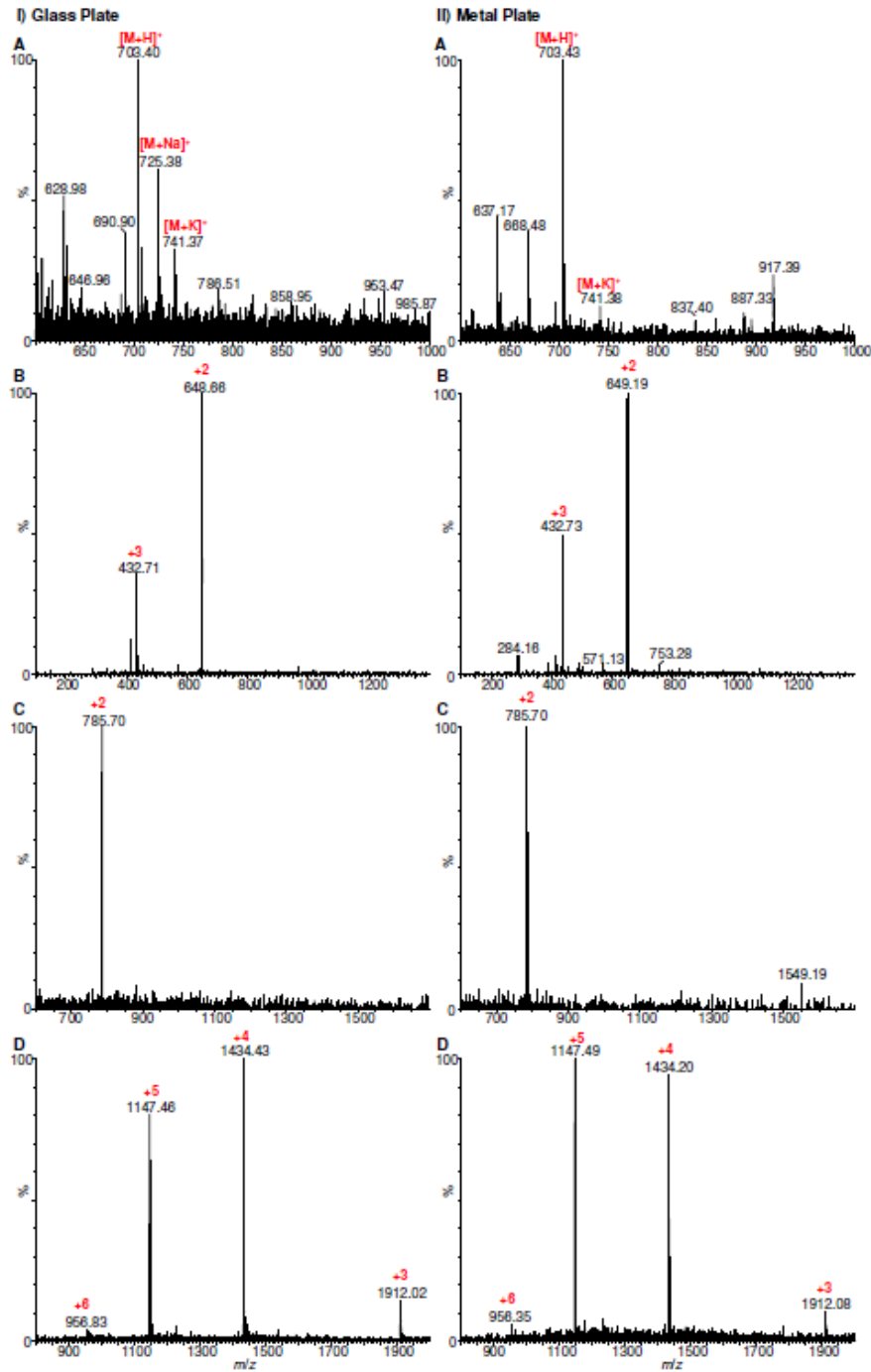
Figure S12. IP-LSI mass spectra of the pure components in the model mixture using 2,5-DHAP matrix prepared in 50:50 ACN:water using low laser energy of "200" from (**I**) glass and (**II**) metal plates.: lipid **A)** sphingomyelin MW 703, peptides **B) a**ngiotensin I MW 1295 and **C)** [Glu-1]-fibrinopeptide B MW 1569, and a protein **D)** bovine insulin MW 5731.
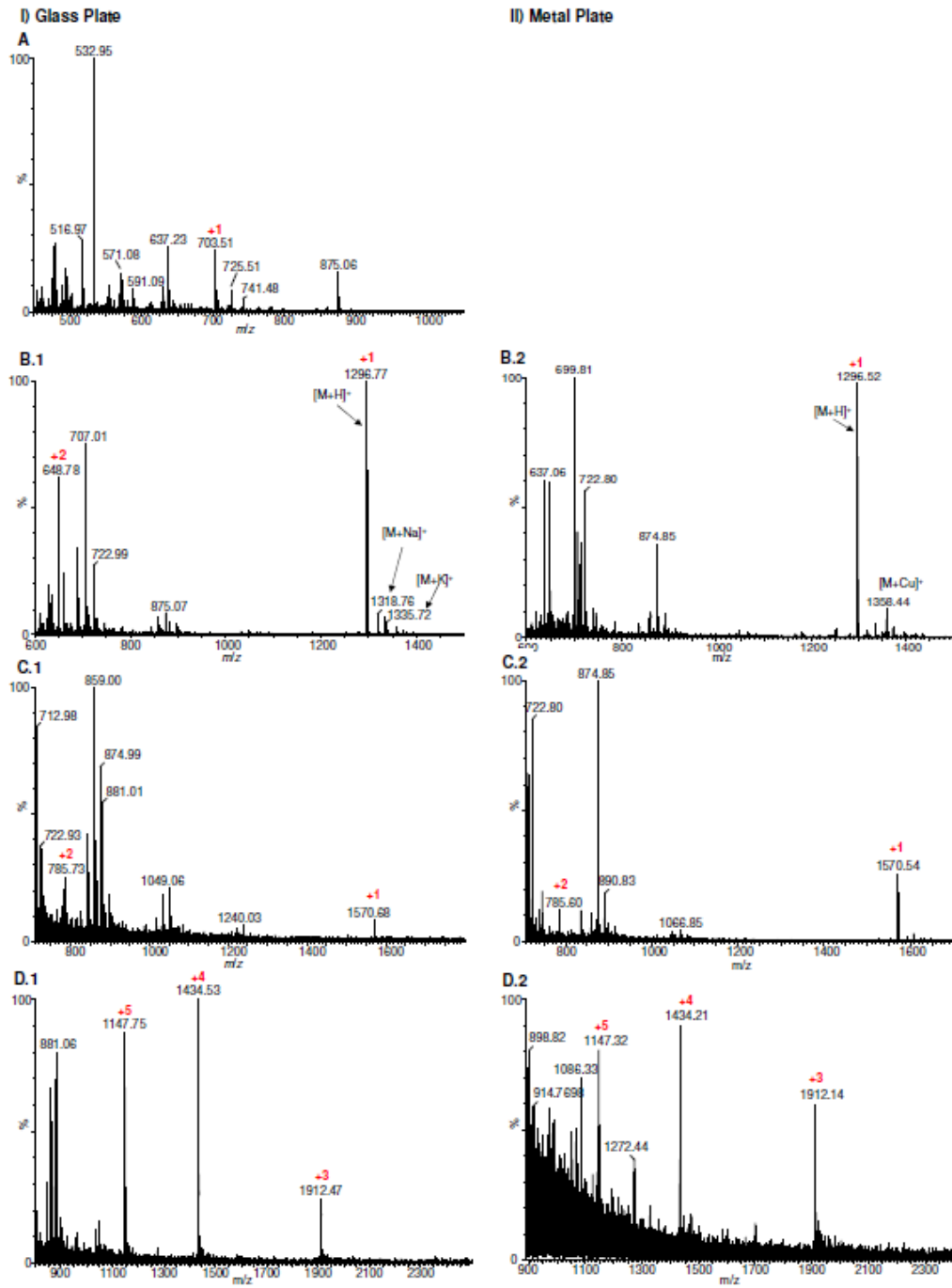
Figure S13. IP-LSI mass spectra of the pure components in the model mixture using 2,5-DHAP matrix prepared in 50:50 ACN:water using laser energy of "500" from (**I**) glass and (**II**) metal plates: lipid (**A**) sphinomyelin (MW 703), peptides (**B**) Angiotensin 1 (MW 1295), (**C**) [Glu-1]-fibrinopeptide B (1569) and a protein (**D**) bovine insulin (MW 5731).
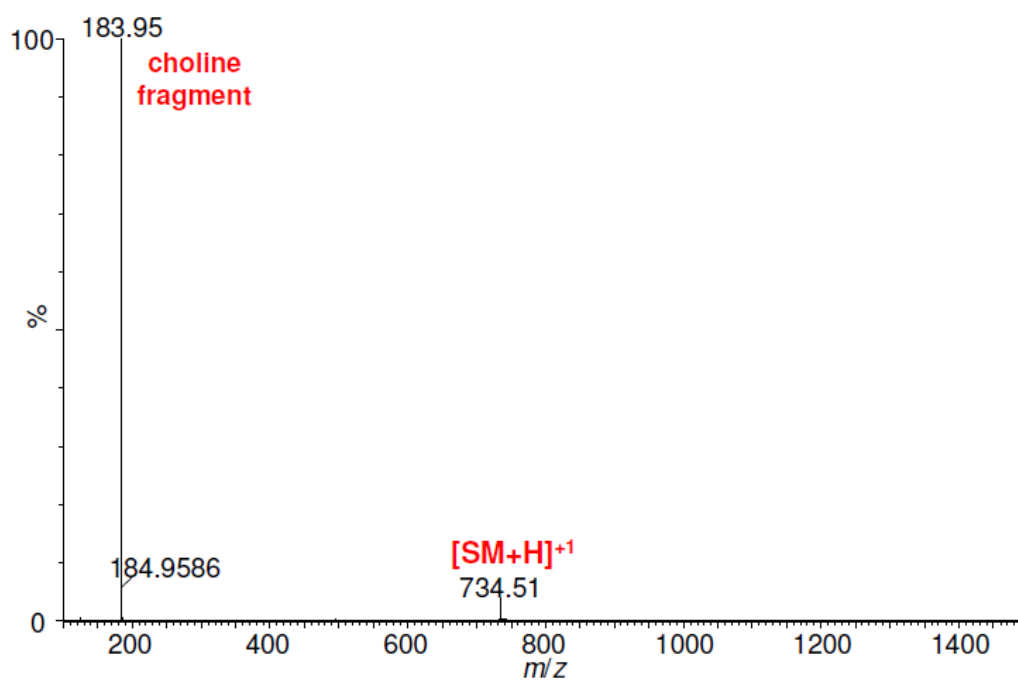
Figure S14. IP-LSI-MS/MS of lipid sphingomyelin (MW 703) using collision induced dissociation acquired directly from an aged mouse brain tissue section spotted with 2,5-DHAP matrix prepared in 50:50 ACN:water. A collision energy of 32 V was applied in the trap cell to produce the choline fragment peak *m/z* 183.
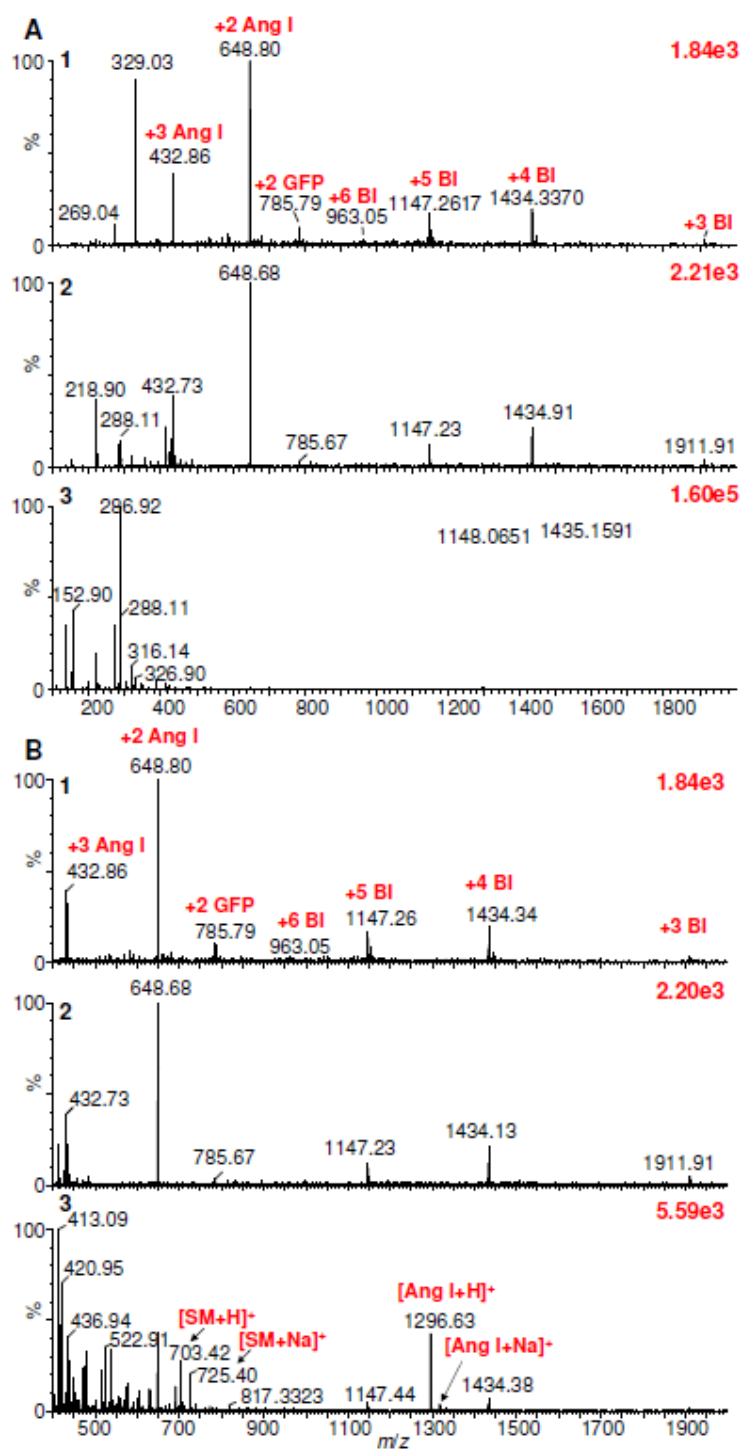
Figure S15. Mass spectra of the model mixture (SM, Ang 1, GFP, and BI) acquired at (**1**) AP-LSI using a UV laser (Nitrogen 337 nm), and at IP-LSI (Nd:Yag 355 nm) using (**2**) "200" and (**3**) "300" laser power. (**A**) Full mass spectra; (**B**) Inset mass spectra from *m/z* 400 to 2000.
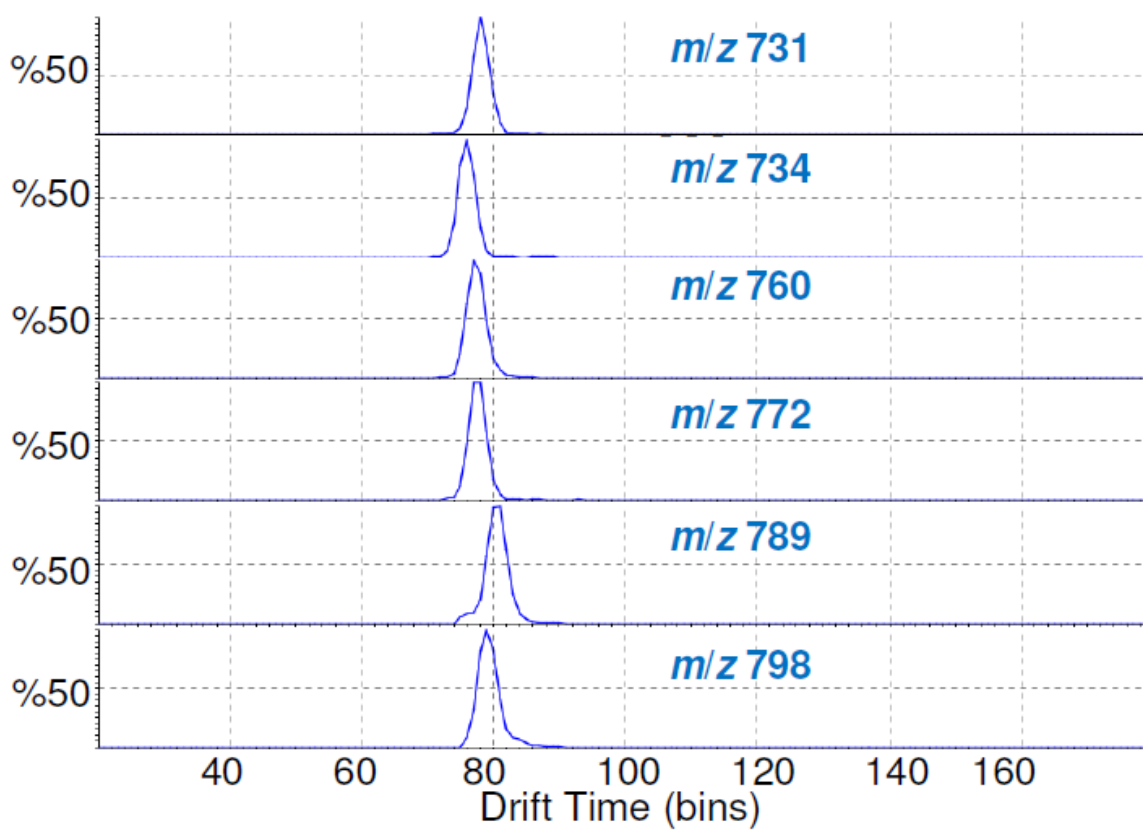
Figure S16. Extracted drift times of the lipids detected from aged delipified mouse brain tissue section spotted with 2,5-DHAP matrix solution in 50:50 ACN:water using IP-LSI-IMS-MS with a laser energy of "500".
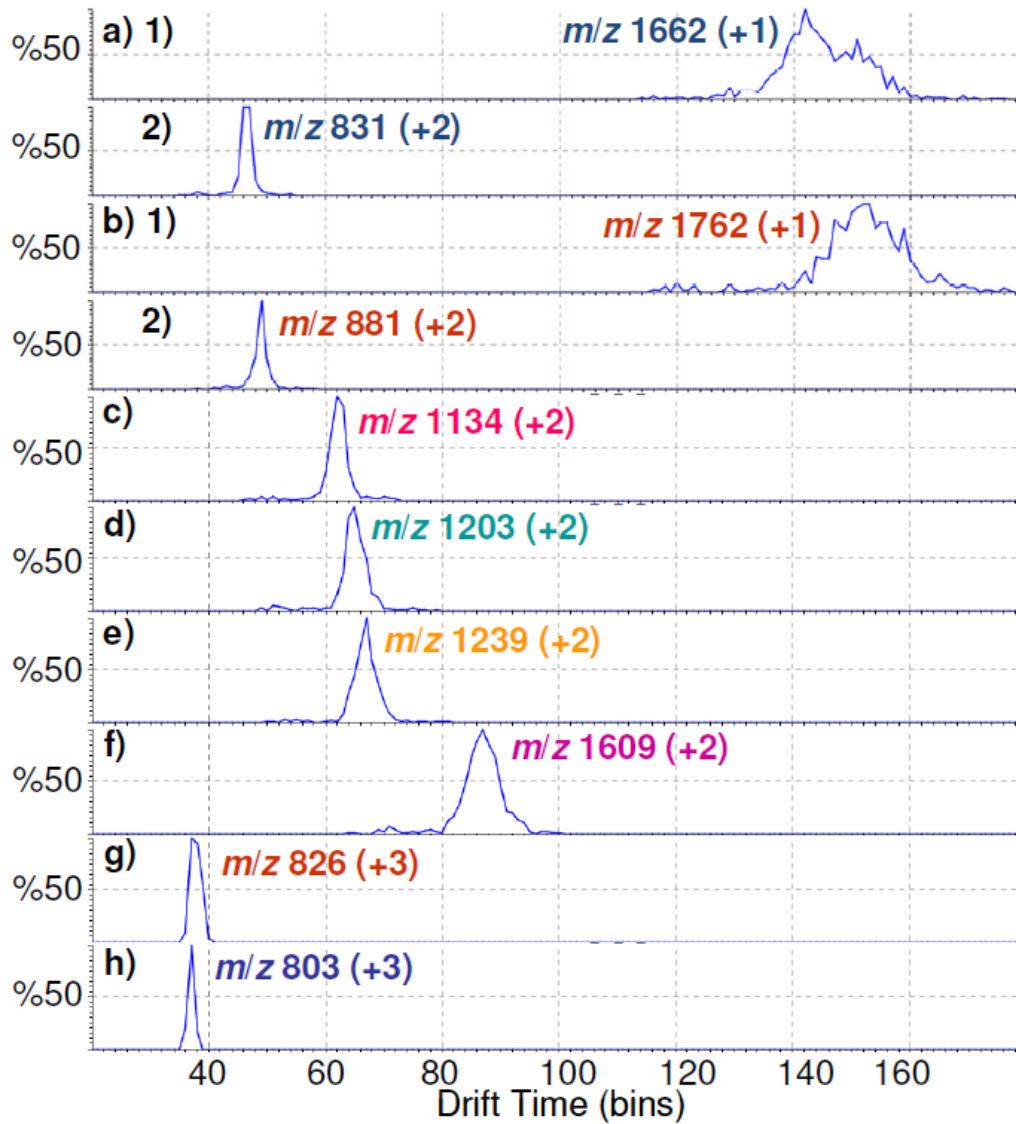
Figure S17. Extracted drift times of the +1, +2 and +3 charged states of peptides detected from aged delipified mouse brain tissue spotted with 2,5-DHAP matrix solution in 50:50 ACN:water using IP-LSI-IMS-MS with a laser energy of "500".
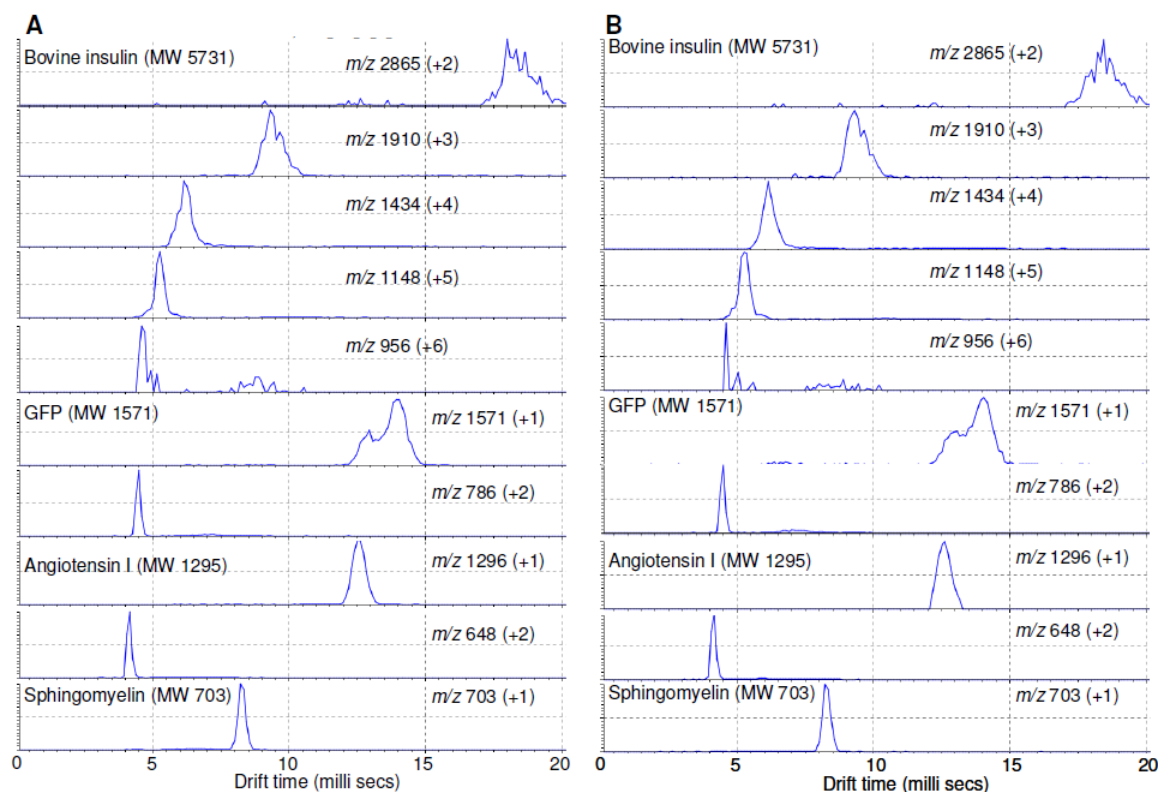
Figure S18. Extracted drift times of the individual component in the model mixture (SM, Ang I, GFP, and BI) acquired using 2,5-DHAP matrix in 50:50 ACN:water. (**A**) Glass plate and (**B**) Metal plate using a laser of 500.
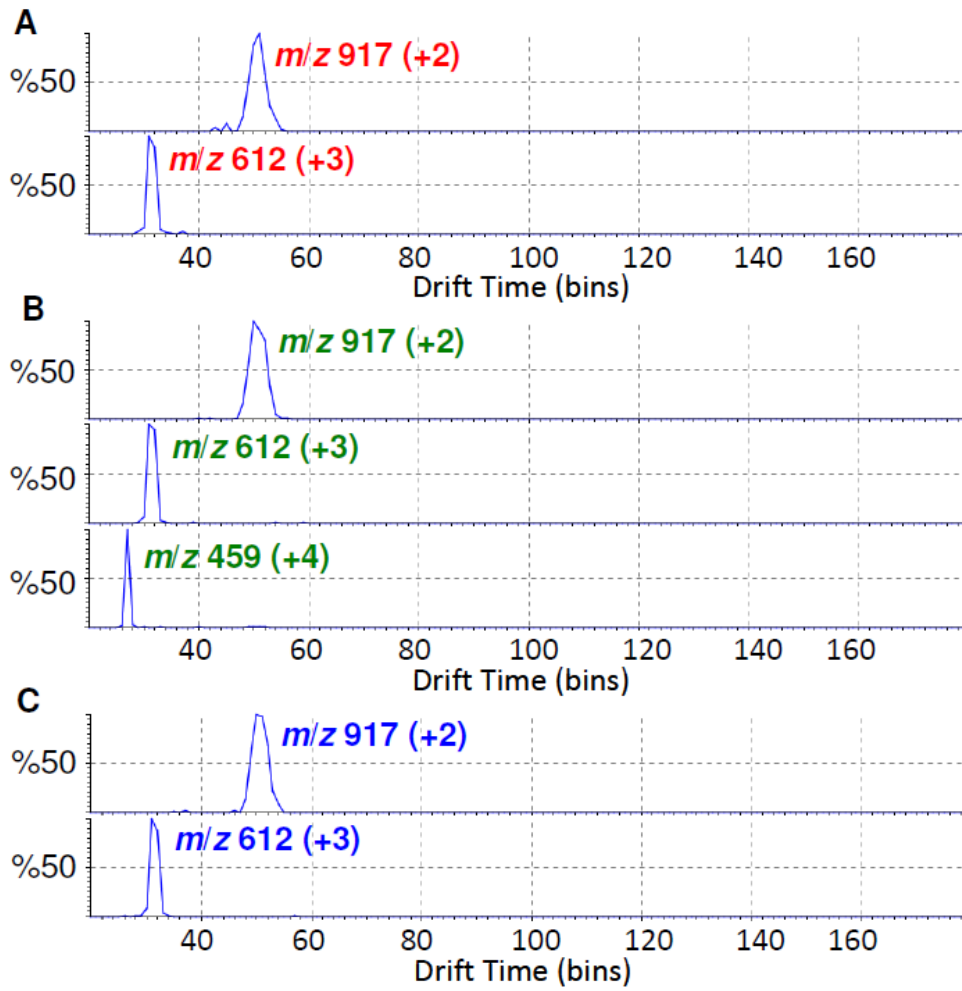
Figure S19. Extracted drift times of the neuropeptide with charge states +2, +3, and +4 (when present): (**A**) from mouse brain tissue section by AP-LSI-IMS-MS, and from the synthesized *N*-acetylated fragment of myelin basic protein obtained by (**B**) AP-LSI-IMSMS and (**B**) ESI-IMS-MS.
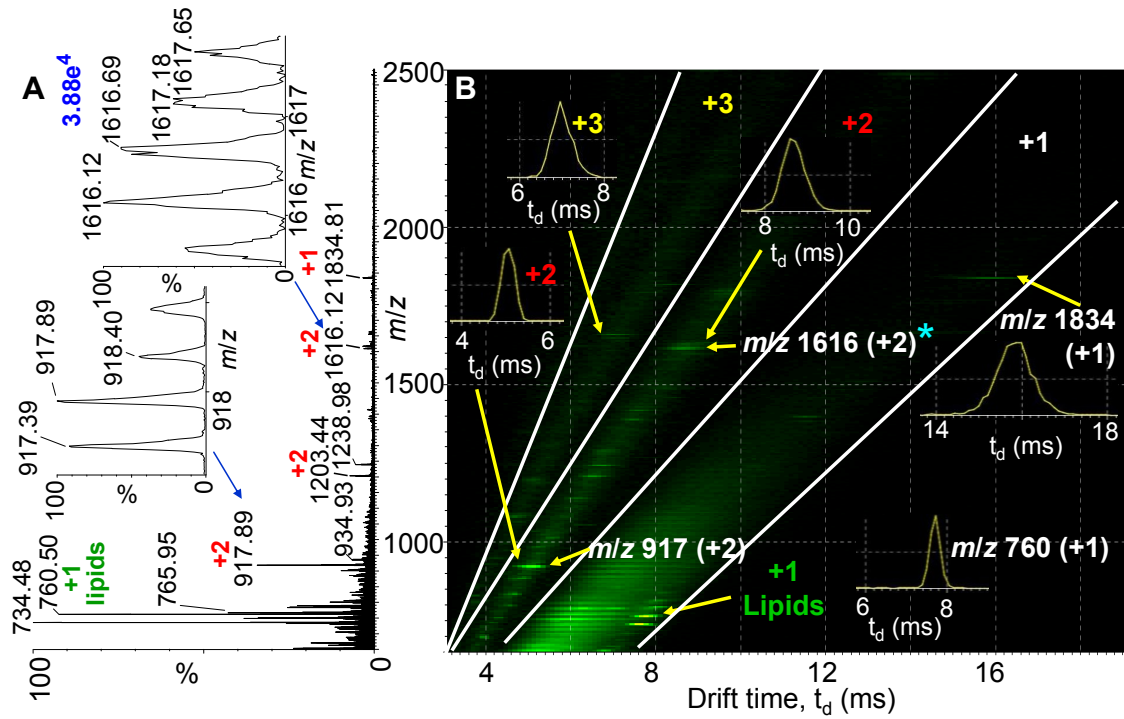
Figure S20: LSIV-IMS-MS (**A**) total mass spectrum and (**B**) two-dimensional plot of drift time *vs. m/z* of delipified mouse brain tissue spotted with 2,5-DHAP matrix and acquired using 'LSI settings'[42,45] on a commercial intermediate pressure MALDI source of the SYNAPT G2 mass spectrometer. Insets show (**A**) isotopic distribution of +2 ions of the identified *N*-acetylated MBP peptide (*m/z* 917.39) and the highest MW detected, ~3.2 kDa (*m/z* 1616.12) (see *****), and (**B**) drift times of +3, +2, and +1 ions.
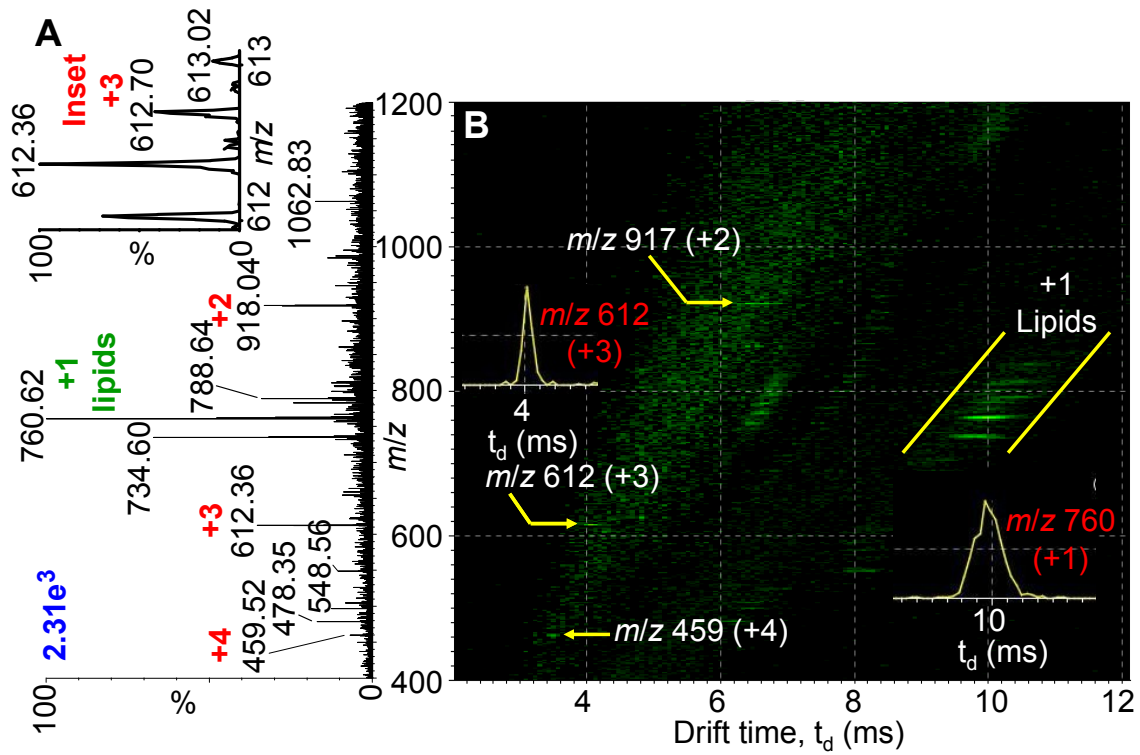
Figure S21: LSII-IMS-MS (**A**) total mass spectrum and (**B**) two-dimensional plot of drift time *vs. m/z* of non delipified mouse brain tissue spotted with 2,5-DHAP matrix and acquired using the nanoESI source of the SYNAPT G2 mass spectrometer with a homebuilt skimmer cone to perform LSII in transmission geometry. Insets show in (**A**) isotopic distribution and (**B**) drift times of +3 charge state ion (*m/z* 612.36) of the identified *N*-acetylated MBP peptide and +1 drift time of a lipid (*m/z* 760.62).

212
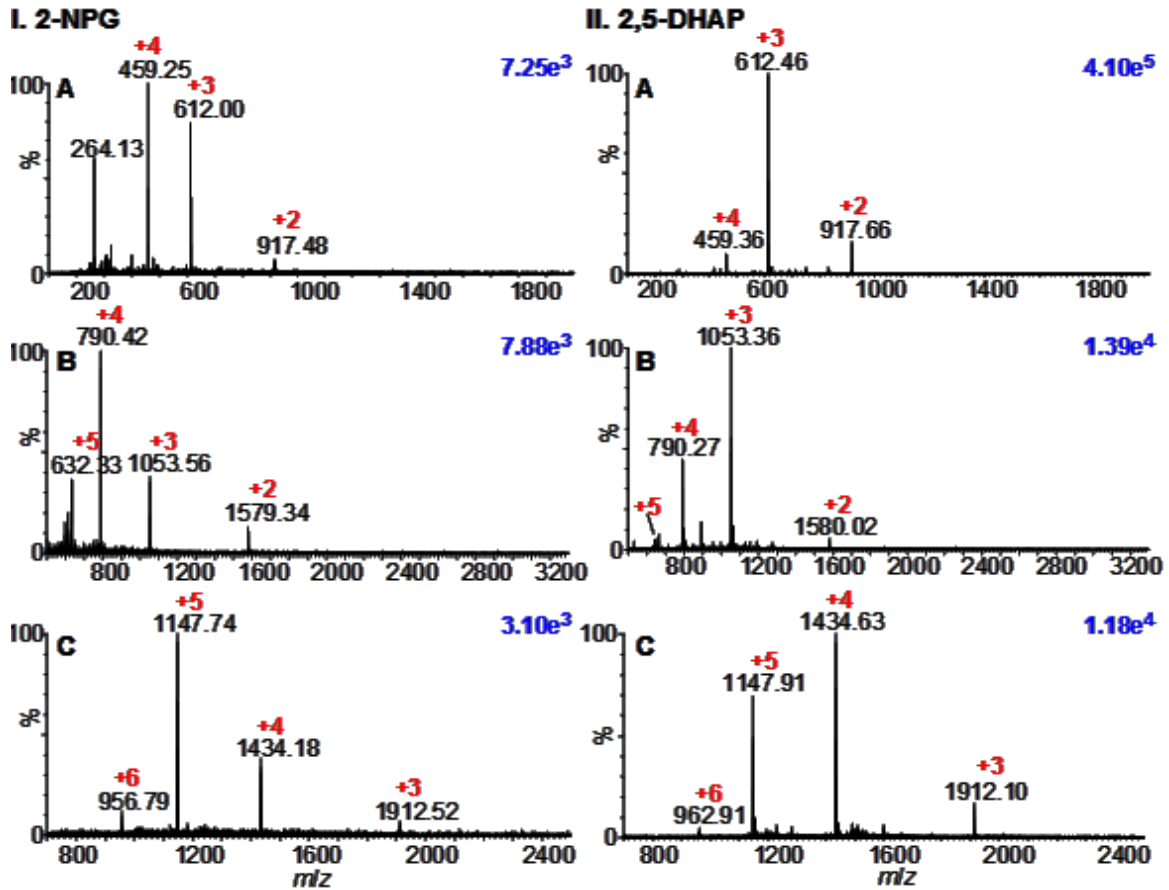
Figure S22: LSIV-MS using (**I**) 2-NPG matrix at low laser power (4.2 J cm^{-2}) and (**II**) 2,5-DHAP matrix at higher laser power (7.3 J cm^{-2}) of (**A**) *N*-acetylated MBP peptide (MW 1833 Da), (**B**) galanin (MW 3150 Da), and (**C**) bovine insulin (MW 5731 Da) acquired using 'LSI settings [42,45] on a commercial intermediate pressure MALDI source of the SYNAPT G2 mass spectrometer.
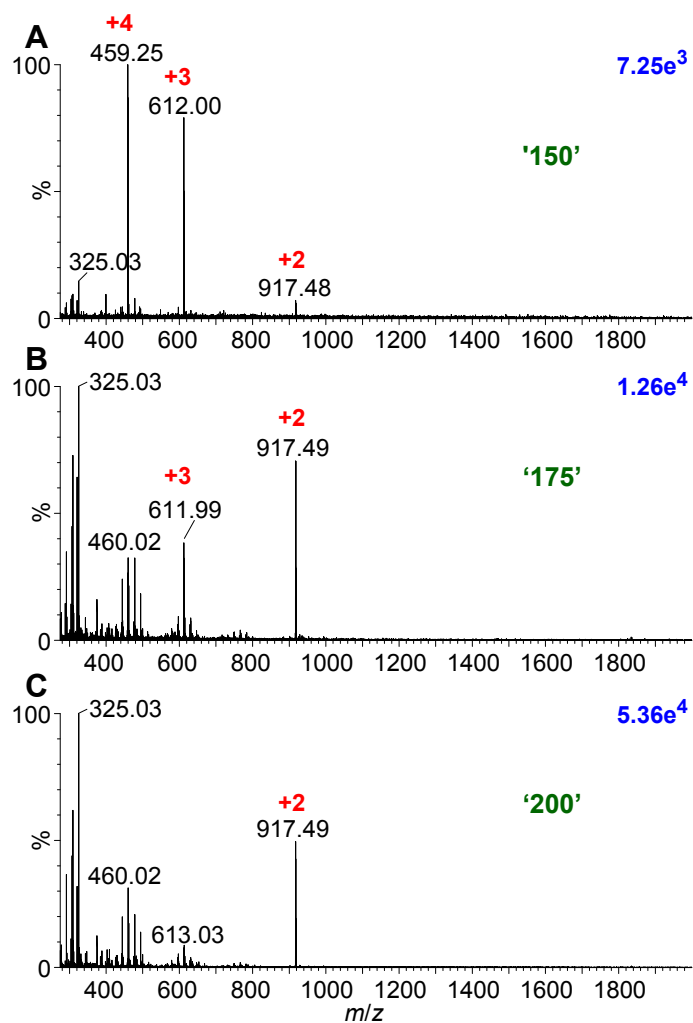
Figure S23: LSIV-MS of *N*-acetylated MBP peptide (MW 1833 Da) with 2-NPG matrix using different laser power: (**A**) 4.2, (**B**) 5.7, and (**C**) 7.3 J cm^{-2} acquired using 'LSI settings [42,45] on a commercial intermediate pressure MALDI source of the SYNAPT G2 mass spectrometer.
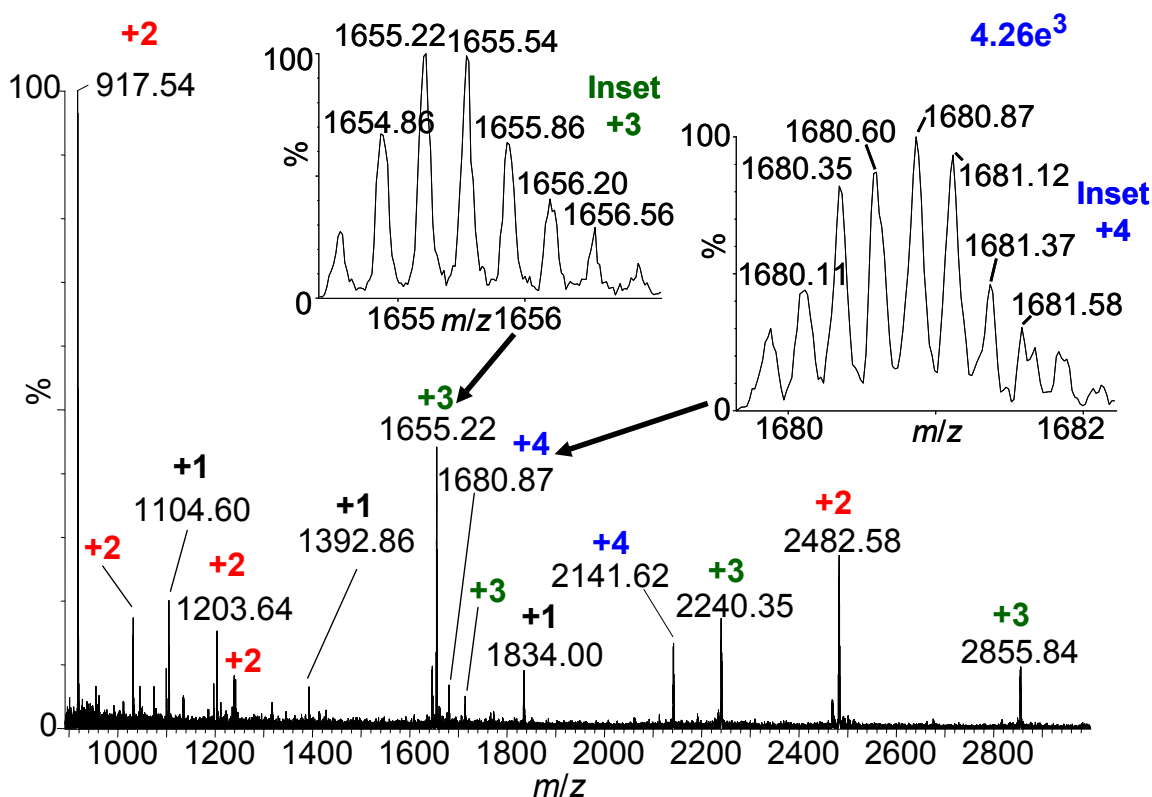
Figure S24: LSIV-IMS-MS of delipified mouse brain tissue spotted with 2-NPG matrix shown in **Figure 2A**. Shown here is the total mass spectrum of the multiply charged peptide and protein ions with the large molecular weight detected, an ~8.6 kDa protein (*m/z* 2855.84) with insets of the isotopic distributions of higher charge states: +3 (*m/z* 1655.22) and +4 (*m/z* 1680.87) ions. Data acquired using 'LSI settings [42,45] on a commercial intermediate pressure MALDI source of the SYNAPT G2 mass spectrometer.
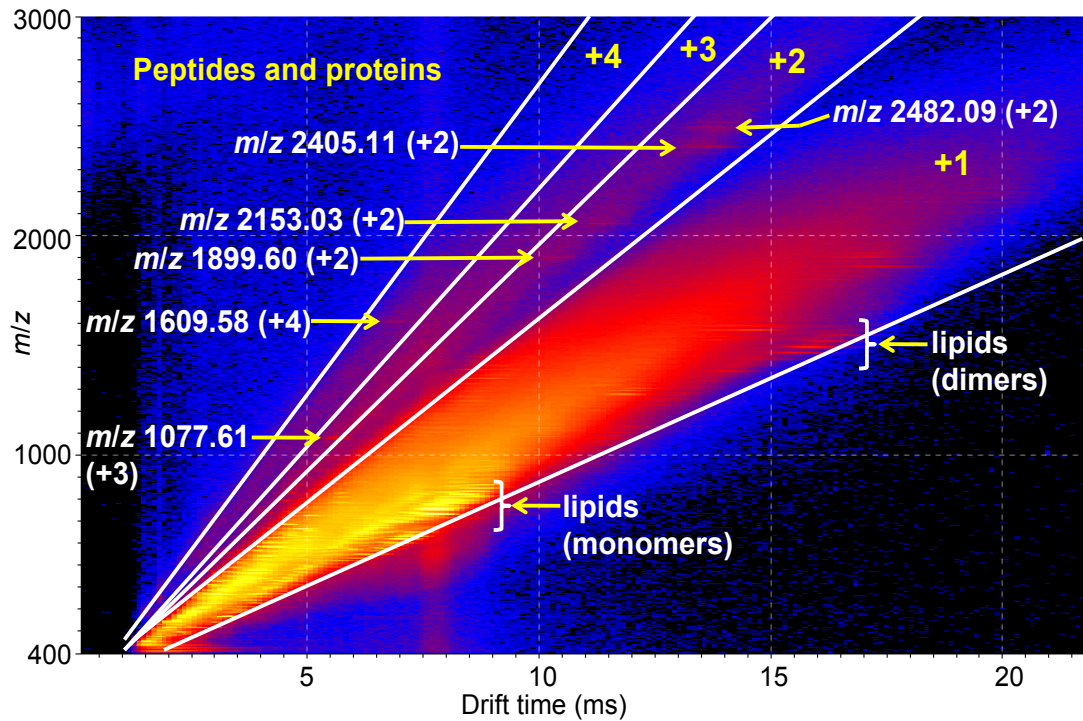
Figure S25: LSIV-IMS-MS two-dimensional plot of drift time *vs.* *m/z* of delipified mouse brain tissue mounted on CHCA precoated glass plate spray coated with binary matrix mixture of 90% 2,5-DHAP and 10% 2-NPG and acquired using 'LSI settings [42,45] on a commercial intermediate pressure MALDI source of SYNAPT G2 mass spectrometer.

APPENDIX C

Matrix Assisted Ionization *Vacuum* Supplementary Information
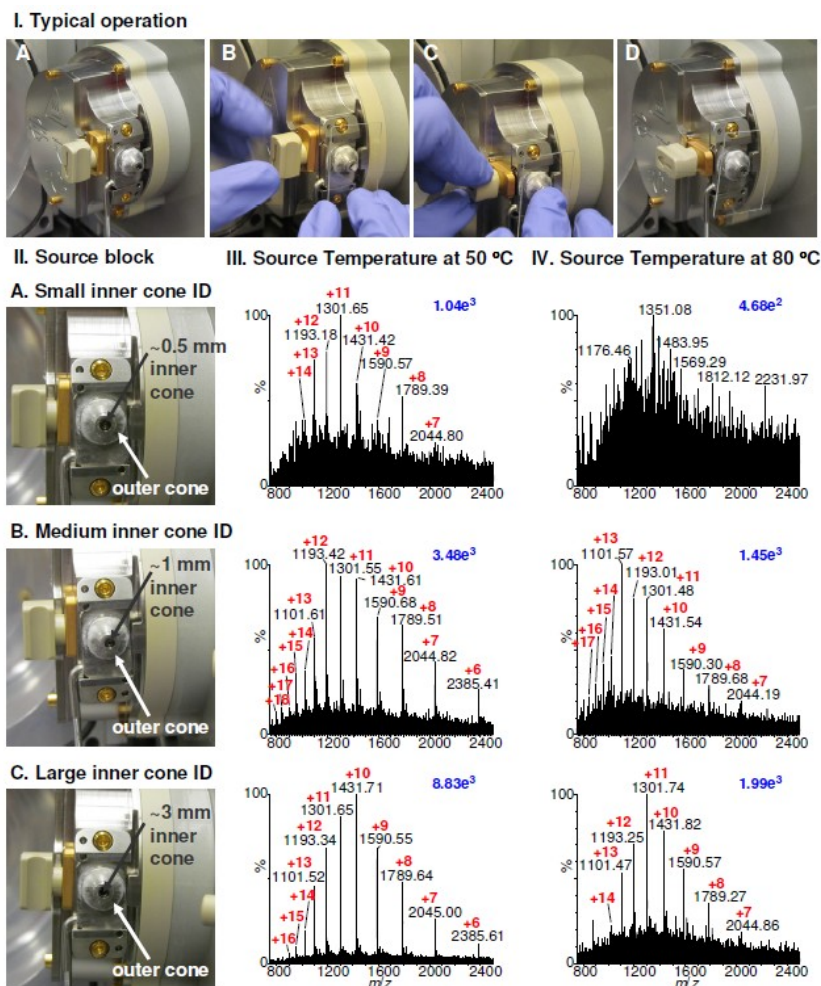
Figure S1. (**I**) Photographs of typical operation of MAIV on the ESI source: (**A**) vacuum valve closed, (**B**) glass on, (**C**) vacuum valve open, (**D**) matrix:analyte sample enters readily mass spectrometer by vacuum forces. This custom designed MAVI source operating from atmospheric pressure conditions is a means of rapid sample introduction to the vacuum of the mass spectrometer. (**II**) MAIV-MS of lysozyme (MW ~14.3 kDa) in 25 mM ammonium acetate buffer in 10% MeOH on the ESI source of SYNAPT G2 using (**I**) a modified skimmer cone with wider outer cone (~4.5 mm ID) and inner cone of (**A**) ~0.5 mm, (**B**) ~1 mm, (**C**) ~3 mm ID using 3-NBN in 50:50 ACN:water with 0.1% FA acquired with a source temperature of (**II**) 50 °C and (**II**) 80 °C. Red numbers indicate the charge state and blue numbers indicate the ion abundance.

A. Total mass spectrum

B. Extracted mass spectra
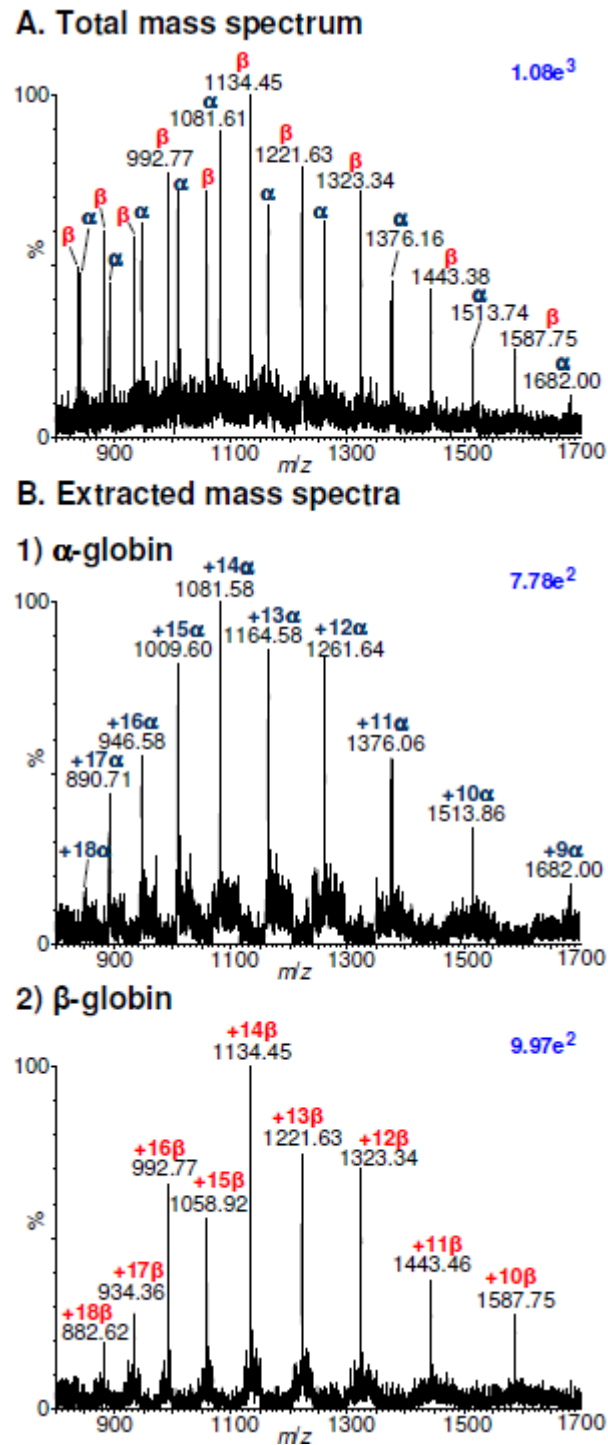
1) α-globin

2) β-globin

Figure S2. MAIV-IMS-MS using ESI source of solvent extracted blood spot from a band aid (**A**) Total mass spectra and (**B**) extracted mass spectra of (**1**) α-globin ions (MW 15126 Da) and (**2**) β-globin (MW 15866 Da) chain of hemoglobin. Data acquired on the SYNAPT G2 using a source temperature of 50 °C.
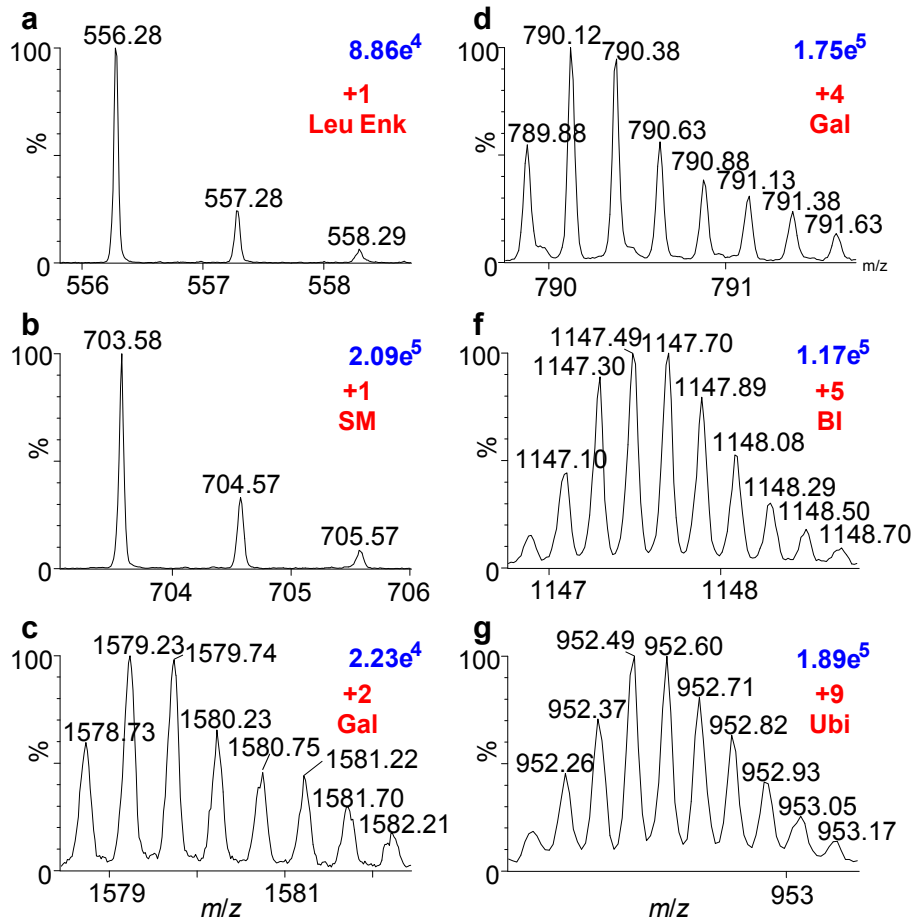
Figure S3. MAIV isotopic distributions from **Figure 1A**: (**a**) leucine enkephalin (+1), (**b**) sphingomyelin (+1), (**c**) galanin (+2), (**d**) galanin (+4), (**e**) bovine insulin (+5), and (**f**) ubiquitin (+9) in the model mixture with 3-NBN matrix. Blue numbers of each spectrum provide an indication of ion abundance and red numbers the charge states.
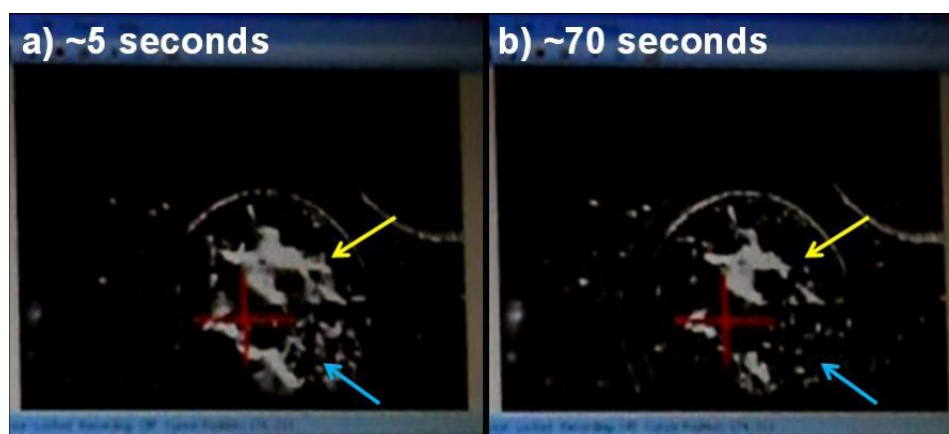
Figure S4. Picture snapshots of matrix:analyte spot with 3-NBN matrix using the MALDI source of SYNAPT G2: (**a**) 5 seconds after indexing sample plate that requires ca. 2 min and (**b**) after additional 70 seconds. Yellow and blue arrows point the areas of the spot where crystals sublimed after 70 seconds in the vacuum source. See online 'MAIV on MALDI source video I' using the intermediate pressure vacuum MALDI source of SYNAPT G2 mass spectrometer.
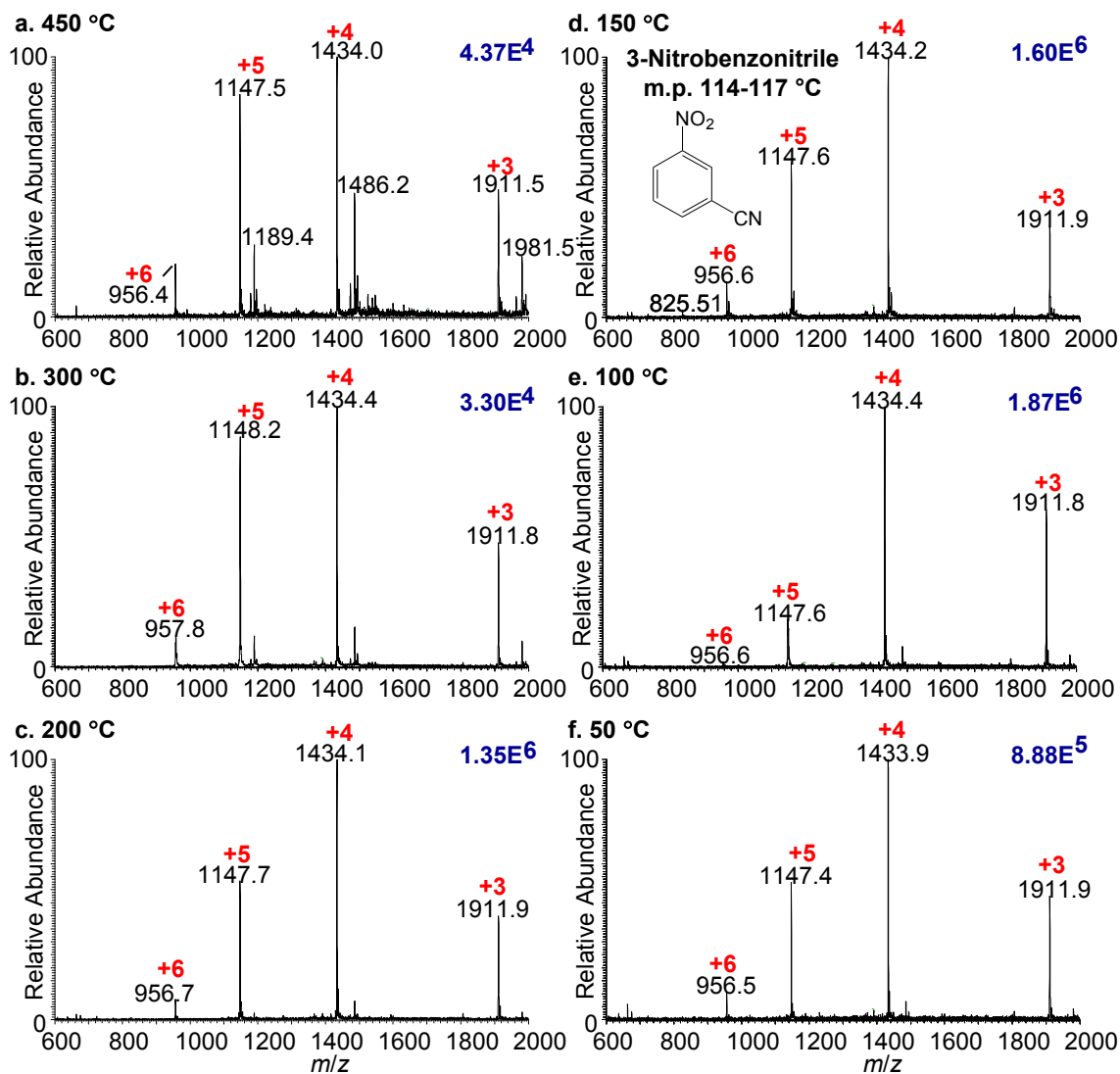
Figure S5. MAII temperature study of 3-NBN in 50:50 ACN:water using acidified bovine insulin (MW 5731 Da) acquired using the LTQ Velos at (**a**) 450 °C, (**b**) 300 °C, (**c**) 200 °C, (**d**) 150 °C, (**e**) 100 °C, and (**f**) 50 °C inlet capillary temperature of the overridden ESI source. Blue numbers of each spectrum provide an indication of ion abundance and red numbers the charge states.
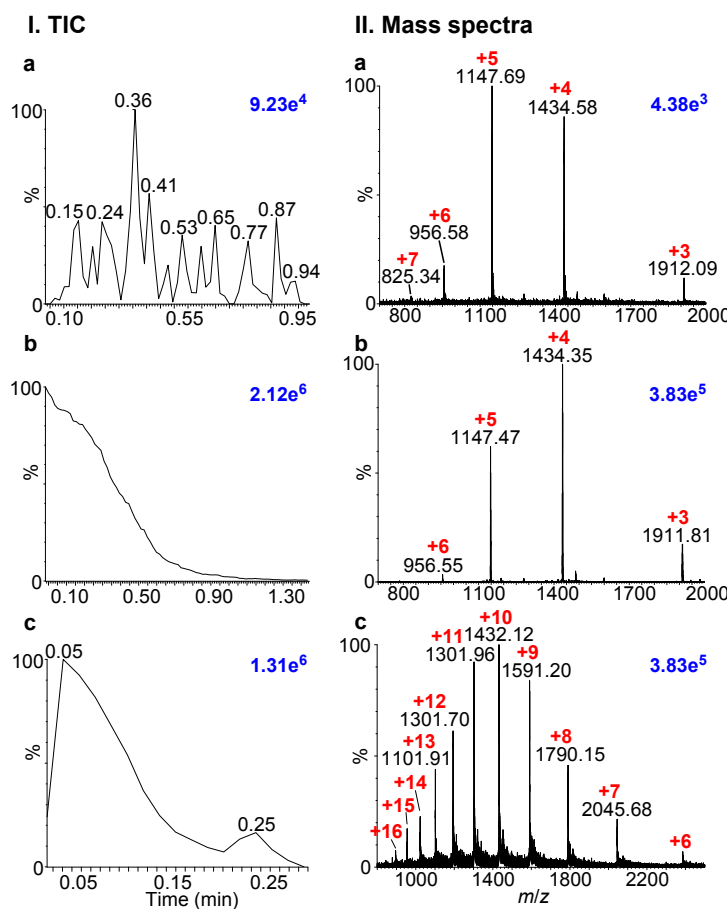
Figure S6. MAIV (**I**) total ion current (**TIC**) and (**II**) mass spectra of bovine insulin (MW 5731 Da) with 3-NBN matrix using a SYNAPT G2 mass spectrometer (**a**) on the commercial ESI source with the custom modified inner and outer cone (**Scheme 1II**) and (**b**) using LSI settings of a commercial SYNAPT G2 intermediate pressure vacuum MALDI source. (**c**) Lysozyme (MW 14.3 kDa) with 3-NBN matrix on custom modified commercial ESI source of SYNAPT G2 with a wider inner and outer cones. Blue numbers in upper right corner of each spectrum provide an indication of ion abundance and red numbers the charge states. See online 'MAIV on ESI source video II' using the custom modified ESI source of SYNAPT G2 mass spectrometer.
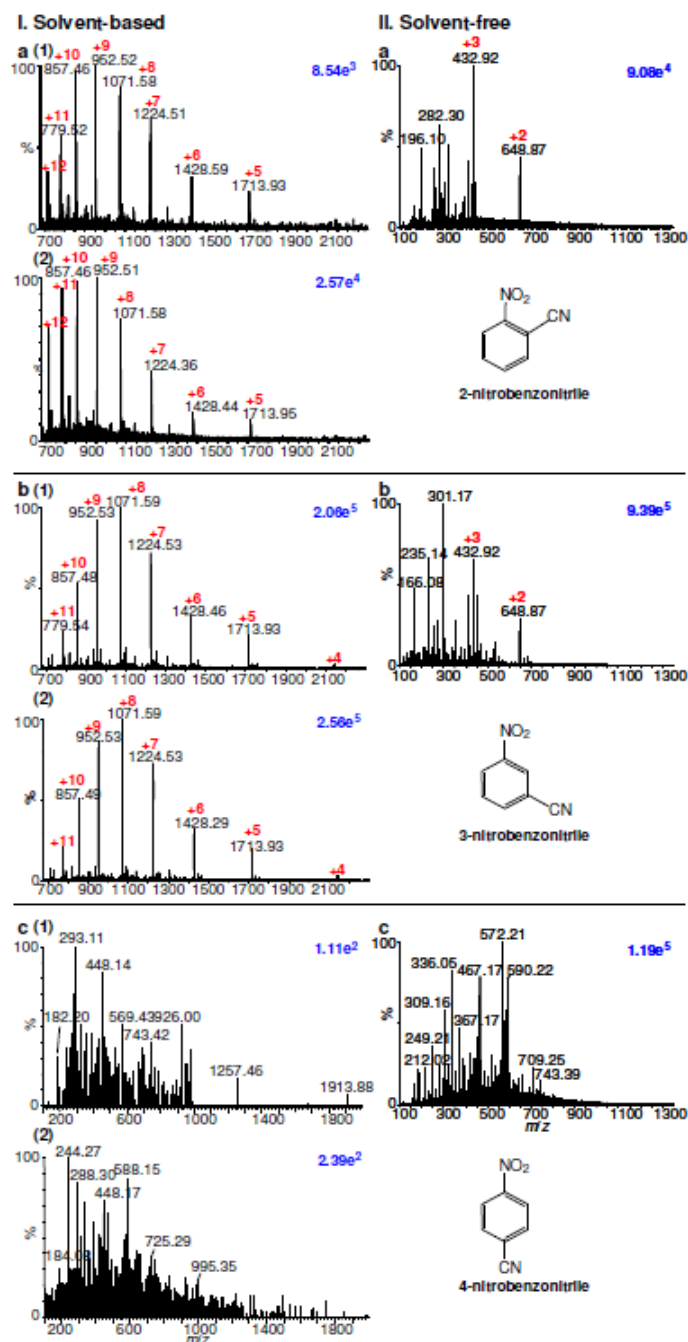
Figure S7. Mass spectra of nitrobenzonitrile (**NBN**) isomers: (**a**) 2-NBN, (**b**) 3-NBN, and (**c**) 4-NBN with (**I**) ubiquitin in water (MW 8561 Da) using solvent-based: (**1**) MAIV and (**2**) with laser, and (**II**) angiotensin I in water (MW 1295 Da) using solvent-free sample preparations acquired using LSI settings of a commercial SYNAPT G2 intermediate pressure vacuum MALDI source. Blue numbers in upper right corner of each spectrum provide an indication of ion abundance and red numbers the charge states.
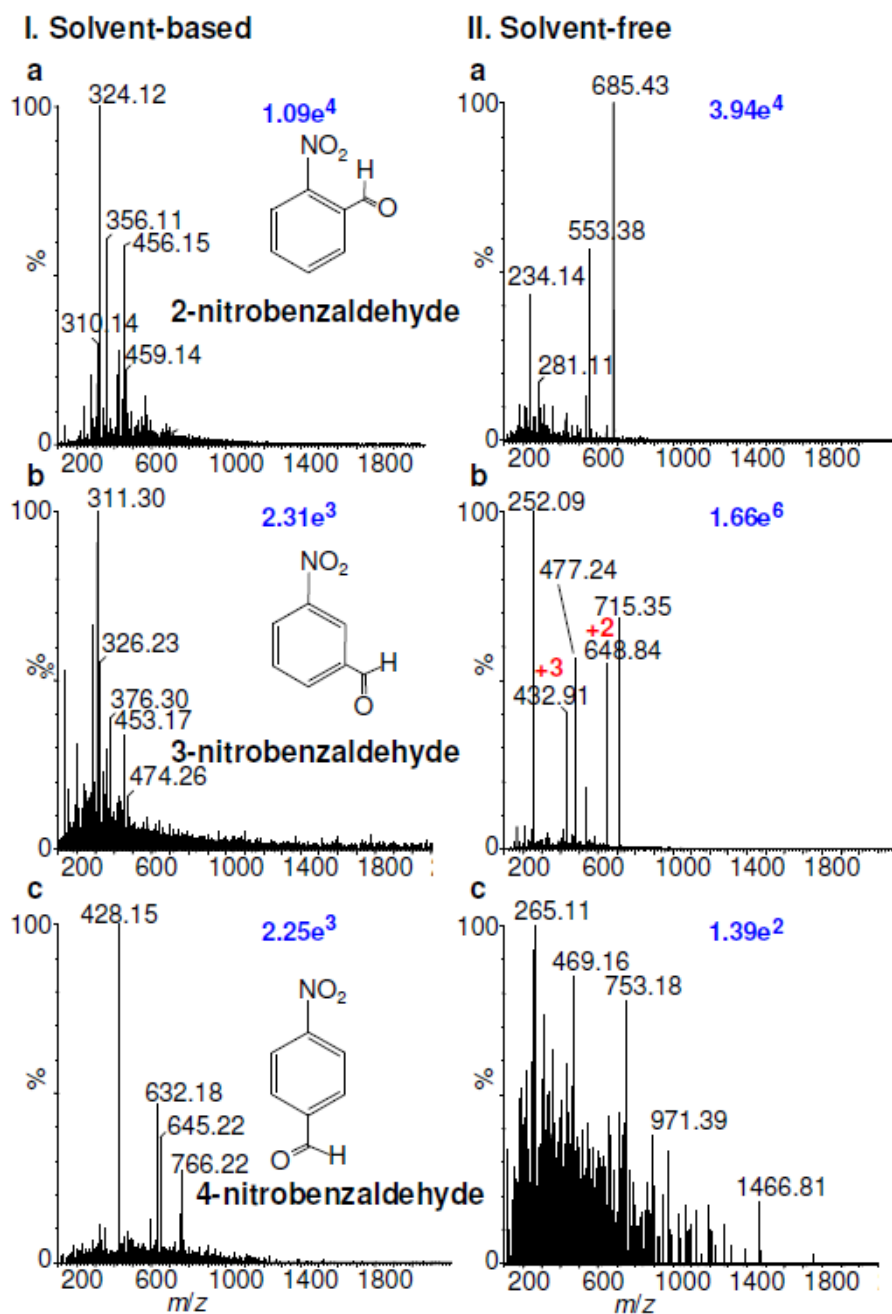
**Figure S8**. Mass spectra of nitrobenzaldehyde isomers: (**a**) 2-nitrobenzaldehyde, (**b**) 3-nitrobenzaldehyde, and (**c**) 4-nitrobenzaldehyde with angiotensin I (MW 1295 Da) using (**I**) solvent-based and (**II**) solvent-free sample preparations acquired using LSI settings of a commercial SYNAPT G2 intermediate pressure vacuum MALDI source. Blue numbers of each spectrum provide an indication of ion abundance and red numbers the charge states.
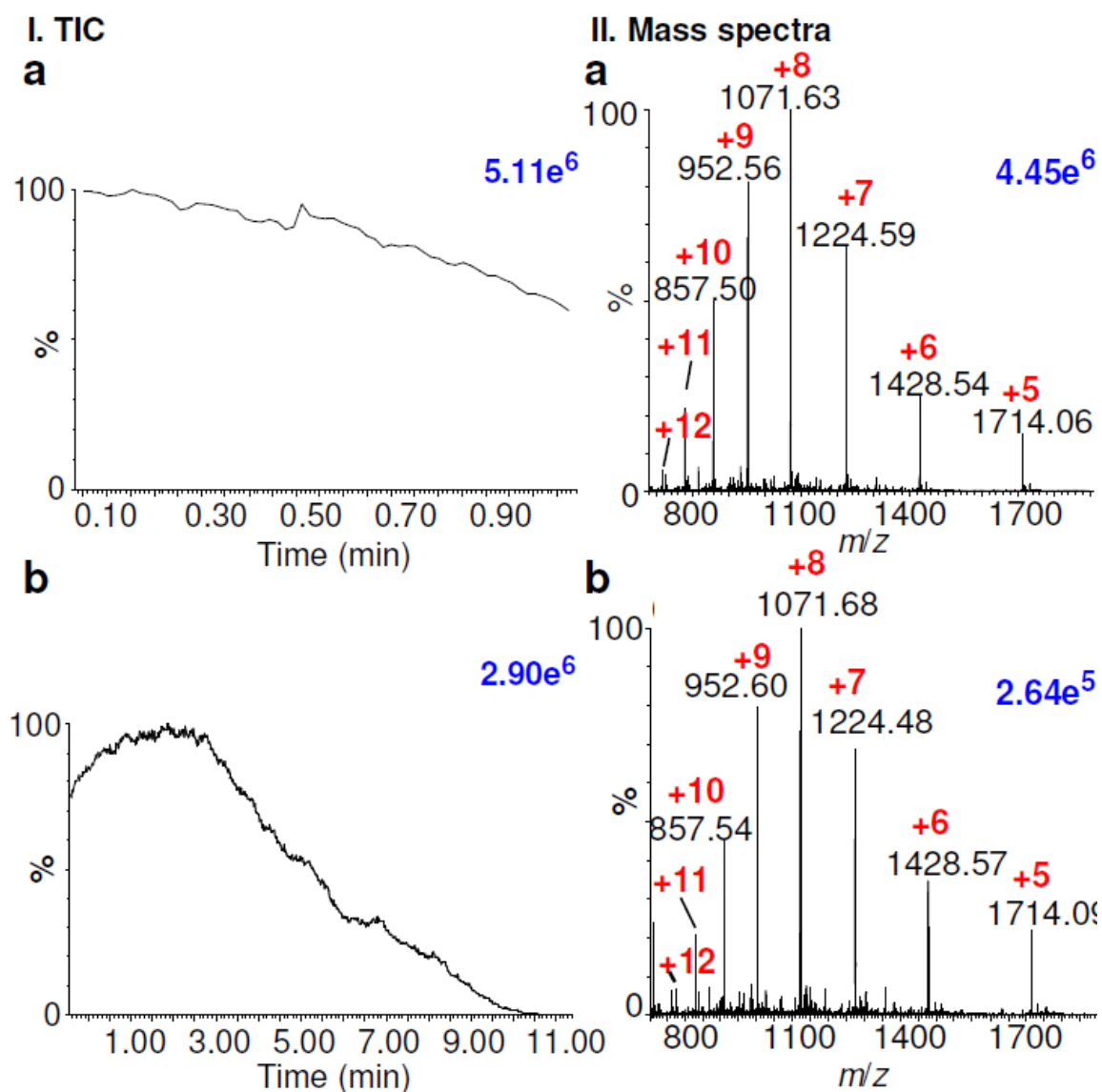
Figure S9. MAIV-MS of ubiquitin in water with 3-NBN matrix in 100% ACN with 0.1% formic acid acquired using LSI settings of a commercial SYNAPT G2 intermediate pressure vacuum MALDI ion source without the use of a laser with matrix:analyte crystals (**a**) wet when loaded in the MALDI source and (**b**) cooled at -80 °C before loading into the vacuum MALDI source: (**I**) total ion current (**TIC**) and (**II**) mass spectra. Blue numbers in upper right corner of each spectrum provide an indication of ion abundance and red numbers the charge states.
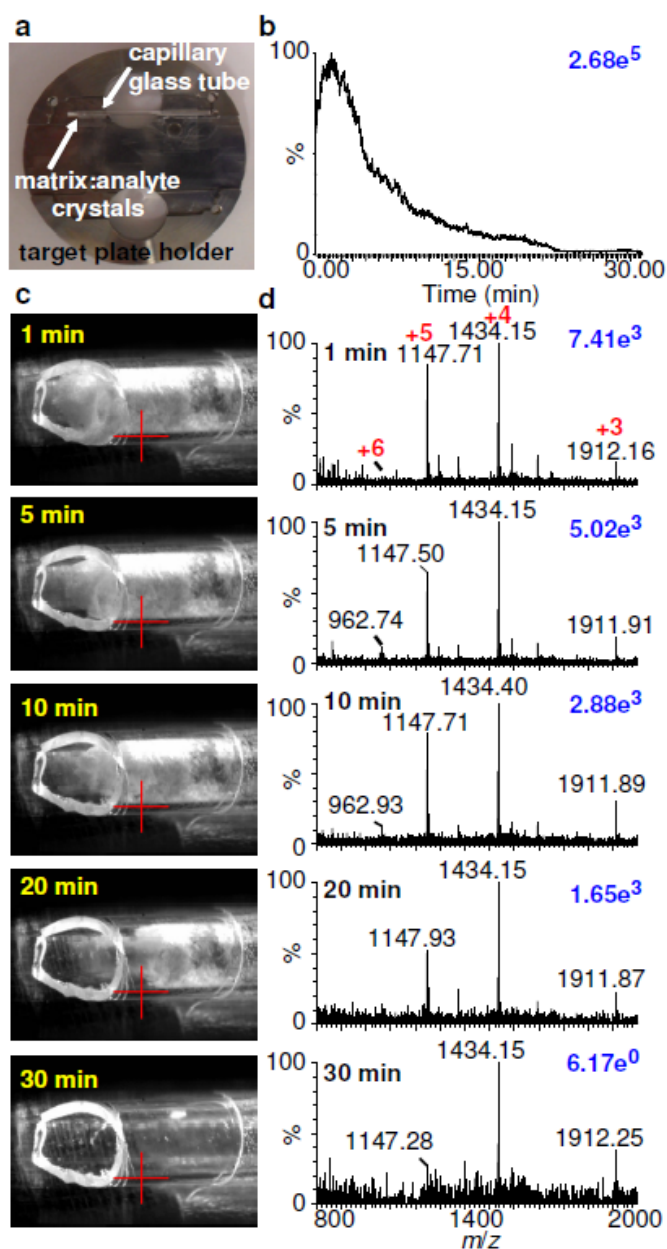
Figure S10. (**a**) Photograph of the target plate holder with the glass capillary tube containing 3-NBN matrix:analyte crystals with acidified bovine insulin (MW 5731 Da), (**b**) total ion current (**TIC**) showing the 30 minute continuous ion production using the glass capillary tube, (**c**) picture capture of the open end of the glass tube containing the matrix:analyte crystals after placing the sample holder inside the intermediate pressure vacuum MALDI source of a commercial SYNAPT G2, and (**d**) mass spectra of bovine insulin at a time period of 1 to 30 min using LSI settings. Blue numbers in upper right corner of each spectrum provide an indication of ion abundance and red numbers the charge states.
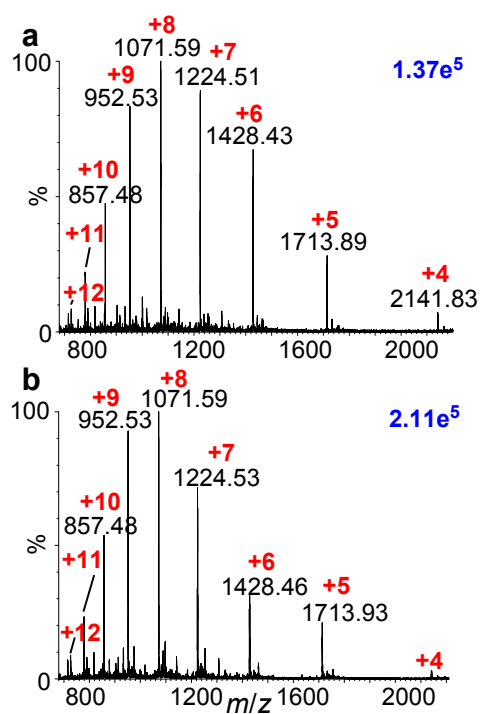
Figure S11. MAIV mass spectra of ubiquitin in water (MW 8561 Da) with 3-NBN in 100% ACN with 0.1% formic acid acquired using LSI settings of the SYNAPT G2 intermediate pressure vacuum MALDI source: (**a**) TOF and (**b**) mobility TOF modes. Blue numbers in upper right corner of each spectrum provide an indication of ion abundance and red numbers the charge states.
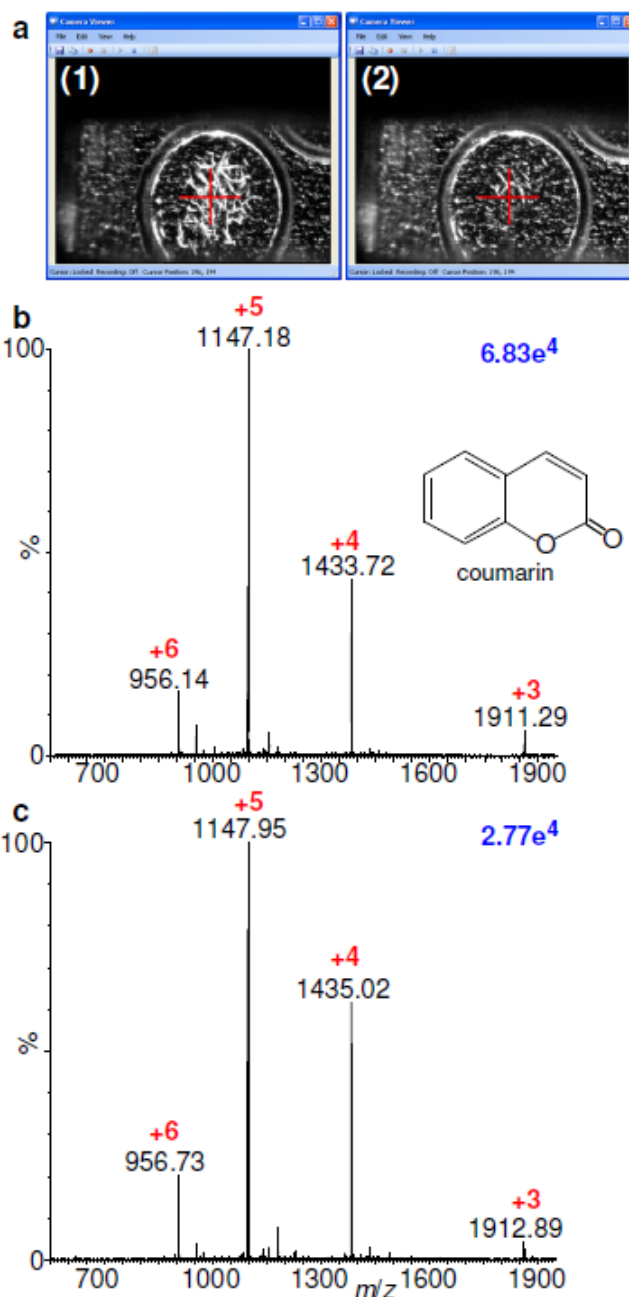
Figure S12. MAIV (**a**) picture snapshots of matrix:analyte spot with coumarin matrix: (**1**) after indexing sample plate and (**2**) after 16 seconds, and mass spectra of 5 pmol bovine insulin with coumarin using (**b**) intermediate pressure vacuum MALDI source and (**c**) custom modified ESI source of SYNAPT G2 mass spectrometer. Blue numbers in upper right corner of each spectrum provide an indication of ion abundance and red numbers the charge states.

I. MAIV on atmospheric pressure ESI source using heat to evaporate 2,5-DHAP matrix:analyte from the surface

a. 80 °C

b. 150 °C
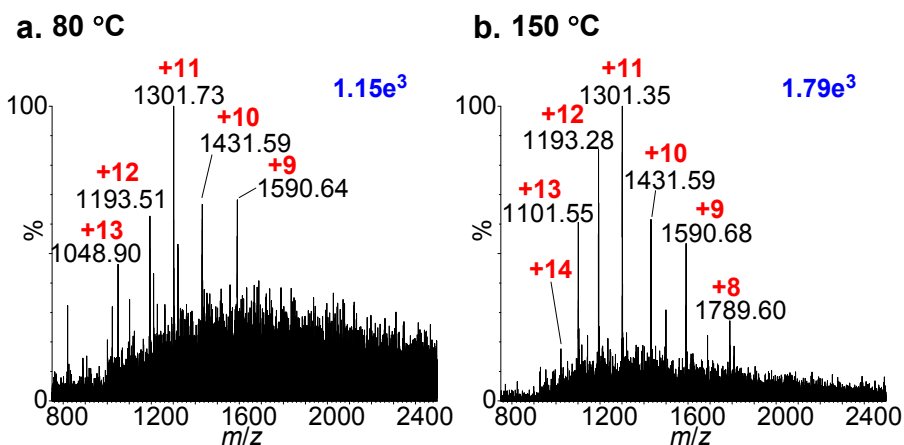
II. LSIV on vacuum MALDI source using a laser for dislodging the 2,5-DHAP matrix:analyte from the surface

a. TIC

b. Mass spectrum
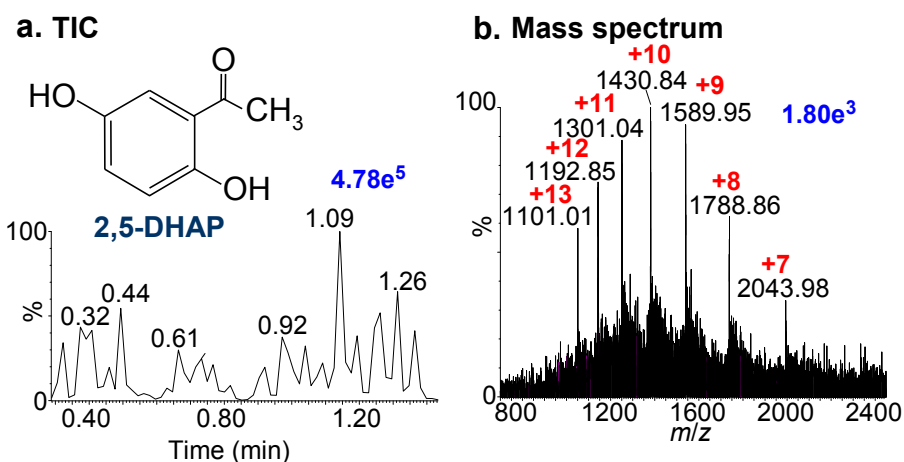
Figure S13. MAIV-MS using 2,5-DHAP for the analyses of lysozyme (MW ~14.3 kDa) in 25 mM ammonium acetate buffer in 10% MeOH; 2,5-DHAP is dissolved in 50:50 ACN:water with 0.1% formic acid. (**I**) ESI source of SYNAPT G2 using a modified skimmer cone with the larger outer (~4.5 mm ID) and inner (~3 mm ID) cones acquired with a source temperature of (**a**) 80 °C and (**b**) 150 °C. (**II**) Intermediate pressure vacuum MALDI source of SYNAPT G2 operated to perform laserspray ionization (**LSIV**): (**a**) total ion current (**TIC**) and (**b**) mass spectrum. As expected for a MALDI matrix, the materials are dislodged by the laser based on sufficient absorption of the matrix at the laser wavelength. A laser power of '230', an arbitrary vendor value ('200' relates to a laser fluence of ~7.3 J cm^{-2} and '250' to ~12.5 J cm^{-2}), was used. Red numbers indicate the charge state and blue numbers indicate the ion abundance.
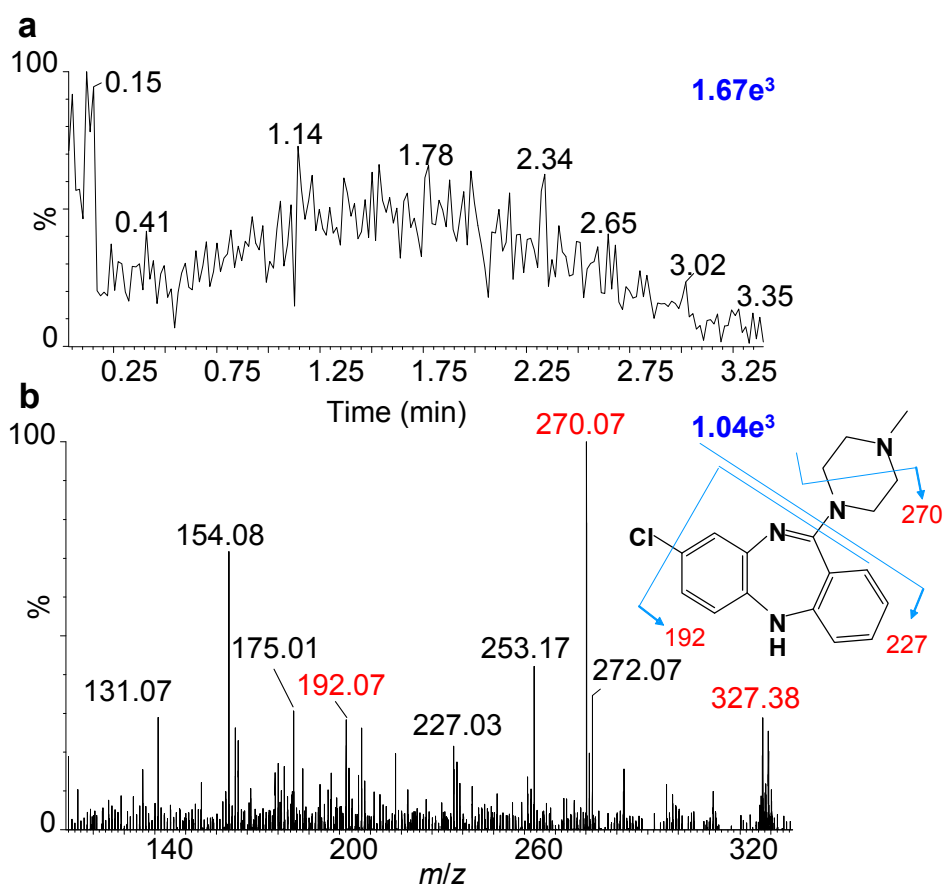
Figure S14. MAIV (**a**) total ion current and (**b**) MS/MS mass spectra using collision-induced fragmentation of 900 attomole clozapine (MW 326 Da) using the 'normal' analyte:matrix spot on target plate cooled on dry ice. Data acquired using 'LSI' settings without the use of a laser on the SYNAPT G2 intermediate pressure vacuum MALDI source. Fragmentation patterns are assigned in red [294]. Blue numbers indicate the ion abundance.
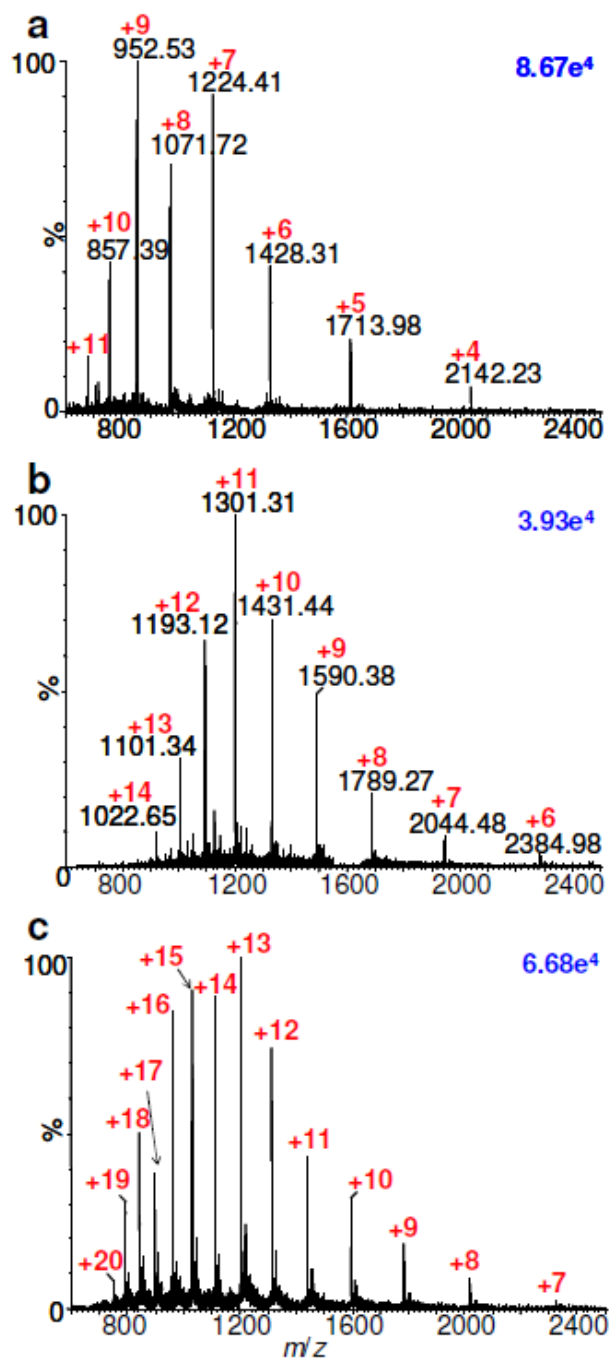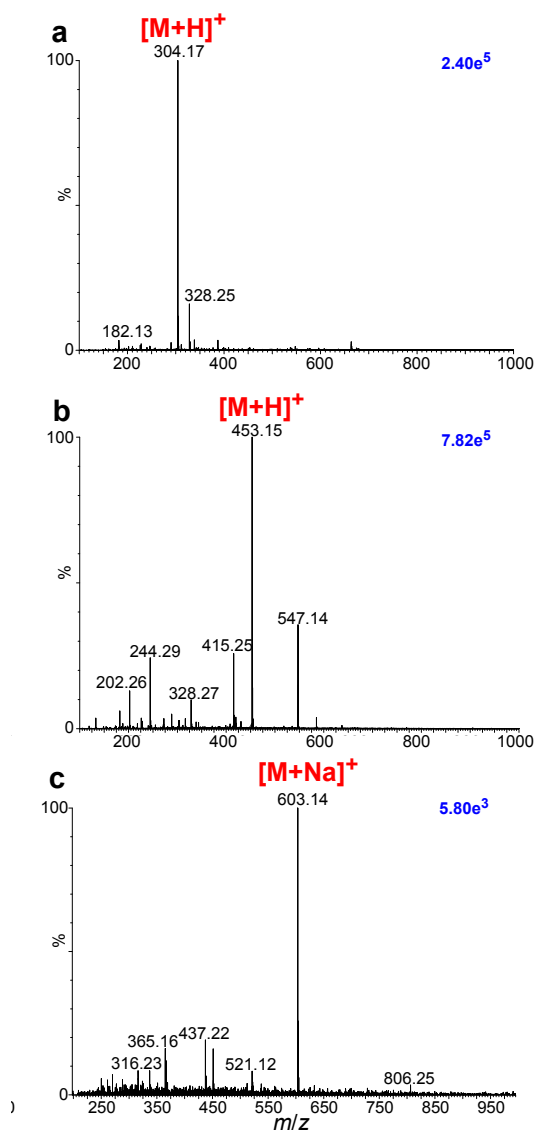
Figure S15. Extracted mass spectra of a mixture of three proteins ionized by MAIV and separated by IMS in the gas phase (**Figure 4II.a)**: (**a**) ubiquitin (MW ~8.6 kDa), (**b**) lysozyme (MW ~14.3 kDa), and (**c**) myoglobin (MW ~17 kDa). Blue numbers in upper right corner of each spectrum provide an indication of ion abundance and red numbers the charge states.

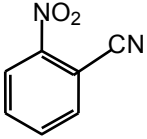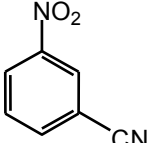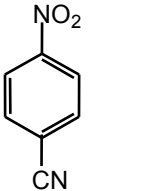**Figure S16.** MAIV-MS of (**a**) cocaine (MW 303 Da), (**b**) pesticide foramsulfuron (MW 452 Da), and (**c**) extracted mass spectrum of 1,2,3,4-tetra-O-acetyl-6-diphenylphosphoryl-β-D-mannopyranose (MW 580 Da) doped with 1 M NaCl with 3-NBN matrix acquired using LSI settings of a commercial SYNAPT G2 intermediate pressure vacuum MALDI source without the use of a laser. Blue numbers in upper right corner of each spectrum provide an indication of ion abundance and red numbers the charge states.
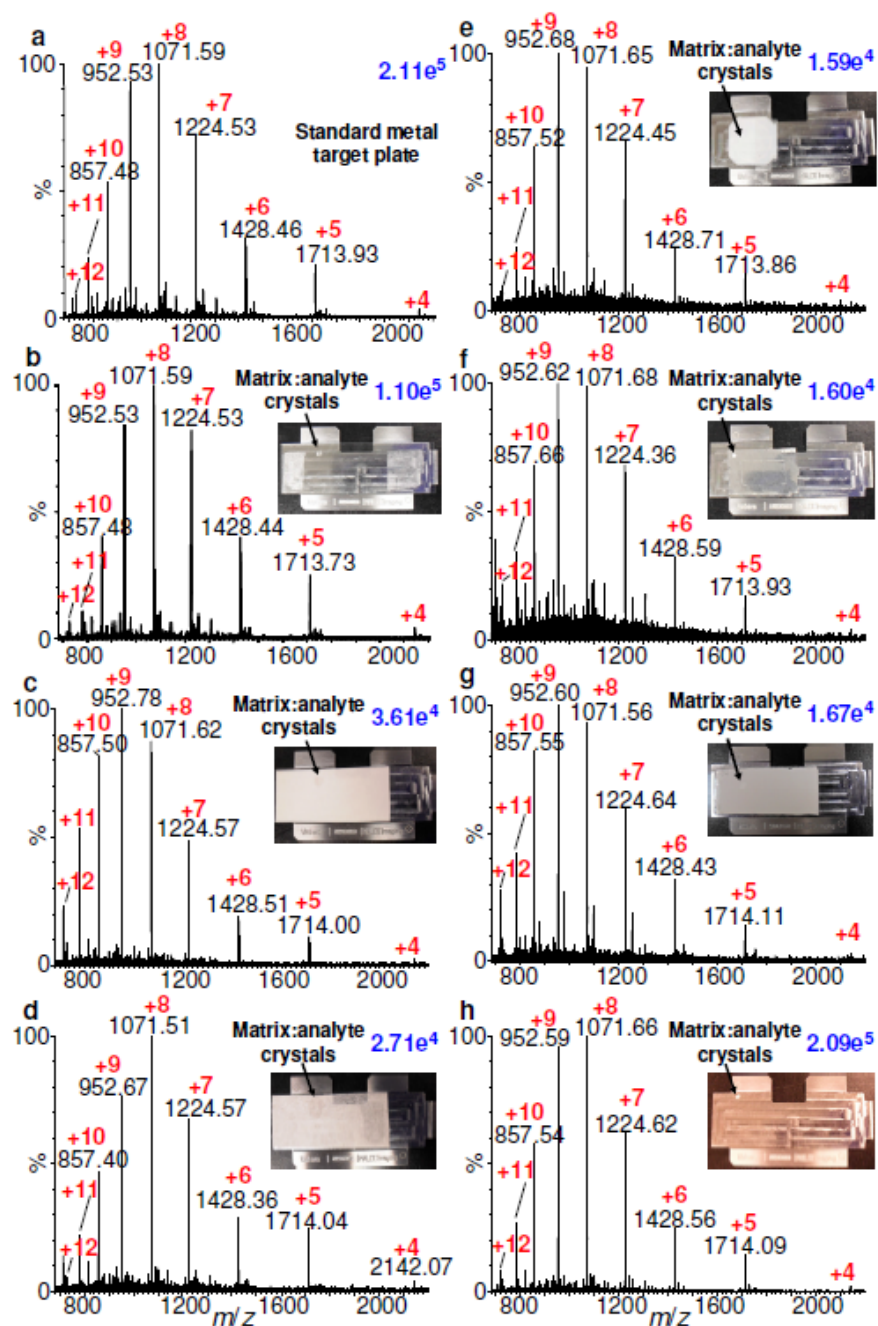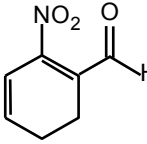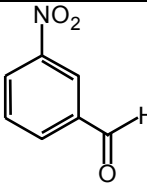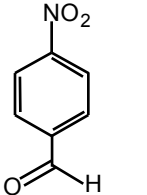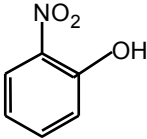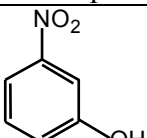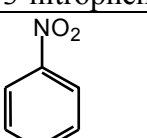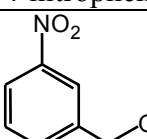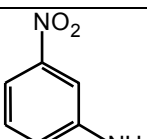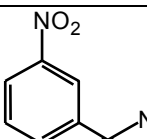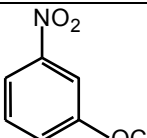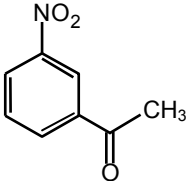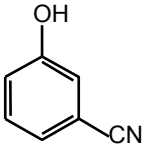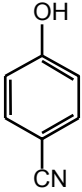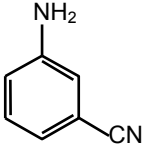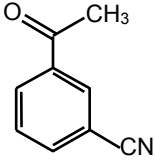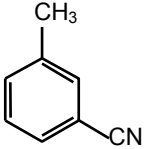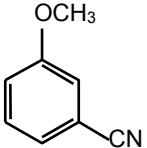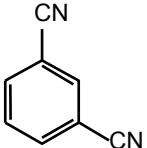
Figure S17. MAIV mass spectra of ubiquitin in water (MW 8561 Da) with 3-NBN in 100% ACN with 0.1% formic acid spotted on **a**) standard metal target plate, **b**) glass plate, **c**) filter paper, **d**) kim wipe tissue, **e**) plastic, **f**) aluminum foil, **g**) thin layer chromatography (TLC) plate, and **h**) glass plate holder. Data acquired using LSI settings of a commercial SYNAPT G2 intermediate pressure vacuum MALDI source without the use of a laser. Blue numbers in upper right corner of each spectrum provide an indication of ion abundance and red numbers the charge states.

Table S1. Summary of matrixes tested at intermediate pressure vacuum using the commercial MALDI source without the use of the laser. I. Compounds with 1,3-substitution, respective isomers, and frequently with one NO2 functionality.

I. Name	Melting point, °C	Observations for angiotensin I as analyte
 2-nitrobenzonitrile	109-111	- crystals formed - sublimed producing multiply charged MAIV ions
 3-nitrobenzonitrile	114-117	- crystals formed - sublimed producing multiply charged MAIV ions
 4-nitrobenzonitrile	144-147	- crystals formed - no analyte ion signal using LSI and MALDI settings without (MAIV) and with a laser (LSIV)
 2-nitrobenzaldehyde	42-44	- no crystals formed - no signal using LSI and MALDI settings without (MAIV) and with a laser (LSIV)
 3-nitrobenzaldehyde	55-58	- no crystals formed using solvent-based sample preparation - sublimed using solvent-free preparation and formed multiply charged MAIV ions
 4-nitrobenzaldehyde	103-106	- crystals formed - no analyte ion signal using LSI and MALDI settings without (MAIV) and with a laser (LSIV)
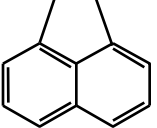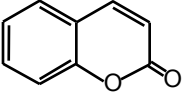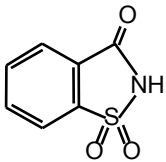
Structure	Melting Point	Observations
2-nitrophenol (NO₂, OH on benzene ring)	n/a	- no crystals formed - no signal using LSI and MALDI settings without (MAIV) and with a laser (LSIV)
3-nitrophenol (NO₂, OH on benzene ring)	96-98	- crystals formed - only +1 analyte charge state using MALDI settings <u>and</u> with laser
4-nitrophenol (NO₂, OH on benzene ring)	110-115	- crystals formed - only +1 analyte charge state using MALDI settings <u>and</u> with laser
3-nitrobenzoic acid (NO₂, COOH on benzene ring)	139-141	- crystals formed - +1 analyte charge state for both LSI and MALDI settings <u>using a laser</u> in both cases
3-nitroaniline (NO₂, NH₂ on benzene ring)	111-114	- crystals formed - no analyte ion signal using LSI and MALDI settings without (MAIV) and with a laser (LSIV)
3-nitrobenzamide (NO₂, CONH₂ on benzene ring)	140-143	- crystals formed - no analyte ion signal using LSI and MALDI settings without (MAIV) and with a laser (LSIV)
3-nitroanisole (NO₂, OCH₃ on benzene ring)	36-38	- no crystals formed - no signal using LSI and MALDI settings without (MAIV) and with a laser (LSIV)
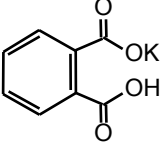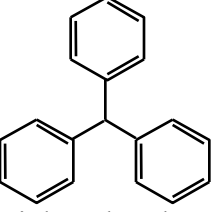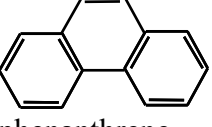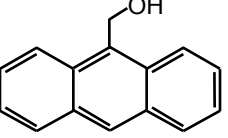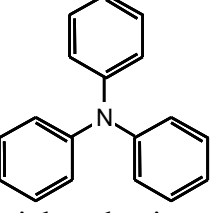
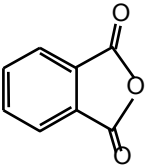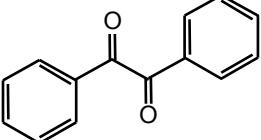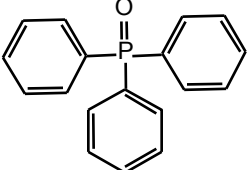|	76-78	- no crystals formed - no signal using LSI and MALDI settings without (MAIV) and with a laser (LSIV)
3-nitroacetophenone		
	78-81	- crystals formed - no analyte ion signal using LSI and MALDI settings without (MAIV) and with a laser (LSIV)
3-cyanophenol		
	110-113	- crystals formed - only +1 analyte charge state using MALDI settings and with laser
4-cyanophenol		
	48-53	- no crystals formed - no signal using LSI and MALDI settings without (MAIV) and with a laser (LSIV)
3-aminobenzonitrile		
	98-100	- crystals formed - no analyte ion signal using LSI and MALDI settings without (MAIV) and with a laser (LSIV)
3-acetylbenzonitrile		
	n/a	- crystals formed - no analyte ion signal using LSI and MALDI settings without (MAIV) and with a laser (LSIV)
m-tolunitrile		
	n/a	- no crystals formed - no signal using LSI and MALDI settings without (MAIV) and with a laser (LSIV)
3-methoxybenzonitrile		

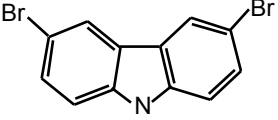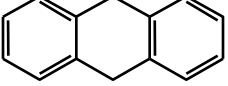|	163-165	- crystals formed - little sublimation but no analyte ion signal using LSI and MALDI settings without (MAIV) and with a laser (LSIV)
CN — benzene ring — CN 1,3-dicyanobenzene		

[1]With poor crystallization the matrix:analyte frequently sublimed/evaporated too rapidly during the 2-min introduction period before the sample holder was at vacuum and the mass spectrometer in operation. LSI and MALDI settings were used for data acquisition.

Table S2. Compounds known to produce triboluminescence.

II. Name	Melting point, °C	Observations for angiotensin I as analyte
pthalic anhyride	131-134	- good crystal formation - no sublimation
benzil	94-95	- good crystal formation - no sublimation
triphenylphosphine oxide	150-157	- atypical crystallization of matrix:analyte mixture - no sublimation
3,6-dibromocarbazole	204-206	- atypical crystallization of matrix:analyte mixture - no sublimation
9,10-dihydroanthracene	103-107	- atypical crystallization of matrix:analyte mixture - no sublimation
acenaphtene	90-94	- atypical crystallization of matrix:analyte mixture - no sublimation
coumarin	68-73	- good crystal formation - sublimed and produced multiply charged MAIV ions
saccharin	226-229	- atypical crystallization of matrix:analyte mixture - no sublimation

potassium hydrogen phthalate	295-300	- atypical crystallization of matrix:analyte mixture - no sublimation
triphenylmethane	92-94	- atypical crystallization of matrix:analyte mixture - no sublimation
phenanthrene	98-100	- atypical crystallization of matrix:analyte mixture - no sublimation
9-anthracenemethanol	n/a	- atypical crystallization of matrix:analyte mixture - no sublimation
triphenylamine	124-128	- atypical crystallization of matrix:analyte mixture - no sublimation
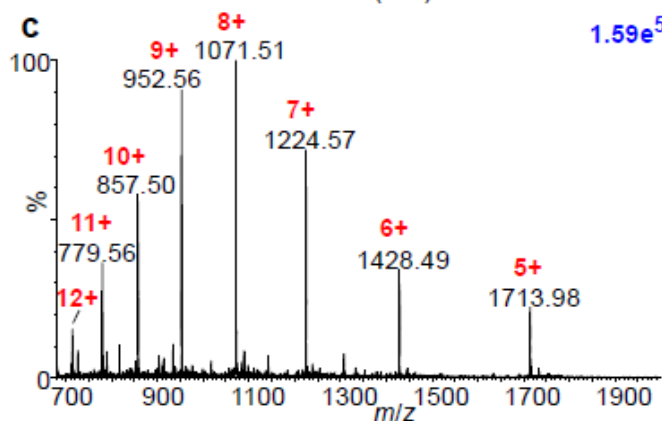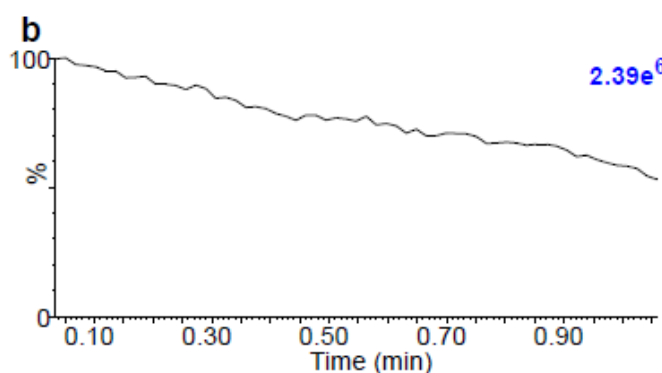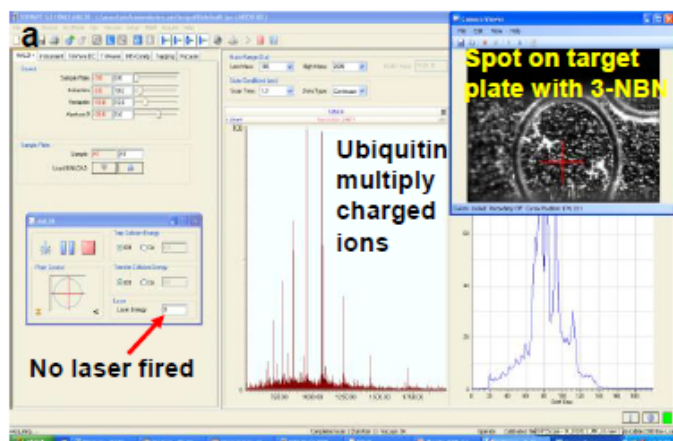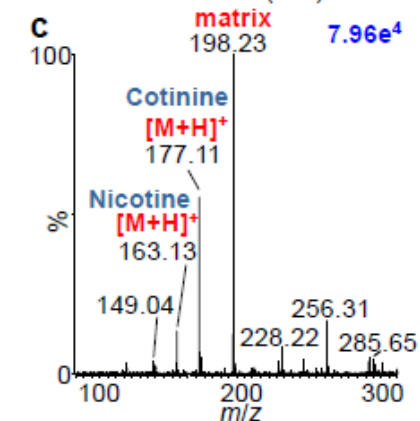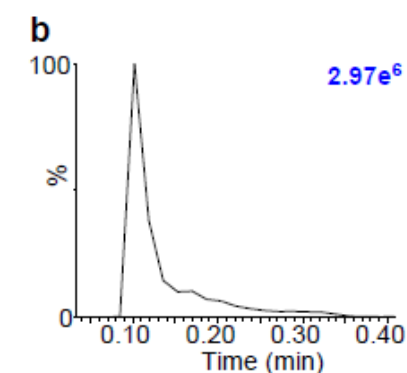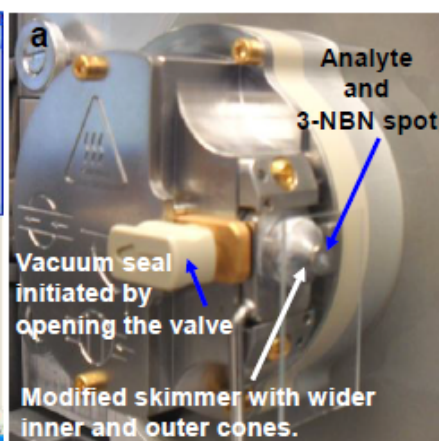
Figure S18: MAIV using the (**I**) intermediate pressure MALDI source: (**a**) Screen shot during MAIV acquisition showing production of multiply charged ions without the use of the laser, (**b**) total ion current (**TIC**), and (**c**) mass spectrum of ubiquitin (MW 8560 Da), and (**II**) custom modified ESI source: (**a**) typical operation, (**b**) TIC, and (**c**) mass spectrum of nicotine standard mixture with 3-NBN matrix and spotted on the glass plate.
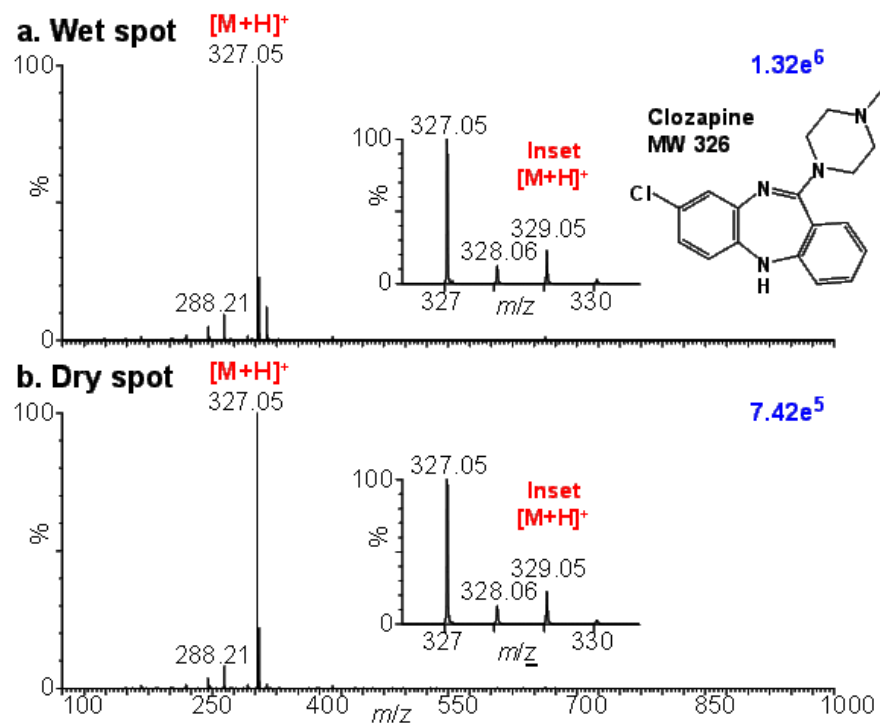
Figure S19: MAIV-MS of a clozapine standard (MW 326 Da) with 3-NBN matrix acquired with (**a**) wet matrix:analyte and (**b**) dry matrix:analyte spots loaded into the intermediate pressure vacuum MALDI source of SYNAPT G2 mass spectrometer using LSI settings. Evaporative cooling that occurs when the solution dries in vacuum is expected to slow sample loss during the time the sample loads. Insets show structure and isotopic distributions of clozapine.
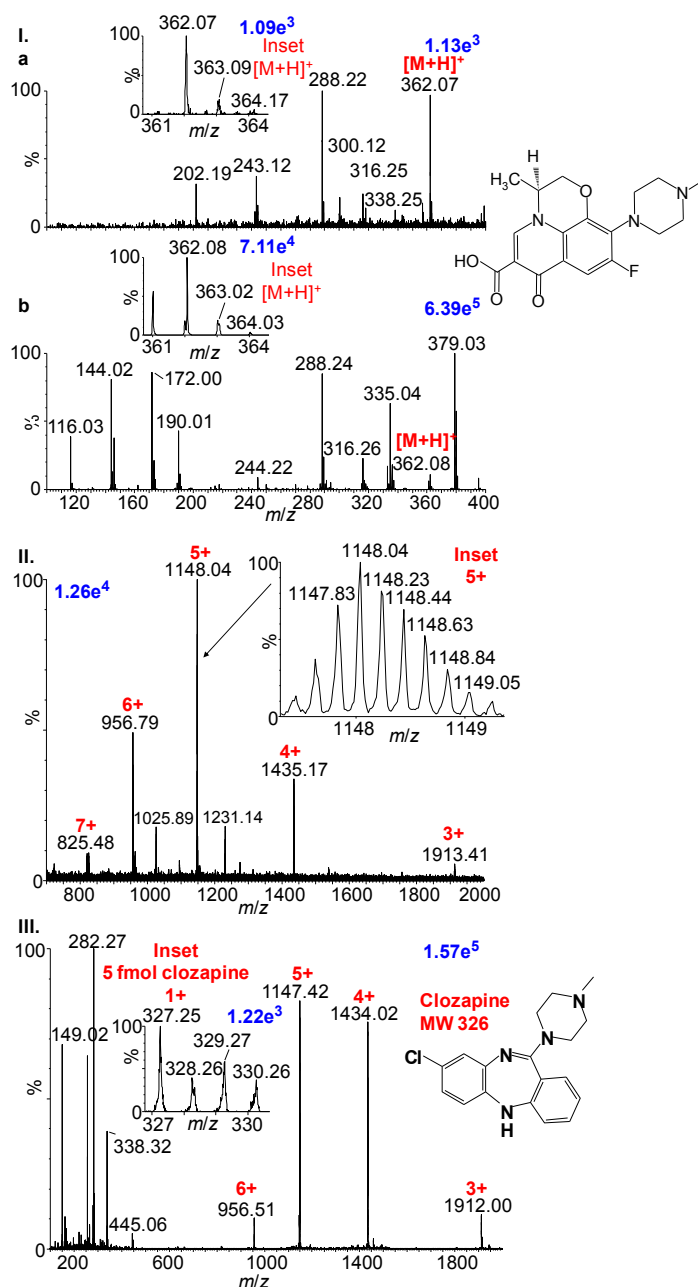
Figure S20: Mass spectra of (**I**) 50 fmol levofloxacin (MW 361 Da) using (**a**) MAIV with 3-NBN matrix and (**b**) MALDI using CHCA matrix acquired using the intermediate pressure MALDI source. MAIV-MS of (**II**) 50 fmol of bovine insulin (MW 5730 Da) with 3-NBN matrix using the custom modified ESI source and (**III**) 5 fmol clozapine (MW 326 Da) and 20 pmol bovine insulin mixture with 3-NBN matrix using the intermediate pressure vacuum MALDI source of the SYNAPT G2 mass spectrometer using LSI settings. Insets show isotopic distributions with structures of (**I**) levofloxacin and (**III**) clozapine.
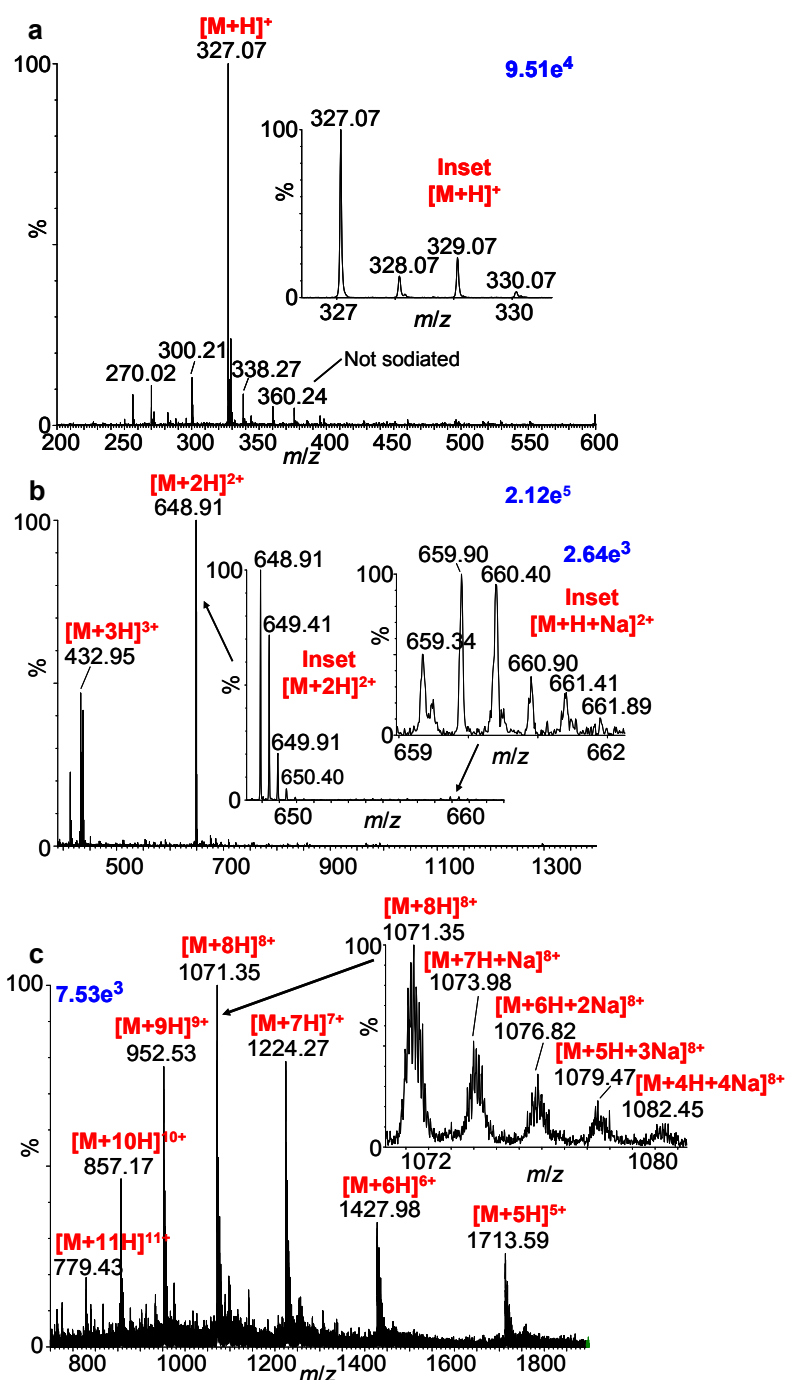
Figure S21. MAIV-MS of (**a**) clozapine (MW 326 Da), (**b**) angiotensin I (MW 1295 Da), and (**c**) ubiquitin (MW 8560 Da) in 1 M NaCl solution with 3-NBN matrix. Data acquired using the intermediate pressure vacuum MALDI source of the SYNAPT G2 mass spectrometer using LSI settings.
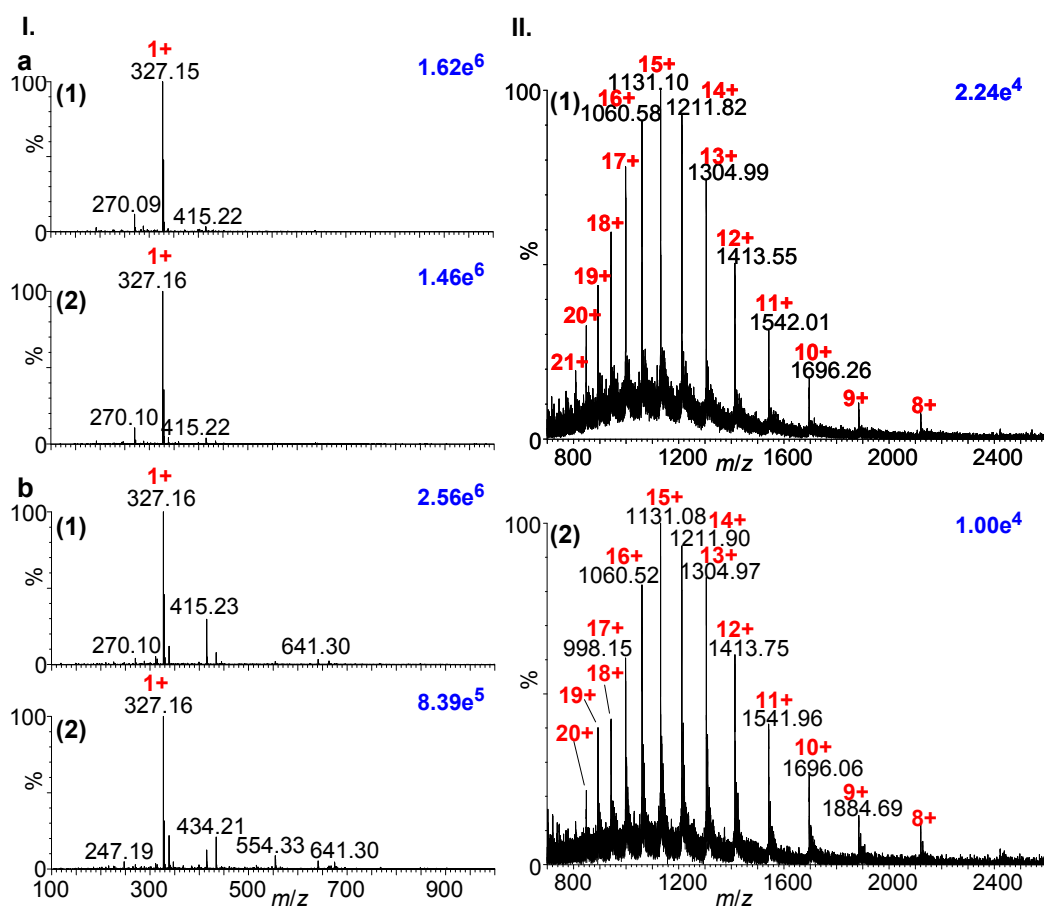
Figure S22. (**I**) Solvent and pH study of 1 pmol clozapine (MW 326 Da) in (**a**) 50:50 methanol:water and (**b**) water with 3-NBN in 100% ACN (**1**) with and (**2**) without acid, and (**II**) pH study of 5 pmol myoglobin in water (MW ~17 kDa) with 3-NBN in 100% ACN (**1**) with and (**2**) without acid. Data acquired using the intermediate pressure vacuum MALDI source of the SYNAPT G2 mass spectrometer using LSI settings.
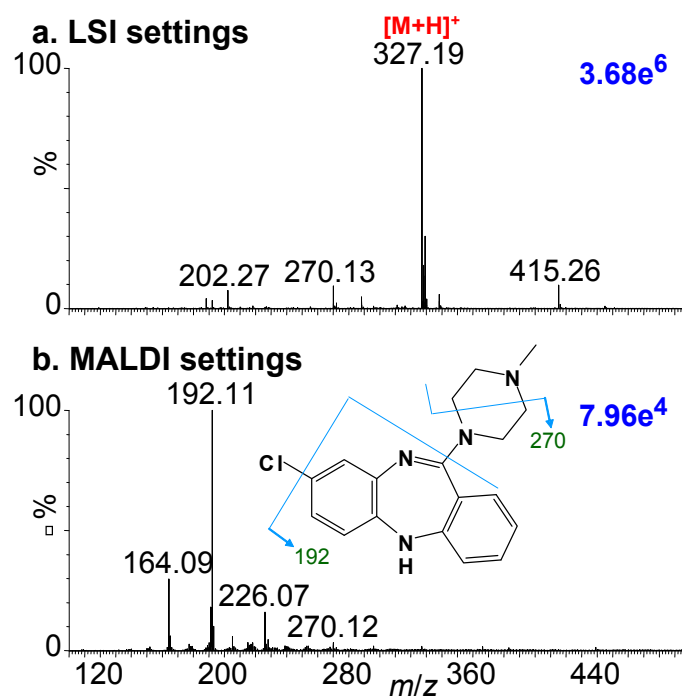
Figure S23. MAIV-MS of 1 pmol clozapine (MW 326 Da) with 3-NBN in 100% ACN with 0.1% formic acid. Data acquired using (**a**) LSI settings and (**b**) MALDI settings of the intermediate pressure vacuum MALDI source of the SYNAPT G2 mass spectrometer.
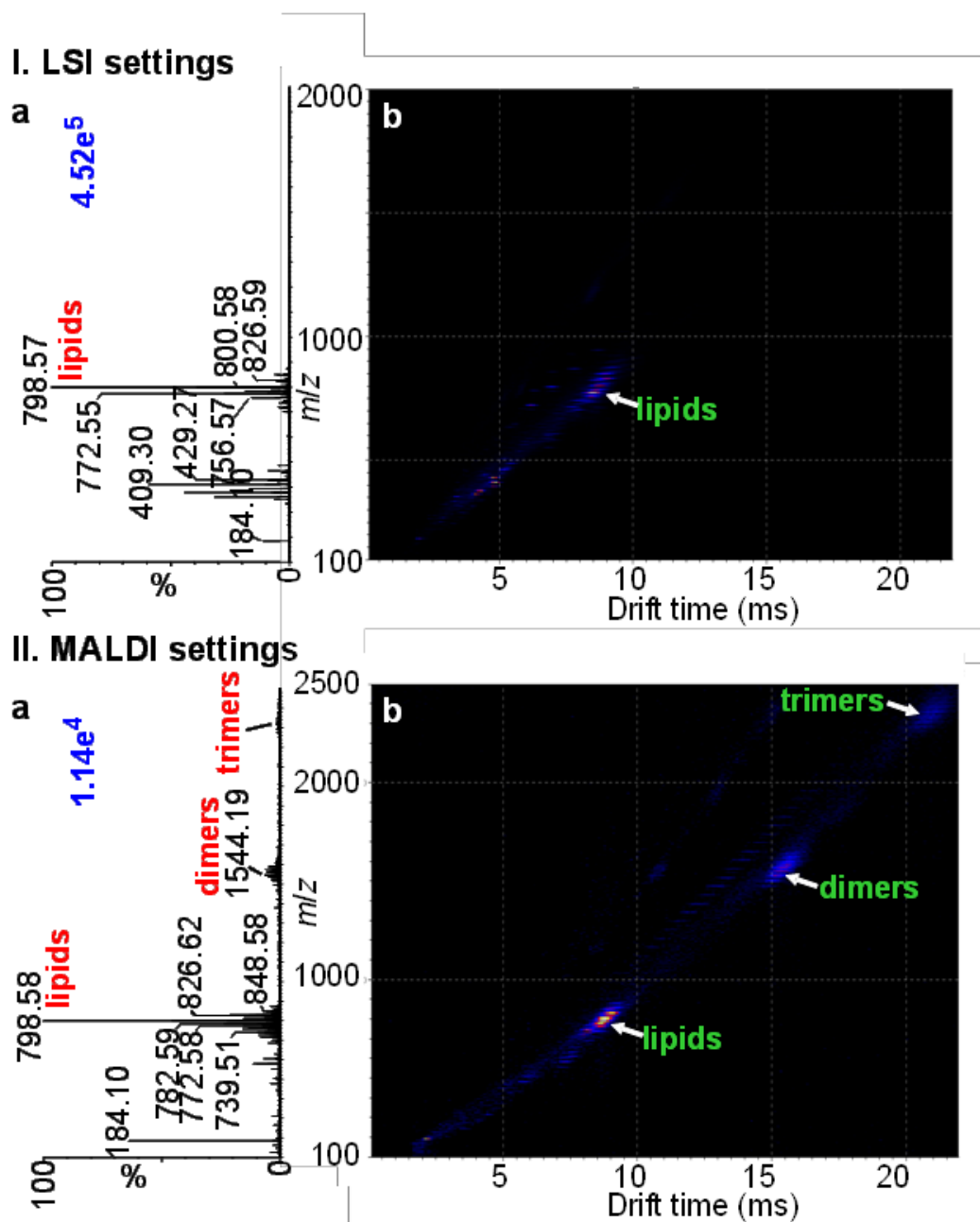
Figure S24: MAIV-IMS-MS of nondelipified mouse brain tissue spotted with 3-NBN matrix acquired using (**I**) LSI settings and (**II**) MALDI settings on the intermediate pressure vacuum MALDI source of the SYNAPT G2 mass spectrometer: (**a**) total mass spectra and (**b**) 2-D plot of drift time *vs. m/z*.
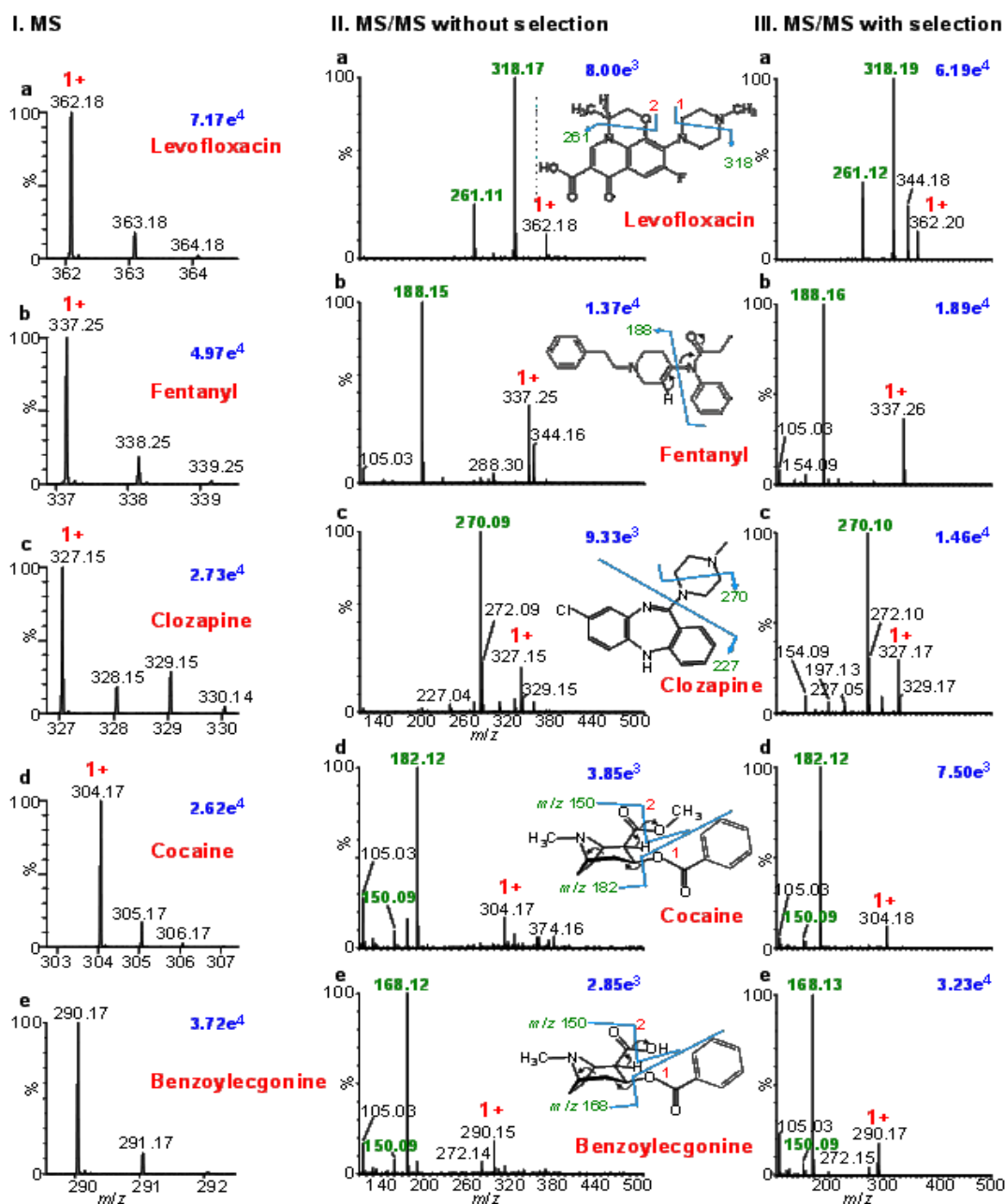
Figure S25: MAIV (**I**) MS and MS/MS mass spectra of small molecule mixture with 3-NBN matrix in the transfer region: (**II**) without selection and extracted from the 2-D plot (**Figure 1.II**) and (**III**) with precursor ion selection of (**a**) levofloxacin [295] (MW 361 Da), (**b**) fentanyl [296] (MW 337 Da), (**c**) clozapine [297] (MW 326 Da), (**d**) cocaine [298] (MW 303 Da), and (**e**) benzoylecgonine [299] (MW 289 Da). Data acquired using the custom modified ESI source of the SYNAPT G2 mass spectrometer. Insets in **II** show structures of the small molecule indicating the fragmentation patterns.
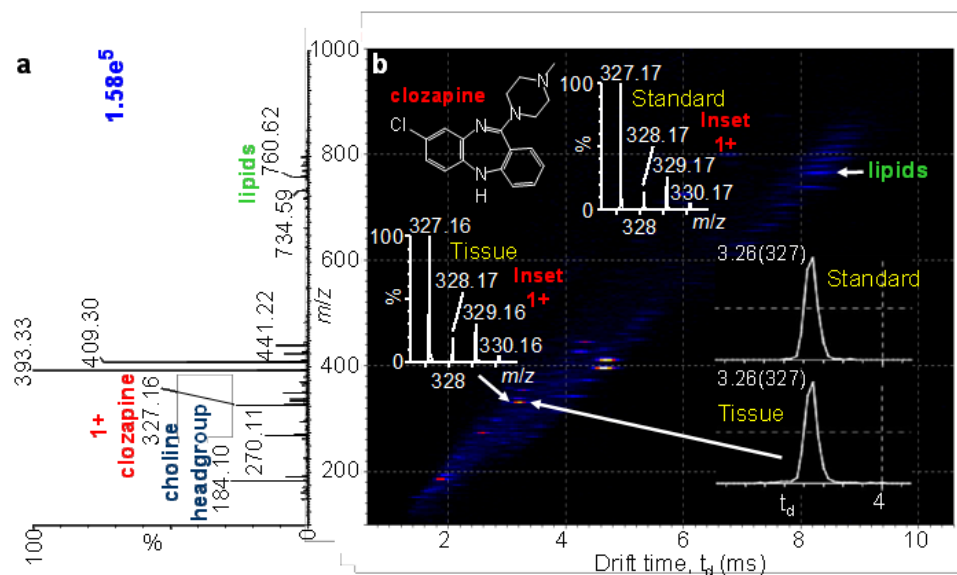
Figure S26: MAIV-IMS-MS of drug treated (90 minutes after receiving 50 mg kg^{-1} of clozapine) mouse brain tissue spotted with 3-NBN matrix: (**a**) total mass spectrum and (**b**) 2-D plot display of drift time *vs. m/z*. Insets in (**b**) show isotopic distributions and drift times of clozapine from tissue and standard. Data acquired using LSI settings of the intermediate pressure vacuum MALDI source of the SYNAPT G2 mass spectrometer.
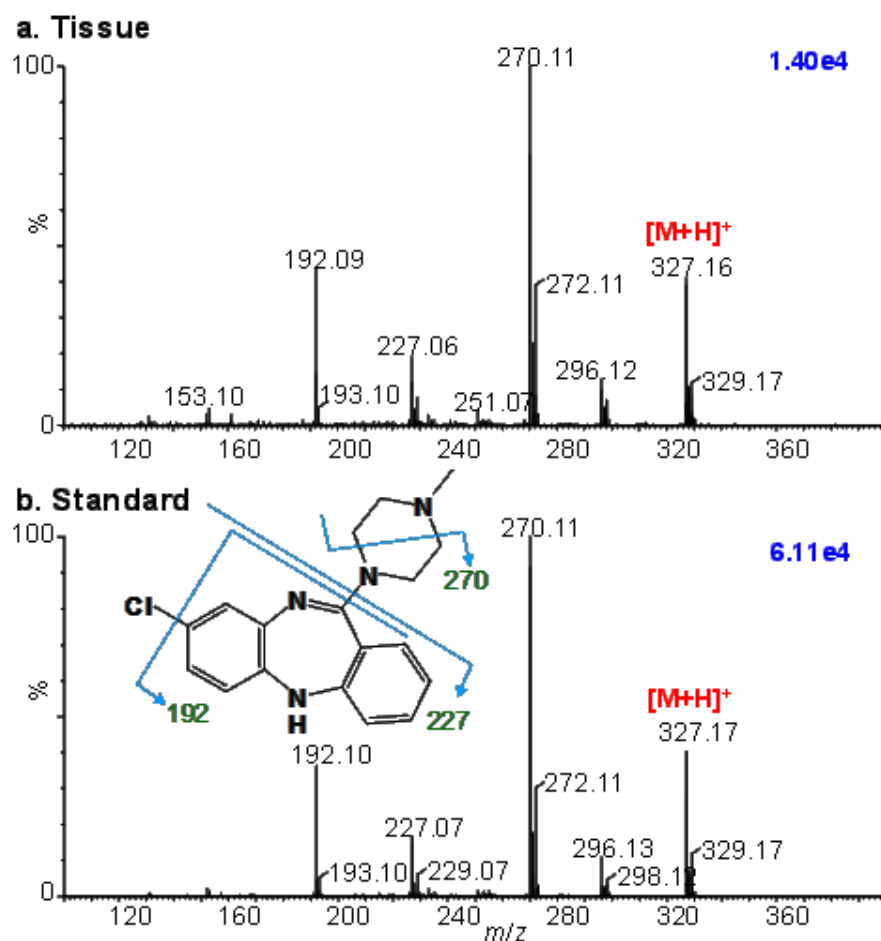
Figure S27: MAIV-IMS-MS/MS of drug clozapine in (**a**) treated mouse brain tissue (90 minutes after receiving 50 mg kg^{-1} of clozapine) spotted with 3-NBN matrix and (**b**) from standard with 3-NBN matrix. Inset in (**b**) shows structure of clozapine indicating fragmentation patterns. Data acquired using LSI settings of the intermediate pressure vacuum MALDI source of the SYNAPT G2 mass spectrometer.
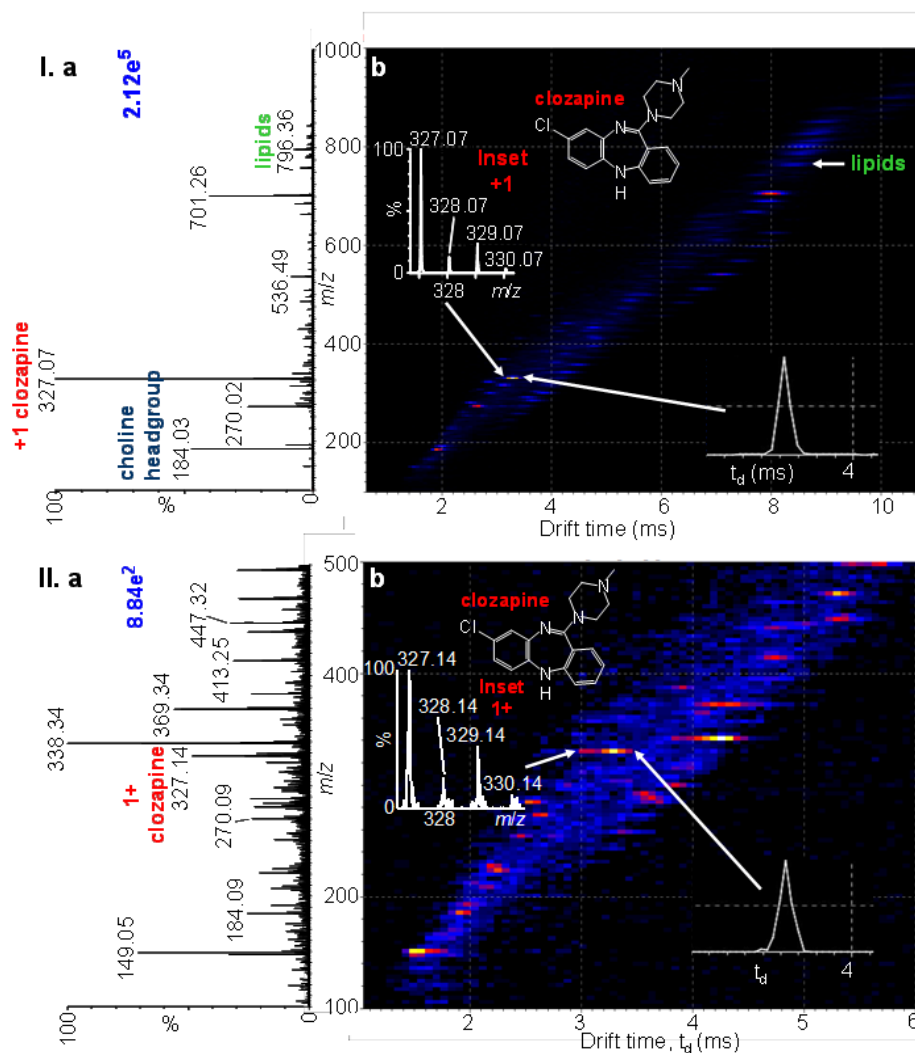
Figure S28: MAIV-IMS-MS of (**I**) clozapine treated mouse tissue removed from glass plate and dipped into the 3-NBN matrix solution and (**II**) plasma of clozapine treated mouse with 3-NBN matrix: (**a**) total mass spectra and (**b**) 2-D plot of drift time *vs. m/z*. Data acquired using LSI settings of the intermediate pressure vacuum MALDI source of the SYNAPT G2 mass spectrometer. Insets in **b** show structure and isotopic distribution of clozapine.
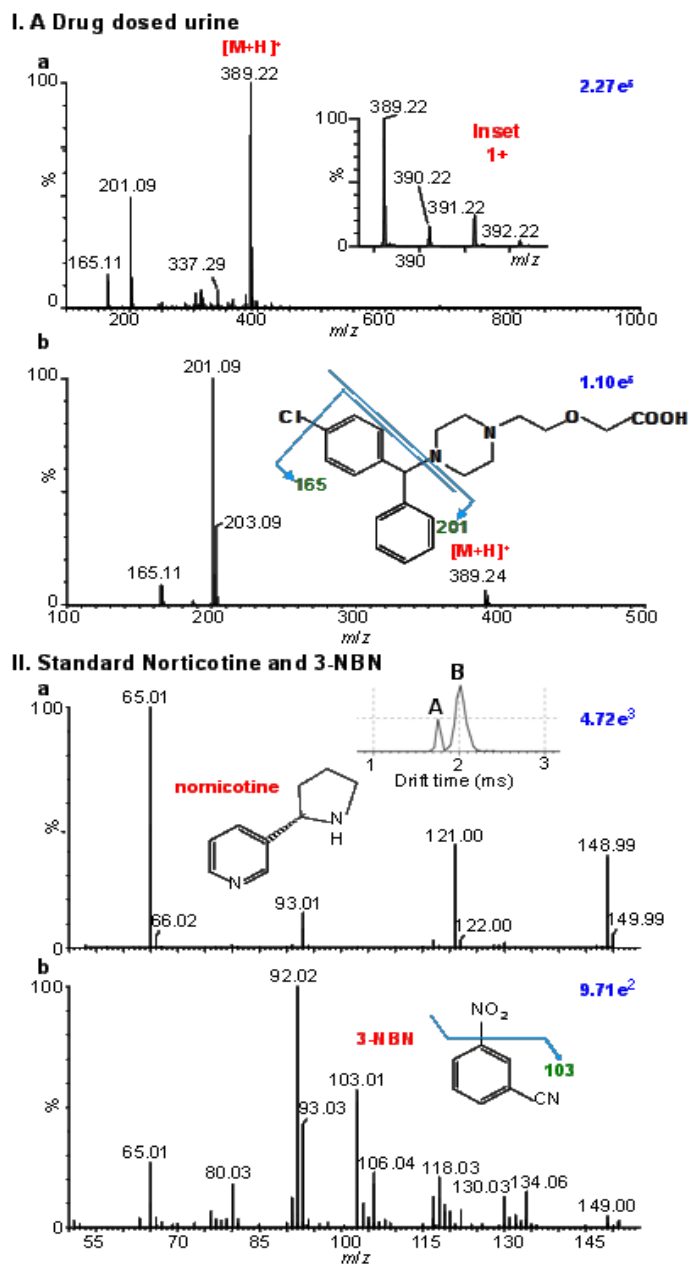
Figure S29: MAIV (**I.a**) cetirizine mass spectra (MW 388 Da) from urine of a drug dosed individual and (**b**) MS/MS of cetirizine tablet, and (**II**) MS/MS of standard (**a**) nornicotine (exact MW 148.0995 Da) and (**b**) 3-NBN (exact MW 148.0267 Da) using LSI settings. Data acquired using the (**I**) intermediate pressure vacuum MALDI source and (**II**) custom modified ESI source of SYNAPT G2 mass spectrometer. Insets in (**I**) show isotopic distribution and structure of cetirizine and (**II**) extracted drift time and structures of nornicotine and 3-NBN.
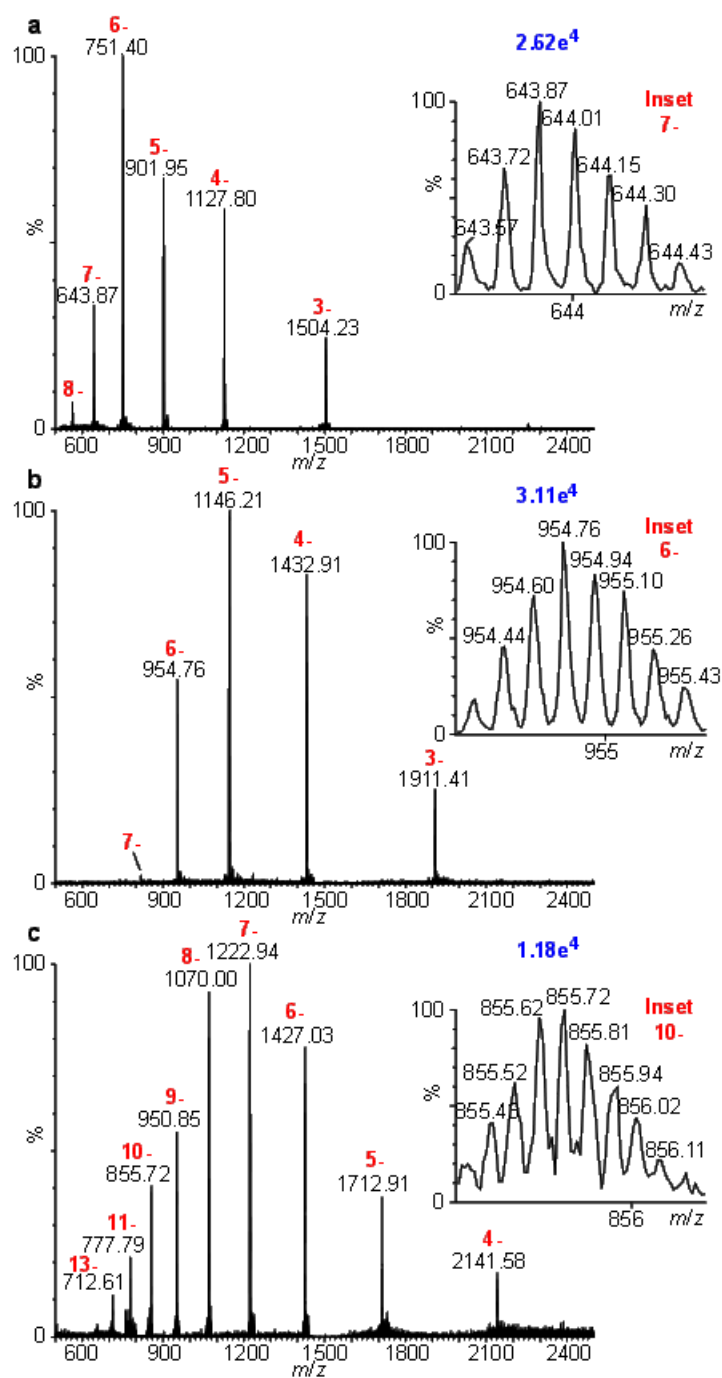
Figure S30: Extracted mass spectra of (**a**) beta amyloid (1-42) (MW 4511 Da), (**b**) bovine insulin (MW 5730 Da), and (**c**) ubiquitin (MW 8560 Da) from the 2-D plot display of drift time *vs. m/z* of the mixture (**Figure 5**) acquired in negative mode using the custom modified ESI source of the SYNAPT G2 mass spectrometer. Insets show isotopic distributions.
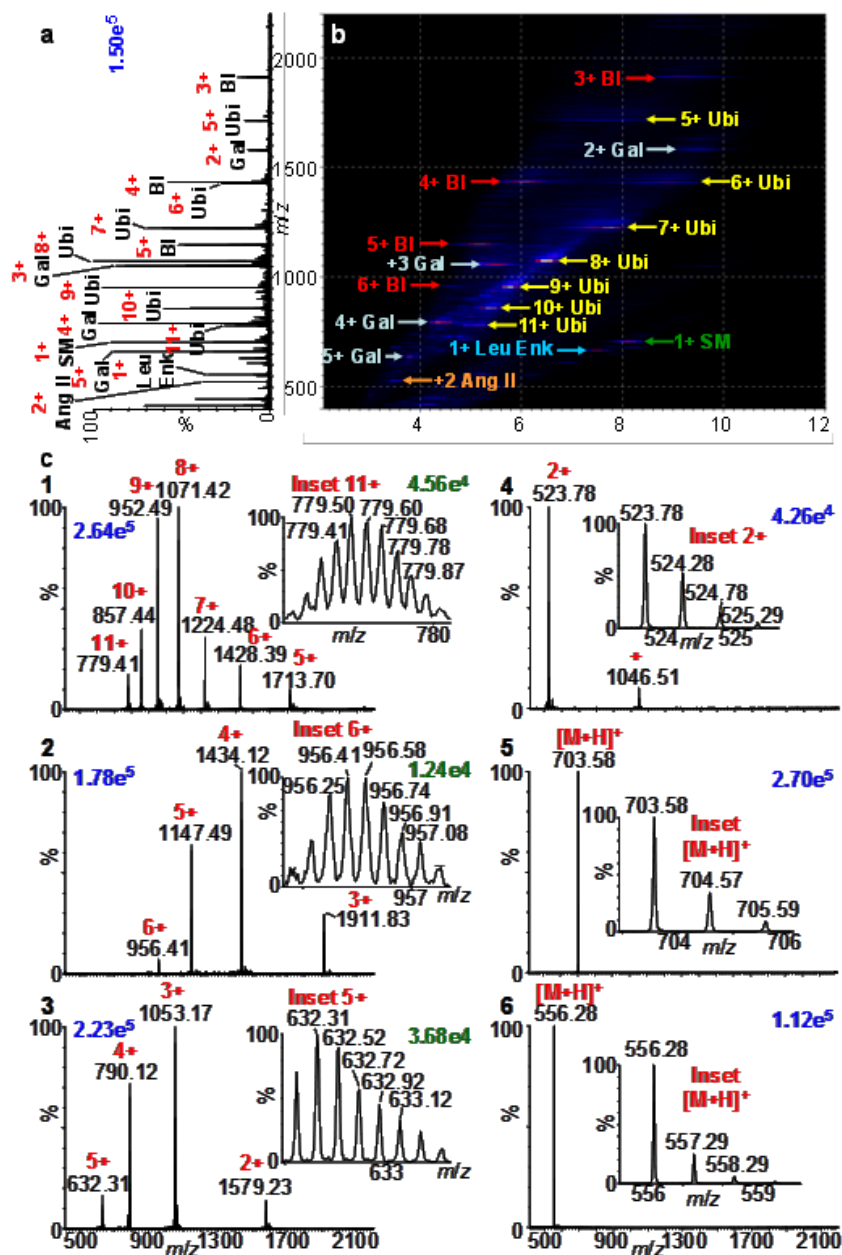
Figure S31: MAIV-IMS-MS of a model mixture of lipids (sphingomyelin MW 702 Da), peptides (leucine enkephalin, MW 555 Da; angiotensin II, MW 1045 Da; galanin, MW 3560 Da), and small proteins (bovine insulin MW 5730 Da, ubiquitin MW 8560 Da) with 3-NBN matrix acquired using the intermediate pressure vacuum MALDI source of the SYNAPT G2 mass spectrometer using LSI settings: (**a**) total mass spectrum, (**b**) 2-D plot display of drift time *vs. m/z,* and (**c**) extracted mass spectra of the components in the mixture. Insets in (**c**) show isotopic distributions.
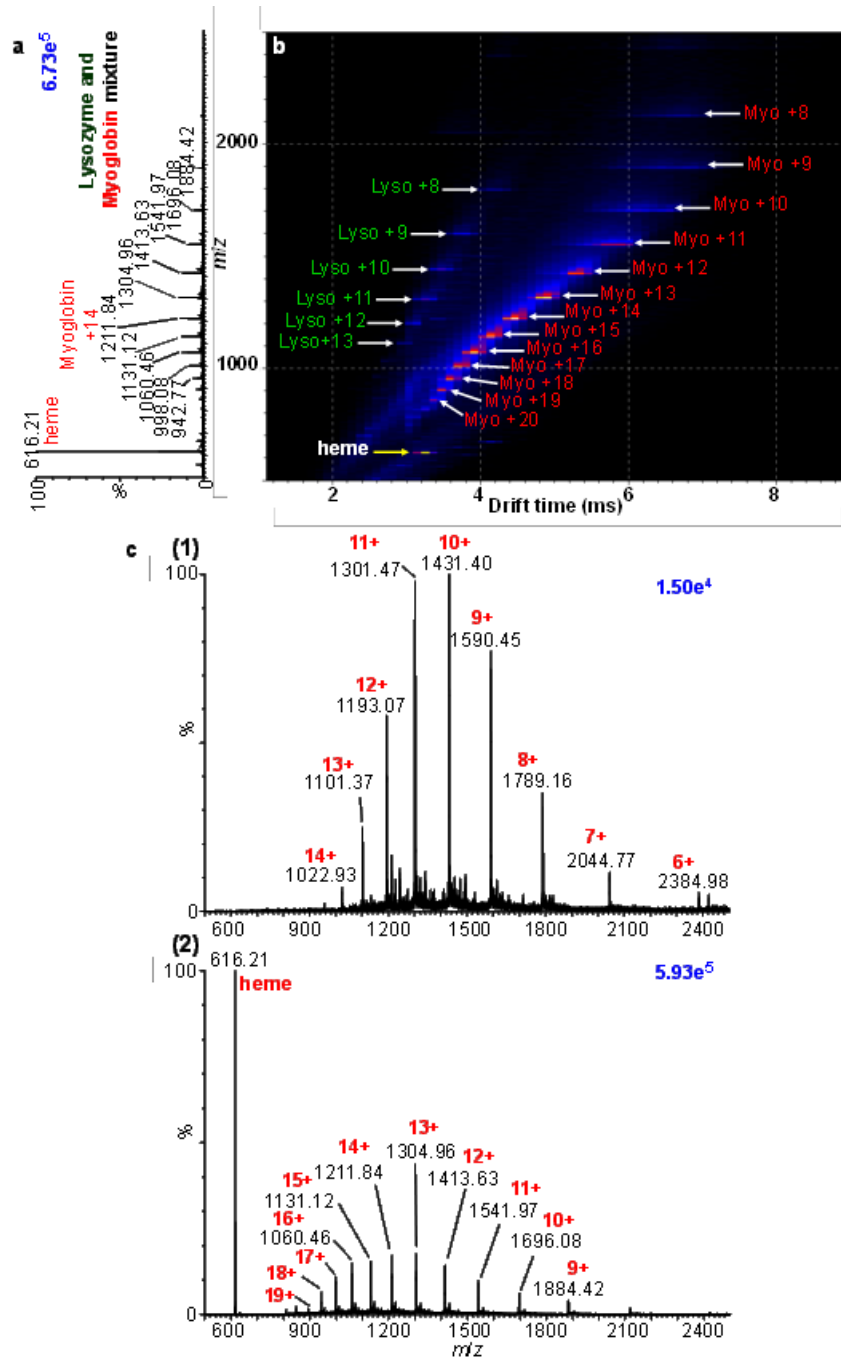
Figure S32: MAIV-IMS-MS (**a**) total mass spectrum, (**b**) 2-D plot display of drift time *vs. m/z,* and (**c**) extracted mass spectra of (**1**) lysozyme (MW 14.3 kDa) and (**2**) myoglobin (MW ~17 kDa) of the mixture (**I**) acquired in positive mode using the intermediate pressure vacuum MALDI source of the SYNAPT G2 mass spectrometer using LSI settings.
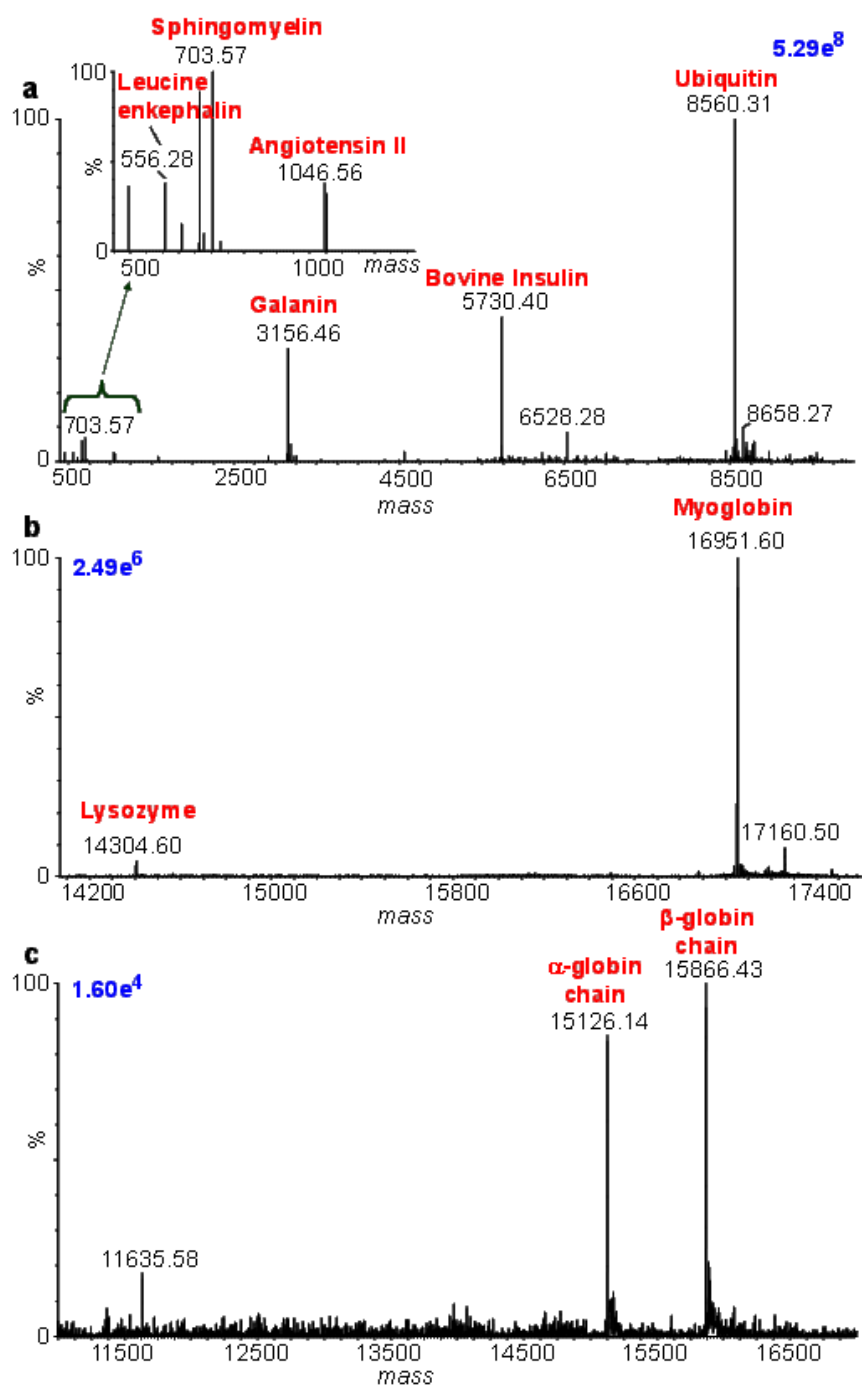
Figure S33: Deconvoluted MAIV mass spectra of (**a**) big model mixture (**Figure S14**), (**b**) protein mixture (**Figure S15**) and (**c**) human plasma (**Figure S17**) using the BayeSpray software from Waters Corporation.
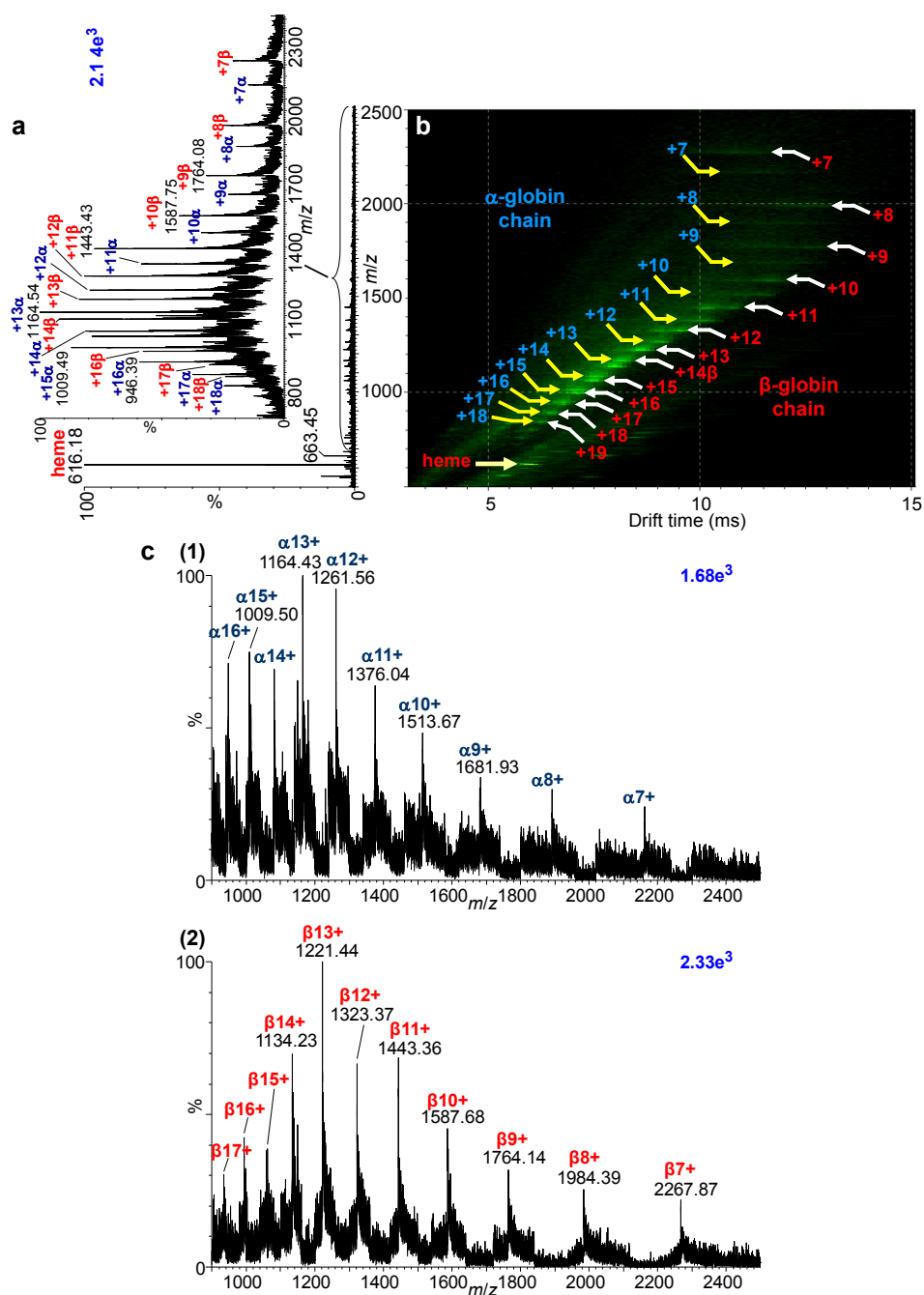
Figure S34: MAIV-IMS-MS (**a**) total mass spectrum with an inset of the extracted mass spectrum of both alpha and beta chains of hemoglobin, (**b**) 2-D plot display of drift time *vs. m/z* and (**c**) extracted mass spectra from (**b**) of (**1**) alpha globin (MW ~ 15.1 kDa) and (**2**) beta globin (MW ~15.9 kDa) of human plasma extracted from bandage with water acquired in positive mode using the intermediate pressure vacuum MALDI source of the SYNAPT G2 mass spectrometer using LSI settings.

256
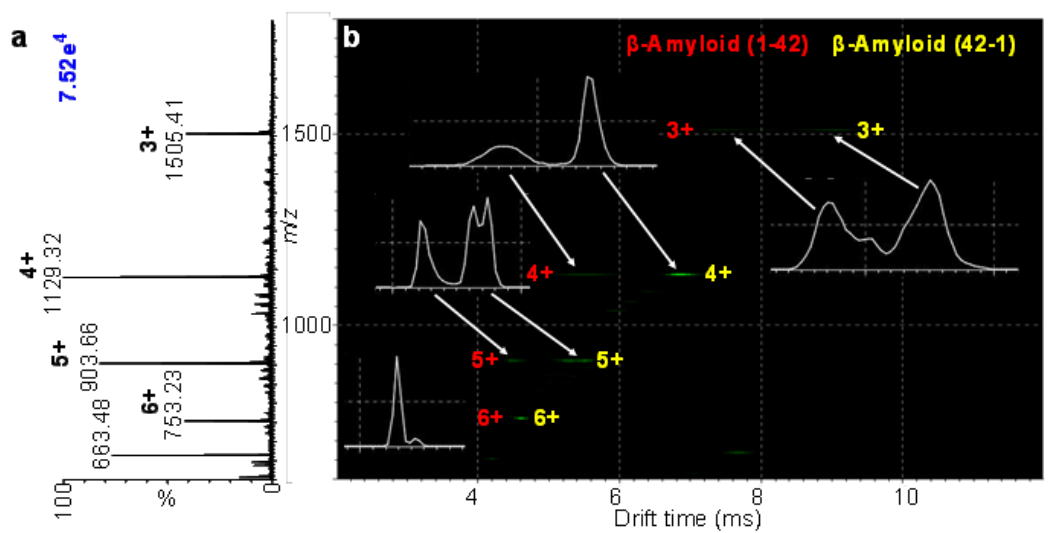
Figure S35: MAIV-IMS-MS of isomeric mixture of beta amyloid (1-42) and (42-1) with 3-NBN matrix: (**a**) total mass spectrum and (**b**) 2-D plot display of drift time *vs. m/z* using the intermediate pressure vacuum MALDI source using LSI settings. Insets in **b** show extracted drift times.
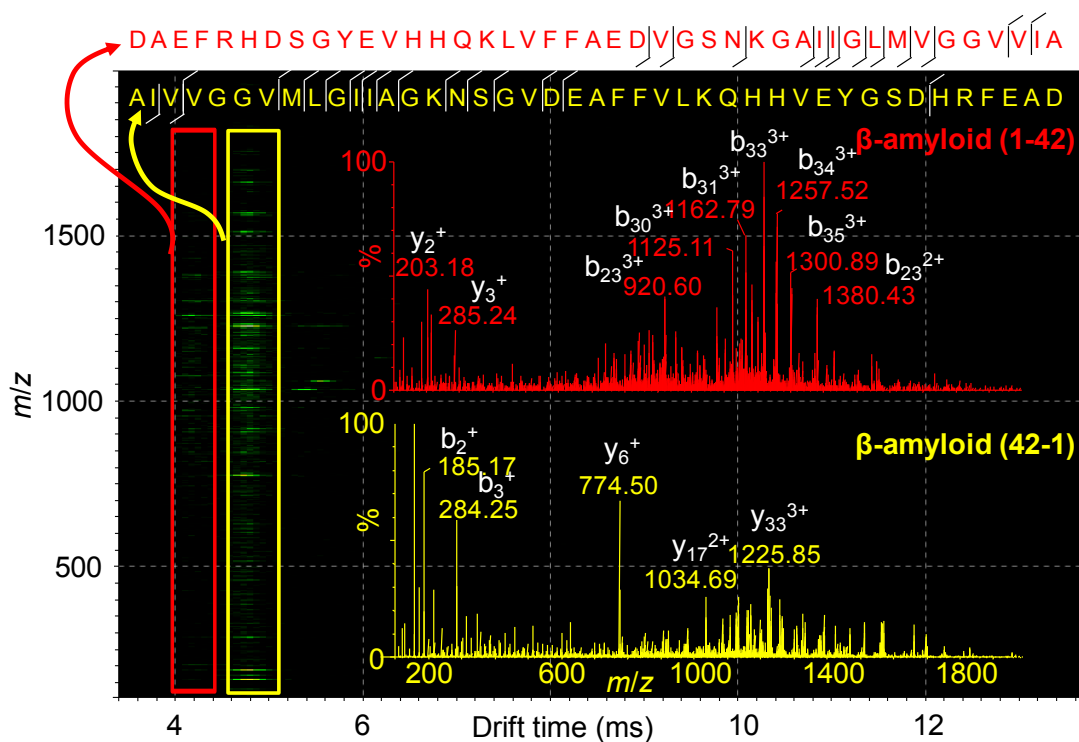
Figure S36: MAIV-IMS-MS/MS 2-D plot display of drift time *vs. m/z* of the isomeric mixture of beta amyloid (1-42) and (42-1) with 3-NBN matrix acquired using the custom modified ESI source of SYNAPT G2 with insets of the extracted MS/MS mass spectra from the 2-D plot of beta amyloid (1-42) (**red**) and (42-1) (**yellow**) (sequence coverage shown on top of the 2-D plot).

APPENDIX D

Copyright Permission

MCP MOLECULAR & CELLULAR
PROTEOMICS

Copyright Permission Policy

These guidelines apply to the reuse of articles, figures, charts and photos in the *Journal of Biological Chemistry, Molecular & Cellular Proteomics* and the *Journal of Lipid Research*.

For authors reusing their own material:

authors need **NOT** contact the journal to obtain rights to reuse their own material. They are automatically granted permission to do the following:

- Reuse the article in print collections of their own writing.
- Present a work orally in its entirety.
- Use an article in a thesis and/or dissertation.
- Reproduce an article for use in the author's courses. (If the author is employed by an academic institution, that institution also may reproduce the article for teaching purposes.)
- Reuse a figure, photo and/or table in future commercial and noncommercial works.
- Post a copy of the paper in PDF that you submitted via BenchPress.

  - Only authors who published their papers under the "Author's Choice" option may post the final edited PDFs created by the publisher to their own/departmental/university Web sites.
  - All authors may link to the journal site containing the final edited PDFs created by the publisher.

Please note that authors must include the following citation when using material that appeared in an ASBMB journal:

"This research was originally published in Journal Name. Author(s). Title. *Journal Name.* Year; Vol:pp-pp. © the American Society for Biochemistry and Molecular Biology."

**SPRINGER LICENSE
TERMS AND CONDITIONS**

May 23, 2013

This is a License Agreement between Ellen Inutan ("You") and Springer ("Springer") provided by Copyright Clearance Center ("CCC"). The license consists of your order details, the terms and conditions provided by Springer, and the payment terms and conditions.

All payments must be made in full to CCC. For payment instructions, please see information listed at the bottom of this form.

License Number	3154950133500
License date	May 23, 2013
Licensed content publisher	Springer
Licensed content publication	Journal of The American Society for Mass Spectrometry
Licensed content title	Laserspray ionization (LSI) ion mobility spectrometry (IMS) mass spectrometry
Licensed content author	Ellen Inutan
Licensed content date	Jan 1, 2010
Volume number	21
Issue number	7
Type of Use	Thesis/Dissertation
Portion	Full text
Number of copies	8
Author of this Springer article	Yes and you are a contributor of the new work
Order reference number	
Title of your thesis / dissertation	Development of Matrix Assisted Ionization Methods for Characterization of Soluble and Insoluble Proteins from Native Environment by Mass Spectrometry
Expected completion date	Aug 2013
Estimated size(pages)	300
Total	0.00 USD
Terms and Conditions	

Introduction

The publisher for this copyrighted material is Springer Science + Business Media. By clicking "accept" in connection with completing this licensing transaction, you agree that the following terms and conditions apply to this transaction (along with the Billing and Payment terms and conditions established by Copyright Clearance Center, Inc. ("CCC"), at the time that you opened your Rightslink account and that are available at any time at http://myaccount.copyright.com).

Copyright Clearance Center

RightsLink®

Home | Account Info | Help

ACS Publications
High quality. High impact.

Title: Laserspray Ionization-Ion Mobility Spectrometry—Mass Spectrometry: Baseline Separation of Isomeric Amyloids without the Use of Solvents Desorbed and Ionized Directly from a Surface

Author: Ellen D. Inutan and Sarah Trimpin

Publication: Journal of Proteome Research

Publisher: American Chemical Society

Date: Nov 1, 2010

Copyright © 2010, American Chemical Society

Logged in as:
Ellen Inutan
Account #:
3000650769

LOGOUT

PERMISSION/LICENSE IS GRANTED FOR YOUR ORDER AT NO CHARGE

BACK | CLOSE WINDOW

Copyright Clearance Center

RightsLink®

Home | Account Info | Help

ACS Publications
High quality High impact.

Title: Commercial Intermediate Pressure MALDI Ion Mobility Spectrometry Mass Spectrometer Capable of Producing Highly Charged Laserspray Ionization Ions

Author: Ellen D. Inutan, Beixi Wang, and Sarah Trimpin

Publication: Analytical Chemistry

Publisher: American Chemical Society

Date: Feb 1, 2011

Copyright © 2011, American Chemical Society

Logged in as:
Ellen Inutan
Account #:
3000650769

LOGOUT

PERMISSION/LICENSE IS GRANTED FOR YOUR ORDER AT NO CHARGE

This type of permission/license, instead of the standard Terms & Conditions, is sent to you because no fee is being charged for your order. Please note the following:

- Permission is granted for your request in both print and electronic formats, and translations.
- If figures and/or tables were requested, they may be adapted or used in part.
- Please print this page for your records and send a copy of it to your publisher/graduate school.
- Appropriate credit for the requested material should be given as follows: "Reprinted (adapted) with permission from (COMPLETE REFERENCE CITATION). Copyright (YEAR) American Chemical Society." Insert appropriate information in place of the capitalized words.
- One-time permission is granted only for the use specified in your request. No additional uses are granted (such as derivative works or other editions). For any other uses, please submit a new request.

BACK | CLOSE WINDOW

Copyright Clearance Center

RightsLink®

Home | Account Info | Help

ACS Publications
High quality. High impact.

Title: Laserspray Ionization Imaging of Multiply Charged Ions Using a Commercial Vacuum MALDI Ion Source

Author: Ellen D. Inutan, James Wager-Miller, Ken Mackie, and Sarah Trimpin

Publication: Analytical Chemistry

Publisher: American Chemical Society

Date: Nov 1, 2012

Copyright © 2012, American Chemical Society

Logged in as:
Ellen Inutan
Account #:
3000650769

LOGOUT

PERMISSION/LICENSE IS GRANTED FOR YOUR ORDER AT NO CHARGE

This type of permission/license, instead of the standard Terms & Conditions, is sent to you because no fee is being charged for your order. Please note the following:

- Permission is granted for your request in both print and electronic formats, and translations.
- If figures and/or tables were requested, they may be adapted or used in part.
- Please print this page for your records and send a copy of it to your publisher/graduate school.
- Appropriate credit for the requested material should be given as follows: "Reprinted (adapted) with permission from (COMPLETE REFERENCE CITATION). Copyright (YEAR) American Chemical Society." Insert appropriate information in place of the capitalized words.
- One-time permission is granted only for the use specified in your request. No additional uses are granted (such as derivative works or other editions). For any other uses, please submit a new request.

BACK | CLOSE WINDOW

**SPRINGER LICENSE
TERMS AND CONDITIONS**

May 23, 2013

This is a License Agreement between Ellen Inutan ("You") and Springer ("Springer") provided by Copyright Clearance Center ("CCC"). The license consists of your order details, the terms and conditions provided by Springer, and the payment terms and conditions.

All payments must be made in full to CCC. For payment instructions, please see information listed at the bottom of this form.

License Number	3154950370385
License date	May 23, 2013
Licensed content publisher	Springer
Licensed content publication	Journal of The American Society for Mass Spectrometry
Licensed content title	Matrix Assisted Ionization in Vacuum, a Sensitive and Widely Applicable Ionization Method for Mass Spectrometry
Licensed content author	Sarah Trimpin
Licensed content date	Jan 1, 2013
Volume number	24
Issue number	5
Type of Use	Thesis/Dissertation
Portion	Full text
Number of copies	8
Author of this Springer article	Yes and you are a contributor of the new work
Order reference number	
Title of your thesis / dissertation	Development of Matrix Assisted Ionization Methods for Characterization of Soluble and Insoluble Proteins from Native Environment by Mass Spectrometry
Expected completion date	Aug 2013
Estimated size(pages)	300
Total	0.00 USD
Terms and Conditions	

Introduction

The publisher for this copyrighted material is Springer Science + Business Media. By clicking "accept" in connection with completing this licensing transaction, you agree that the following terms and conditions apply to this transaction (along with the Billing and Payment terms and conditions established by Copyright Clearance Center, Inc. ("CCC"), at the time that you opened your Rightslink account and that are available at any time at http://myaccount.copyright.com).

SPRINGER LICENSE
TERMS AND CONDITIONS

May 23, 2013

This is a License Agreement between Ellen Inutan ("You") and Springer ("Springer") provided by Copyright Clearance Center ("CCC"). The license consists of your order details, the terms and conditions provided by Springer, and the payment terms and conditions.

All payments must be made in full to CCC. For payment instructions, please see information listed at the bottom of this form.

License Number	3154950509176
License date	May 23, 2013
Licensed content publisher	Springer
Licensed content publication	International Journal for Ion Mobility Spectrometry
Licensed content title	The potential for clinical applications using a new ionization method combined with ion mobility spectrometry-mass spectrometry
Licensed content author	Ellen D. Inutan
Licensed content date	Jan 1, 2013
Volume number	16
Issue number	2
Type of Use	Thesis/Dissertation
Portion	Full text
Number of copies	8
Author of this Springer article	Yes and you are a contributor of the new work
Order reference number	
Title of your thesis / dissertation	Development of Matrix Assisted Ionization Methods for Characterization of Soluble and Insoluble Proteins from Native Environment by Mass Spectrometry
Expected completion date	Aug 2013
Estimated size(pages)	300
Total	0.00 USD

Terms and Conditions

Introduction
The publisher for this copyrighted material is Springer Science + Business Media. By clicking "accept" in connection with completing this licensing transaction, you agree that the following terms and conditions apply to this transaction (along with the Billing and Payment terms and conditions established by Copyright Clearance Center, Inc. ("CCC"), at the time that you opened your Rightslink account and that are available at any time at http://myaccount.copyright.com).

BIBLIOGRAPHY

[1]   Yamashita, M.; Fenn, J. Electrospray Ion Source. Another Variation on the Free-Jet Theme. *J. Phys. Chem.* **1984**, *88*, 4451-4459.

[2]   Tanaka, K.; Waki, H.; Ido, Y.; Akita, S.; Yoshida, Y.; Yoshida, T.; Matsuo, T. Protein and polymer analyses up to *m/z* 100,000 by laser ionization time-of- flight mass spectrometry. *Rapid Commun. Mass Spectrom.* **1988**, *2*, 151-153.

[3]   Karas, M.; Hillenkamp, F. Laser desorption ionization of proteins with molecular masses exceeding 10,000 daltons. *Anal. Chem.* **1988**, *60*, 2299-2301.

[4]   Aebersold, R.; Goodbelt, D.R. Mass Spectrometry in Proteomics. *Chem. Rev.* **2001**, *101*, 269-295.

[5]   Hillenkamp, F.; Karas, M.; Beavis, R.C.; Chait, B.T.T. Matrix-assisted laser desorption/ionization mass spectrometry of biopolymers. *Anal. Chem.* **1991**, *63*, 1193A-1202A.

[6]   Zhang, H.; Caprioli, R.M. Direct Analysis of Aqueous Samples by Matrix-assisted Laser Description Ionization Mass Spectrometry Using Membrane Targets Precoated with Matrix. *J. Mass Spectrom.* **1996**, *31*, 690-692.

[7]   Caprioli, R.M.; Farmer, T.B.; Gile, J. Molecular imaging of biological samples: Localization of peptides and proteins using MALDI-TOF MS. *Anal. Chem.* **1997**, *69*, 4751-4760.

[8]   Stoeckli, M.; Chaurand, P.; Hallahan, D.E.; Caprioli, R.M. Imaging Mass Spectrometry: A New Technique Applied to Mammalian Brain Tumor Protein Expression. *Nat. Med.* **2001**, *7*, 493-496.

[9]   Wu, C.C.; Yates III, J.R. The Application of Mass Spectrometry to Membrane Proteins. *Nat. Biotech.* **2003**, *21*, 262-267.

[10]   Trimpin, S.; Brizzard, B. Analysis of Insoluble Proteins. *Biotechniques* **2009**, *46*, 409-419.

[11]   Stevens, T.J.; Arkin, I.T. Do more complex organisms have greater proportion of membrane proteins in their genomes? *Proteins* **2000**, *39*, 417-420.

[12]   Wallin, E.; Von Heijne, G. Genome-wide analysis of integral membrane proteins from eubacterial, archaean, and eukaryotic organisms. *Protein Sci.* **1998**, *7*, 1029-1038.

[13]   Rohner, T.C.; Staab, D.; Stoeckli, M. Spatial and spectral correlations in MALDI mass spectrometry images by clustering and multivariate analysis. *Mech. Ageing Dev.* **2005**, *126*, 177-185.

[14]   Stefani, M.; Dobson, C.M. Protein aggregation and aggregate toxicity: new insights into protein folding, misfolding diseases, and biological evolution. *J. Mol. Med.* **2003**, *81*, 678-699.

[15]   Pierson, J.; Norris, J.L.; Aerni, H.R.; Svenningsson, P.; Caprioli, R.M.; Andren, P.E. Molecular profiling of experimental Parkinson's disease: Direct analysis of peptides and proteins on brain tissue sections by MALDI mass spectrometry. *J. Proteome Res.* **2004**, *3*, 289-295.

[16]   Stauber, J.; Lemaire, R.; Franck, J.; Bonnel, D.; Croix, D.; Day, R.; Wisztorski, M.; Fournier, I.; Salzet, M. MALDI imaging of formalin-fixed paraffin-embedded

tissues: application to model animals of Parkinson disease for biomarker hunting. *J. Proteome Res.* **2008**, 7, 969-978.

[17] Quist, A.; Doudevski, I.; Lin, H.; Azimova, R.; Ng, D.; Frangione, B.; Ghiso, J.; Lal, R. Amyloid ion channels: A common structural link for protein-misfolding disease. *Proc. Nat'l Acad. Sci. USA* **2005**, *102*, 10427-10432.

[18] Stefani, M.; Dobson, C.M. Protein aggregation and aggregate toxicity: New insights into protein folding, misfolding diseases, and biological evolution. *J. Mol. Med.* **2003**, *81*, 678-699.

[19] Savas, J.N.; Stein, B.D.; Wu, C.C.; Yates, J.R. Mass spectrometry accelerates membrane protein analysis. *Trends Biochem. Sci.* **2011**, *36*, 388-396.

[20] Vestal, M.L. The Future of Biological Mass Spectrometry. *J. Am. Soc. Mass Spectrom.* **2011**, *22*, 953-959.

[21] Laiko, V.V.; Baldwin, M.A.; Burlingame, A.L. Atmospheric Pressure MALDI-MS. *Anal. Chem.* **2000**, *72*, 652-657.

[22] Doroshenko, V.M.; Laiko, V.V.; Taranenko, N.I.; Berkout, V.D.; Lee, H.S. Recent developments in atmospheric pressure MALDI mass spectrometry. *Int. J. Mass Spectrom.* **2002**, *221*, 39-58.

[23] Vestal, M.L. Modern MALDI Time-of-flight mass spectrometry. *J. Mass Spectrom.* **2009**, *44*, 303-317.

[24] Sheehan, E.W.; Willoughby, R.C. (June 13, **2006**) U. S. Patent 7,060,976.

[25] Willis, D.A.; Grosu, V. Microdroplet Deposition by Laser-Induced Forward Transfer. *Appl. Phys. Lett.* **2005**, *86*, 244103.

[26]   Galicia, M.C.; Vertes, A.; Callahan, J.H. Atmospheric pressure matrix-assisted laser desorption/ionization in transmission geometry. *Anal. Chem.* **2002**, *74*, 1891-1895.

[27]   Trimpin, S.; Herath, T.N.; Inutan, E.D.; Cernat, S.A.; Wager-Miller, J.; Mackie, K.; Walker, J.M. Field-free Transmission Geometry Atmospheric Pressure Matrix-Assisted Laser Desorption/Ionization for Rapid Analysis of Unadulterated Tissue Samples. *Rapid Commun. Mass Spectrom.* **2009**, *23*, 3023-3027.

[28]   Trimpin, S.; Inutan, E.D.; Herath, T.N.; McEwen, C.N.: Matrix-assisted laser desorption/ionization mass spectrometry method for selectively producing either singly or multiply charged molecular ions. *Anal. Chem.* **2010**, *82*, 11-15.

[29]   Trimpin, S.; Inutan, E.D.; Herath, T.N.; McEwen, C.N. Laserspray Ionization - A New AP-MALDI Method for Producing Highly Charged Gas-Phase Ions of Peptides and Proteins Directly from Solid Solutions. *Mol. Cell. Proteomics* **2010**, *9*, 362-367.

[30]   Trimpin, S. A Perspective on MALDI Alternatives - Total solvent-free analysis and electron transfer dissociation of highly charged ions by laserspray ionization. *J. Mass Spectrom.* **2010**, *45*, 471-485.

[31]   McEwen, C.N.; Trimpin, S. An Alternative Ionization Paradigm for Atmospheric Pressure Mass Spectrometry: Flying Elephants from Trojan Horses. *Int J. Mass Spectrom.* **2011**, *300*, 167-172.

[32]   Handschuh, M.; Nettesheim, S.; Zenobi, R. Laser-induced molecular desorption and particle ejection from organic films. *Appl. Surf. Sci.* **1999**, *137*, 125-135.

[33]   Cai, Y.; Peng, W.P.; Kuo, S.J.; Sabu, S.; Han, C.C.; Chang, H.C. Optical Detection and Charge State Analysis of MALDI-Generated Particles with Molecular Masses Greater than 5 MDa. *Anal. Chem.* **2002**, *74*, 4434-4440.

[34]   Musapelo, T.; Murray, K.K. Particle Formation in Ambient MALDI Plumes. *Anal. Chem.* **2011**, *83*, 6601-6608.

[35]   Knochenmuss, R.; Zhigilei, L.V. Molecular Dynamics Model of Ultraviolet Matrix-assisted Laser Desorption/Ionization Including Ionization Processes. *J. Phys. Chem. B* **2005**, *109*, 22947-22957.

[36]   Zhigilei, L.V.; Garrison, B.J. Microscopic Mechanism of Laser Ablation of Organic Solids in the Thermal and Stress Confinement Irradiation Regimes. *J. Appl. Phys.* **2000**, *88*, 1281-1298.

[37]   Zhigilei, L.V. Dynamics of the Plume Formation and Parameters of the Ejected Clusters in Short-pulse Laser Ablation. *Appl. Phys. A* **2003**, *76*, 339-350.

[38]   Zhigilei, L.V.; Kodali, P.B.; Garrison, B. On the threshold behavior in laser ablation of organic solids. *J. Chem. Phys. Lett.* **1997**, *276*, 269-273.

[39]   McEwen, C.N.; Pagnotti, V.S.; Inutan, E.D.; Trimpin, S. New Paradigm in Ionization: Multiply Charged Ion Formation from a Solid Matrix without a Laser or Voltage. *Anal. Chem.* **2010**, *82*, 9164-9168.

[40]   Li, J.; Inutan, E.D.; Wang, B.; Lietz, C.B.; Green, D.R.; Manly, C.D.; Richards, A.L.; Marshall, D.D.; Lingenfelter, S.; Ren, Y.; Trimpin, S. Matrix assisted ionization: New aromatic and non-aromatic matrix compounds producing multiply charged lipid, peptide, and protein ions in the positive and negative mode

observed directly from surfaces. *J. Am. Soc. Mass Spectrom.* **2012**, *23*, 1625-1643.

[41] McEwen, C.N.; Larsen, B.S.; Trimpin, S. Laserspray Ionization on a Commercial AP-MALDI Mass Spectrometer Ion Source: Selecting Singly or Multiply Charged Ions. *Anal. Chem.* **2010**, *82*, 4998-5001.

[42] Inutan, E.D.; Wang, B.; Trimpin, S. Commercial intermediate pressure MALDI ion mobility spectrometry mass spectrometer capable of producing highly charged laserspray ionization ions. *Anal. Chem.* **2011**, *83*,678-684.

[43] Inutan, E.D.; Wager-Miller, J.; Mackie, K.; Trimpin, S. Laserspray Ionization Imaging of Multiply Charged Ions using a Commercial Vacuum MALDI Ion Source. *Anal. Chem.***2012**, *84*, 9079-9084.

[44] Trimpin, S.; Ren, Y.; Wang, B.; Lietz, C.B.; Richards, A.L.; Marshall, D.D.; Inutan, E.D. Extending the Laserspray Ionization Concept to Produce Highly Charged Ions at High Vacuum on a Time-of-Flight Mass Analyzer. *Anal. Chem.* **2011**, *83*, 5469-5475.

[45] Trimpin, S.; Wang, B.; Inutan, E.D.; Li, J.; Lietz, C.B.; Harron, A.; Pagnotti, V.S.; Sardelis, D.; McEwen, C.N. A Mechanism for Ionization of Nonvolatile Compounds in Mass Spectrometry: Considerations from MALDI and InletIonization. *J. Am. Soc. Mass Spectrom.* **2012**, *23*, 1644-1660.

[46] Inutan, E.D.; Trimpin, S. Matrix Assisted Ionization Vacuum, a New Ionization Method for Biological MaterialsAnalysis using Mass Spectrometry. *Mol. Cell Proteomics* **2013**, *12*, 792-796.

[47]   Trimpin, S.; Inutan, E.D. Matrix Assisted Ionization in Vacuum, a Sensitive and Widely Applicable Ionization Method for Mass Spectrometry. *J. Am. Soc. Mass Spectrom.* **2013**, DOI: 10.1007/s13361-012-0571-z.

[48]   Inutan, E.D.; Richards, A.L.; Wager-Miller, J.; Mackie, K.; McEwen, C.N.; Trimpin, S. Laserspray Ionization - A New Method for Protein Analysis Directly from Tissue at Atmospheric Pressure and with Ultra-High Mass Resolution and Electron Transfer Dissociation Sequencing. *Mol. Cell. Proteomics* **2011**, *10*, 1-8.

[49]   Inutan, E. D.; Trimpin, S. Laserspray ionization (LSI) ion mobility spectrometry (IMS) mass spectrometry (MS). *J. Am. Soc. Mass Spectrom.* **2010**, *21*, 1260-1264.

[50]   Inutan, E.D.; Trimpin, S. Laserspray ionization-ion mobility spectrometry-mass spectrometry: Baseline separation of isomeric amyloids without the use of solvents desorbed and ionized directly from a surface. *J. Proteome Res.* **2010**, *9*, 6077-6081.

[51]   Dole, M.; Mack, L.L.; Hines, R.L.; Mobley, R.C.; Ferguson, L.D.; Alice, M. B. Molecular beams of macroions. *J. Chem. Phys.* **1968**, *49*, 2240-2249.

[52]   Iribarne, J.V.; Thomson, B.A. On the evaporation of small ions from charged droplets. *J. Chem. Phys.* **1976**, *64*, 2287-2294.

[53]   Vestal, M.L. Studies of ionization mechanisms involved in thermo- spray LC-MS. *Int. J. Mass Spectrom. Ion Phys.* **1983**, *46*, 193-196.

[54]   Karas, M.; Gluckmann, M.; Schafer, J. Ionization in matrix-assisted laser desorption/ionization: singly charged molecular ions are the lucky survivors. *J. Mass Spectrom.* **2000**, *35*, 1-12.

[55] Karas, M.; Kruger, R. Ion formation in MALDI: the cluster ionization mechanism. *Chem. Rev.* **2003**, *103*, 427-440.

[56] Kennedy, E.T.; Costello, J.T.; Mosnier, J.P. New experiments in photoabsorption studies of singly and multiply charged ions. *J. Electron Spectrosc.* **1996**, *79*, 283-288.

[57] Kononikhin, A.S.; Nikolaev, E.N.; Frankevich, V.; Zenobi, R. Multiply charged ions in matrix-assisted laser desorption/ionization generated from electrosprayed sample layers. *Eur. J. Mass Spectrom.* **2005**, *11*,257-259.

[58] Syka, J.E.; Coon, J.J.; Schroeder, M.J.; Shabanowitz, J.; Hunt, D.F. Peptide and protein sequence analysis by electron transfer dissociation mass spectrometry. *Proc. Natl. Acad. Sci. U.S.A.* **2004**, *101*, 9528-9533.

[59] Clemmer, D. E.; Jarrold, M. F. Ion mobility measurements andtheir applications to clusters and biomolecules. *J. Mass Spectrom.* **1997**, *32*, 577-592.

[60] Wu, C.; Klasmeier, J.; Hill, H. H. Atmospheric pressure ion mobilityspectrometry of protonated and sodiated peptides. *Rapid Commun. Mass Spectrom.***1999**, *13*, 1138-1142.

[61] Wyttenbach, T.; Bowers, M. T. Gas-phase conformations: The ion mobility/ion chromatography method. *Top.Curr. Chem.* **2003**, *225*,207-232.

[62] McLean, J. A.; Ruotolo, B. T.; Gillig, K. J.; Russell, D. H. Ion mobilitymassspectrometry: A new paradigm for proteomics. *Int. J. Mass Spectrom.* **2005**, *240*, 301-315.

[63]   Pringle, S. D.; Giles, K.; Wildgoose, J. L.; Williams, J. P.; Slade, S. E.; Thalassinos, K.; Bateman, R. H.; Bowers, M. T.; Scrivens, J. H. An investigation of the mobility separation of some peptide and protein ions using a new hybrid quadrupole/travelling wave IMS/oa-ToF instrument. *Int. J. Mass Spectrom.* **2007**, *261*, 1-12.

[64]   Liu, X.; Valentine, S. J.; Plasencia, M. D.; Trimpin, S.; Naylor, S.;Clemmer, D. E. Mapping the Human Plasma Proteome by SCXLC-IMS-MS. *J. Am. Soc. Mass Spectrom.* **2007**, *18*, 1249-1264.

[65]   Trimpin, S.; Plasencia, M. D.; Isailovic, D.; Clemmer, D. E. ResolvingOligomers from Fully Grown Polymers with IMS-MS. *Anal. Chem.* **2007**,*79*, 7965-7974.

[66]   Trimpin, S.; Clemmer, D. E. Ion mobility spectrometry/massspectrometry snapshots for assessing the molecular compositionsof complex polymeric systems. *Anal. Chem.* **2008**, *80*, 9073-9083.

[67]   Trimpin, S.; Tan, B.; Bohrer, B. C.; O'Dell, D. K.; Merenbloom, S. I.; Pazos, M. X.; Clemmer, D. E.; Walker, J. M. Profiling of phospholipids and related lipid structures using multidimensional ion mobility spectrometry-mass spectrometry. *Int. J. Mass Spectrom.* **2009**, *287*, 58-69.

[68]   Mitchell, J., Jr.; Deveraux, H. D. Determination of traces of organic compounds in the atmosphere: role of detectors in gas chromatography. *Anal. Chim. Acta* **1978***, 52***,** 45-52.

[69]   Sweeting, L. M.; Cashel, M. L.; Rosenblatt, M. M. Triboluminescence spectra of organic crystals are sensitive to conditions of acquisition. *J. Lumin.* **1992***, 52***, 281-291.

[70]   Sweeting, L. M. Triboluminescence with and without air. *Chem. Mater.* **2001***, 13*, 854-870.

[71]   Inutan, E.D.; Wager-Miller, J.; Narayan, S.; Mackie, K.; Trimpin, S. The Potential for Clinical Applications using a New Ionization Method Combined with Ion Mobility Spectrometry-Mass Spectrometry. *Int. J. Ion Mobility Spectrom.* **2013**, *16*, 145-159.

[72]   Trimpin, S.; Rouhanipour, A.; Az, R.; Rader, H.J.; Mullen, K. New aspects in matrix-assisted laser desorption/ionization time-of-flight mass spectrometry: A universal solvent-free sample preparation. *Rapid Commun. Mass Spectrom.* **2001**, *15*, 1364-1373.

[73]   Trimpin, S.; McEwen, C.N. Multisample preparation methods for the solvent-free MALDI-MS analysis of synthetic polymers. *J. Am. Soc. Mass Spectrom.* **2007**, *18*, 377-381.

[74]   Seeley, E.H.; Oppenheimer, S.R.; Mi, D.; Chaurand, P.; Caprioli, R.M. Enhancement of protein sensitivity for MALDI imaging mass spectrometry after chemical treatment of tissue sections. *J. Am. Soc. Mass Spectrom.* **2008**, *19*, 1069-1077.

[75]   Garrett, T.J.; Yost, R.A. Analysis of intact tissue by intermediate-pressure MALDI on a linear ion trap mass spectrometer. *Anal. Chem.* **2006**, *78*, 2465-2469.

[76]   Clarke, S.L.; Vasanthakumar, A.; Anderson, S.A.; Pondarre, C.; Koh, C.M.; Deck, K. M.; Pitula, J.S.; Epstein, C.J.; Fleming, M.D.; Eisenstein, R.S. Iron-responsive degradation of iron-regulatory protein 1 does not require the Fe–S cluster. *EMBO J.* **2006**, *25*, 544-553.

[77]   Navratil, M.; Mabbott, G.A.; Arriaga, E.A. Chemical microscopy applied to biological systems. *Anal. Chem.* **2006**, *78*, 4005- 4019.

[78]   Trimpin, S.; Mixon, A.E.; Stapels, M.D.; Kim, M.Y.; Spencer, P.S.; Deinzer, M.L. Identification of endogenous phosphorylation sites of bovine medium and low molecular weight neurofilament proteins by tandem mass spectrometry. *Biochemistry* **2004**, *43*, 2091-2105.

[79]   Gunawardena, H.P.; Emory, J.F.; McLuckey, S.A. Phosphopeptide anion characterization via sequential charge inversion and electron-transfer dissociation. *Anal. Chem.* **2006**, *78*, 3788-3793.

[80]   Zubarev, R.A.; Kelleher, N.L.; McLafferty, F.W. Electron capture dissociation of multiply charged protein cations. A nonergodic process. *J. Am. Chem. Soc.* **1998**, *120*, 3265-3266.

[81]   Zubarev, R.A.; Horn, D.M.; Fridriksson, E.K.; Kelleher, N.L.; Kruger, N.A.; Lewis, M.A.; Carpenter, B.K.; McLafferty, F.W. Electron capture dissociation for

structural characterization of multiply charged protein cations. *Anal. Chem.* **2000**, *72*, 563-573.

[82] Knochenmuss, R.; Zenobi, R. MALDI ionization: the role of in-plume processes. *Chem. Rev.* **2003**, *103*, 441–452.

[83] Knochenmuss, R.A. Ion formation mechanisms in UV-MALDI. *Analyst* **2006**, *131*, 966-986.

[84] Gluckmann, M.; Pfenninger, A.; Kruger, R.; Thierolf, M.; Karas, M.; Horneffer,V.; Hillenkamp, F.; Strupat, K. Mechanisms in MALDI analysis: surface interaction or incorporation of analytes? *Int. J. Mass Spectrom.* **2001**, *210/211*, 121-132.

[85] Fournier, I.; Brunot, A.; Tabet, J.C.; Bolbach, G. Delayed extraction experiments using a repulsive potential before ion extraction: Evidence of clusters as ion precursors in UV-MALDI. Part I: Dynamical effects with the matrix 2,5-dihydroxybenzoic acid. *Int. J. Mass Spectrom.* **2002**, *213*, 203-215.

[86] Knochenmuss, R.A Quantitative model of ultraviolet matrix-assisted laser desorption/ionization including analyte ion generation. *Anal. Chem.* **2003**, *75*, 2199-2207.

[87] Chang, W.C.; Huang, L.C.; Wang, Y.S.; Peng, W.P.; Chang, H.C.; Hsu, N.Y.; Yang, W.B.; Chen, C.H. Matrix-assisted laser desorption/ionization (MALDI) mechanism revisited. *Anal.Chim.Acta* **2007**, *582*, 1-9.

[88]   Zhou, J.; Lee, T. D. Charge state distribution shifting of protein ions observed in matrix-assisted laser desorption ionization mass spectrometry. *J. Am. Soc. Mass Spectrom.* **1995**, *6*, 1183-1189.

[89]   Ovaberg, A.; Karas, M.; Hillenkamp, F. Matrix-assisted laser desorption of large biomolecules with a TEA-CO_2-laser. *Rapid Commun. Mass Spectrom.* **1991**, *5*, 128-131.

[90]   Sampson, J.S.; Hawkridge, A.M.; Muddiman, D.C. Development and characterization of an ionization technique for analysis of biological macromolecules: Liquid matrix-assisted laser desorption electrospray ionization. *Anal. Chem.* **2008**, *80*, 6773-6778.

[91]   Grimm, R.L.; Beauchamp, J.L. Field-induced droplet ionization mass spectrometry. *J. Phys. Chem. B* **2003**, *107*, 14161-14163.

[92]   Hiraoka, K. Laser spray: Electric field-assisted matrix-assisted laser desorption/ionization. *J. Mass Spectrom.* **2004**, *39*, 341-350.

[93]   Coon, J.J.; Ueberheide, B.; Syka, J.E.; Dryhurst, D.D.; Ausio, J.; Shabanowitz, J.; Hunt, D.F. Protein identification using sequential ion/ion reactions and tandem mass spectrometry. *Proc. Nat'l. Acad. Sci. U.S.A.* **2005**, *102*, 9463-9468.

[94]   Krutchinsky, A.N.; Chait, B.T. On the nature of the chemical noise in MALDI mass spectra. *J. Am. Soc. Mass Spectrom.* **2002**, *13*, 129-134.

[95]   Katta, V.; Rockwood, A.L.; Vestal, M.L. Field limit for ion evaporation from charged thermospray droplets. *Int. J. Mass Spectrom. Ion Proc.* **1991**, *103*, 129-148.

[96]   Trimpin, S.; Deinzer, M.L. Solvent-free MALDI-MS for the analysis of β-amyloid peptides via the mini-ball mill approach: qualitative and quantitative improvements. *J. Am. Soc. Mass Spectrom.* **2007**, *18*, 1533-1543.

[97]   Trimpin, S.; Wijerathnea, K.; McEwen, C.N. Rapid methods of polymer and polymer additives identification: multi-sample solvent-free MALDI, pyrolysis at atmospheric pressure, and atmospheric solids analysis probe mass spectrometry. *Anal. Chim. Acta* **2009**, *654*, 20-25.

[98]   Horneffer, V.; Dreisewerd, K.; Ludemann, H.C.; Hillenkamp, F.; Lage, M.; Strupat, K. Is the incorporation of analytes into matrix crystals a prerequisite for matrix-assisted laser desorption/ionization mass spectrometry? A study of five positional isomers of dihydroxybenzoic acid. *Int. J. Mass Spectrom.* **1999**, *185-187*, 859-870.

[99]   Trimpin, S.; Rader, H.J.; Mullen, K. Investigation of theoretical principles for MALDI-MS derived from solvent-free sample preparation. Part I: preorganization. *Int. J. Mass Spectrom.* **2006**, *253*, 13-21.

[100] Mikesh, L.M.; Ueberheide, B.; Chi, A.; Coon, J.J.; Syka, J.E.; Shabanowitz, J.; Hunt D.F. The utility of ETD mass spectrometry in proteomic analysis. *Biochim. Biophys. Acta* **2006**, *1764*, 1811-1822.

[101] Bohrer, B.C.; Merenbloom, S.I.; Koeniger, S.L.; Hilderbrand, A.E.; Clemmer, D.E. Biomolecule Analysis by Ion Mobility Spectrometry. *Ann. Rev. Anal. Chem.* **2008**, *1*, 293-327.

[102] Kanu, A.B.; Hill, H.H. Ion Mobility Spectrometry Detection for Gas Chromatography. *J. Chromatogr. A* **2008**, *1177*, 12-27.

[103] McLean, J.A.; Ruotolo, B.T.; Gillig, K.J.; Russell, D.H. Ion Mobility-Mass Spectrometry: A New Paradigm for Proteomics. *Int. J. Mass Spectrom.* **2005**, *240*, 301-315.

[104] Kaur-Atwal, G.; O'Connor, G.; Aksenov, A.A.; Bocos-Bintintan, V.; Paul Thomas, C.L.; Creaser, C.S. Chemical Standards for Ion Mobility Spectrometry: A Review. *Int. J. Ion Mobility Spectrom.* **2009**, *12*, 1-14.

[105] Pringle, S.D.; Giles, K.; Wildgoose, J.L.; Williams, J.P.; Slade, S.E.; Thalassinos, K.; Bateman, R.H.; Bowers, M.T.; Scrivens, J.H. An investigation of the mobility separation of some peptide and protein ions using a new hybrid quadrupole/travelling wave IMS/oa-ToF instrument. *Int. J. Mass Spectrom.* **2007**, *261*, 1-12.

[106] Koeniger, S.L.; Merenbloom, S.I.; Sevugarajan, S.; Clemmer, D.E. Transfer of Structural Elements from Compact to Extended States in Unsolvated Ubiquitin. *J. Am. Chem. Soc.* **2006**, 128, 11713-11719.

[107] Koeniger, S.L.; Merenbloom, S.I.; Clemmer, D.E. Evidence for Many Resolvable Structures within Conformation Types of Electrosprayed Ubiquitin Ions. *J. Phys. Chem. B* **2006**, *110*, 7017-7021.

[108] Koeniger, S.L.; Clemmer, D.E. Resolution and Structural Transitions of Elongated States of Ubiquitin. *J. Am. Soc. Mass Spectrom.* **2007**, *18*,322-331.

[109] Valentine, S.J.; Counterman, A.E.; Clemmer, D.E. Conformer-Dependent Proton-Transfer Reactions of Ubiquitin Ions. *J. Am. Soc. Mass Spectrom.* **1997**, *8*, 954-961.

[110] Chaurand, P.; Schriver, K.E.; Caprioli, R.M. Instrument design and characterization for high resolution MALDI-MS imaging of tissue sections. *J. Mass Spectrom.* **2007**, *42*, 476-89.

[111] McDonnell, L.A.; Heeren, R.M.A. Imaging mass spectrometry. *Mass Spectrom. Rev.* **2007**, *26*, 606-643.

[112] Fournier, I.; Wisztorski, M.; Salzet, M. Tissue imaging using MALDI-MS: A new frontier of histopathology proteomics. *Expert Rev. Proteomics* **2008**, *5*, 413-424.

[113] Trimpin, S.; Herath, T.N.; Inutan, E.D.; Wager-Miller, J.; Kowalski,P.; Claude, E.; Walker, J.M.; Mackie, K. Automated solvent-free matrix deposition for tissue imaging by mass spectrometry. *Anal.Chem.* **2010**, *82*, 359-367.

[114] Li, J.; Taraszka, J.A.; Counterman, A.E.; Clemmer, D.E. Influenceof solvent composition and capillary temperature on the conformations of electrosprayed ions: Unfolding of compact ubiquitin conformers from pseudonative and denatured solutions. *Int. J. Mass. Spectrom.* **1999**, *185/186/187*, 37-47.

[115] Badman, E.R.; Hoaglund-Hyzer, C.S.; Clemmer, D.E. Dissociation of different conformations of ubiquitin ions. *J. Am. Soc. Mass Spectrom.* **2002**, *13*, 719-723.

[116] Grasso, G.; Mineo, P.; Rizzarelli, E.; Spoto, G. MALDI, AP/MALDI and ESI techniques for the MS detection of amyloid β-peptides. *Int. J.Mass Spectrom.* **2009**, *282*, 50-55.

[117] Shen, C.L.; Murphy, R.M. Solvent effects on self-assembly of_β-amyloid peptide. *Biophys. J.* **1995**, *69*, 640-651.

[118] Bernstein, S.L.; Wyttenbach, T.; Baumketner, A.; Shea, J.; Bitan,G.; Teplow, D.B.; Bowers, M.T. Amyloid β-protein: Monomer structure and early aggregation states of Aβ 42 and its Pro19 alloform. *J. Am. Chem. Soc.* **2005**, *127*, 2075-2084.

[119] Butterfield, D.A.; Boyd-Kimball, D. The critical role of methionine 35 in Alzheimer's amyloid beta-peptide (1-42) - induced oxidative stress and neurotoxicity. *Biochem. Biophys. Acta* **2005**, *1703*, 149-156.

[120] Fournier, I.; Wisztorski, M.; Salzet, M. Tissue imaging using MALDI-MS: a new frontier of histopathology proteomics. *Expert Rev. Proteomics* **2008**, *5*, 413-424.

[121] Bedair, M.; Sumner, L.W. Current and emerging mass spectrometry technologies for metabolomics. *Trends Anal. Chem.* **2008**, *27*, 238-250.

[122] Jackson, S.N.; Ugarov, M.; Egan, T.; Post, J.D.; Langlais, D.; Schultz, J.A.; Woods, A.S. MALDI-ion mobility-TOFMS imaging of lipids in rat brain tissue. *J. Mass Spectrom.* **2007**, *42*, 1093-1098.

[123] Stoeckli, M.; Chaurand, P.; Hallahan, D.E.; Caprioli, R.M. Imaging mass spectrometry: A new technology for the analysis of protein expression in mammalian tissues. *Nat. Med.* **2001**, *7*, 493-496.

[124] Chaurand, P.; Schwartz, S.A.; Caprioli, R.M. Imaging mass spectrometry: A new tool to investigate the spatial organization of peptides and proteins in mammalian tissue sections. *Curr. Opin. Chem. Biol.* **2002**, *6*, 676-681.

[125] Khatib-Shahidi, S.; Andersson, M.; Herman, J.L.; Gillespie, T.A.; Caprioli, R.M. Direct molecular analysis of whole-body animal tissue sections by imaging MALDI mass spectrometry. *Anal. Chem.* **2006**, *78*, 6448-6456.

[126] Chaurand, P.; Cornett, D.S.; Caprioli, R.M. Molecular imaging of thin mammalian tissue sections by mass spectrometry. *Curr. Opin. Biotechnol.* **2006**, *17*, 431- 436.

[127] Ostrowski, S.G.; Van Bell, C.T.; Winograd, N.; Ewing, A.G. Mass spectrometric imaging of highly curved membranes during Tetrahymena mating. *Science* **2004**, *305*, 71-73.

[128] Winograd, N. The magic of cluster SIMS. *Anal.Chem.* **2005**, *77*,142A-149A.

[129] Jones, E.A.; Lockyer, N.P.; Vickerman, J.C. Depth profiling brain tissue sections with a 40 keV C-60(+) primary ion beam. *Anal. Chem.* **2008**, *80*, 2125-2132.

[130] Chaurand, P.; Schwartz, S.A.; Caprioli, R.M. Assessing protein patterns in disease using imaging mass spectrometry. *J. Proteome Res.* **2004**, *3*, 245-252.

[131] Zimmerman, T.A.; Monroe, E.B.; Sweedler, J.V. Adapting the stretched sample method from tissue profiling to imaging. *Proteomics* **2008**, *8*, 3809-3815.

[132] Deininger, S.O.; Suckau, D.; Becker, M.; Schuerenberg, M. MALDI-tissue imaging at high resolution and speed: Essential steps towards its applications in histology. *Proc. of the 57th ASMS Conference on Mass Spectrometry and Allied Topics*, Philadelphia, May 31–June 4, **2009**.

[133] Touboul, D.; Piednoe, H.; Voisin, V.; De La Porte, S.; Brunelle, A.; Halgand, F.; Laprevote, O. Changes in phospholipid composition within the dystrophic muscle

by matrix-assisted laser desorption/ionization mass spectrometry and mass spectrometry imaging. *Eur. J. Mass Spectrom.* **2004**, *10*, 657-664.

[134] Chaurand, P.; Schwartz, S.A.; Caprioli, R.M. Profiling and imaging proteins in tissue sections by MS. *Anal. Chem.* **2004**, *76*, 86A-93A.

[135] Han, H.; Xia, Y.; Yang, M.; McLuckey, S.A. Rapidly alternating transmission mode electron-transfer dissociation and collisional activation for the characterization of polypeptide ions. *Anal. Chem.* **2008**, *80*, 3492-3497.

[136] Landgraf, R.R.; Prieto Conaway, M.C.; Garrett, T.J.; Stacpoole, P.W.; Yost, R.A. Imaging of lipids in spinal cord using intermediate pressure matrix-assisted laser desorption-linear ion trap/Orbitrap MS. *Anal. Chem.* **2009**, *81*, 8488-8495.

[137] Zydel, F.; Trimpin, S.; McEwen, C.N. Laserspray ionization using an atmospheric solids analysis probe for sample introduction. *J. Am. Soc. Mass Spectrom.* **2010**, *21*, 1889-1892.

[138] Richards, A.L.; Marshall, D.D.; Inutan, E.D.; McEwen, C.N.; Trimpin, S. *Rapid Commun. Mass Spectrom.* **2011**, *25*, 1-4.

[139] Takats, Z.; Wiseman, J.M.; Gologan, B.; Cooks, R.G. Mass spectrometry sampling under ambient conditions with desorption electrospray ionization. *Science* **2004**, *306*, 471-473.

[140] Laiko, V.V.; Moyer, S.C.; Cotter, R.J. Atmospheric pressure MALDI/ion trap mass spectrometry. *Anal. Chem.* **2000**, *72*, 5239-5243.

[141] Perkins, D.N.; Pappin, D.J.; Creasy, D.M.; Cottrell, J.S. Probability-based protein identification by searching sequence data- bases using mass spectrometry data. *Electrophoresis* **1999**, *20*, 3551-3567.

[142] Chaurand, P.; Norris, J.L.; Cornett, D.S.; Mobley, J.A.; Caprioli, R.M. New developments in profiling and imaging of proteins from tissue sections by MALDI mass spectrometry. *J. Proteome Res.* **2006**, *5*, 2889-2900.

[143] Kaleta, B.K.; van der Wiel, I.M.; Stauber, J.; Guzel, C.; Kros, J.M.; Luider,T.M.; Heeren, R.M. Sample preparation issues for tissue imaging by imaging MS. *Proteomics* **2009**, *9*, 2622-2633.

[144] Schwartz, S.A.; Reyzer, M.L.; Caprioli, R.M. Direct tissue analysis using matrix-assisted laser desorption/ionization mass spectrometry: Practical aspects of sample preparation. *J. Mass Spectrom.* **2003**, *38*, 699-708.

[145] Chaurand, P.; Schriver, K.E.; Caprioli, R.M. Instrument design and characterization for high resolution MALDI-MS imaging of tissue sections. *J. Mass Spectrom.* **2007**, *42*, 476-489.

[146] Caldwell, R.L.; Caprioli, R.M. Tissue profiling by mass spectrometry: A review of methodology and applications. *Mol. Cell. Proteomics* **2005**, *4*, 394-401.

[147] Hortin, G.L. The MALDI-TOF mass spectrometric view of the plasma proteome and peptidome. *Clin. Chem.* **2006**, *52*, 1223-1237.

[148] Batoy, S.M. A.B.; Akhmetova, E.; Miladinovic, S.; Smeal, J.; Wilkins, C.L. Developments in MALDI mass spectrometry: the quest for the perfect matrix *Appl. Spectrosc. Rev.* **2008**, *43*, 485-550.

[149] Weidner, S.M.; Trimpin, S. Mass Spectrometry of Synthetis Polymers. *Anal. Chem.* **2010**, *82*, 4811-4829.

[150] Trimpin,S. A perspective on MALDI alternatives total solvent-free analysis and electron transfer dissociation of highly charged ions by laserspray ionization. *J. Mass Spectrom.* **2010**, *45*, 471-485.

[151] Handschuh, M.; Nettesheim, S.; Zenobi, R. Laser-induced molecular desorption and particle ejection from organic films. *Appl. Surf. Sci.* **1999**, *137*, 125-135.

[152] Alves, S.; Fournier, F.; Afonso, C.; Wind, F.; Tabet, J.C. Gas-phase ionization/desolvation processes and their effect on protein charge state distribution under matrix-assisted laser desorption/ionization conditions. *Eur. J. Mass Spectrom.* **2006**, *12*, 369-383.

[153] Wenzel, T.; Sparbier, K.; Mieruch, T.; Kostrzewa, M. *Rapid Commun. Mass Spectrom.* **2006**, *20*, 785-789.

[154] Krause, J.; Stoeckli, M.; Schlunegger, U. P. Studies on the selection of new matrices for ultraviolet matrix-assisted laser desorption/ionization time-of-flight mass spectrometry. *Rapid Commun. Mass Spectrom.* **1996**, *10*, 1927-1933.

[155] Cohen, L. R. H.; Strupat, K.; Hillenkamp, F. Analysis of quaternary protein ensembles by matrix assisted laser desorption/ionization mass spectrometry. *J. Am. Soc. Mass Spectrom.* **1997**, *8*, 1046-1052.

[156] Wortmann, A.; Pimenova, T.; Alves, S.; Zenobi, R. Investigation of the first shot phenomenon in MALDI mass spectrometry of protein complexes. *Analyst* **2007**, *132*, 199-207.

[157] Woods, A. S.; Ugarov, M.; Egan, T.; Koomen, J.; Gillig, K. J.; Fuhrer, K.; Gonin, M.; Schultz, J. Lipid/peptide/nucleotide separation with MALDI-ion mobility-TOF MS. *Anal. Chem.* **2004**, *76*, 2187-2195.

[158] Jackson, S. N.; Wang, H. J.; Woods, A. S.; Ugarov, M.; Egan, T.; Schultz, J. A. Direct Tissue Analysis of Phospholipids in Rat Brain Using MALDI-TOFMS and MALDI-Ion Mobility-TOFMS. *J. Am. Soc. Mass. Spectrom.* **2005**, *16*, 133-138.

[159] Jackson, S. N.; Ugarov, M.; Egan, T.; Post, J. D.; Langlais, D.; Schultz, J. A.; Woods, A. S. MALDI-ion mobility-TOFMS imaging of lipids in rat brain tissue. *J. Mass Spectrom.* **2007**, *42*, 1093-1098.

[160] McLean, J. A.; Ridenour, W. B.; Caprioli, R. M. Profiling and imaging of tissues by imaging ion mobility-mass spectrometry. *J. Mass Spectrom.* **2007**, *42*, 1099-1105.

[161] Djidja, M.; Francese, S.; Loadman, P. M.; Sutton, C. W.; Scriven, P.; Claude, E.; Snel, M. F.; Franck, J.; Salzet, M.; Clench, M. R. Detergent addition to tryptic digests and ion mobility separation prior to MS/MS improves peptide yield and protein identification for in situ proteomic investigation of frozen and formalin-fixed paraffin-embedded adenocarcinoma tissue sections. *Proteomics* **2009**, *9*, 2750-2763.

[162] Ridenour, W.B.; Kliman, M.; McLean, J.A.; Caprioli, R.M. Structural characterization of phospholipids and peptides directly from tissue sections by MALDI traveling-wave ion mobility-mass spectrometry. *Anal. Chem.* **2010**, *82*, 1881-1889.

[163] Bush, M. F.; Hall, Z.; Giles, K.; Hoyes, J.; Robinson, C. V.; Ruotolo, B. T. Collision cross sections of proteins and their complexes: a calibration framework and database for gas-phase structural biology. *Anal. Chem.* **2010**, *82*, 9557-9565.

[164] Lee, S.; Ewing, M. A.; Nachtigall, F. M.; Kurulugama, R. T.; Valentine, S. J.; Clemmer, D. E. Determination of cross sections by overtone mobility spectrometry: evidence for loss of unstable structures at higher overtones. *J. Phys. Chem. B* **2010**, *114*, 12406-12415.

[165] Leary, J. A.; Schenauer, M. R.; Stefanescu, R.; Andaya, A.; Ruotolo, B. T.; Robinson, C. V.; Thalassinos, K.; Scrivens, J. H.; Sokabe, M.; Hershey, J. W. B. Methodology for measuring conformation of solvent-disrupted protein subunits using T-WAVE ion mobility MS: an investigation into eukaryotic initiation factors. *J. Am. Soc. Mass. Spectrom.* **2009**, *20*, 1699-1706.

[166] Fenn, L. S.; Kliman, M.; Mahsut, A.; Zhao, S. R.; McLean, J. A. Characterizing ion mobility-mass spectrometry conformation space for the analysis of complex biological samples. *Anal. Bioanal. Chem.* **2009**, *394*, 235-244.

[167] Williams, J. P.; Lough, J. A.; Campuzano, I.; Richardson, K.; Sadler, P. J. Use of ion mobility mass spectrometry and a collision cross-section algorithm to study an organometallic ruthenium anticancer complex and its adducts with a DNA oligonucleotide. *Rapid Commun. Mass Spectrom.* **2009**, *23*, 3563-3569.

[168] Shvartsburg, A. A.; Noskov, S. Y.; Purves, R. W.; Smith, R. D. Pendular proteins in gases and new avenues for characterization of macromolecules by ion mobility spectrometry. *Proc. Natl. Acad. Sci. U.S.A.* **2009**, *106*, 6495-6500.

[169] Scarff, C. A.; Thalassinos, K.; Hilton, G. R.; Scrivens, J. H. Travelling wave ion mobility mass spectrometry studies of protein structure: biological significance and comparison with X-ray crystallography and nuclear magnetic resonance spectroscopy measurements. *Rapid Commun. Mass Spectrom.* **2008**, *22*, 3297-3304.

[170] Kim, H.; Kim, H. I.; Johnson, P. V.; Beegle, L. W.; Beauchamp, J. L.; Goddard, W. A.; Kanik, I. Experimental and Theoretical Investigation into the Correlation between Mass and Ion Mobility for Choline and Other Ammonium Cations in N_2. *Anal. Chem.* **2008**, *80*, 1928-1936.

[171] Trimpin, S.; Plasencia, M.; Isailovic, D.; Clemmer, D. E. Resolving oligomers from fully grown polymers with IMS-MS. *Anal. Chem.* **2007**, *79*, 7965-7974.

[172] Tao, L.; McLean, J. R.; McLean, J. A.; Russell, D. H. A collision cross-section database of singly-charged peptide ions. *J. Am. Soc. Mass Spectrom.* **2007**, *18*, 1232-1238.

[173] Smith, D. P.; Giles, K.; Bateman, R. H.; Radford, S. E.; Ashcroft, A. E. Monitoring copopulated conformational states during protein folding events using electrospray ionization-ion mobility spectrometry-mass spectrometry. *J. Am. Soc. Mass Spectrom.* **2007**, *18*, 2180-2190.

[174] Colgrave, M. L.; Bramwell, C. J.; Creaser, C. S. Nanoelectrospray ion mobility spectrometry and ion trap mass spectrometry studies of the non-covalent complexes of amino acids and peptides with polyethers. *Int. J. Mass Spectrom.* **2003**, *229*, 209-216.

[175] Hoaglund, C. S.; Valentine, S. J.; Sporleder, C. R.; Reilly, J. P.; Clemmer, D. E. Three-dimensional ion mobility/TOFMS analysis of electrosprayed biomolecules. *Anal. Chem.* **1998**, *70*, 2236-2242.

[176] von Helden, G.; Wyttenbach, T.; Bowers, M. T. Inclusion of a MALDI ion source in the ion chromatography technique: conformational information on polymer and biomolecular ions. *Int. J. Mass Spectrom. Ion Processes* **1995**, *146/147*, 349-364.

[177] Senko, S. W.; McLafferty, F. W. Mass spectrometry of macromolecules: has its time now come? *Annu. Rev. Biophys. Biomol. Struct.* **1994**, *23*, 763-785.

[178] Vidova, V.; Pól, J.; Volny, M.; Novak, P.; Havlícek, V.; Wiedmer, S.K.; Holopainen, J.M. Visualizing spatial lipid distribution in porcine lens by MALDI imaging high-resolution mass spectrometry. *J. Lipid Res.* **2010**, *51*, 2295-2302.

[179] Tennessen, J.A.; Woodhams, D.C.; Chaurand, P.; Reinert, L.K.; Billheimer, D.; Shyr, Y.; Caprioli, R.M.; Blouin, M.S.; Rollins-Smith, L.A. Variations in the expressed antimicrobial peptide repertoire of northern leopard frog (< i> Rana pipiens</i>) populations suggest intraspecies differences in resistance to pathogens. *Dev. Com. Immunol.* **2009**, *33*, 1247-1257.

[180] Van Remoortere, A.; van Zeijl, R.J.M.; van den Oever, N.; Franck, J.; Longuespee, R.; Wisztorski, M.; Salzet, M. MALDI imaging and profiling MS of higher mass proteins from tissue. *J. Am. Soc. Mass Spectrom.* **2010**, *21*, 1922-1929.

[181] Schwamborn, K.; Caprioli, R.M. Molecular imaging by mass spectrometry-looking beyond classical histology. *Nat. Rev. Cancer* **2010**, *10*, 639-646.

[182] Rauser, S.; Marquardt, C.; Balluff, B.; Deininger, S.; Albers, C.; Belau, E.; Hartmer, R.; Suckau, D.; Specht, K.; Ebert, M.P.; Schmitt, M.; Aubele, M.; Hofler, H.; Walch, A. Classification of HER2 receptor status in breast cancer tissues by MALDI imaging mass spectrometry. *J. Proteome Res.* **2010**, *9*, 1854-1863.

[183] Chandra, S.; Lorey, D.R. SIMS ion microscopy in cancer research: single cell isotopic imaging for chemical composition, cytotoxicity, and cell cycle regulation. *Cell Mol. Biol.* **2001**, *47*, 503-518.

[184] Chandra, S.; Lorey, D.R.; II; Smith, D.R. Quantitative subcellular secondary ion mass spectrometry (SIMS) imaging of boron-10 and boron-11 isotopes in the same cell delivered by two combined BNCT drugs: in vitro studies on human glioblastoma T98G cells. *Radiat. Res.* **2002**, *157*, 700-710.

[185] Sjovall, P.; Lausmaa, J.; Johansson, B. Mass spectrometric imaging of lipids in brain tissue. *Anal.Chem.* **2004**, *76*, 4271-4278.

[186] Touboul, D.; Kollmer, F.; Niehuis, E.; Brunelle, A.; Laprevote,O. Improvement of Biological Time-of-Flight-Secondary Ion Mass Spectrometry Imaging with a Bismuth Cluster Ion Source *J. Am. Soc. Mass Spectrom.* **2005**, *16*, 1608-1618.

[187] Jones, E.A.; Lockyer, N.P.; Vickerman, J.C. Mass spectral analysis and imaging of tissue by ToF-SIMS—The role of buckminsterfullerene, C_{60}^{+}, primary ions. *Int. J. Mass Spectrom.* **2007**, *260*, 146-157.

[188] Maarten Altelaar, A.F.; van Minnen, J.; Jiménez, C.R.; Heeren,R.M.A.; Piersma, S.R. Direct molecular imaging of Lymnaea stagnalis nervous tissue at subcellular spatial resolution by mass spectrometry. *Anal. Chem.* **2005**, *77*, 735-741.

[189] McDonnel, L.; Piersma, S.R.; Maarten Altelaar, A.F.; Mize, T.H.; Luxembourg, S.L.; Verhaert, P.D.E.M.; van Minnen, J.; Heeren, R.M.A. Subcellular imaging mass spectrometry of brain tissue. *J. Mass Spectrom.* **2005**, *40*, 160-168.

[190] Altelaar, A.F.M.; Klinkert, I.; Jalink, K.; de Lange, R.P.J.; Adan, R.A.H.; Heeren, R.M.A.; Piersma, S.R. Gold-enhanced biomolecular surface imaging of cells and tissue by SIMS and MALDI mass spectrometry. *Anal. Chem.* **2006**, *78*, 734-742.

[191] Wiseman, J. M.; Puolitaival, S. M.; Takats, Z.; Cooks, R. G.; Caprioli, R. M. Mass spectrometric profiling of intact biological tissue by using desorption electrospray ionization. *Angew. Chem., Int. Ed.* **2005**, *44*, 7094-7097.

[192] Wiseman, J. M.; Ifa, D. R.; Song, Q.; Cooks, R. G. Tissue imaging at atmospheric pressure using desorption electrospray ionization (DESI) mass spectrometry. *Angew. Chem. Int. Ed.* **2006**, *45*, 7188-7192.

[193] Wiseman, J. M.; Ifa, D. R.; Zhuc, Y.; Kissingerc, C. B.; Manicke, N. E.; Kissingera, P. T.; Cooks, R. G. Desorption electrospray ionization mass spectrometry: Imaging drugs and metabolites in tissues. *Proc. Natl. Acad. Sci. U.S.A.* **2008**, *105*, 18120-18125.

[194] Lietz, C. B.; Richards, A. L.; Ren, Y.; Trimpin, S. Inlet ionization: protein analyses from the solid state without the use of a voltage or a laser producing up

to 67 charges on the 66 kDa BSA protein. *Rapid Commun. Mass Spectrom.* **2011**, *25*, 3453-3456.

[195] Richards, A. L.; Lietz, C. B.; Wager-Miller, J.; Mackie, K.; Trimpin, S. Imaging mass spectrometry in transmission geometry. *Rapid Commun. Mass Spectrom.* **2011**, *25*, 815-820.

[196] Richards, A. L.; Lietz, C. B.; Wager-Miller, J.; Mackie, K.; Trimpin, S. Localization and imaging of gangliosides in mouse brain tissue sections by laserspray ionization inlet. *J. Lipid Res.* **2012**, *53*, 1390-1398.

[197] Frankevich, V.; Nieckarz, R.; Sagulenko, P.; Barylyuk, K.; Levitsky, L.; Agapov, A.; Perlova, T.; Gorshkov, M.; Tarasova, I.; Zenobi, R. Probing the mechanisms of ambient ionization by laser-induced fluorescence spectroscopy. *Rapid Commun. Mass Spectrom.* **2012**, *26*, 1567-1572.

[198] Sidman, R. L.; Kosaras, B.; Misra, B. M.; Senft, S. L. High Resolution Mouse Brain Atlas, 1999. Website: http://www.hms. harvard.edu/research/brain/atlas.html (accessed June 9, 2012).

[199] Rosinke, B.; Strupat, K.; Hillenkamp, F.; Rosenbusch, J.; Dencher, N., Kruger, U.; Galla, H. J. Matrix-assisted laser desorption/ionization mass-spectrometry (MALDI-MS) of membrane-proteins and noncovalent complexes. *J. Mass Spectrom.* **1995***, 30*, 1462-1468.

[200] Bich, C.; Zenobi, R. Mass spectrometry of large complexes. *Curr. Opin. Struct. Biol.* **2009**, *19*, 632–639.

[201]   Wei, J.; Buriak, J.; Siuzdak, G. Desorption-ionization mass spectrometry on porous silicon. *Nature 1999*, *399*, 243-246.

[202]   Karas, M.; Bahr, U.; Strupat, K.; Hillenkamp, F.; Tsarbopoulos, A.; Pramanik, B. N. Matrix dependence of metastable fragmentation of glycoproteins in MALDI-TOF mass spectrometry. *Anal. Chem.* **1995**, *667*, 675-679.

[203]   Nemes, P.; Vertes, A. Laser ablation electrospray ionization for atmospheric pressure, in vivo, and imaging mass spectrometry. *Anal. Chem.* **2007**, *79*, 8098-8106.

[204]   Hopper, J. T. S.; Oldham, N. J. Collision induced unfolding of protein ions in the gas phase studied by ion mobility-mass spectrometry: the effect of ligand binding on conformational stability. *J. Am. Soc. Mass Spectrom.* **2009**, *20*, 1851-1858.

[205]   Luxembourg, S. L.; McDonnell, L. A.; Duursma, M. C.; Guo, X. H.; Heeren, R. M. A. Effect of local matrix crystal variations in matrix-assisted ionization techniques for mass spectrometry. *Anal. Chem.* **2003**, *75***,** 2333-2341.

[206]   Tholey, A.; Heinzle, E. Ionic (liquid) matrices for matrix-assisted laser desorption/ionization mass spectrometry-applications and perspectives. *Anal. Bioanal. Chem.* **2006***, 386*, 24-37.

[207]   Jaskolla, T. W.; Lehmann, W. D.; Karas, M. 4-Chloro-alpha-cyanocinnamic acid is an advanced, rationally designed MALDI matrix. *Proc. Natl. Acad. Sci. U.S.A.* **2008***, 105*, 12200-12205.

[208]   Tu, T.; Gross, M. L. Miniaturizing sample spots for matrix-assisted laser desorption/ionization mass spectrometry. *Trends Anal. Chem.* **2009***, 28*, 833-841.

[209] Kuprowski, M. C.; Boys, B. L.; Konermann, L. Analysis of protein mixtures by electrospray mass spectrometry: effects of conformation and desolvation behavior on the signal intensities of hemoglobin subunits. *J. Am. Soc. Mass Spectrom.* **2007**, *18*, 1279-1285.

[210] Merchant, M.; Weinberger, S.R. Recent advancements in surfaceenhanced laser desorption/ionization-time of flight-mass spectrometry. *Electrophoresis* **2000**, *21*, 1164-1177.

[211] Sunner, J.; Dratz, E.; Chen, Y.C. Graphite surface-assisted laser desorption/ionization time-of-flight mass spectrometry of peptides and proteins from liquid solutions. *Anal. Chem.* **1995**, *67*, 4335-4342.

[212] Wei, J.; Buriak, J.M.; Siuzdak, G. Desorption-ionization mass spectrometry on porous silicon. *Nature* **1999**, *399*, 243-246.

[213] Hutchens, T.W.; Yip, T.T. New desorption strategies for the mass spectrometric analysis of macromolecules. *Rapid Commun. Mass Spectrom.* **1993**, *7*, 576-580.

[214] Gebhardt, C.R.; Tomsic, A.; Schruder, H.; Durr, M.; Kompa, K.L. Matrix-free formation of gas-phase biomolecular ions by soft clusterinduced desorption. *Angew. Chem. Int. Ed.* **2009**, *48*, 4162-4165.

[215] Yamada, I.; Matsou, J.; Toyoda, N.; Kirkpatrick, A. Materials processing by gas cluster ion beams. *Mater. Sci. Eng. R* **2001**, *34*, 231-295.

[216] Cheng, J.; Wucher, A.; Winograd, N. Molecular depth profiling with cluster ion beams. *J. Phys. Chem. B* **2006**, *110*, 8329-8336.

[217]   Weibel, D.; Wong, S.; Lockyer, N.; Blenkinsopp, P.; Hill, R.; Vickerman, J.C. A C60 primary ion beam system for time of flight secondary ion mass spectrometry: Its development and secondary ion yield characteristics. *Anal. Chem.* **2003**, *75*, 1754-1764.

[218]   Page, J.S.; Tang,; Kelly, R.T.; Smith, R.D. Subambient pressure ionization with nanoelectrospray source and interface for improved sensitivity in mass spectrometry. *Anal. Chem.* **2008**, *80*, 1800-1805.

[219]   Hakansson, K.; Zubarev, R.A.; Coorey, R.V.; Talrose, V.L.; Hakansson, P. Interaction between explosive and analyte layers in explosive matrix-assisted plasma desorption mass spectrometry. *Rapid Commun. Mass Spectrom.* **1999**, *13*, 1169-1174.

[220]   Zubarev, R.A.; Hakansson, P.; Sundqvist, N.; Talrose, V.L. Enhancement of the molecular ion yield in plasma desorption mass spectrometry using explosive matrices. *Rapid Commun. Mass Spectrom.* **1997**, *11*, 63-70.

[221]   Pagnotti, V.S; Chubatyi, N.D.; McEwen, C.N. Solvent assisted inlet ionization: An ultrasensitive new liquid introduction ionization method for mass spectrometry. *Anal. Chem.* **2011**, *83*, 3981-3985.

[222]   Wang, B.; Inutan, E.D.; Trimpin, S. A new approach to high sensitivity liquid chromatography-mass spectrometry of peptides using nanoflow solvent assisted inlet ionization. *J. Am. Soc. Mass Spectrom.* **2012**, *23*, 442-445.

[223] Wang, B.; Lietz, C.B.; Inutan, E.D.; Leach, S.; Trimpin, S. Producing highly charged ions without solvent using laserspray ionization: A total solvent-free analysis approach at atmospheric pressure. *Anal. Chem.* **2011**, *83*, 4076-4084.

[224] Saunders, C. Charge separation mechanisms in clouds. *Space Sci. Rev.* **2008**, *137*, 335-353.

[225] Cheng, R.J. Water drop freezing: Ejection of microdroplets. *Science* **1970**, *170*, 1395-1396.

[226] Zink, J.I. Triboluminescence. *Accts. Chem. Res.* **1978**, *11*, 289-295.

[227] Lin, S.H.; Wutz, D.; Ho, Z.Z. Eyring, H. Mechanism of triboluminescence. *Proc. Natl. Acad. Sci. U.S.A.* **1980**, *77*, 1245-1247.

[228] Zink, J.I.; Klimt, W. Triboluminescence of coumarin-fluorescence and dynamic spectral features excited by mechanical-stress. *J. Am. Chem. Soc.* **1974**, *96*, 4690-4692.

[229] Sabbah, R.; Elwatik, K. Thermodynamic study of anthrone, coumarin, and phenazine. *J. Thermal Anal.* **1992**, *38*, 803-809.

[230] Smith, R.M. The mass spectrum of cocaine. *J. Forensic Sci.* **1997**, *42*, 475-480.

[231] Jagerdeo, E.; Abdel-Rehim, M. Screening of cocaine and its metabolites in human urine samples by direct analysis in real-time source coupled to time-of-flight mass spectrometry after online preconcentration utilizing microextraction by packed sorbent. *J. Am. Soc. Mass Spectrom.* **2009**, *20*, 891-899.

[232] McEwen, C.N.; McKay, R.G.; Larsen, B.S. Analysis of solids, liquids, and biological tissues using solids probe introduction at atmospheric pressure on commercial LC/MS instruments. *Anal. Chem.* **2005**, *77*, 7826-7831.

[233] Pieper, R.; Su.Q.; Gatlin C.L.; Huang, S.T.; Anderson, N.L.; Steiner, S. Multi-component immunoaffinity subtraction chromatography: an innovative step towards a comprehensive survey of the human plasma proteome. *Proteomics* **2003**, *3*, 422-432.

[234] Pieper, R.; Gatlin, C.L.; McGrath, A.M.; Makusky, A.J.; Mondal, M.; Seonarain, M.; Field, E.; Schatz, C.R.; Estock, M.A.; Ahmed, N.; Anderson, N.G.; Steiner, S. Characterization of the human urinary proteome: a method for high-resolution display of urinary proteins on two-dimensional electrophoresis gels with a yield of nearly 1400 distinct protein spots. *Proteomics* **2004**, *4*, 1159-1174.

[235] Wang, H.; Hanash, S. Multi-dimensional liquid phase based separations in proteomics. *J. Chromatog. B* **2003**, *787*, 11-18.

[236] Shushan, B. A review of clinical diagnostic applications of liquid chromatography–tandem mass spectrometry. *Mass Spectrom. Rev.* **2010**, *29*, 930-944.

[237] Kasper, D.C.; Herman, J.; De Jesus, V.R.; Mechtler, T.P.; Metz, T.F.; Shushan, B. The application of multiplexed, multidimensional ultra-high-performance liquid chromatography/tandem mass spectrometry to the high-throughput screening of lysosomal storage disorders in newborn dried bloodspots. *Rapid Commun. Mass Spectrom.* **2010**, *24*, 986-994.

[238] Ang, C.S.; Rothacker, J.; Patsiouras, H.; Gibbs, P.; Burgess, A.W.; Nice, E.C. Use of multiple reaction monitoring for multiplex analysis of colorectal cancer-associated proteins in human feces. *Electrophoresis* **2011**, *32*, 1926-1938.

[239] Zhang, X.; Fang, A.; Riley, C.P.; Wang, M.; Regnier, F.E.; Buck, C. Multi-dimensional liquid chromatography in proteomics. *Ana.l Chim. Acta* **2010**, *664*, 101-113.

[240] Issaq, H.J. The role of separation science in proteomics research. *Electrophoresis* **2001**, *22*, 3629-3638.

[241] Zhang, J.; Xu, X.; Gao, M.; Yang, P.; Zhang, X. Comparison of 2-D LC and 3-D LC with post-and pre-tryptic-digestion SEC fractionation for proteome analysis of normal human liver tissue. *Proteomics* **2007**, *7*, 500-512.

[242] Dixon, S.P.; Pitfield, I.D.; Perrett, D. Comprehensive multidimensional liquid chromatographic separation in biomedical and pharmaceutical analysis: a review. *Biomedical Chromatog.* **2006**, *20*, 508-529.

[243] Han, H.; Miyoshi, Y.; Ueno, K.; Okamura, C.; Tojo, Y.; Mita, M.; Lindner, W.; Zaitsu, K.; Hamase, K. Simultaneous determination of daspartic acid and d-glutamic acid in rat tissues and physiological fluids using a multi-loop two-dimensional HPLC procedure. *J. Chromatog. B* **2011**, *879*, 3196-3202.

[244] Liu, W.; Liu, B.; Cai, Q.; Li, J.; Chen, X.; Zhu, Z. Proteomic identification of serum biomarkers for gastric cancer using multidimensional liquid chromatography and 2D differential gel electrophoresis. *Clinica Chim. Acta* **2012**, *413*, 1098-1106.

[245] Zerefos, P.G.; Aivaliotis, M.; Baumann, M.; Vlahou, A. Analysis of the urine proteome via a combination of multidimensional approaches. *Proteomics* **2012**, *12*, 391-400.

[246] Gray, T.R.; Shakleya, D.M.; Huestis, M.A. A liquid chromatography tandem mass spectrometry method for the simultaneous quantification of 20 drugs of abuse and metabolites in human meconium. *Anal. Bioanal. Chem.* **2009**, *393*, 1977-1990.

[247] Isailovic, D.; Plasencia, M.D.; Gaye, M.M.; Stokes, S.T.; Kurulugama, R.T.; Pungpapong, V.; Zhang, M.; Kyselova ,Z.; Goldman, R.; Mechref, Y.; Novotny, M.V.; Clemmer, D.E. Delineating diseases by IMSMS profiling of serum N-linked glycans. *J. Proteome Res.* **2012**, *11*, 576-585.

[248] Kanu, A.B.; Dwivedi, P.; Tam, M.; Matz, L.; Hill, H.H. Jr. Ion mobility-mass spectrometry. *J Mass. Spectrom.* **2008**, *43*, 1-22.

[249] Baumketner, A.; Bernstein, S.L.; Wyttenbach, T.; Bitan, G.; Teplow, D.B.; Bowers, M.T.; Shea, J.E. Amyloid beta-protein monomer structure: a computational and experimental study. *Protein Sci.* **2006**, *15*, 420-428.

[250] Wu, C.; Siems, W.F.; Klasmeier, J.; Hill, H.H. Separation of isomeric peptides using electrospray ionization/high-resolution ion mobility spectrometry. *Anal. Chem.* **2000**, *72*, 391–395.

[251] Ruotolo, B.T.; Verbeck, G.F.; Thomson, L.M.; Woods, A.S.; Gillig, K.J.; Russell, D.H. Distinguishing between phosphorylated and nonphosphorylated peptides with ion mobility−mass spectrometry. *J. Proteome Res.* **2002**, *1*, 303-306.

[252] Hoaglund, C.S.; Valentine, S.J.; Sporleder, C.R.; Reilly, J.P.; Clemmer, D.E. Three-dimensional ion mobility/TOFMS analysis of electrosprayed biomolecules. *Anal. Chem.* **1998**, *70*, 2236-2242.

[253] Thalassinos, K.; Slade, S.E.; Jennings, K.R.; Scrivens, J.H.; Giles, K.; Wildgoose, J.; Hoyes, J.; Bateman, R.H.; Bowers, M.T. Ion mobility mass spectrometry of proteins in a modified commercial mass spectrometer. *Int. J. Mass Spectrom.* **2004**, *236*, 55-63.

[254] Ruotolo, B.T.; Giles, K.; Campuzano, I.; Sandercock, A.M.; Bateman, R.H.; Robinson, C.V. Evidence for macromolecular protein rings in the absence of bulk water. *Science* **2005**, *310*, 1658-1661.

[255] Bernstein, S.L.; Dupuis, N.F.; Lazo, N.D.; Wyttenbach, T.; Condron, M.M.; Bitan, G.; Teplow, D.B.; Shea, J.E.; Ruotolo, B.T.; Robinson, C.V.; Bowers, M.T. Amyloid-β protein oligomerization and the importance of tetramers and dodecamers in the aetiology of Alzheimer's disease. *Nat. Chem.* **2009**, *1*, 326-331.

[256] Benesch, J.L.; Ruotolo, B.T.; Simmons, D.A.; Robinson, C.V. Protein complexes in the gas phase: technology for structural genomics and proteomics. *Chemical Rev.-Columbus* **2007**, *107*, 3544-3567.

[257] Seo Y, Andaya A, Leary JA (2012) Preparation, separation, and conformational analysis of differentially sulfated heparin octasaccharide isomers using ion mobility mass spectrometry. *Anal. Chem.* **2012**, *84*, 2416-2423.

[258] Niñonuevo, M.R.; Leary, J.A. Ion mobility mass spectrometry coupled with rapid protein threading predictor structure prediction and collision-induced dissociation for probing chemokine conformation and stability. *Anal. Chem.* **2012**, *84*, 3208–3214.

[259] Giles, K.; Williams, J.P.; Campuzano, I. Enhancements in travelling wave ion mobility resolution. *Rapid Commun. Mass Spectrom.* **2011**, *25*, 1559–1566.

[260] Li, H.; Giles, K.; Bendiak, B.; Kaplan, K.; Siems, W.F.; Hill, H.H. Jr. Resolving structural isomers of monosaccharide methyl glycosides using drift tube and traveling wave ion mobility mass spectrometry. *Anal. Chem.* **2012**, *84*, 3231-3239.

[261] Chawner, R.; McCullough, B.; Giles, K.; Barran, P.E.; Gaskell, S.J.; Eyers, C.E. A QconCAT standard for calibration of ion mobility mass spectrometry systems. *J. Proteome Res.* **2012**, *11*, 5564-5572.

[262] Jungmann, J.H.; Heeren, R.M.A. Emerging technologies in mass spectrometry imaging. *J. Proteomics* **2012**, *75*, 5077-5092.

[263] Reid, G.E.; McLuckey, S.A. Top down protein characterization via tandem mass spectrometry. *J Mass Spectrom.* **2002**, *37*, 663-675.

[264] Moss, C.L.; Chamot-Rooke, J.; Nicol, E.; Brown, J.; Campuzano, I.; Richardson, K.; Williams, J.P.; Bush, M.F.; Bythell, B.; Paizs, B.; Turecek, F. Assigning structures to gas-phase peptide cations and cation-radicals. An infrared multiphoton dissociation, ion mobility, electron transfer, and computational study of a histidine peptide ion. *The J. Phys. Chem. B* **2012**, *116*, 3445-3456.

[265] Cody, R.B.; Laramee, J.A.; Durst, H.D. Versatile new ion source for the analysis of materials in open air under ambient conditions. *Anal. Chem.* **2005**, *77*, 2297-2302.

[266] Shiea, J.; Huang, M.Z.; Hsu, H.J.; Lee, C.Y.; Yuan, C.H.; Beech, I.; Sunner, J. Electrospray-assisted laser desorption/ionization mass spectrometry for direct ambient analysis of solids. *Rapid Commun. Mass Spectrom.* **2005**, *19*, 3701–3704.

[267] Sampson, J.S.; Hawkridge, A.M.; Muddiman, D.C. Generation and detection of multiply-charged peptides and proteins by Matrix-Assisted Laser Desorption Electrospray Ionization (MALDESI) fourier transform ion cyclotron resonance mass spectrometry. *J. Am. Soc. Mass Spectrom.* **2006**, *17*, 712–1716.

[268] Pagnotti, V.S.; Inutan, E.D.; Marshall, D.D.; McEwen, C.N.; Trimpin, S. Inlet ionization: a new highly sensitive approach for liquid chromatography-mass spectrometry of small and large molecules. *Anal. Chem.* **2011**, *83*, 7591–7594.

[269] Chubatyi, N.D.; Pagnotti, V.S.; Bentzley, C.M.; McEwen, C.N. High sensitivity steroid analysis using liquid chromatography/solvent-assisted inlet ionization mass spectrometry. *Rapid Commun. Mass Spectrom.* **2012**, *26*, 887–892.

[270] Hoaglund-Hyzer, C.S.; Lee, Y.J.; Counterman, A.E.; Clemmer, D.E. Coupling ion mobility separations, collisional activation techniques, and multiple stages of MS for analysis of complex peptide mixtures. *Anal. Chem.* **2002**, *74*, 992-1006.

[271] Ferrige, A.G.; Seddon, M.J.; Green, B.N.; Jarvis, S.A.; Skilling, J.; Staunton, J. Disentangling electrospray spectra with maximum entropy. *Rapid Commun. Mass Spectrom.* **1992**, *6*, 707-711.

[272] Eibisch, M.; Zellmer, S.; Gebhardt, R.; Suss, R.; Fuchs, B.; Schiller, J. Phosphatidylcholine dimers can be easily misinterpreted as cardiolipins in complex lipid mixtures: a matrix-assisted laser desorption/ionization time-of-flight mass spectrometric study of lipids from hepatocytes. *Rapid Commun. Mass Spectrom.* **2011**, *25*, 2619-2626.

[273] James, P.F.; Perugini, M.A.; O'Hair, R.A.J. Sources of artefacts in the electrospray ionization mass spectra of saturated diacylglycerophosphocholines: From condensed phase hydrolysis reactions through to gas phase intercluster reactions. *J. Am. Soc. Mass Spectrom.* **2006**, *17*, 384-394.

[274] Vestal, M.L.; Juhasz, P.; Martin, S.A. Delayed extraction MALDI TOF MS. *Rapid Commun. Mass Spectrom.* **1995**, *9*, 1044–1050.

[275] Shariatgorji, M.; Nilsson, A.; Goodwin Richard, J.A.; Svenningsson, P.; Schintu, N,, Banka, Z.; Kladni, L.; Hasko, T.; Szabo, A.; Andren, P.E. Deuterated matrix-assisted laser desorption ionization matrix uncovers masked mass spectrometry imaging signals of small molecules. *Anal. Chem.* **2012**, *84*, 7152-7157.

[276] Sun, J.; Baker, A.; Chen, P. Profiling the indole alkaloids in yohimbe bark with ultra-performance liquid chromatography coupled with ion mobility quadrupole time-of-flight mass spectrometry. *Rapid Commun. Mass Spectrom.* **2011**, *25*, 2591-2602.

[277] Plumb, R.S.; Johnson, K.A.; Rainville, P.; Smith, B.W.; Wilson, I.D.; Castro-Perez, J.M.; Nicholson, J.K. UPLC/MSE; a new approach for generating

molecular fragment information for biomarker structure elucidation. *Rapid Commun. Mass Spectrom.* **2006**, *20*, 1989–1994.

[278] Bateman, K.P.; Castro-Perez, J.; Wrona, M.; Shockcor, J.P.; Yu, K.; Oballa, R.; Nicoll-Griffith, D.A. MSE with mass defect filtering for in vitro and in vivo metabolite identification. *Rapid Commun. Mass Spectrom.* **2007**, *21*, 1485-1496.

[279] Ronci, M.; Bonanno, E.; Colantoni, A.; Pieroni, L.; Di Ilio, C.; Spagnoli, L.G.; Federici, G.; Urbani, A. Protein unlocking procedures of formalin-fixed paraffin-embedded tissues: Application to MALDITOF Imaging MS investigations. *Proteomics* **2008**, *8*, 3702-3714.

[280] Cheng, F.Y.; Blackburn, K.; Lin, Y.M.; Goshe, M.B.; Williamson, J.D. Absolute protein quantification by LC/MSE for global analysis of salicylic acid-induced plant protein secretion responses. *J. Proteome Res.* **2009**, *8*, 82-93.

[281] Castro-Perez, J.M.; Kamphorst, J.; DeGroot, J.; Lafeber, F.; Goshawk, J.; Yu, K.; Shockcor, J.P.; Vreeken, R.J.; Hankemeier, T. Comprehensive LC− MSE lipidomic analysis using a shotgun approach and its application to biomarker detection and identification in osteoarthritis patients. *J. Proteome Res.* **2010**, *9*, 2377-2389.

[282] Finamore, F.; Pieroni, L.; Ronci, M.; Marzano, V.; Mortera, S.L.; Romano, M.; Cortese, C.; Federici, G.; Urbani, A. Proteomics investigation of human platelets by shotgun nUPLC-MSE and 2DE experimental strategies: a comparative study. *Blood Transfusion* **2010**, *8*, S140-S148.

[283] Prasad, B.; Garg, A.; Takwani, H.; Singh, S. Metabolite identification by liquid chromatography-mass spectrometry. *Trends Anal. Chem*. **2011**, *30*, 360-387.

[284] Bijlsma, L.; Sancho, J.V.; Hernández, F.; Niessen, W. Fragmentation pathways of drugs of abuse and their metabolites based on QTOF MS/MS and MSE accurate-mass spectra. *J. Mass Spectrom.* **2011**, *46*, 865-875.

[285] Martins-de-Souza, D.; Guest, P.C.; Guest, F.L.; Bauder, C.; Rahmoune, H.; Pietsch, S.; Roeber, S.; Kretzschmar, H.; Mann, D.; Baborie, A.; Bahn, S. Characterization of the human primary visual cortex and cerebellum proteomes using shotgun mass spectrometry-data-independent analyses. *Proteomics* **2012**, *12*, 500-504.

[286] Cha, I.S.; Kwon, J.; Park, S.H.; Nho, S.W.; Jang, H.B.; Park, S.B.; del Castillo, C.S.; Hikima, J.; Aoki, T.; Jung, T.S. Kidney proteome responses in the teleost fish Paralichthys olivaceus indicate a putative immune response against Streptococcus parauberis. *J. Proteomics* **2012**, *75*, 5166-5175.

[287] Dong, W.; Wang, P.; Meng, X.; Sun, H.; Zhang, A.; Wang, W.; Dong, H.; Wang, X.J. Ultra-performance liquid chromatography–high definition mass spectrometry analysis of constituents in the root of radix stemonae and those absorbed in blood after oral administration of the extract of the crude drug. *Phytochemical Anal.* **2012**, *23*, 657-667.

[288] Barbara, J.E.; Kazmi, F.; Muranjan, S.; Toren, P.C.; Parkinson, A. High-resolution mass spectrometry elucidates metabonate (False Metabolite) formation

from alkylamine drugs during in vitro metabolite profiling. *Drug Metabolism Disposition* **2012**, *40*, 1966-1975.

[289] Aluise, C.D.; Robinson, R.A.; Becket, T.L.; Murphy, M.P.; Cai, J.; Pierce, W.M.; Markesbery, W.R.; Butterfield, D.A. Preclinical Alzheimer disease: brain oxidative stress, Aβ peptide and proteomics. *Neuro Disease* **2010**, *39*, 221–228.

[290] Roher, A.E.; Lowenson, J.D.; Clarke, S.; Woods, A.S.; Cotter, R.J.; Gowing, E.; Ball, M.J. β-Amyloid-(142) is a major component of cerebrovascular amyloid deposits: implications for the pathology of Alzheimer disease. *Proc. Nat'l. Acad. Sci. U. S. A.* **1993**, *90*, 10836-10840.

[291] Pan, J.; Han, J.; Borchers, C.H.; Konermann, L. Conformerspecific hydrogen exchange analysis of a beta(1–42) oligomers by top-down electron capture dissociation mass spectrometry. *Anal. Chem.* **2011**, 83, 5386-5393.

[292] Kraus, M.; Bienert, M.; Krause, E. Hydrogen exchange studies on Alzheimer's amyloid-beta peptides by mass spectrometry using matrix-assisted laser desorption/ionization and electrospray ionization. *Rapid Commun. Mass Spectrom.* **2003**, *17*, 222-228.

[293] Ceuppens, R.; Dumont, D.; Van Brussel, L.; Van de Plas, B.; Daniels, R.; Noben, J.P.; Verhaert, P.; Van der Gucht, E.; Robben, J.; Clerens, S.; Arckens, L. Direct profiling of myelinated and demyelinated regions in mouse brain by imaging mass spectrometry. *Int. J. Mass Spectrom.* **2007**, *260*, 185-194.

[294] Weinmann, W.; Müller, C.; Vogt, S.; Frei, A. LC-MS-MS analysis of the neuroleptics clozapine, flupentixol, haloperidol, penfluridol, thioridazine, and

zuclopenthixol in hair obtained from psychiatric patients. *J. Anal. Toxic* **2002**, *26*, 303-307.

[295]   Bao, D.; Truong, T.T.; Renick, P.J.; Pulse, M.E.; Weiss, W.J. Simultaneous determination of rifampicin and levofloxacin concentrations in catheter segments from a mouse model of a device-related infection by liquid chromatography/electrospray ionization tandem mass spectrometry. *J. Pharma. Biomed. Anal.* **2008**, *46*, 723-727.

[296]   Wichitnithad, W.; McManus, T.J.; Callery, P.S. Identification of isobaric product ions in electrospray ionization mass spectra of fentanyl using multistage mass spectrometry and deuterium labeling. *Rapid. Commun. Mass Spectrom.* **2010**, *24*, 2547-2553.

[297]   Weinmann, W.; Müller, C.; Vogt, S.; Frei, A. LC-MS-MS analysis of the neuroleptics clozapine, flupentixol, haloperidol, penfluridol, thioridazine, and zuclopenthixol in hair obtained from psychiatric patients. *J. Anal. Toxic* **2002**, *26*, 303-307.

[298]   Smith, R.M. The Mass Spectrum of Cocaine. *J. Forensic Sci.* **1997**, *42*, 475-480.

[299]   Wood, M.; Laloup, M.; Ramirez;F.M.M.; Jenkins, K.M.; Young, M.S.; Ramaekers, J.G.; De Boeck, G.; Samyn, N. Quantitative analysis of multiple illicit drugs in preserved oral fluid by solid-phase extraction and liquid chromatography-tandem mass spectrometry. *Forensic Sci. Int.* **2005**, *150*, 227-228.

ABSTRACT

DEVELOPMENT OF MATRIX ASSISTED IONIZATION METHODS FOR CHARACTERIZATION OF SOLUBLE AND INSOLUBLE PROTEINS FROM NATIVE ENVIRONMENTS BY MASS SPECTROMETRY

by

ELLEN DELA VICTORIA INUTAN

August 2013

Advisor: Prof. Sarah Trimpin

Major: Chemistry (Analytical)

Degree: Doctor of Philosophy

Matrix-assisted laser/desorption ionization (**MALDI**) and electrospray ionization (**ESI**) have made a huge impact in the analysis of biological materials. ESI has gained its popularity involving liquid based analysis, efficient fragmentation, chromatographic and electrophoretic separations but has a limitation for solubility restricted materials and surface analysis. MALDI is applicable to large biomolecule analysis and for surface methods useful for tissue imaging but is limited for structural characterization due to poor fragmentation and is ill suited for liquid based separation methods. The research presented here relates to new ionization methods that encompass the benefits of ESI and MALDI. These novel ionization methods produce multiply charged ions similar to ESI but directly from surfaces similar to MALDI. The formation of multiply charged ion extends the mass range of high performance mass spectrometers with advanced features

for structural characterization such as ultra-high mass resolution and mass accuracy, and electron transfer dissociation. The surface method approach enables the detection, characterization, and identification of compounds directly from native environments such as tissue. The use of gas phase ion mobility separation reduces spectral complexity and improves the dynamic range of the experiment. Among the three novel ionization methods presented, MAIV has the potential to analyze fragile molecules and protein complexes, and is applicable for both atmospheric pressure and vacuum conditions. The laser-based method, LSII has the potential to improve the spatial resolution for tissue imaging and LSIV to enhance sensitivity.

AUTOBIOGRAPHICAL STATEMENT

ELLEN D. INUTAN

Education

August 2013	Ph.D., Chemistry (*anticipated*) Wayne State University, USA
October 2001	M.S., Chemistry; Mindanao State University-Iligan Instititute of Technology, Philippines
April 1994	B.S., Chemistry; Mindanao State University-Iligan Instititute of Technology, Philippines

Awards and Honors

2012-2013	Rumble Fellowship Award from Graduate School
2012	David Boltz Award in Analytical Chemistry
2012	Summer Dissertation Fellowship Award from Graduate School
2011-2012	Schaap Fellowship Award from Department of Chemistry
2010-2011	Rumble Fellowship Award from Graduate School
2010	Honor Citation for Teaching Service in Chemistry
2009	Best Oral Presentation Award, Anachem Symposium
2009	Honor Citation for Teaching Service in Chemistry

Relevant Publications (*denotes corresponding author)

1) **Inutan, E.D.**; Wager-Miller, J.; Narayan, S.; Mackie, K.; Trimpin, S.* *Int. J. Ion Mobility Spectrom.* **2013**, *16*, 145-159.
2) Trimpin, S.*; **Inutan, E.D.** *J. Am. Soc. Mass Spectrom.* **2013**, *24*, 722-732.
3) Trimpin, S.*; **Inutan, E.D.** *Anal. Chem.* **2013**, *85*, 2005-2009.
4) **Inutan, E.D.**; Trimpin, S*. *Mol. Cell. Proteomics* **2013**, *12*, 792-796.
5) **Inutan, E. D.**; Wager-Miller, J.; Mackie, K.; Trimpin, S.* *Anal. Chem.* **2012**, *84*, 9079–9084.
6) Trimpin, S.*; Wang, B.; **Inutan, E.D.**; Li, J.; Lietz, C.B.; Harron, A.; Pagnotti, V.S.; Sardelis, D.; McEwen, C.N.* *J. Am. Soc. Mass Spectrom.* **2012**, *23*, 1644-1660.
7) Li, J.; **Inutan, E. D.**; Wang, B.; Lietz, C. B.; Green, D. R.; Manly, C. D.; Richards, A. L.; Marshall, D. D.; Lingenfelter, S.; Ren, Y.; Trimpin, S.* *J. Am. Soc. Mass Spectrom.* **2012**, *23*, 1625-1643.
8) **Inutan, E.D.**; Wang, B.; Trimpin, S.* *Anal. Chem.* **2011**, *83*, 678-684.
9) **Inutan, E.D.**; Richards, A.L.; Wager-Miller, J.; Mackie, K.; McEwen, C.N.; Trimpin, S.* *Mol. Cell Proteomics* **2011**, *10*, 1-8.
10) **Inutan, E.D.**; Trimpin, S.* *J. Proteome Res.* **2010**, *9*, 6077-6081.
11) **Inutan, E.D.**; Trimpin, S*. *J. Am. Soc. Mass Spectrom.* **2010**, *21*, 1260-1264.
12) Trimpin, S.*; **Inutan, E.D.**; Herath, T.N.; McEwen, C.N. *Mol. Cell. Proteomics* **2010**, *9*, 362-367.
13) Trimpin, S.*; **Inutan, E.D**.; Herath, T.N.; McEwen, C.N. *Anal. Chem.* **2010**, *82*, 11-15.

Book Chapter (Co-Authored)

Inutan, E.D., Claude, E., and Trimpin, S.* Total Solvent-free Analysis, Charge Remote Fragmentation, and Structures of Highly Charged Laserspray Ions using IMS-MS, Ion Mobility Spectrometry: Theory and Applications, Taylor and Francis Group, **2010**.